Advanced Technologies Enabling Unlicensed Spectrum Utilization in Cellular Networks

Bolin Chen

Department of Electronic and Electrical Engineering
University of Sheffield

This thesis is submitted for the approval of the
Doctor of Philosophy

September 2018

Acknowledgements

This four-year PhD is full of adventures and challenges at the same time. Everything went differently from what I was expecting, yet nothing ended as what I was fearing for. From my perspective, PhD study is not just about learning new things and applying them in our research fields. We also learn to deal with all the unexpected changes and frustration that might occur at any moment in our research and in other aspects of our lives. During these four years, I grew up as a researcher and as a person, with a lot of ups and downs, embracing numerous magic moments and cruel reality. When this journey finally comes to the end, I feel extremely grateful for all the chain reactions one after another that have brought me where I belong. For that, I would like to give my deepest gratitude to all the people who have accompanied me through this part of my life and offered me their kindest support.

First of all, I would like to thank my supervisor Prof.Jie Zhang, for being a very wise, cool and supportive supervisor, who gives inspiration and guide instead of giving instructions. I really enjoyed all the brainstorming discussions, from which I learned thinking about research problems from different perspectives and in a broader picture. I would also like to thank my second supervisor Dr. Xiaoli Chu, for her support and help during these years.

I would like to give my special thanks to Prof. Di Yuan, for inviting me to visit his group in Linköping University, which turns out to be a life-changing decision in many ways. And my other collaborators, Dr. Nikolaos Pappas, Dr. Zheng Chen, Dr. Yuan Gao, Dr. Jiming Chen, Dr. Lei You, Dr. Ioannis Avgoustis, Dr. Qing He and Dr. Lei Lei, with whom I had very nice collaboration experience and learned many things about research. Many thanks for the support from the European Commission for the H2020 DECADE. Nice cooperation! Many thanks to my officemates and all my friends in Sheffield, Norrkoping, Shenzhen, previous and current colleagues, for making every workday full of laughter and interesting discussions.

Last but not least, All these hard work during my PhD will not mean anything without mentioning the support from my parents and other family members. I would not have made it this far without their encouragement and sacrifice. Thanks Mom and Dad, wish you are always in a good mood. Thanks Yingzhuzhu, wish our love will last forever. God bless us.

Abstract

As the rapid progress and pleasant experience of Internet-based services, there is an increasing demand for high data rate in wireless communications systems. Unlicensed spectrum utilization in Long Term Evolution (LTE) networks is a promising technique to meet the massive traffic demand. There are two effective methods to use unlicensed bands for delivering LTE traffic. One is offloading LTE traffic to Wi-Fi. An alternative method is LTE-unlicensed (LTE-U), which aims to directly use LTE protocols and infrastructures over the unlicensed spectrum. It has also been pointed out that addressing the above two methods simultaneously could further improve the system performance.

However, how to avoid severe performance degradation of the Wi-Fi network is a challenging issue of utilizing unlicensed spectrum in LTE networks. Specifically, first, the inter-system spectrum sharing, or, more specifically, the coexistence of LTE and Wi-Fi in the same unlicensed spectrum is the major challenge of implementing LTE-U. Second, to use the LTE and Wi-Fi integration approach, mobile operators have to manage two disparate networks in licensed and unlicensed spectrum. Third, optimization for joint data offloading to Wi-Fi and LTE-U in multi-cell scenarios poses more challenges because inter-cell interference must be addressed.

This thesis focuses on solving problems related to these challenges. First, the effect of bursty traffic in an LTE and Wi-Fi aggregation (LWA)-enabled network has been investigated. To enhance resource efficiency, the Wi-Fi access point (AP) is designed to operate in both the native mode and the LWA mode simultaneously. Specifically, the LWA-mode Wi-Fi AP cooperates with the LTE base station (BS) to transmit bearers to the LWA user, which aggregates packets from both LTE and Wi-Fi. The native-mode Wi-Fi AP transmits Wi-Fi packets to those native Wi-Fi users that are not with LWA capability. This thesis proposes a priority-based Wi-Fi transmission scheme with congestion control and studied the throughput of the native Wi-Fi network, as well as the LWA user delay when the native Wi-Fi user is under heavy traffic conditions. The results provide fundamental insights in the throughput and delay behavior of the considered network. Second, the above work has been extended to larger topologies. A stochastic geometry model has been used to model and analyze the performance of an MPTCP Proxy-based LWA network with intra-tier and cross-tier dependence. Under the considered network model and the activation conditions of LWA-mode Wi-Fi, this thesis has obtained three approximations for the density of active LWA-mode Wi-Fi APs through different approaches. Tractable analysis is provided for

the downlink (DL) performance evaluation of large-scale LWA networks. The impact of different parameters on the network performance have been analyzed, validating the significant gain of using LWA in terms of boosted data rate and improved spectrum reuse. Third, this thesis also takes a significant step of analyzing joint multi-cell LTE-U and Wi-Fi network, while taking into account different LTE-U and Wi-Fi inter-working schemes. In particular, two technologies enabling data offloading from LTE to Wi-Fi are considered, including LWA and Wi-Fi offloading in the context of the power gain-based user offloading scheme. The LTE cells in this work are subject to load-coupling due to inter-cell interference. New system frameworks for maximizing the demand scaling factor for all users in both Wi-Fi and multi-cell LTE networks have been proposed. The potential of networks is explored in achieving optimal capacity with arbitrary topologies, accounting for both resource limits and inter-cell interference. Theoretical analyses have been proposed for the proposed optimization problems, resulting in algorithms that achieve global optimality. Numerical results show the algorithms' effectiveness and benefits of joint use of data offloading and the direct use of LTE over the unlicensed band. All the derived results in this thesis have been validated by Monte Carlo simulations in Matlab, and the conclusions observed from the results can provide guidelines for the future unlicensed spectrum utilization in LTE networks.

Contents

Acknowledgements **i**

List of Publications **v**

List of Figures **vii**

List of Tables **xi**

List of Abbreviations **xii**

1 Introduction **1**

1.1 Motivation of Using Unlicensed Spectrum 1

1.2 Analysis on Related Features of LTE and Wi-Fi 3

1.2.1 LTE Carrier Aggregation with Unlicensed Band 3

1.2.2 LTE and Wi-Fi MAC Protocols 6

1.2.3 Coexistence Issues and Enablers 8

1.2.4 Key Factors of Performance Difference between LTE-LAA and Wi-Fi . . 10

1.2.5 Co-channel Interference 13

1.2.6 Summary and Guidelines 14

1.3 Motivations of this Thesis 16

1.3.1 Modeling and Analysis of LTE and Wi-Fi Aggregation using Both Queueing Theory and Stochastic Geometry 16

1.3.2 Resource Optimization for Joint Data Offloading to Wi-Fi and LTE-U in Load-coupled and Multi-cell Networks 18

1.4 Main Contributions and Outline of the Thesis 21

2 Literature Review **24**

2.1 Introduction 24

2.2 Comparative Study of Existing Surveys on LTE and This Chapter 25

2.3 Current Research on Directly Extending LTE to the Unlicensed Band 28
2.3.1 Recent Related Works 28
2.3.2 Coexistence Mechanisms in Markets without LBT Requirement 34
2.3.3 Coexistence Mechanisms in Markets with LBT Requirement 39
2.3.4 Summary and Guidelines 41
2.4 Current Research on LTE and Wi-Fi Integration 44
2.4.1 LTE-WLAN Aggregation 45
2.4.2 LTE-Wi-Fi Path Aggregation based on Multipath TCP 47
2.4.3 Advantages of LTE-WLAN Integration 47
2.5 Modelling Considerations for LTE and Wi-Fi Inter-working System 48
2.5.1 With or Without an Anchor in the Licensed Band 48
2.5.2 Radio Link-Level or TCP-level LTE-WLAN Integration 48
2.5.3 Comparison of Standardization Statuses 49
2.5.4 Further Research Directions 50
2.6 Deployment Scenarios for the Coexistence and Scenario-oriented Decision-making 51
2.6.1 Influential Factors for the Classification of SC Scenarios 51
2.6.2 Representative Deployment Scenarios 55
2.6.3 An Example of Scenario-oriented Coexistence Design with Representative Performance Evaluation Metrics and Scenarios 57
2.7 Conclusion 63

3 LTE-WLAN Aggregation: A Packet Level Analysis 64
3.1 Introduction 64
3.1.1 Background 64
3.1.2 Main Results and Chapter Organization 64
3.2 System Model 66
3.2.1 Network Model 66
3.2.2 Priority Based Wi-Fi Transmission Scheme 67
3.2.3 Physical Layer Model 69
3.3 Network Performance Metrics 70
3.3.1 Service Probability for the Queues 70
3.3.2 Native Wi-Fi throughput 72
3.3.3 LWA UE Delay 72
3.4 Analysis of Native Wi-FI Network Throughput and LWA UE Delay 73
3.4.1 Analysis of the Queues 73

3.4.2 Analysis of the Native Wi-Fi Throughput . . . 77
3.4.3 Analysis of the LWA UE Delay . . . 78
3.5 Numerical Results . . . 79
3.5.1 Native Wi-Fi Throughput . . . 80
3.5.2 LWA UE Delay . . . 83
3.6 Conclusion . . . 84

4 Modeling and Analysis of MPTCP Proxy-based LTE-WLAN Path Aggregation 85
4.1 Introduction . . . 85
4.2 System Model . . . 86
4.3 Performance Analysis . . . 91
4.3.1 Success Probability Analysis . . . 91
4.3.2 Cellular Rate Improvement . . . 94
4.3.3 Area Spectral Efficiency Improvement of the WiFi Band . . . 95
4.4 Numerical Results . . . 96
4.4.1 LWPA-mode WiFi Link Success Probability . . . 97
4.4.2 WiFi ASE Improvement . . . 97
4.4.3 Cellular Rate Improvement . . . 98
4.5 Conclusion . . . 99

5 Resource Optimization for Joint LWA and LTE-U in Load-coupled and Multi-Cell Networks 100
5.1 Introduction . . . 100
5.2 System Model and Problem Formulation . . . 101
5.2.1 Network Model . . . 101
5.2.2 LTE Load Coupling . . . 102
5.2.3 Rate and Resource Characterization for Wi-Fi . . . 104
5.2.4 Problem Formulation . . . 104
5.3 Solution Approach . . . 105
5.4 Simulation Results . . . 107
5.5 Conclusion . . . 110

6 Performance Optimization for Joint Wi-Fi Offloading and LTE-U in Multi-Cell Networks 111
6.1 Introduction . . . 111
6.1.1 Background and Motivation . . . 111

6.1.2 Main Results and Chapter Organization 111
6.2 System Model 113
6.2.1 Network Model 113
6.2.2 LTE Load Coupling 114
6.2.3 Rate and Resource Characterization for Wi-Fi 116
6.3 Problem Formulation and Description 117
6.4 Problem Reduction with Restricted UE Offloading Scheme 119
6.5 Optimization Under Restricted UE Offloading Scheme 122
6.6 Simulation Results 125
6.7 Conclusion 128

7 Conclusions and Outlook **129**
7.1 General Conclusions 129
7.2 Highlight and Future Research Directions 130

Bibliography **135**

List of Publications:

Journal papers:

1. **B. Chen**, J. Chen, Y. Gao and J. Zhang. "Coexistence of LTE-LAA and Wi-Fi on 5 GHz With Corresponding Deployment Scenarios: A Survey", IEEE Communications Surveys & Tutorials, $19(1)$, $7-32$, Jan. 2017. (Chapter 1, 2)

2. **B. Chen**, N. Pappas, D. Yuan and J. Zhang. "Throughput and Delay Analysis of LWA with Bursty Traffic and Randomized Flow Splitting", IEEE Access, $7(1)$, $24667-24678$, Feb. 2019. (Chapter 3)

3. **B. Chen** and L. You and D. Yuan and N. Pappas and J. Zhang. "Resource Optimization for Joint LWA and LTE-U in Load-coupled and Multi-Cell Networks", IEEE Communications Letters, $23(2)$, $330-333$, Feb. 2019. (Chapter 5)

4. **B. Chen**, L. You, D. Yuan and J. Zhang. "Performance Optimization for Joint Wi-Fi Offloading and LTE-U in Multi-Cell Networks", IEEE Transactions on Wireless Communications, to appear, Apr. 2019. (Chapter 6)

Conference papers:

1. **B. Chen**, J. Chen and J. Zhang. "Scenario-Oriented Small Cell Network Design for LTE-LAA and Wi-Fi Coexistence on 5 GHz", IEEE International Workshop on Computer Aided Modeling and Design of Communication Links and Networks (CAMAD), IEEE, Lund, Sweden, Jun. 2017. (Chapter 1)

2. **B. Chen**, Z. Chen, N. Pappas, D. Yuan and J. Zhang. "Bringing LTE to Unlicensed Spectrum: Technical Solutions and Deployment Considerations". IEEE International Workshop on Computer Aided Modeling and Design of Communication Links and Networks (CAMAD), IEEE, Barcelona, Spain, Sept. 2018. (Chapter 1)

3. **B. Chen**, N. Pappas, Z. Chen, D. Yuan and J. Zhang. "LTE-WLAN Aggregation with Bursty Data Traffic and Randomized Flow Splitting", IEEE International Conference on Communications (ICC), IEEE, Shanghai, May. 2019. (Chapter 3)

4. **B. Chen**, Z. Chen, N. Pappas, D. Yuan and J. Zhang. "Modeling and Analysis of MPTCP Proxy-based LTE-WLAN Path Aggregation", IEEE Global Communications Conference (GLOBECOM), IEEE, Singapore, Dec. 2017. (Chapter 4)

5. Y. Gao, **B. Chen**, X. Chu and J. Zhang. "Resource Allocation in LTE-LAA and WiFi Coexistence: a Joint Contention Window Optimization Scheme", IEEE Global Communications Conference (GLOBECOM), IEEE, Singapore, Dec. 2017.

List of Figures

1.1 5 GHz unlicensed spectrum under consideration. 4

1.2 Integration of LTE licensed and LTE unlicensed. UE refers to user. . . . 4

1.3 Two categories of ICIC users: a) Cell Center User (CCU); b) Cell Edge User (CEU). CCUs are distributed in the gray region. CEUs are distributed in the color regions. CCU's frequency reuse factor is 1. The frequency reuse factor for CEU is 3. Different colors represent different frequencies. 9

1.4 Co-channel interference from LTE SC/UE to Wi-Fi AP/STA. 13

2.1 Three steps of coexistence mechanism centralized by CSAT: a) CHS; b) OSDL; and c) CSAT. 33

2.2 Messages exchange between Co-located LTE and Wi-Fi radios. 35

2.3 Two categories of CSAT periods. (a) CSAT ON periods; (b) CSAT OFF periods. The usage of the channel by LTE-LAA radio can be reduced by pulling its transmission power back or bring the cyclic ON/OFF ratio down, and vice versa. The introduction of data punctured subframes can be used to reduce latency by dividing the CSAT ON periods into two parts: the short CSAT ON periods and the short CSAT OFF periods. . . 37

2.4 An example of CCA placement option. A subframe S (e.g., subframe 9) consists of a GP, several slots for CCA placement and a node for CUBS for the remaining symbols. A GP is provided prior to the CCA placement to guarantee the idle time. If the CCA procedure succeeds, the node will seize and hold the medium until the start of the next subframe S, and CUBS may block the transmission signals of other users nearby. 39

2.5 Illustration of DTX periods and DL CCA intervals. If the first CCA lose contention, the eNB will not transmit, nor will it perform any CCA until the next transmission period, either. On the contrary, if it wins contention, while the second CCA procedures fail during one DTX period, the transmission will stop until a subsequent second CCA indicates that the radio frequency band is available again. 41
2.6 LTE-WLAN integration operation scenarios: (a) Non-collocated LWA operation scenario; (b) Collocated LWA operation scenario; (c) LWPA operation scenario. EPC refers to evolved packet core. 45
2.7 Ideal/non-ideal backhaul deployments. 53
2.8 Four LTE-LAA deployment scenarios designed by 3GPP: a) scenario 1: carrier aggregation between licensed macro cell (F1) and unlicensed SC (F3); b) scenario 2: carrier aggregation between licensed SC (F2) and unlicensed SC (F3) without macro cell coverage; 3) scenario 3: licensed macro cell and SC (F1), with carrier aggregation between licensed SC (F1) and unlicensed SC (F3); 4) scenario 4: carrier aggregation between licensed macro cell (F1), licensed SC (F2) and unlicensed SC (F3) if there is ideal backhaul among macro cell and SC. 55
2.9 Office or CBD buildings. 58
2.10 Scenario-oriented coexistence design for a realistic scenario. 59
2.11 Two performance evaluation scenarios designed by 3GPP: a)indoor scenario; b) outdoor scenario, where the licensed carriers for the SC and macro cell are different. 60

3.1 An example LWA network. LWA splits data units of the same bearer over the LTE and Wi-Fi link simultaneously. The AP W serves LWA purpose, and also operates as the native-mode Wi-Fi AP. The BS transmitter has queue LW and queue LU_L with packets intended to W and U_L, respectively. The AP transmitter has queue WU_L and queue WU_W containing the messages that are destined to U_L and U_W, respectively. . 65
3.2 The operation of W in the described protocol. 68
3.3 The Discrete Time Markov Chain which models the i-th queue evolution ($i \in \{LU_L, LW, WU_L\}$). When $i \in \{LU_L, LW\}$, $M \to \infty$ holds. . . . 72
3.4 $\mathcal{P}(Q_{WU_L} = 0)$ vs. $q_{W,W}$. 79

3.5 $\mathcal{P}(1 \leqslant Q_{WU_L} \leqslant M)$ vs. $q_{W,W}$. 80
3.6 $\mathcal{P}(Q_{WU_L} = 0)$ vs. $q_{U_L,W}$. 81
3.7 $\mathcal{P}(1 \leqslant Q_{WU_L} \leqslant M)$ vs. $q_{U_L,W}$. 81
3.8 Native Wi-Fi throughput vs. $q_{U_L,W}$. 81
3.9 Native Wi-Fi throughput vs. $q_{W,W}$. 81
3.10 LWA UE delay vs. $q_{U_L,W}$. 82
3.11 LWA-mode Wi-Fi link delay vs. $q_{U_L,W}$. 82

4.1 Two-RAT HetNet consisting of LTE BSs, active LWPA-mode Wi-Fi APs, inactive LWPA-mode Wi-Fi APs in the cellular RAT, and closed-access Wi-Fi APs in the WLAN RAT. The backhaul is shown by the dotted lines. AP1 and AP2 are active LWPA-mode Wi-Fi APs since they both meet the conditions. AP3 and AP6 are not available for LWPA mode because they are closed-access Wi-Fi. Although AP4 and AP5 are open-access Wi-Fi, they are inactive LWPA-mode Wi-Fi APs because there is no cellular user closer to AP5 than distance R, while the distance between AP4 and the active Wi-Fi AP3 is shorter than δ. 87
4.2 Density of active LWPA WiFi APs vs. user density with $p = 0.2, 0.5, 0.8$ and $\delta = 50$ m. 90
4.3 Guard Zone with radius δ of a typical active LWPA-mode WiFi AP centered at the origin with its users uniformly distributed in a disk $B(0, R)$. According to the system model, no active open-access or closed-access WiFi AP can lie in the circle of radius δ centered at the origin, thus the distance from the nearest WiFi AP to the typical LWPA user is at least $\delta - l$. 92
4.4 LWPA-mode Wi-Fi link success probability vs. θ with $p = \{0.2, 0.5, 0.8\}$, $\delta = 50$ m. 94
4.5 Wi-Fi ASE improvement vs. guard zone radius with $p = \{0.2, 0.5, 0.8\}$. 95
4.6 Wi-Fi ASE improvement vs. user density with $p = \{0.2, 0.5, 0.8\}$, and here δ= 50 m. 96
4.7 Cellular rate improvement vs. guard radius with $p = \{0.2, 0.5, 0.8\}$. . . 97
4.8 Cellular rate improvement vs. user density with $p = \{0.2, 0.5, 0.8\}$, and here $\delta = 50$ m. 98

5.1 System model for LTE-U and LWA. 101
5.2 Optimum α with respect to the number of LTE UEs per Wi-Fi AP. . . . 108
5.3 Percentage improvement of HB over NON in respect of available θ. . . 109

6.1 System model for joint LTE-U and Wi-Fi Offloading. 113
6.2 Percentage improvement of HB and WO over NON in respect of the number of offloadable LTE UEs per Wi-Fi AP. 126
6.3 Percentage improvement of HB and RS over NON in respect of the percentage of available unlicensed spectrum. 127
6.4 Percentage improvement of HB over NON in respect of the percentage of available θ. 128

List of Tables

2.1 Comparative Study of our work with existing surveys on LTE 27
2.2 Comparative study of coexistence schemes 29
2.3 Progress in LTE Unlicensed Standardization 31
2.4 Typical LTE-LAA and Wi-Fi coexistence testing and results 32
2.5 Comparative study of LBT and Duty-cycling 42
2.6 5 GHz sub-bands for indoor/outdoor environment in some countries . . 52

3.1 Formulation symbols. 66
3.2 System Parameters. 79

List of Abbreviations

3GPP	3rd Generation Partnership Project
ABS	Almost Blank Subframe
ACK	Acknowledgement Packet
AP	Access Point
BS	Base Station
CBD	Central Business District
CCA	Clear Channel Assessment
CCU	Cell Center User
CEU	Cell Edge User
CHS	Channel Selection
CoMP	Coordianated Multi-point
CQI	Channel Quality Indicator
CRS	Cell-specific Reference Signal
CR	Cognitive Radio
CSAT	Carrier Sense Adaptive Transmission
CSMA/CA	Carrier Sense Multiple Accesses Collision Avoidance
CTS	Clear to Send
CUBS	Channel Usage Beacon Signals
DCF	Distributed Coordination Function

DL	Downlink
DTX	Discontinuous Transmission
eICIC	enhanced ICIC
eNB	evolved NodeB
FCC	Federal Communications Commission
FDMA	Frequency Division Multiple Access
GP	Guard Period
HARQ	Hybrid Automatic Repeat Request
HetNet	Heterogeneous Network
ICIC	Inter-cell Interference Coordination
LBT	Listen-Before-Talk
LOS	Line of Sight
LTE-A	LTE Advanced
LTE-LAA	LTE-licensed Assisted Access
LTE-U	LTE-Unlicensed
LTE	Long Term Evolution
LWA	LTE-WLAN Radio Level Aggregation
LWPA	LTE-WLAN Path Aggregation
M2M	Machine-to-machine
MAC	Medium Access Control
MCS	Modulation and Coding Scheme
MHCP	Matern Hard-coreProcess
MPTCP	Multipath Transmission Control Protocol
MSA	Multi-stream Aggregatio

OFDM	Orthogonal Frequency Division Multiplexing
OSDL	Opportunistic SDL
PCell	Primary Cell
PDCCH	PHY DL Control Channel
PDSCH	PHY DL Shared Channel
PHY	Physical Layer
PPDU	Physical Protocol Data Unit
PPP	Poisson Point Process
PSD	Power Spectral Density
PSS	Primary Synchronization Signal
PUCCH	PHY UL Control Channel
PUSCH	PHY UL Shared Channel
PU	Primary User
QoS	Quality of Service
RAN	Radio Access Network
RAT	Radio Access Technology
RF	Radio Frame
RRH	Remote Radio Head
RRM	Radio Resource Management
RS-CS	Resource Specific Cell Selection
RTS	Request to Send
SCell	Secondary Cell
SC	Small Cell
SDL	Supplemental DL

SINR	Signal to Interference plus Noise Ratio
SON	Self-organizing Network
SSS	Secondary Synchronization Signal
STA	Station
SU	Secondary User
TDD	Time-Division-Duplexed
UE	User
UL	Uplink
UNII	Unlicensed National Informational Infrastructure
WLAN	Wireless Local Area Network

Chapter 1

Introduction

1.1 Motivation of Using Unlicensed Spectrum

Due to the exponentially growing mobile data traffic caused by increasing number of devices and content-centric applications, the demands for higher network capacity and efficiency are continuously augmenting. Higher network capacity can be achieved by seeking additional spectrum resources, achieving higher spectral efficiency thus, improving the spatial reuse of communication resources. While the new licensed frequency bands are becoming insufficient and expensive, some unlicensed spectrum are under-utilized in current cellular networks. One possible solution to address the increasing wireless data demand is data offloading from licensed Long Term Evolution (LTE) networks to the unlicensed spectrum [1]. Recent works on data aggregation at the LTE base station (BS) allow for better control of offloading with improved performance at both system and user levels while leveraging the existing LTE features.

The current mobile networks are facing great capacity challenges. Benefits promised by the coexistence of Wi-Fi and LTE networks in unlicensed spectrum have started to attract interest from the research community [2]. For example, LTE causes less adjacent channel interference to a Wi-Fi system compared to another Wi-Fi system [3]. In other words, LTE is a better neighbour than another Wi-Fi system in terms of adjacent channel coexistence with a Wi-Fi system. On the other hand, as stated in [4, 5], combined LTE and Wi-Fi can unquestionably increase the traffic load in the band, the contention for spectrum resources, and the congestion if the coexistence of LTE and Wi-Fi is not satisfactorily arranged.

To be clear, the reason to adopt LTE in 5 GHz is not to unseat Wi-Fi, but to increase

the spectral efficiency and capacity of the 5 GHz band, and to do so with the technology that is fully integrated within the mobile operators networks. In fact, it is envisioned that Wi-Fi and LTE will exhibit complementary benefits that can be leveraged for an efficient integration. On the one hand, due to the uncontrolled nature of Wi-Fi, the competition for resources among a large number of hotspot users can yield dramatically poor throughputs. Offloading some of this traffic to the well-managed LTE network becomes necessary. On the other hand, due to cross-tier and co-tier interference among LTE networks, some of the traffic can also be offloaded from LTE networks to the Wi-Fi band, so as to alleviate the interference and ease congestion.

There are two main approaches for unlicensed bands utilization in LTE networks: 1) data offloading to the IEEE 802.11 based Wireless Local Area Network (WLAN) via LTE-WLAN integration; and 2) the direct usage of LTE based networks over the unlicensed spectrum. New technologies for integration of Wi-Fi as an integral part of 3rd Generation Partnership Project (3GPP) radio access network (RAN) have been proposed, allowing seamless integration of unlicensed spectrum in the LTE network without significant modification on the Wi-Fi architecture. Recently, Radio link level integration includes LTE-WLAN Aggregation (LWA), which is currently being standardized by 3GPP. For LWA, Wi-Fi works as another carrier managed by the LTE network to convey traffic. Another LTE-WLAN integration solution is at Transmission Control Protocol (TCP) level, i.e., LTE-WLAN Path Aggregation (LWPA) based on Multipath TCP (MPTCP) [6]. MPTCP can split data and transmit them through both LTE and Wi-Fi networks, concurrently. In this mode, each of the connections can be managed separately without the knowledge of each other's presence. In general, LTE-WLAN integration allows the operators to leverage the existing cellular network deployments and the established base of Wi-Fi deployments.

One motivating factor in using LTE in unlicensed spectrum directly is the use of the same core radio technology across both licensed and unlicensed bands, as the data offloading can be enabled in a seamless fashion. Two technologies to augment an existing LTE licensed band interface with unlicensed band transmissions have emerged: LTE-Licensed Assisted Access (LTE-LAA) [3], a 3GPP standards-based solution, and LTE-Unlicensed (LTE-U) [7], proposed by the LTE-U forum. There is also another technique called MulteFire. MulteFire incorporates a full LTE core network in unlicensed spectrum without requiring an LTE anchor in licensed spectrum.

The above solutions have attracted considerable attention from both academic and industrial communities. Each solution has its respective merits, and is suitable for different deployment scenarios. For example, some operators with a large installed base of Wi-Fi access points (APs) may prefer LTE-WLAN integration, while others who have a strong dependency on LTE cellular infrastructure might prefer the direct use of LTE in unlicensed spectrum. Extending LTE to the unlicensed bands will need mechanisms for fair coexistence with other unlicensed technologies such as Wi-Fi. To use the LTE-WLAN integration approach mobile operators have to manage two disparate networks in licensed and unlicensed spectrum.

1.2 Analysis on Related Features of LTE and Wi-Fi

For a better understanding of unlicensed spectrum utilization in cellular networks, brief summaries of several related features of the two technologies, i.e., LTE and Wi-Fi are reviewed in this section.

1.2.1 LTE Carrier Aggregation with Unlicensed Band

5 GHz Unlicensed Spectrum under Consideration

For the sake of clearer channel conditions, wider spectrum, and easier implementation, the unlicensed frequency band of common interest in 3GPP is the 5 GHz UNII band mainly used by IEEE 802.11-based WLAN, or Wi-Fi currently [8].

With regard to the availability of 5 GHz spectrum, different countries have their regional requirements on 5 GHz UNII band in the form of regulations or rules. As shown in Fig.1.1, the spectrum 5.15-5.35 GHz (UNII-1, UNII-2A) is available in the US, Europe, Japan and China. 5.47-5.725GHz (UNII-2C) is open for unlicensed wireless access for the US, Europe and Japan. In addition, 5.725-5.85 GHz (UNII-3) is available for the US, China, and being considered as new spectrum additions to extend unlicensed use in Europe. Furthermore, there are still 195 MHz bands (proposed UNII-2B 5.35-5.47 GHz and proposed UNII-4 5.85-5.925 GHz) that could be available in the US, Europe and China in the future [9].

3GPP has decided to focus initially on the 5 GHz band, but some other unlicensed bands are still available. For example, LTE-LAA could easily expand to 2.4 GHz, though this band is already congested and hence unlikely to protect its LTE-LAA investment

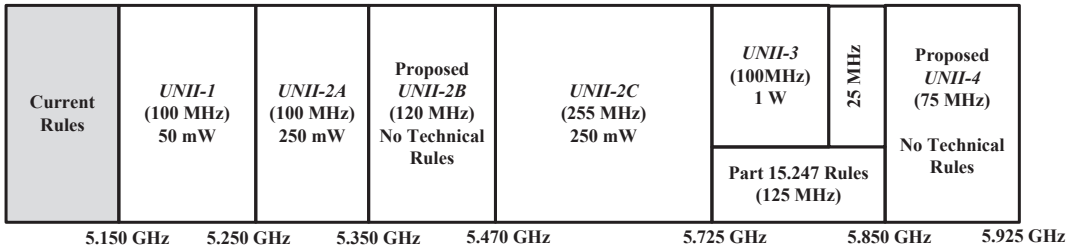

Figure 1.1: 5 GHz unlicensed spectrum under consideration.

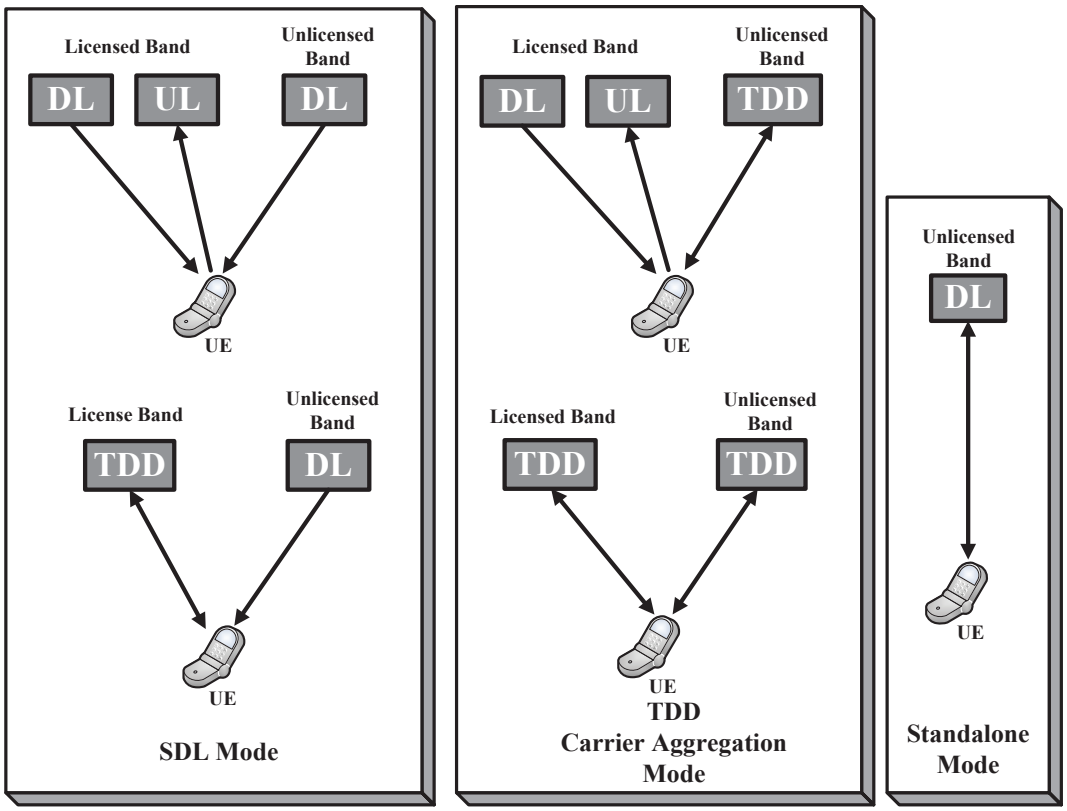

Figure 1.2: Integration of LTE licensed and LTE unlicensed. UE refers to user.

currently. The 60 GHz band is another possible target, but the range is too limited to be used in the enterprise or in public venues [10].

The main purpose of aggregating LTE to the unlicensed bands is that it gives operators access to a new band. Meanwhile, there are other licensed bands available that can be used to add capacity to cellular networks. The 3.5 GHz band, for example, is an attractive option. Due to its short coverage radius, the 3.5 GHz band is not suited for Macro deployments, but it works well as an under-layer for SCs that, unlike co-channel deployments, does not create interference with the Macro layers [10].

LTE-LAA and LTE-U

It should be taken into account that the transmission relying only on unlicensed spectrum is unstable since the nature of being unlicensed makes it hard to provide guaranteed Quality of Service (QoS) [8]. Therefore, it seems unreasonable to ignore the usage of licensed spectrum during the extension of LTE spectrum access. To allow users to access both licensed and unlicensed spectrum and to study the use of unlicensed band under a unified LTE network infrastructure, LTE-LAA is initiated as part of 3GPP LTE Release 13 [11, 12]. According to the design, LTE-LAA in unlicensed spectrum is an extension of the LTE carrier aggregation protocol [13–16]. LTE-LAA on unlicensed band is always combined with licensed band LTE and is replacing the current terminology of LTE-U [8], which is a natural extension of LTE carrier aggregation to unlicensed band as a part of secondary carriers. Besides using unlicensed spectrum targeting at 5 GHz UNII band at present, LTE-LAA tends to include every kind of technology that would augment licensed spectrum operation [17].

As it requires fewer modifications from licensed LTE compared to LTE-LAA, LTE-U will be the first version of LTE unlicensed to be available in commercial deployments. However, because it does not implement LBT mechanisms, LTE-U can only be used in markets where regulation does not require LBT, such as China, Korea, India and the USA. LTE-LAA, on the other hand, is the version of LTE in unlicensed band that 3GPP standardizes in Release 13. It supports LBT in addition to carrier aggregation. LTE-LAA is set to become a global standard as it strives to meet regulatory requirements worldwide. Nevertheless, because the standardization work had not been completed until March 2016, commercialization will take longer than for LTE-U. For details refering to the LBT mechanisms, see section 1.2.3. For more details about LTE carrier aggregation, refer to [18–22].

Integration of LTE Licensed and LTE Unlicensed

As stated above, if there is additional capacity demand, to manage the different component carriers, carrier aggregation may be employed with one carrier serving as the Primary Cell (PCell) and others serving as Secondary Cells (SCells)[23, 24]. The unlicensed spectrum may be employed by cellular systems in different ways, distinguished by the supplementary and control channel configurations shown in Fig. 1.2. In some systems, the aggregation is based on what is supported in 3GPP Release 12 [25]. In this

case, the second carrier would be a Time-Division-Duplexed (TDD) carrier or Supplemental DL (SDL) only. In the SDL mode, the unlicensed band is used to carry data traffic originally staying in the licensed spectrum, while the UL and control channel remain in the licensed spectrum. In the TDD carrier aggregation mode, the unlicensed band is capable of carrying data traffic in both UL and DL directions while the control channel remains in the licensed spectrum. In other systems, the unlicensed spectrum may be employed in a standalone configuration, with all carriers operating in the unlicensed spectrum exclusively. A representative LTE-based technology for unlicensed spectrum without licensed anchor channel is called MuLTEfire alliance, which is formed by Nokia and Qualcomm. It is a solution that may be attractive to cable operators, wireless Internet service providers or hotspot network operators who lack licensed spectrum. This mode has not been discussed in 3GPP yet.

1.2.2 LTE and Wi-Fi MAC Protocols

In this part, I briefly review the load-based Wi-Fi and frame-based LTE MAC layers.

LTE MAC Protocol

The key enabling technology of LTE systems is orthogonal frequency division multiple access. For better QoS control, transmission spectral efficiency and inter-cell coordination, transmission in LTE has to follow a continuous stream of a deterministic frame structure, i.e., a Radio Frame (RF). An LTE RF consists of ten 1 ms subframes, each one is further divided into two 0.5 ms slots [18, 19, 26, 27]. For further details about LTE frame structure, refer to [20, 21, 28–30].

The LTE system adopts a centralized MAC protocol, which includes a dynamic resource scheduler that allocates physical resources on PHY DL Shared Channel (PDSCH) for data traffic. The scheduler takes into account the traffic volume, the QoS requirement, and the radio channel conditions when sharing the physical resources among mobile devices. For DL data transmissions, the eNBs transmits the PDSCH resource assignments and their Modulation and Coding Scheme (MCS), on PHY DL Control Channel (PDCCH), and the data packet on the PDSCH accordingly. The mobile device needs to monitor its PDCCH in the control region to discover its grant. Once its PDCCH is detected, the mobile device decodes PDSCH on allocated resources using the MCS provided. For more details about LTE MAC protocol and radio resource management, refer

to [18, 26, 31].

Wi-Fi MAC Protocol

A Wi-Fi node, on the contrary, with no need for centralized controller, will first sense the channel whenever it has a pending transmission. The MAC layer of Wi-Fi is based on the Carrier Sense Multiple Accesses with Collision Avoidance (CSMA/CA) mechanism [32], so Wi-Fi systems do not require a centralized controller as is needed in LTE systems [33]. The basic idea of CSMA/CA is to sense the channel to determine whether the wireless medium is busy or not. Only if the channel is sensed to be not busy, or idle, is a Wi-Fi station (STA) permitted to transmit. The CSMA/CA mechanism particularly used in the IEEE 802.11 MAC is also known as the Distributed Coordination Function (DCF), which enables multiple Wi-Fi STAs to access the channel according to the order they start sensing the channel [34, 35].

DCF is very effective when the medium is not heavily loaded, since it allows STAs to transmit with minimum delay. However, there is always a chance of collision, i.e., several STAs transmitting at the same time, due to the fact that these STAs sense the medium free and decide to transmit at once. In order to overcome this problem, Wi-Fi uses a collision avoidance mechanism. As a matter of fact, if the medium is free for a specified time, defined as distributed inter frame space, the STA is then allowed to transmit, the receiving STA will check the cyclic redundancy check of the received packet and send an Acknowledgement Packet (ACK). Receipt of the ACK means that no collision occurred. Besides the above mechanism, IEEE 802.11 Wi-Fi standard also defines a virtual carrier sense mechanism. When an STA is willing to transmit a packet, it will first transmit a short control packet called Request to Send (RTS). As a response to the RTS, the destination STA will send a Clear to Send (CTS) back. All STAs receiving RTS/CTS will set their virtual carrier sense indicator, and will use this information together with the physical carrier sense when sensing the medium. For more details about DCF and related collision avoidance mechanisms, refer to [32].

The fundamental difference between LTE and Wi-Fi MAC layers has caused some issues on the coexistence of the two systems [36]. I will focus on coexistence challenges and enablers as well as the choice of LTE-LAA and Wi-Fi in section 1.2.3 and section 1.2.4 respectively.

1.2.3 Coexistence Issues and Enablers

The main challenge for the coexistence of LTE-LAA and Wi-Fi is while operating LTE-LAA in the presence of Wi-Fi making use of the same band, the performance of Wi-Fi systems will be significantly affected, while the performance of LTE is nearly unchanged since Wi-Fi moves to silence mode due to the CSMA/CA mechanism. That is due to the fact that these two technologies use different channel usage and access procedures. LTE is designed based on the assumption that one operator has exclusive control of a given spectrum. It will continuously transmit with minimum time gap even in the absence of data traffic. LTE also has an almost continuously transmitting protocol, as well as a periodically transmitting protocol to transfer a variety of control and reference signals. Wi-Fi, on the contrary, is designed to coexist with other technologies through random backoff and channel sensing. As a result, Wi-Fi users will have little chance to sense a clear channel and transmit. For more details about LTE channel usage and access procedures, refer to [22, 31, 37–41].

Studying the MAC implementation of Wi-Fi system can help understand how LTE and Wi-Fi systems can coexist with each other. In fact, the LBT scheme introduced by [42] and [43] is a simplified version of DCF. In order to enable the coexistence of LTE-LAA and Wi-Fi in unlicensed bands, in such markets where the LBT is mandatory, the coexistence of these two systems can be enabled by LBT enforced on LTE-LAA in unlicensed bands [36].

Two design options of LTE-LAA LBT, asynchronous LBT and synchronous LBT, have been proposed in [44]. The main difference between them lies in that the asynchronous LBT is based on the current DCF protocol. In this case, the LBT scheme might use IEEE 802.11 RTS/CTS signals to ensure that the channel is idle just at that moment. However, synchronous LBT can be seen as a special version of asynchronous LBT, wherein, data subframes are synchronized with the licensed LTE carrier. This LBT approach may need a smaller number of changes in the LTE specification, and use Inter-cell Interference Coordination (ICIC) already defined in LTE releases to manage the interference among LTE base STAs [45].

A simple way to explain ICIC is based on the scheme of Fig. 1.3. The users are divided into two categories, one is CCU shown in Fig. 1.3(a), and the other is CEU shown in Fig. 1.3(b). CCUs are the users distributed in the gray region of Fig. 1.3, and CEUs are the users distributed in the red, green and blue areas. CCU can use all the

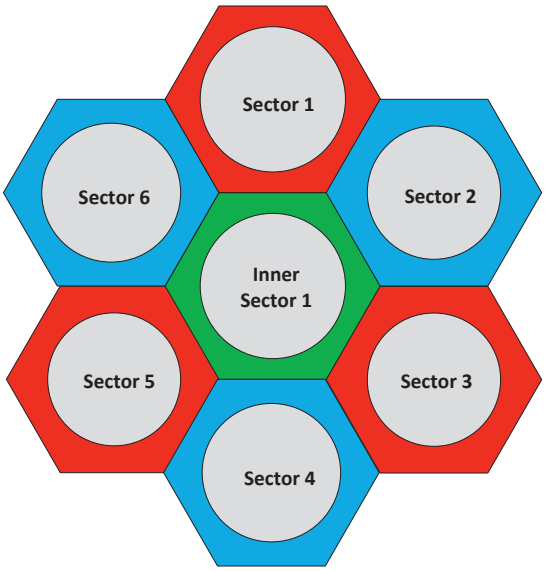

Figure 1.3: Two categories of ICIC users: a) Cell Center User (CCU); b) Cell Edge User (CEU). CCUs are distributed in the gray region. CEUs are distributed in the color regions. CCU's frequency reuse factor is 1. The frequency reuse factor for CEU is 3. Different colors represent different frequencies.

frequency points to communicate with the base STA, while CEU must use corresponding specified frequency points to ensure orthogonality between different cells. CEUs can be assigned a higher transmission power for the frequency reuse factor greater than 1. The frequency points are not overlapped at the edges so the adjacent cell interference is small. CCUs frequency reuse factor is 1 for the cases where path loss is small and transmission power is low. Therefore the interference to the adjacent cells is not high either. More details about ICIC can be found in [46–48].

Furthermore, LTE advanced in unlicensed spectrum can also use a coexistence mechanism centralized by CSAT, which is in spirit very similar to DCF.

Moreover, enhanced ICIC (eICIC) in 3GPP Release 10 [25], which is designed to mitigate intra-frequency interference by using various measures in the power, frequency, and also time domain, introduces a concept of ABSs to manage coexistence of the two technologies [49]. ABSs are LTE subframes with reduced DL transmission activity or power. The eICIC in time domain introduces a Resource Specific Cell Selection (RSCS) method. The concept is to have certain sub-frames during which the Macro-eNB is not allowed to transmit data allowing the Pico cell edge users suffering high interference

from the Macro-eNB, to be served with better conditions. Transmissions from Macro-eNBs are periodically muted during entire sub-frame. The users associated with the Pico cell can send their data during such an ABS and avoid interference from the Macro cell. In fact the muting is not completed since certain control signals still need to be transmitted even in the muted sub-frames to avoid radio link failure.

1.2.4 Key Factors of Performance Difference between LTE-LAA and Wi-Fi

Mobile operators are assessing LTE-LAA in the 3GPP standardization. At the same time, Wi-Fi also relies on for enterprise and residential offload, carrier Wi-Fi, or hotspot access, and the use of this technology expanding as Wi-Fi becomes more preferable while using unlicensed spectrum for opportunistic access. Since LTE in unlicensed band will be deployed mostly in SC topologies, often in indoor locations, operators can face a complex decision of choosing between LTE-LAA and Wi-Fi especially when they plan for an SC deployment [10]. In some deployment scenarios, if practical commercial factors are taken into account, LTE-LAA or Wi-Fi should be used alone in 5 GHz band without considering coexistence issue. Even if the coexistence issue is considered, LTE-LAA and Wi-Fi deployments should also depend on their own features. Therefore, comparison of performance between LTE-LAA and Wi-Fi becomes necessary. In order to emphasize key points, I choose several items of representative performance to illustrate the difference between two RANs.

Spectral Efficiency

The following factors are responsible for the improved spectral efficiency of LTE-LAA over Wi-Fi:

a) **Robust transmission schemes:** As stated before, LTE is a synchronous system and uses scheduling-based channel access rather than contention-based random access. LTE-LAA adopts centralized MAC layer to schedule multi-user transmissions based on the user feedback information of the channel qualities, achieving multi-user frequency-selective diversity gain [19, 27, 30].

b) **Effective interference management:** Interference coordination and avoidance mechanisms, i.e., eICIC and Coordinated Multi-point (CoMP) are adopted in LTE systems to reduce interference and improve spectrum efficiency. CoMP transmission and re-

ception actually refer to a wide range of techniques that requires close coordination among a number of geographically separated eNBs. They dynamically coordinate to provide joint scheduling and transmissions as well as proving joint processing of the received signals. In this way a user at the edge of a cell is able to be served by two or more eNBs to improve signals reception and transmission as well as increase throughput particularly under cell edge conditions [22, 25, 26, 29].

c) **Carrier aggregation to manage traffic across licensed and unlicensed channels:** LTE carrier aggregation technology, aggregating both licensed bands and unlicensed band, will bring in several benefits. First, higher throughput can be achieved with the help of a wider bandwidth. Second, aggregating multiple carriers not only increases spectrum but also includes trunking gains from dynamically scheduling traffic across the entire spectrum. This in turn increases cell capacity and network efficiency as well as improves the experience for all users. Third, carrier aggregation also leads to an optimum utilization of the operator's spectrum resources. The majority of operators has fragmented spectrum covering different bands and bandwidth. Carrier aggregation helps combine these into more valuable spectrum resource [20, 31, 40].

d) **Better mobility and coverage support:** As stated in section 1.2.2, LTE-LAA users are operated within a unified architecture since LTE access methods can be used on both licensed and unlicensed spectrum [8]. First, a unified architecture means the same core network, and the same integrated authentication, management, and security procedures. Second, synchronization on both spectrum types means that interference bursts can be handled better. Last but not least, PCells can always provide ubiquitous coverage for one user. Only horizontal handover is needed between SC and Macro cell [37, 38, 41].

e) **HARQ versus ARQ:** As for the difference of retransmission mechanisms between LTE and Wi-Fi, LTE can make full use of time-domain receiver diversity with the help of Hybrid Automatic Repeat Request (HARQ) at MAC layer, which has a higher efficiency than single-loop ARQ with ACK used by Wi-Fi due to the receiver combination of retransmissions and small overhead [12]. For ARQ, if the received data has an error (as detected by ARQ) then it is discarded, and a new transmission is requested from the sender. For HARQ, if the received data has an error then the receiver buffers the data and requests a re-transmission from the sender. In this case the

eNB will perform a retransmission, sending the same copy of the lost packet. Then, the user will try to decode the packet combining the retransmission with the original version, and will send an ACK message to the eNB upon a successfully decoding [18, 21, 22].

Link adaption

In terms of link adaption, Wi-Fi uses open-loop link adaption without asking for Channel Quality Indicator (CQI) feedback, hence it is incapable of catching up with fast channel/interference fluctuation. On the contrary, LTE can choose resource blocks based on the received CQI [50]. Another impact of using dynamic link adaption based on instantaneous CQI feedback is that, if both technologies employ the same power, the Power Spectral Density (PSD) for LTE is higher than that for Wi-Fi. PSD describes how power of a signal or time series is distributed over frequency, as defined in [51]. This also means, to attain the same PSD, the power consumption of LTE will be much lower than that of Wi-Fi. Power consumption often refers to the electrical energy over time supplied to operate an electrical appliance.

Performance stability

As stated in section 1.2.1, for LTE-LAA, licensed and unlicensed bands are integrated on the same SC, and only the PCell can carry the control signallings which are granted the highest priority among the nine QoS class identifiers the LTE has defined. The control channel messages are transmitted properly between the base STAs (BSs) and the users. Those features make LTE-LAA be able to better facilitate the opportunistic unlicensed access. Wi-Fi systems, on the contrary, is not efficient especially when the network is heavily loaded [18, 19, 21].

Additional Wi-Fi Advantages

Compared to LTE-LAA, Wi-Fi has several advantages. Besides its robust standardization and established ecosystem, an additional advantage is its wide AP footprint in the enterprise and in public venues [10]. This installed base can be used as a springboard for SC deployment. Being able to co-locate SCs where Wi-Fi APs already exist can speed up deployments and reduce cost and complexity in the above two scenarios. On the contrary, while combining unlicensed and licensed LTE strategy, a mobile operator may find

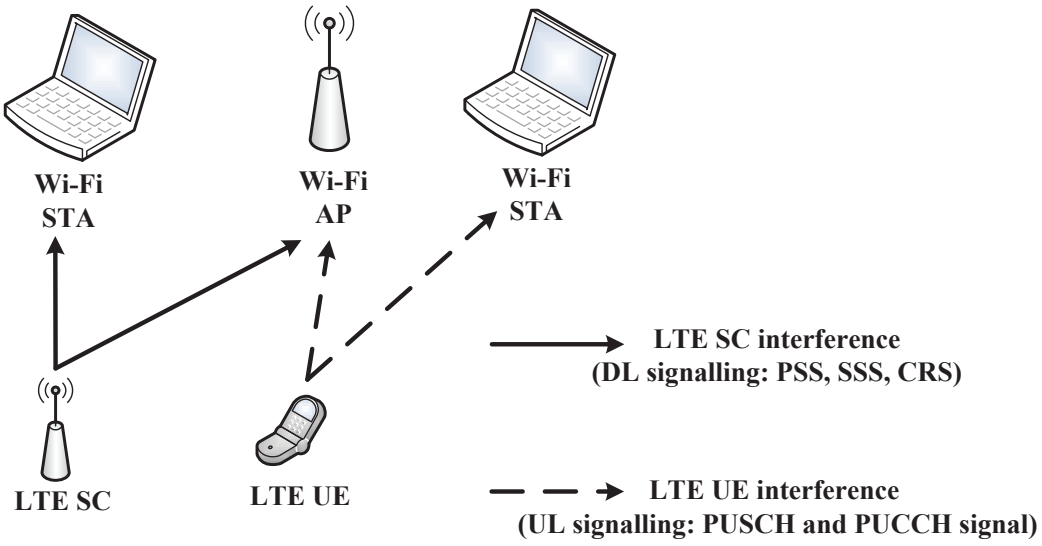

Figure 1.4: Co-channel interference from LTE SC/UE to Wi-Fi AP/STA.

it more complex to gain access to these premises, because enterprise and public venues managers already have their own Wi-Fi networks. An operator wanting to install LTE unlicensed might be taken as an aggressive competitor, especially if the fair coexistence of LTE-LAA and Wi-Fi is not trusted [52].

1.2.5 Co-channel Interference

Interference Sources

Fig. 1.4 shows two sources of potential co-channel interference caused by LTE-LAA to the Wi-Fi APs in cases where LTE-LAA SCs are deployed with Wi-Fi APs together [53]. One source of co-channel interference is DL signaling from the LTE SC. This signaling includes not only broadcasted synchronization and discovery such as the Primary Synchronization Signal (PSS), Secondary Synchronization Signal (SSS) and Cell-specific Reference Signal (CRS), but also data transmissions to users. This interference will impact the Wi-Fi AP as well as the STA. Another source of co-channel interference is UL signaling including control information such as the PHY UL Shared Channel (PUSCH) signal and PHY UL Control Channel (PUCCH) signal from the user.

Interference Management in Unlicensed Bands

One crucial issue for LTE-LAA and Wi-Fi coexistence mechanisms reviewed above is the so-called interference management, including interference detection, measurement and mitigation/avoidance, etc.

Take the LTE-LAA interference management in unlicensed bands for Wi-Fi operation for example. One method for improving the quality of interference management has been provided in [17]. The basic idea is to compare the signal energy monitored by Wi-Fi devices with a known waveform signature corresponding to LTE-LAA operation. The comparison result works as an indicator to help identify the presence of an LTE-LAA interferer on the communication channel in the current frequency band.

In particular, first, the Wi-Fi AP monitors signalling energy on a communication channel in a frequency band associated with its typical operations, such as the 5 GHz. Wi-Fi is able to monitor signalling energy within its frequency band of operation by using its own WLAN receiver circuitry. Second, once the measurements are collected, the Wi-Fi AP can compare the monitored signal energy with a known waveform signature corresponding to LTE and identify therefrom the presence of any LTE interfaces. For example, PSS and SSS signals are sent on the center subcarriers of all component carriers in the last Orthogonal Frequency Division Multiplexing (OFDM) symbol of the 1st slot and 11th slot in every RF by the LTE SC. The periodicity of the signaling energy output in center frequency bins can accordingly be matched in pattern to identify the presence of nearby LTE SCs based on a PSS and SSS signature pattern. Then, the interference identification may be repeated over a period of time to produce reliable pattern matching results. Finally, once an LTE interferer has been identified, the Wi-Fi AP may perform further match processing on the resulting signal energy pattern to classify the type of interference [53].

1.2.6 Summary and Guidelines

Lessons learnt from LTE and Wi-Fi MAC Comparison

In general, LTE and Wi-Fi adopt different MAC layers.

From the aspect of channel access and channel usage schemes, for LTE systems, there are no sensing and backoff procedures. Instead, in LTE systems designed for licensed bands, there indeed exists a centralized controlling architecture, which always allocates

one resource unit to the user that can maximize the target metric in every subframe. A Wi-Fi node, on the contrary, with no need for centralized controller, will first sense the channel whenever it has a pending transmission.

What's more, for Wi-Fi systems, channel is occupied only when packets need to be transmitted. Since LTE frames are contiguous, channels are always in the ON periods.

Furthermore, channel access in LTE systems are centrally scheduled, so the collision avoidance mechanisms adopted in Wi-Fi is not required in this case.

The Choice of LTE-LAA and Wi-Fi

In addition to the key factors of performance difference between LTE-LAA and Wi-Fi summarized in section 1.2.4, there are still two issues with the heaviest weight of consideration during the choice procedure:

a) Wi-Fi still needs enhancement in coverage, mobility and network efficiency like what LTE offers [54]. Unlike Wi-Fi, LTE network is well integrated to the existing operator network, thus solving almost all authentication, operations and management and QoS issues [55]. LTE also simplifies network management and tracking of key performance indicators through a single RAN [56]. Unfortunately, due to various types of restriction upon large-scale transformation towards Wi-Fi, it seems impossible to achieve the purpose of above-mentioned enhancement on Wi-Fi performance in the foreseeable future.

b) Wi-Fi has been widely used with traditional merits in low cost and easy deployment, making the integration of Wi-Fi in LTE networks possible today. Furthermore, the commercial availability of LTE-LAA in mobile devices requires a couple of years [10].

When operating in a channel shared with Wi-Fi or another LTE-LAA network, LTE's performance advantages are reduced by interference or by the introduction of coexistence mechanisms. For more details about how coexistence mechanisms affect performance of LTE-LAA and Wi-Fi, refer to section 2.3.4.

In view of their own benefits, the choice of Wi-Fi or LTE-LAA should depend on the environment and power considerations. The detailed environment classifications are being elaborated in section 2.3. Furthermore, it is also related to the experience of operators and even financial and other factors.

As stated, LTE carrier aggregation with 5 GHz unlicensed band has been pointed out by the industry as a candidate solution to offload cellular traffic to the unlicensed band, while another way for network operators to utilize unlicensed spectrum is to use the Wi-Fi radio access technology (RAT). Operators may face a complex decision of choosing between LTE and Wi-Fi in the unlicensed spectrum. Therefore, a comparison between techniques with LTE or Wi-Fi in the unlicensed bands becomes essential.

This section includes an overview of the recent existing literature on LTE and Wi-Fi coexistence in 5 GHz. For details about performance evaluation workflow, scenarios and metrics, refer to section 2.3.3.

1.3 Motivations of this Thesis

1.3.1 Modeling and Analysis of LTE and Wi-Fi Aggregation using Both Queueing Theory and Stochastic Geometry

Early studies of LWA mainly focus on the prototype and architecture design [57, 58]. The feasibility of licensed and unlicensed carriers aggregation has been verified experimentally in [59]. The authors in [60] present a traffic aggregation-based LWA flow control algorithm. Reference [61] implements the radio resource management layer for LWA. The layer 2 structure for LWA to achieve the compatibility with Wi-Fi is proposed in [62]. The authors in [63] investigate the load balancing and user assignment solutions for LWA. Techniques for traffic splitting and aggregation at the radio layer have also been considered in the literature. References [64, 65] investigate aggregation and path selection mechanisms that maximize the network utility. The LWA and Wi-Fi offloading scheme are jointly considered in [66], which also strikes the balance between user payment and quality of service (QoS).

The aforementioned LWA studies are based on one common assumption: a Wi-Fi AP serving LWA purpose is only able to offload bearers from LTE, and does not have its own user equipments (UEs) to serve. In reality, a Wi-Fi AP can operate in both the native mode and the LWA mode simultaneously [57, 67]. Specifically, the LWA-mode Wi-Fi AP cooperates with the LTE BS to transmit bearers to the LWA UE, which aggregates packets from both LTE and Wi-Fi. The native-mode Wi-Fi AP transmits Wi-Fi packets to the native Wi-Fi UEs, which do not serve the LWA purpose. Hence the problem arises of how to transmit different messages for one AP to different UEs. The conventional

approach is to set up orthogonal channels in terms of time/frequency etc [68]. However, this approach is inefficient and not optimal in terms of achievable rates [69]. More importantly, collisions may be inevitable because of imperfect knowledge of the channel occupancy state. As an alternative, a method called superposition coding proposed in [70, 71] can be used to remove the orthogonality constraint in a transmission by one AP to both the LWA UE and the native Wi-Fi UE. The superposition coding method is considered as a promising technique for enhancing resource efficiency, and it achieves the capacity on a scalar Gaussian broadcast channel [72].

Nevertheless, spectrum sharing between the native-mode AP and the LWA-mode AP inevitably creates interference among concurrent transmissions. Accounting for the interference caused by the native Wi-Fi network and affecting the LWA UE, an appropriate access protocol needs to be carefully designed such that the QoS of the LWA UE will not be adversely degraded. The authors in [73, 74] develop the scheduling polices for the low-priority node under partial channel state information. In [75], a random access protocol is proposed, where low-priority nodes make transmission attempts with a given probability. The study [75] is based on the general multi-packet reception (MPR) channel model proposed in [76, 77], which captures the interference at the physical layer more efficiently compared to the traditional channel model, as in the former a transmission may still succeed even in the presence of interference. References [78, 79] study the interference created by the spectrum sharing between high-priority and low-priority nodes in the MPR channel among current transmissions. Reference [80] analyzes the throughput of the low-priority network where MPR capability is adopted in a cognitive network with the high-priority node under certain conditions. The authors in [81] optimize the throughput with deadline constraints on a single low-priority node accessing a multi-channel system.

In this thesis, we consider a shared access Wi-Fi network inspired by the cognitive radio network paradigm. More specifically, the high-priority node (i.e., the LWA-mode Wi-Fi AP) is allowed to access the channel whenever it is needed. However, the low-priority node (i.e., the native-mode Wi-Fi AP) will randomly access the channel when the queue size of the LWA-mode Wi-Fi AP is below a congestion limit, so as not to create harmful interference to the LWA UE. How to investigate the performance of such systems remains open. Recently, there is growing interest in the delay analysis or the combination of throughput and delay analysis in LWA-enabled networks [82–85]. How-

ever, most of the existing studies focus on the case under the saturated traffic assumption. In fact, based on the queueing theory, the analysis of the delay of networks with bursty sources cannot be easily seen with the saturated traffic assumption [86]. In general, how to design the random access protocol accounting for both the throughput of the native Wi-Fi network and the delay of the LWA-enabled network with bursty LWA traffic has not been addressed yet.

In addition, a mathematical approach would be helpful for a fundamental understanding of the performance of LWA. Recently, stochastic geometry has become a powerful tool for modeling cellular and Wi-Fi systems with large random topologies. In [87], the coverage probability and the average Shannon rate were derived for macro cellular networks with BSs distributed according to a *Poisson Point Process* (PPP). This work has been extended to heterogeneous cellular networks (HetNets) [88–90]. Stochastic geometry can also model Carrier Sense Multiple Access with Collision Avoidance (CSMA/CA)-based Wi-Fi networks. When using CSMA/CA as the MAC protocol, due to the carrier sensing range, there is a minimum guaranteed distance between concurrent transmitters operating in the same frequency band. *Matérn Hard-core Process* (MHCP) has become a commonly used model for the distribution of simultaneously transmitting nodes where two points cannot coexist with a separating distance shorter than a predefined parameter [91–93]. Thus, MHCP can capture the repulsion between two coexisting nodes. Another commonly used model for networks with inter-tier repulsion is the *Poisson Hole Process* (PHP), which can capture the inter-tier correlation when a secondary node cannot be within a predefined distance to a primary node [94–97]. In a Device-to-Device (D2D) underlaid cellular network where the activation conditions of D2D nodes depend on the locations of neighbors in both cellular and D2D tiers [98], the effect of two-tier dependence on the network throughput has been characterized in [99].

1.3.2 Resource Optimization for Joint Data Offloading to Wi-Fi and LTE-U in Load-coupled and Multi-cell Networks

Offloading traffic to the unlicensed spectrum is a recent trend [1]. Two approaches for LTE are data offloading to Wi-Fi via LWA or Wi-Fi offloading. [16] and LTE-U [8]. Existing works have addressed LWA/Wi-Fi offloading or LTE-U. We consider performance optimization with joint LWA and LTE-U.

With multi-cell LTE, interference is present. Reference [100] uses stochastic geom-

etry to analyze the coexistence performance of multi-cell LTE and Wi-Fi. By the nature of stochastic geometry, the results do not apply for analyzing networks with specific given topology, which is focused in our work. Another mathematical characterization for interference modeling is the load-coupling model [101]. The load of a cell is defined to be the proportion of consumed time-frequency resources, and its value is used as the severity of generated interference. This model has been widely used [102–105]. It has been verified in [104] through system level simulations that this model is sufficiently accurate for multi-cell network performance analysis.

How to avoid severe performance degradation of the Wi-Fi network is a challenging issue of implementing joint Wi-Fi offloading and LTE-U. First, one needs to carefully design the amount of offloaded traffic to avoid over saturation in the Wi-Fi network, especially when Wi-Fi has limited resource for external offloading. Various offloading schemes have been proposed to improve the system performance [106–111]. Among them, Wi-Fi offloading in the context of user equipment (UE) association has been investigated in [106, 111]. Second, the inter-system spectrum sharing, or, more specifically, the coexistence of LTE and Wi-Fi in the same unlicensed spectrum is the major challenge of implementing LTE-U. As shown in system-level simulation studies, e.g., [112], Wi-Fi throughput can be significantly degraded by the LTE-U interference if no adaption is made for LTE protocol. This is because Wi-Fi moves to silent mode when sensing a busy channel used by LTE-U due to the contention-based scheme [113]. Orthogonal spectrum sharing schemes have been proposed in [3, 114–118] to deal with LTE and Wi-Fi coexistence issue, and can be guaranteed by the listen before talk (LBT) protocol [3] or the duty-cycle method [114]. It is shown that Wi-Fi can be protected with LBT or adaptive duty-cycle [1].

In this work, we consider multi-cell LTE networks and therefore inter-cell interference is present. The authors in [111] jointly address traffic offloading and spectrum sharing between LTE and Wi-Fi in a single-cell case. However, resource allocation in multi-cell scenarios faces more challenges compared to the single-cell case. The crucial aspect of multi-cell scenarios consists of capturing the mutual interference among cells. In [116–118], stochastic geometry has been used to analyze the coexistence performance of Wi-Fi and multi-cell LTE networks. Hence the results do not apply for analyzing network with specific given topology, which is focused in our work. To the best of our knowledge, resource allocation for joint Wi-Fi offloading in the context of

UE association and LTE-U with inter-system spectrum sharing in multi-cell networks without restrictions on network topology has not been addressed yet.

To enable the network-wide performance evaluation with arbitrary network topology, a modelling approach named load-coupling has been proposed by [101]. The inter-cell interference in [101] is modeled via characterizing the coupling relationship of allocated resource among cells. The cell load here refers to the proportion of consumed time-frequency resource in each cell. The load-coupling model has been widely used in the literature [102, 103, 105, 119–121]. Among them, [119] proposes a utility maximization framework for data offloading to Wi-Fi. The works [102, 103, 119, 120] assume fixed UE association in load-coupled heterogeneous network (HetNet) even though proper UE association plays a critical role in achieving enhanced network performance, especially in Wi-Fi offloading scenarios. Recently, the authors in [105, 121] consider UE association in load-coupled HetNet. However, most of the existing efforts do not study the properties of load-coupling when the amount of resource is variable. Recently in [122], we address resource optimization in load-coupled networks with spectrum sharing. However, the system model does not consider offloading LTE UEs to Wi-Fi. How to model joint optimization of UE association and inter-system spectrum sharing in joint Wi-Fi and load-coupled LTE networks and how to solve the resulting problems to optimality have remained open so far.

One way of evaluating the performance with respect to capacity is to compute how much of the UE demand can be scaled up subject to the constraint on the maximum network resource. Given a baseline demand distribution, for fairness-based capacity enhancement, the problem can be investigated by measuring the maximum demand scaling factor for all UEs, while accounting for the resource limits, such as in [102, 122, 123]. The solution method in above three works is based on solving a conditional eigenvalue problem for a non-linear system. However, references [102, 122, 123] employ a restricted setup of ours. The method in their works does not generalize to the case of scaling up the demand for UEs in networks with variable UE association and/or amount of resource, as the generalized problem does not map to computing the eigenvalue anymore. Besides, in load-coupled networks with Wi-Fi offloading and LTE-U, the interplay among load-coupling, UE association and inter-system spectrum sharing needs to be captured. Whether or not the maximum capacity with respect to demand scaling of joint Wi-Fi and load-coupled LTE networks with both Wi-Fi offloading and LTE-U can

be efficiently and effectively computed remains unknown.

1.4 Main Contributions and Outline of the Thesis

The main contributions of this thesis can be summarized as follows.

LTE carrier aggregation with 5 GHz unlicensed national informational infrastructure band has been pointed out by the industry as a good solution to handle the rapidly increasing amounts of data traffic. To provide fair coexistence of LTE-LAA and Wi-Fi on 5 GHz, several coexistence mechanisms have already been proposed. **Chapter 2** provides the world's first comprehensive survey of the coexistence of LTE-LAA and Wi-Fi on 5 GHz with corresponding deployment scenarios. I first analyze coexistence-related features of those two technologies, including motivation, LTE carrier aggregation with unlicensed band, LTE and Wi-Fi medium access control protocols comparison, coexistence challenges and enablers, performance difference between LTE-LAA and Wi-Fi, as well as co-channel interference. Second, I further extensively discuss current considerations about the coexistence of LTE-LAA and Wi-Fi. Third, influential factors for the classification of small cell scenarios, as well as four representative scenarios are investigated in detail. Then I explore a relatively smooth technical route for solving coexistence-related problems, which practically takes features of a specific scenario as the base for designing deployment mode of LTE-LAA and/or Wi-Fi. A scenario-oriented decision making procedure for the coexistence issue and the analysis on an example deployment scenario, including design and performance evaluation metrics focusing on the concept of the scenario-oriented coexistence are presented. I finally forecast further research trends on the basis of our conclusion.

LTE-WLAN Path Aggregation (LWPA) based on MPTCP has been under standardization procedure as a promising and cost-efficient solution to boost Downlink (DL) data rate and handle the rapidly increasing data traffic. **Chapter 3** aims at providing tractable analysis for the DL performance evaluation of large-scale LWPA networks with the help of tools from stochastic geometry. We consider a simple yet practical model to determine under which conditions a native WLAN AP will work under LWPA mode to help increasing the received data rate. Using stochastic spatial models for the distribution of WLAN APs and LTE BSs, we analyze the density of active LWPA-mode WiFi APs in the considered network model, which further leads to closed-form expressions on the DL data rate and area spectral efficiency (ASE) improvement. Our numerical results illus-

trate the impact of different network parameters on the performance of LWPA networks, which can be useful for further performance optimization.

Chapter 4 investigates the effect of bursty traffic in an LTE and Wi-Fi aggregation (LWA)-enabled network. The LTE BS routes packets of the same IP flow through the LTE and Wi-Fi link independently. I motivate the use of superposition coding, so as to allow the Wi-Fi AP serving the purpose of LWA can simultaneously operate as the native-mode AP that serves Wi-Fi users only. With respect to the existing works on LWA, the novelty of our study consists in a random access protocol allowing the native-mode AP to access the channel with probabilities that depend on the queue size of the LWA-mode AP, such that it does not impede the performance of the LWA-enabled network. I analyze the throughput of the native Wi-Fi network and the delay experienced by the LWA users, accounting for the native-mode AP access probability, the traffic flow splitting between LTE and Wi-Fi, and the operating mode of the LWA user with both LTE and Wi-Fi interfaces. The results provide fundamental insights in the throughput and delay behavior of such systems, which are essential for further investigation in larger topologies.

Chapter 5 considers performance optimization of multi-cell networks with LWA and LTE-U with sharing of the unlicensed band. Theoretical results are derived to enable an algorithm to approach the optimum. Numerical results show the algorithms effectiveness and benefits of joint use of LWA and LTE-U.

Chapter 6 takes a significant step of analyzing joint Wi-Fi offloading and LTE-U in multi-cell scenarios. For unlicensed spectrum utilization in cellular networks, most of the existing efforts have addressed separately Wi-Fi offloading or LTE-U with sharing of unlicensed bands occupied by Wi-Fi. Besides, compared to the single-cell case, optimization for joint Wi-Fi offloading and LTE-U in multi-cell scenarios is much more challenging because inter-cell interference must be addressed. I explore the potential of networks in achieving optimal capacity with arbitrary topologies, accounting for resource limits and inter-cell interference. Towards this goal, I consider an optimization problem, aiming at maximumly scaling up the capacity for all user equipments (UEs), by jointly optimizing UE association and inter-system spectrum sharing. I first consider a restricted optimization problem, which is then proved to lead to no loss of optimality and generality. Next, theoretical results are derived to enable an algorithm that achieves global optimality for this restriction. Numerical results show the algorithms effective-

ness and benefits of joint use of Wi-Fi offloading and LTE-U.

Chapter 7 concludes the thesis. I summarize the contribution as well as the highlights of this thesis. The perspectives regarding the future work related to the topics presented in this thesis has also been discussed. To be more specific, I discussed future research directions malily related to medium sharing algorithms design, realistic scenarios and mechanisms consideration, further coexistence optimization, advanced traffic flow and aggregation schemes, as well as realistic coexistence mechanisms to be considered in the joint Wi-Fi and multi-cell LTE networks.

Chapter 2

Literature Review

2.1 Introduction

As the rapid progress and pleasant experience of Internet-based services, there is an increasing demand for high data rate in wireless communications systems such that the growth of mobile traffic in the next decade is over one thousand times [124]. However, since the usable licensed spectrum is of limited physical extent, new licensed frequency bands are becoming rare and expensive. To respond to increased wireless communication capacity demand, the innovation focusing on such techniques that enable better use of different types of spectrum for traffic offload, including unlicensed bands, is urgently needed [2]. It is assumed that up to thirty percent of broadband access in cellular networks can be offloaded to unlicensed bands, primarily Wi-Fi networks until now [125].

The extension of LTE-LAA over 5 GHz UNII band and the requirement to provide fair coexistence of LTE-LAA with other technologies working on 5 GHz are two major observations of the ongoing discussion on the 3GPP [8, 126]. While considering the coexistence of Wi-Fi and LTE-LAA in 5 GHz UNII spectrum, designers should ensure that LTE-LAA can coexist with Wi-Fi fairly and friendly in unlicensed band by complying with regulatory requirements of the local government in a region. In some markets, like the US, Korea and China, there is no Listen-Before-Talk (LBT) requirement. Without changing LTE air interface protocol, coexistence with Wi-Fi in those scenarios can be realized for LTE Release 10-12 by using specific techniques such as CSAT. In markets like Europe and Japan where LBT is required, however, LTE air interface would need changes with the introduction of LBT feature potentially in 3GPP Release 13 [127].

To the best of our knowledge, current research mainly aims at such mechanisms as

capable of enabling the coexistence of LTE-LAA and Wi-Fi. It should be noticed that the coexistence performance of LTE-LAA and Wi-Fi in 5 GHz UNII spectrum would vary a lot in different deployment scenarios. Take the early coexistence results in [55, 128] for example, the ratio of the DL throughput gain of LTE-LAA to that of Wi-Fi would be different if the simulation scenario changes from outdoor to indoor. The throughput also differs when an operator chooses to place Picocells uniformly or in a hotspot region[127]. Both LTE-LAA and Wi-Fi have their own benefits and cannot be replaced by each other at the moment [54]. The performance of either LTE-LAA or Wi-Fi should be maintained and not be affected by each other while deployed in 5 GHz spectrum together.

Focusing on those important issues, this chapter surveys the coexistence of LTE-LAA and Wi-Fi on 5 GHz with corresponding deployment scenarios, and introduces a scenario-oriented decision-making method for coexistence. The rest of this chapter is organized in the following manner. In section 2.2, a comparative study of existing LTE surveys and this chapter is provided. In section 1.2, relevant features of Wi-Fi and LTE-LAA are overviewed. In section 2.3, I first overview the coexistence mechanisms related researches. Then I review the LTE-LAA and Wi-Fi coexistence testing and results to present a picture of the research stage in the community. We also investigate the current coexistence mechanisms in both markets where LBT is required or not, so as to evaluate their influence on wireless service. In addition, I also provide lessons learnt from different coexistence mechanisms comparison and Cognitive Radio (CR), as well as propose recommendations and guidelines for ensuring fairness. In section 2.6, I analyze eight key influential factors for the classification of SC scenarios, demonstrate several representative scenarios, and dissect an example of deployment scenario to highlight the concept of the scenario-oriented coexistence for different access applications. I further recommend performance evaluation scenarios and metrics. In section 2.5.4, I discuss future research trends. Finally, I conclude in section 2.7.

2.2 Comparative Study of Existing Surveys on LTE and This Chapter

In order to provide a broader perspective, as well as to give directions to readers about the key distributions of this survey, I illustrate a comparative study of the existing surveys

on LTE and this chapter.

Here I investigate several representative surveys reviewing the LTE-related technologies from different aspects. Authors in [19] first review the evolution of LTE physical (PHY) layer control channels. Moreover, in [18, 20, 31], authors focus on radio resource management (RRM) for LTE and LTE Advanced (LTE-A) from different angles. To be more specific, authors in [18] demonstrate Heterogeneous Networks (HetNets), particularly on femto cells and relay nodes. In [31], authors study RRM for spectrum aggregation. Resource allocation and link adaptation are overviewed in [20]. What's more, in [26, 29, 30, 39–41], authors review the Uplink (UL) or Downlink (DL) scheduling from different angles. In particular, authors in [26] classify LTE UL scheduling from the perspective of Machine-to-machine (M2M) communications. In [29], authors demonstrate cooperative UL transmissions beyond LTE-A system. In [30], authors summary UL scheduling in LTE and LTE-A. Authors in [40] demonstrate DL packet scheduling in LTE cellular network. Multi-cell coordinated scheduling, particularly inter-cell interference mitigation techniques for DL and UL are reviewed in [39]. As a supplement to [39], multi-cell scheduling strategies in LTE and LTE-A are also overviewed in [41]. In addition, there are also some surveys discussing corresponding techniques enabling communications in LTE networks. In [21], authors review M2M communications in the context of LTE and LTE-A. Authors in [27] review Device-to-Device communications in LTE networks. Security aspects for LTE and LTE-A networks are overviewed in [37]. In [38], authors also review the mobility management support in LTE-A networks. Authors discuss alternatives to improve the operation of the random access channel of LTE and LTE-A in [22].

Unlike these surveys which are targeted only for a single Radio Access Network (RAN), i.e., LTE, this chapter focuses on the study of LTE-LAA and Wi-Fi coexistence in 5 GHz, including coexistence-related features, coexistence considerations, deployment scenarios for the coexistence and scenario-oriented decision making. Table 2.1 shows a brief summary of the related survey papers on LTE and this article.

Table 2.1: Comparative Study of our work with existing surveys on LTE

Item	Key word	Description
Our work	Coexistence	A comprehensive survey on LTE-LAA and Wi-Fi coexistence in 5 GHz 1. analysis on coexistence-related features of LTE-LAA and Wi-Fi; 2. current research on LTE-LAA and Wi-Fi coexistence considerations; 3. deployment scenarios for the coexistence and scenario-oriented decision-making; 4. challenges and further research directions.
[19]	PHY	The evolution of LTE PHY layer control channels: 1. an overview of the legacy LTE control channel and challenges; 2. the new solutions provided by LTE Release 11; 3. limitations of the new design.
[18]	RRM	RRM for LTE/LTE-A HetNets, particularly for femtocells and relay nodes: 1. key challenges from HetNet; 2. radio resource management schemes; 3. schemes classification and comparison according to approaches.
[20]	RRM	Resource allocation and link adaptation in LTE and LTE-A: 1. the units for resource allocation modes and purposes; 2. the way the resource allocations are encoded under these different modes; 3. methods of link adaption; 4. the control signaling encoding for link adaption; 5. the encoding of channel state feedback.
[31]	RRM	RRM for spectrum aggregation in LTE-A: 1. spectrum aggregation techniques; 2. radio resource management aspects and algorithms to support carrier aggregation; 3. technical challenges for future research on aggregation in LTE-A.
[26]	UL/DL scheduling	Classification of LTE UL scheduling techniques from the perspective of machine-to-machine communications: 1. power efficiency; 2. QoS support; 3. multi-hop connectivity; 4. scalability for massive number of users.
[29]	UL/DL scheduling	Cooperative UL transmissions of systems beyond the LTE-A initiative: 1. single-carrier Frequency Division Multiple Access (FDMA) and the localized FDMA comparison; 2. the philosophy of both user cooperation and cooperative single-carrier FDMA; 3. benefits of relying in LTE-A.
[30]	UL/DL scheduling	UL scheduling in LTE and LTE-A: 1. scheduling in LTE and LTE-A; 2. schemes that address the scheduling problem; 3. an evaluation methodology to be as a basis for comparison between scheduling.
[39]	UL/DL scheduling	Multi-cell coordinated scheduling and multiple-input multiple-output techniques in LTE: 1. single user multiple-input multiple-output; 2. multi user multiple-input multiple-output; 3. inter-cell interference mitigation techniques for DL and UL; 4. potential research challenges on physical limitation of user equipment, feed back consideration and enhanced codebook-based transmission.
[40]	UL/DL scheduling	DL packet scheduling in LTE cellular networks: 1. the design of a resource allocation algorithm for LTE networks; 2. a survey on the most recent techniques, including channel-unaware strategies, channel-aware/QoS-unaware strategies, channel-aware/QoS-aware strategies, semi-persistent scheduling for voice over Internet phone support and energy-aware strategies; 3. performance comparisons of the above well-known schemes.
[41]	UL/DL scheduling	Multi-cell scheduling strategies in LTE and LTE-A: the evolution of interference management.
[21]	Techniques enabling communications	Machine-to-machine communications in the context of the LTE and LTE-A: 1. architectural enhancements for providing machine-to-machine services; 2. the signal overheads and various QoS requirements in machine-to-machine communications; 3. application scenarios; 4. machine-to-machine challenges over LTE/LTE-A and issues on random access overhead control.
[27]	Techniques enabling communications	Device-to-Device communication in LTE networks: related research works ranging from technical papers to experimental prototypes to standard activities.
[37]	Techniques enabling communications	Security aspects for LTE and LTE-A networks: 1. an overview of the security aspects of the LTE and LTE-A networks; 2. the security vulnerabilities in the architecture; 3. the design of LTE and LTE-A networks; 4. the existing solutions to security problems.
[38]	Techniques enabling communications	Mobility management support in the presence of femtocells in LTE-A: 1. key aspects and research challenges of mobility management support 2. mobility management procedures in the LTE-A system; 3. handover decision algorithms
[22]	Techniques enabling communications	Alternatives to improve the operation of the random access channel of LTE and LTE-A: 1. discussion of the limits of LTE and LTE-A to handle M2M applications; 2. performance evaluation of the energy efficiency of the random access mechanism of LTE; 3. existing improvements of the random access channel, including optimized MAC, access class barring, separation of random access resources and distributed queuing for M2M applications.

2.3 Current Research on Directly Extending LTE to the Unlicensed Band

In light of the aforementioned challenges, this section first overviews the recent related works to present a stage picture of the research in the community. What's more, representative coexistence mechanisms with and without LBT features will be investigated from the markets perspective. In addition, I further summarize and compare between these two kinds of schemes in terms of MAC/PHY modification requirement, advantages and disadvantages. Moreover, I illustrate lessons learnt from cognitive radio, as well as recommendations and guidelines for ensuring fairness.

2.3.1 Recent Related Works

This section includes an overview of the recent existing literature on LTE and Wi-Fi coexistence in 5 GHz. For details about performance evaluation workflow, scenarios and metrics, refer to section 2.3.3.

An Overview of Coexistence Mechanisms Related researches

There are some existing works studying the coexistence mechanisms of LTE-LAA and Wi-Fi networks in very recent years. Relevant studies in this chapter are overviewed in a logical manner.

The community first analyzes the problem of LTE-LAA and Wi-Fi coexistence. For example, in [112], coexistence of LTE-LAA and Wi-Fi in the TV white space band is studied. Simulation results show that in situations where LTE and Wi-Fi nodes are randomly deployed, Wi-Fi throughput can be significantly degraded by LTE interference. In [140], the results show that channel sharing between Wi-Fi and LTE is unfair for the Wi-Fi network to a great extent.

To solve the above challenges, the basic idea of enabling the fair coexistence of LTE-LAA and Wi-Fi networks by adjusting LTE MAC protocols is proposed. In [42], it concludes that LTE-LAA can gain high throughput performance without harming Wi-Fi performance with the proposed MAC mechanisms. However, this conclusion only holds when the coexistence channel model can accurately simulate the interference condition between LTE-LAA and Wi-Fi transmission. Papers like [24] mathematically model how LTE would behave if quite period was added to it. They calculated the probability of

Table 2.2: Comparative study of coexistence schemes

Item	Scheme	Descriptions	Characteristics/limitations
[54]	LTE UL power control	**The design of an LTE UL power control** with an interference-aware power operating point.	1. LTE power control procedures are specified and established by 3GPP TS 36.213 [129]. 2. LTE UL power control defines UE transmit powers so that path loss and interference are compensated. 3. Not suitable in dense deployment scenarios.
[3]	LBT	**The design of three LBT design options:** 1. LBT without random backoff; 2. LBT with random backoff in a contention window of fixed size; 3. LBT with random backoff in a contention window of variable size (The 3rd option is also adopted by [130–132]).	1. Lower collision probability means higher Wi-Fi throughput. 2. The collision probability to the Wi-Fi can be adjusted by the contention window size. 3. Wi-Fi performance itself benefits from a variable backoff periods.
[36]	LBT	**A specific LBT scheme considering two data rate stages:** 1. At high data rate stage, if packet collision occurs, the equipment will not transmit, and LTE-LAA will automatically go to low data rate stage; 2. At low data rate stage, LTE-LAA will use a lower modulation and coding selection.	1. Much simpler compared to previous LBT schemes. 2. Not included in the 3GPP discussion. 3. The definition about high/low data rate stage is not easy to use.
[42, 43]	LBT	**The design of a LBT scheme similar to Wi-Fi**: 1. Based on the Wi-Fi DCF protocol; 2. Similar to Wi-Fi CSMA mechanism (section 2.3.3).	1. Only holds when the coexistence channel model can accurately simulate the interference condition. 2. This LBT approach needs a large number of changes in the LTE specification.
[44]	LBT	**The design of two LBT options:** 1. asynchronous LBT (similar to [42, 43]); 2. synchronous LBT (data subframes are synchronized with the licensed LTE carrier).	1. The asynchronous LBT scheme might use IEEE 802.11 RTS/CTS signals to ensure that the channel is idel; 2. The synchronous LBT scheme may need a smaller number of changes in the LTE specification, and use ICIC to manage the interference among LTE STAs.
[133, 134]	LBT	**The design of two LBT options:** 1. frame-based LBT, where the equipment has an idle period after transmission; 2. load-based LBT, where the equipment checks the channel, and transmits if the channel is idle (also adopted by [135], where LTE-LAA further incorporates a backoff defer period after a busy channel has just become free).	1. Since LTE operates with the fixed frame period, the frame-based LBT is easy to be applied in LTE if a fixed frame period for frame-based LBT can be defined. 2. Load-based LBT takes the advantages over frame-based LBT in channel access opportunities because the transmitter can continuously detect the channel.
[136, 137]	LTE muting	**Assigning channel time** to every competing entity including idle periods, successful transmissions and collisions for the Wi-Fi network.	1. Wi-Fi performance will degrade because Wi-Fi UEs may spend. much time in backoff. 2. The above problem can be solved if LTE-LAA can exploit the silent time. 3. ABS can be exploited as a base (section 2.3.2) in order to avoid interference from LTE-LAA to Wi-Fi.
[138, 139]	CHS	**CHS** performs scanning procedures to classify the different channels based on their conditions. (section 2.3.2)	1. Sufficient if the traffic density is low. 2. Not available if there is no clean channel.
[24]	CSAT	The key idea of **CSAT** is to define a time division multiplexing cycle for the LTE-LAA transmission in a short term (section 2.3.2).	1. As a supplement to CHS 2. For characteristics and limitations, refer to Table 2.5

Wi-Fi's back-off delay is less than LTE-LAA quite period. However, in this chapter, authors only consider pure statistical approach, and eliminate PHY layer effects as well as hidden/exposed terminal problems. Papers like [141] suggest to divide transmission burst time. This means that the BSs must know the exact number of nodes of LTE-LAA and Wi-Fi. This is challenging if nodes overhear each other.

Then, coexistence mechanisms designed for markets with or without LBT require-

ment are proposed. Table 2.2 shows a comparative study of coexistence schemes proposed so far. Papers like [12, 42, 129, 135, 142] introduce coexistence algorithm by implementing contention based algorithms in LTE-LAA, i.e., LBT, and add collision avoidance algorithms to LTE-LAA. Specifically, 3GPP is working on the introduction of LBT in the 3GPP standards. Progress in LTE-LAA standardization is shown in Table 2.3. 3GPP has also defined an LTE-LAA coexistence mechanism in TS 36.213 [129]. An extensive coexistence study of different coexistence mechanism has also been summarized in 3GPP TR 36.889 [142]. However, as will be stated in section 2.3.4, LBT introduces extra delay due to the contention time overhead, which can lead to inefficient channel usage.

For markets with no LBT requirement, authors in [138, 139] propose a Channel Selection (CHS) mechanism to enable the coexistence of LTE-LAA and Wi-Fi. However, as discussed in section 2.3.2, LTE-LAA has to hold until the channel becomes idle again in scenarios where no clean channel is available. As a supplement to CHS, CSAT is proposed in [24]. The advantage and drawback of CSAT as well as other duty-cycle mechanisms can be found in section 2.3.1. An approach using LTE UL power control to solve the coexistence issue of LTE-LAA and Wi-Fi networks is studied in [54]. Simulation results show that the proposed power control mechanism can improve the performance of both types of networks. However, power control mechanism can not solve coexistence problem of LTE-LAA and Wi-Fi in dense deployment scenarios.

An Overview of LTE-LAA and Wi-Fi coexistence testing and results

LTE-LAA and Wi-Fi coexistence physical equipment studies and simulations have been presented by a number of industry players. Their testing activities are hardly in the form of apples-to-apples comparisons, particularly in recent comments to the Federal Communications Commission (FCC). That is due to the fact that different companies are calling the other's test methodologies skewed toward their preferred results. What's more, testing organised by the industry consortium LTE-U Forum is mainly focused on mechanisms designed for markets without LBT requirement. On the contrary, testing organised by 3GPP are aimed at markets with LBT requirement. Unlike the former two others, test works organised by Wi-Fi stakeholders is focused on ensuring that technologies share unlicensed spectrum fairly with Wi-Fi. This section summarizes what different companies have concluded based on their evaluations from different angles.

Table 2.3: Progress in LTE Unlicensed Standardization

Time	Description
Dec. 2013	Qualcomm and Ericsson presentation of the initial proposal for LTE-U at a 3GPP meeting.
Jan. 2014	A 3GPP unofficial meeting with companies and operators presenting their perspectives on the use of LTE in 5 GHz.
Mar. 2014	**Outcomes include:** 1. A plan to set up a study item in September 2014. 2. Adoption of LTE-LAA designation Agreement to focus on the 5 GHz band. 3. Commitment to finding a global solution. 4. Establishment of fair coexistence with Wi-Fi and among LTE operators.
Sep. 2014	3GPP approves LAA-LTE as a study item for Release 13. The main goal is to determine the changes needed for fair coexistence of LTE-LAA and Wi-Fi. **The relevant study covers:** 1. Regulatory requirement 2. Deployment Scenarios 3. Design targets and functionalities 4. Coexistence evaluation and methodology **Required functionalities include:** 1. LBT mechanism 2. Dynamic frequency selection for radar avoidance 3. Carrier selection 4. Transmit power control
Mar. 2016	Complete **LTE-LAA related Updates:** 1. LBT coexistence mechanisms implementation design 2. The paring of unlicensed transmission with licensed band **Other LTE Unlicensed Updates:** 1. LTE-WLAN Aggregation (LWA) is included in Release 13. 2. New functionality to improve mobility management. 3. eNB management in integrated LTE and Wi-Fi network. 4. 3GPP has approved Enhanced LTE-LAA and Enhanced LWA in Release 14, targeting completion by June 2017.

In comments to the FCC, there are different kinds of suggestions. The first kind is to leave the development of coexistence mechanisms to industry cooperation with the broader unlicensed community, e.g. IEEE 802.11 and the Wi-Fi Alliance rather than regulatory intervention. For instance, in [143], tests are conducted in an RF isolation chamber with programmable attenuators, with single Wi-Fi AP-client pairs and a single LTE-LAA eNB. Only LTE-LAA transmissions in the unlicensed bands were considered. It concludes that the failure to coexist effectively can be attributed to two factors. One is the effect of LTE-LAA's duty-cycling mechanism on Wi-Fi operation, as will be discussed in section 2.3.4. Another is the lack of effective coexistence mechanisms in

Table 2.4: Typical LTE-LAA and Wi-Fi coexistence testing and results

Item	Organiser	Characteristics/conclusions
[143]	FCC	**The first representative suggestion:** 1. Leave the development of coexistence mechanisms to industry cooperation with the broader unlicensed community. 2. The failure to coexist effectively can be attributed to: a. Duty-cycling's effect on Wi-Fi; b. Lack of coexistence mechanism at moderate levels.
[144]	FCC	**The second representative suggestion:** 1. Congests [143]'s second conclusion. 2. LTE-LAA is a better neighbor to one Wi-Fi than other Wi-Fi devices.
[145]	FCC	**Neutral opinion compared to [143, 144]**: 1. Unfair to compare Wi-Fi's performance in an interference-free environment to its performance in the presence of LTE-LAA. 2. Instead, a more fair comparison is to evaluate Wi-Fi's performance in the presence of other Wi-Fi nodes. 3. Different vendors will be impacted quite differently in the presence of LTE in 5 GHz.
[7]	LTE-U Forum	**For markets without LBT**: 1. Simulation models are not published. 2. LTE-LAA behaves as a comparable neighbor to Wi-Fi compared to Wi-Fi as a neighbor, while LTE-LAA significantly outperforms Wi-Fi. 3. All tests in [7] are based on the current IEEE 802.11ac standard.
[142]	3GPP	**For markets with LBT**: 1. It is possible for LTE-LAA with LBT scheme in 5 GHz to be a good neighbor to Wi-Fi. 2. All testing activitis in [142] are based on the current IEEE 802.11ac standard. 3. Recommendations based on testing: a. Some LBT schemes should be configurable within limits b. LTE-LAA should support UL LBT.
[146]	Wi-Fi Alliance	**A future test plan:** 1. Tests are developed to ensure fairness to Wi-Fi. 2. How LTE-LAA equipment passes those tests is immaterial.

scenarios where LTE-LAA and Wi-Fi devices receive signals from each other at moderate levels. It even states that LTE-LAA does not have an effective coexistence technique to handle scenarios in which LTE-LAA and Wi-Fi devices hear each other at moderate levels (below -62 dBm) and, as a consequence, Wi-Fi can be crippled in such scenarios. Nevertheless, the accuracies of this claim have been contested by [144], which reflects the second kind of suggestion that LTE-LAA is a better neighbor to Wi-Fi than other Wi-Fi devices. There are also some neutral opinions. In [145], a series of tests and demonstrations using eight Wi-Fi routers and gradually changing nodes in form of Wi-Fi or LTE-LAA have been done, arguing that it is unfair to compare Wi-Fi's performance in an interference-free environment to its performance in the presence of LTE-LAA. Instead, a more fair comparison is to evaluate Wi-Fi's performance in the presence of other Wi-Fi nodes. One thing [145] makes clear is that different vendors will be impacted quite differently in the presence of LTE over unlicensed band. There is further a very large set of FCC fillings within this area [147]. Furthermore, in [7], a significant amount of LTE-

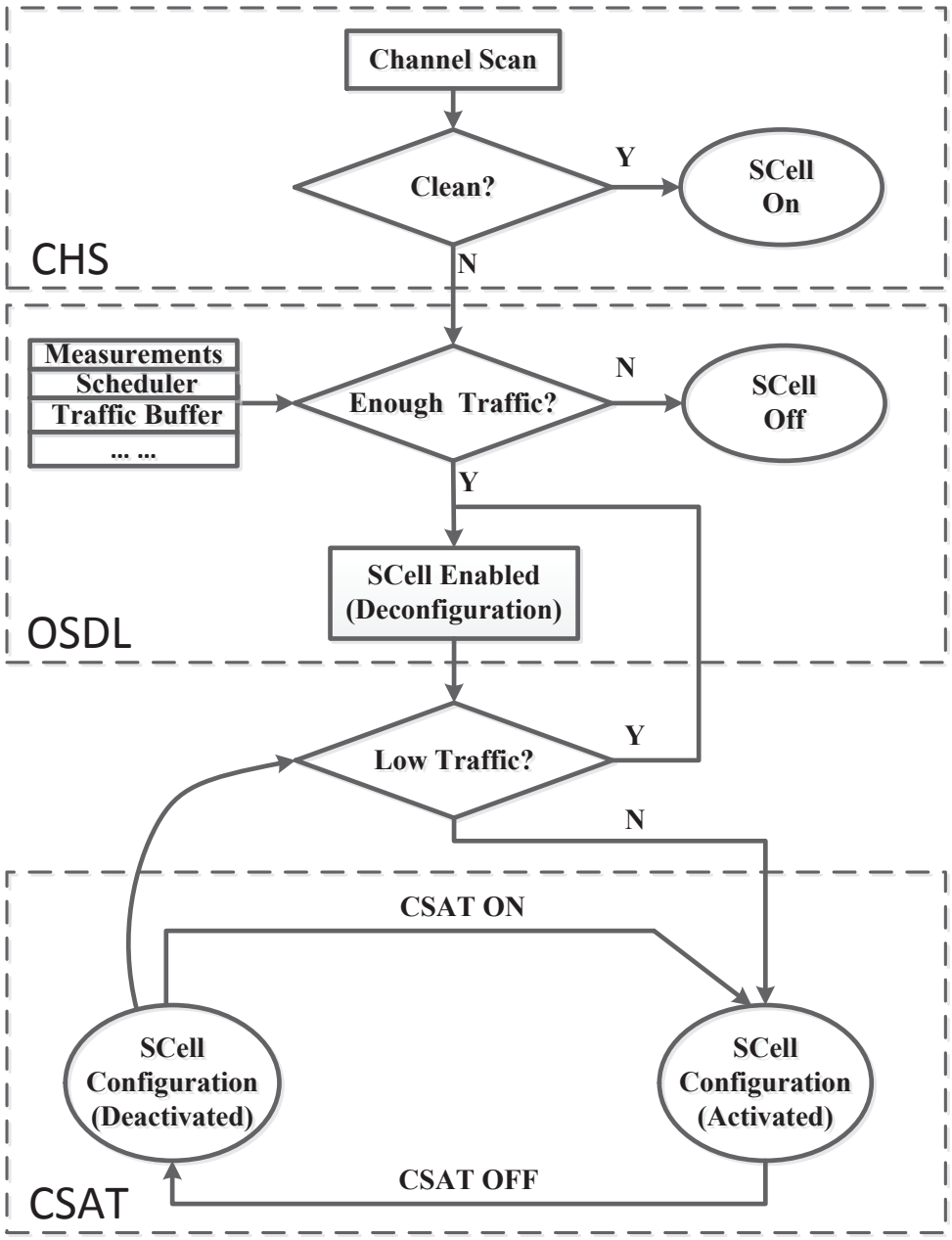

Figure 2.1: Three steps of coexistence mechanism centralized by CSAT: a) CHS; b) OSDL; and c) CSAT.

U forum testing and technical documentation can be found. However, the most crucial details such as the simulation models are proprietary. The testing has shown result that LTE-LAA behaves as a comparable neighbor to Wi-Fi compared to Wi-Fi as a neighbor, while LTE-LAA significantly outperforms Wi-Fi. All tests in [7] are based on the current IEEE 802.11ac standard.

In addition, in [142], the testing work organised by 3GPP presents the results of a study on the operation of LTE in unlicensed spectrum as an SCell. It shows that with proper and robust coexistence mechanisms, it is possible for LTE-LAA with LBT scheme in 5 GHz to be a good neighbor to Wi-Fi. For example, LTE-LAA causes less adjacent channel interference to a Wi-Fi system compared to another Wi-Fi system. 3GPP also provides some recommendations for the coexistence study in the future based on the testing result. First, it is recommended that the key parameters of the LBT scheme such as contention windows and defer periods should be configurable within limits to enable fair coexistence with other technologies operating in unlicensed spectrum. Second, it also shows that LTE-LAA should support UL LBT at the UE.

What's more, to ensure that LTE-LAA and Wi-Fi will coexist well and to address stakeholder questions and concerns, LTE-U Forum has been collaborating with Wi-Fi stakeholders, e.g. the Wi-Fi Alliance, CableLabs and others in the cable industry. In particular, Wi-Fi Alliance has posted the current test plan [146], and also posted the coexistence guidance [148]. In [146], tests are developed to ensure fairness to Wi-Fi, and how LTE-LAA equipment passes those tests is immaterial and is not specified. Table 2.4 gives the details of each work.

2.3.2 Coexistence Mechanisms in Markets without LBT Requirement

In those markets where no LBT is required, with carefully designed coexistence mechanisms, resource sharing between LTE-LAA and Wi-Fi in unlicensed band could be managed fairly without modifying Release 10/11 PHY/MAC standards. LTE-LAA duty cycling is proposed to release resources to the Wi-Fi network. One practical way to implement duty cycling is using coexistence mechanism centralized by CSAT [2, 127]. Another feasible methodology is assisted by ABS [112, 140, 149].

Coexistence Mechanism Centralized by CSAT

One example cellular operation consisting of three different techniques has been given in [150]. As shown in Fig. 2.1, the whole workflow can be divided into three steps. Originally, the CHS performs scanning procedures to classify the different channels based on their conditions. If a clean channel is identified, a corresponding SCell (e.g., LTE-LAA) can be operated without concerning co-channel communications. In practice, if a form of interference is found in the current operating channel, the LTE-LAA transmission will

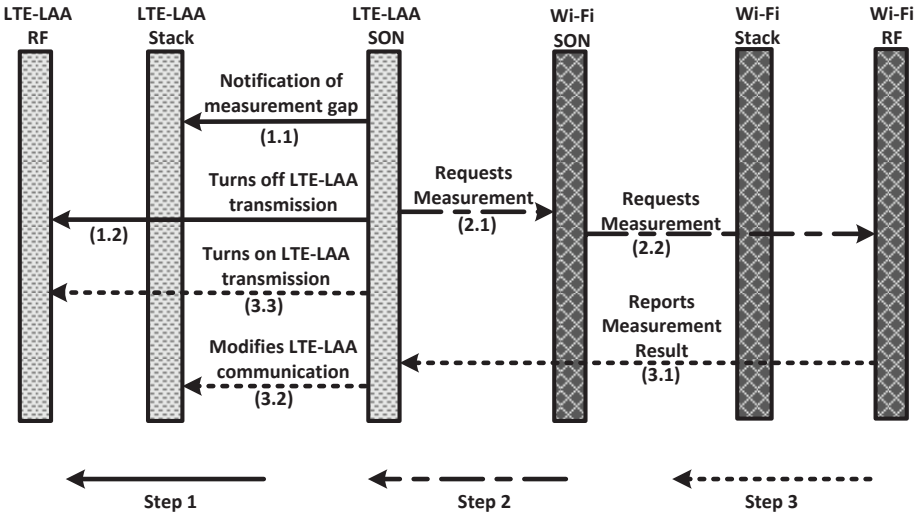

Figure 2.2: Messages exchange between Co-located LTE and Wi-Fi radios.

be switched to a cleaner one with less interference by using LTE Release 10/11 procedures. Note the interference level in this example can be measured by energy detection for the sake of simplicity, as is done in [151], where interference types and sources are not considered. On the other hand, in consideration of the existence of multiple incumbent wireless technologies besides Wi-Fi in the unlicensed spectrum such as radar signal and satellite signal, a scheme of high level interference detection of which the sensitivity is improved by collecting the information of the sources types and quantities can be performed [8].

CHS is often sufficient to meet the Wi-Fi and LTE-LAA coexistence requirement as long as the traffic density is low [127]. On the contrary, in areas of dense deployments, where no clean channel is available, a further process, i.e., Opportunistic SDL (OSDL) should be utilized to reduce the impact on co-channel communications. Input from CHS algorithms as well as from various measurements, traffic buffers and schedulers is optional by OSDL to find out whether there exists enough traffic to support a secondary carrier or not. If the answer is 'YES', an SCell supporting relevant secondary carrier can be initially enabled in a deconfigured state, then be configured and activated with the help of additional process such as CSAT which is designed to improve the coexistence performance. Otherwise, if no enough traffic is available, SCell will be disabled [150].

CSAT has been proposed initially by Qualcomm for LTE-LAA MAC scheduling [127]. During CSAT operation, the SCell remains configured. However, once the traffic

level drops below a certain threshold, the SCell will return to the deconfiguration state. The key idea of CSAT is to define a time division multiplexing cycle for the transmission of LTE-LAA in a short duration of time, where CSAT is enabled, namely CSAT ON periods, during which it is available for an SC to transmit at a relatively high power. While in the rest part, also known as CSAT OFF periods, although remains configured, the SC will operate at a relatively low power or even gate off in order to avoid competing with Wi-Fi [8].

Measurements of resource utilization performed by user devices and/or small BSs can be utilized as reference materials to help adapt the CSAT parameters accordingly [127, 150, 151]. In another word, one Radio Access Technology (RAT) (e.g., LTE-LAA) needs to request a measurement from another RAT (e.g., Wi-Fi) and to identify its utilization based on the received signals. Fig. 2.2 shows an example of about how messages exchange between two different RATs during measurements time [150]. The whole workflow also consists of three steps. In the first step, the LTE-LAA Self-organizing Network (SON) sends a message to the LTE-LAA stack to notify that a measurement gap is upcoming on the shared unlicensed band and then commands the LTE-LAA radio to temporarily turn off transmission on the unlicensed band. The purpose of this part is to guarantee that LTE-LAA transmission will not interfere with measurements during this time. Sequentially, LTE-LAA SON requests the co-located Wi-Fi SON that a measurement be taken on the unlicensed band by sending a message, which will then command Wi-Fi RF to measure how Wi-Fi is utilizing the unlicensed band currently. In the final step, the measurement report including the results of the measurements goes back to the LTE-LAA SON, which may send permission to LTE-LAA RF and LTE-LAA stack separately in order to turn on LTE-LAA transmission and modify communication.

By adjusting those parameters such as the cyclic on/off ratio and transmission powers during the CSAT ON or OFF periods based on the current signaling conditions, resource sharing between LTE-LAA and Wi-Fi in the same unlicensed spectrum can be optimized, thus leads to a better coexistence performance. Take a representative CSAT communications scheme shown in Fig. 2.3 for example [150], if the utilization of a given channel by Wi-Fi devices needs to be high, the usage of the channel by LTE-LAA radio can be reduced by pulling its transmission power back or bring the cyclic on/off ratio down, and vice versa.

The CSAT ON/OFF period duration also differs in various solutions. In some articles

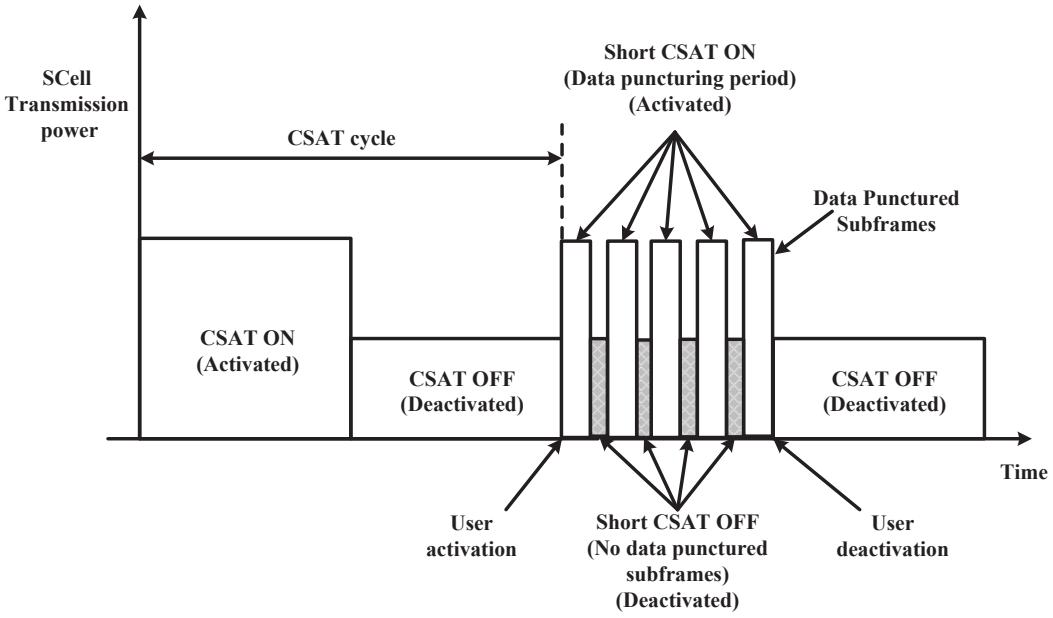

Figure 2.3: Two categories of CSAT periods. (a) CSAT ON periods; (b) CSAT OFF periods. The usage of the channel by LTE-LAA radio can be reduced by pulling its transmission power back or bring the cyclic ON/OFF ratio down, and vice versa. The introduction of data punctured subframes can be used to reduce latency by dividing the CSAT ON periods into two parts: the short CSAT ON periods and the short CSAT OFF periods.

like [150] this length of the CSAT cycle is designed to be greater than 200 ms to guarantee a sufficient opportunity for user devices to measure the channel condition at least one time. What's more, longer CSAT cycle means higher capacity because of less overhead in carrier activation [2]. On the flipside, shorter CSAT cycle reduces latency impact to delay sensitive traffic on Wi-Fi. Like what coexistence specification from LTE-U forum says, the maximum length of CSAT ON/OFF period is 50 ms [7]. Unfortunately, it is contradictory indeed about this time length issue, so far no authoritative result has been reached. In general, coexistence mechanisms centralized by CSAT herein may enjoy several advantages. One example is, as mentioned before, it ensures fair and efficient channel sharing between LTE-LAA node and Wi-Fi APs making use of CHS, OSDL and CSAT as a group. Another big benefit is that such mechanism does not bring any change to the underlying RAT communication protocol [127, 150]. It is no doubt that a weakness remains in CSAT itself, namely its longer latency compared to CSMA. To solve this problem, in one aspect, primary channel occupation by Wi-Fi APs needs to be prevented by CSAT [127]. On the other hand, data punctured subframes inserted period-

ically in Fig. 2.3 is also capable of minimizing latency impact [2]. In particular, the data punctured subframes makes the CSAT ON period shown ahead be able to be divided into two parts: the short CSAT ON period, i.e., the data puncturing period, and the short CSAT OFF period, i.e., the time period where no data will be transmitted.

Coexistence Mechanism Assisted by ABS

Another mechanism called LTE muting in spirit similar to CSAT has also been proposed, which is summarized as avoiding different RATs accessing the channel at the same time, i.e., in n of every 5 subframes, LTE-LAA needs to be turned off, and Wi-Fi users will replace LTE-LAA nodes in using channel resource [8]. Another example of fair allocation scheme is to assign equal channel time to every competing entity including idle periods, successful transmissions and collisions for the Wi-Fi network [136]. Moreover, Wi-Fi users may spend a lot of time in backoff if there are a lot of users trying to access the network at the same time. The Wi-Fi performance would not necessarily degrade if LTE-LAA could exploit those silent times [137]. In those examples, the communication among different network techniques, utilized to adapt CSAT parameters and cannot always be ensured when devices belong to different operators, is not required. These time-sharing coexistence techniques requiring LTE silent periods would exploit ABSs, a key feature introduced in Release 10 as a base [112]. ABSs are LTE subframes with reduced DL transmission activity or power. By muting the transmission power of the SCs in certain subframes, interference caused by Macro eNBs to Pico eNBs would be less in HetNets [8, 112]. Building on this work, a probability for LTE-LAA to access the channel is defined in [152–154]. A survey involving the summary of an example coexistence mechanism assisted by ABS has also been published [112]. It is concluded that LTE-LAA activities in unlicensed spectrum can be controlled with the help of a modified version of ABS, where UL and/or DL subframes can be silenced, and no LTE common reference signals are included. It is shown that Wi-Fi is able to reuse the blank subframes ceded by LTE, and that throughput increases with the number of null-subframes. However, since LTE throughput decreases almost proportionally to the number of ceded blank subframes, a tradeoff is established. Additional LTE performance degradation may be observed if blank subframes are nonadjacent, since Wi-Fi transmissions are not completely confined within LTE silent modes. However, if the duration and occurrence of LTE blank subframes is reported to Wi-Fi during the negotiation phase, Wi-Fi nodes

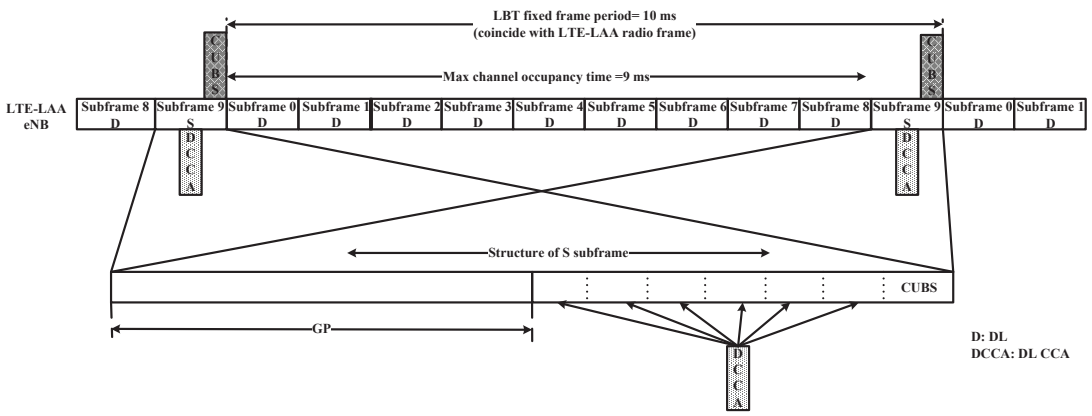

Figure 2.4: An example of CCA placement option. A subframe S (e.g., subframe 9) consists of a GP, several slots for CCA placement and a node for CUBS for the remaining symbols. A GP is provided prior to the CCA placement to guarantee the idle time. If the CCA procedure succeeds, the node will seize and hold the medium until the start of the next subframe S, and CUBS may block the transmission signals of other users nearby.

may be able to conveniently confine their transmissions within blank subframes and thus avoid interference with LTE.

2.3.3 Coexistence Mechanisms in Markets with LBT Requirement

In many markets where LBT requirement exists, various modifications are required to adapt LTE PHY/MAC. For example, LBT using CCA to determine if a particular channel is available is needed to meet regional requirement. The concept of beacon signal is also introduced to reserve the channel for transmission following LBT [127].

A node having data to transmit should perform a CCA first to determine the availability of the spectrum band, i.e., whether the channel is clean or already occupied by other signals transmitted by other operators or radar. If clean channel is available, this CCA procedure will contend for use of the radio frequency spectrum band. Upon the successful first CCA procedure, one or more additional CCA procedures will be performed during Discontinuous Transmission (DTX) periods to determine continued availability of the radio frequency spectrum band [12, 155].

Fig. 2.4 shows a case of CCA placement options in an example of DL frame structure [156]. Subframe S (e.g., subframe 9) may be used to hold the succeeding transmission resources. It may work as CCA, DTX, or Channel Usage Beacon Signals (CUBS). A subframe S consists of a Guard Period (GP), several slots for CCA placement and a node

for CUBS for the remaining symbols. A GP is provided prior to the CCA placement to guarantee the idle time. The number of slots for CCA placement varies in different papers, even as little as 2 in [139]. However, as is emphasized in [156], the number of slots for CCA placement may be referred to as a CCA reuse factor, which can be 3, 4, 7, 9 or 12. The reuse factor adopted in Fig. 2.4 is 7. If the CCA procedure succeeds, which means the node will grab and hold the medium until the start of the next subframe S, CUBS may block the transmission signals of other users nearby by notifying other nodes also performing CCA later in the same subframe S that the medium has been occupied.

It is necessary to set CCA threshold appropriately for the purpose of protecting nearby WLAN transmissions. The ability for devices to coexist is highly dependent upon their ability to detect another at lower RF levels. Raising the threshold helps protect smaller area around eNB and implies sensing. However, if the LBT threshold is too high, the case with LBT will become ineffective since it turns to be equivalent to the one without LBT. Lowing the threshold will lead to wider covering area, but reducing the chance for the eNB to transmit at the same time [12]. The CCA threshold also varies with two types of CCA techniques designed in IEEE 802.11 specification, energy based CCA and preamble based CCA. In the former case, the transmitter only measures the total received power and does not require any knowledge of the signal structure or packet format. The preamble based CCA, on the other hand, is the one achieved by a cross correlation module. In IEEE 802.11, the transmitter will declare the channel as busy when the total received power is larger than -62 dBm while using energy based CCA in 20 MHz. This threshold value changes to -82 dBm while using preamble based CCA. Since in LTE-LAA, either energy based CCA or preamble based CCA, or even both may be used, CCA threshold should also be set carefully in different scenarios [157].

During example DTX periods shown in Fig. 2.5 [155], upon the successful first CCA procedure, one or more second CCA procedures may be performed to determine continued availability of the radio frequency band. If the first CCA does not succeed, the eNB will not transmit, nor will it perform any CCA until the next transmission period, either. On the contrary, if it succeeds, while the second CCA procedures fail during one DTX period, the transmission will stop until a subsequent second CCA indicates that the radio frequency band is available again.

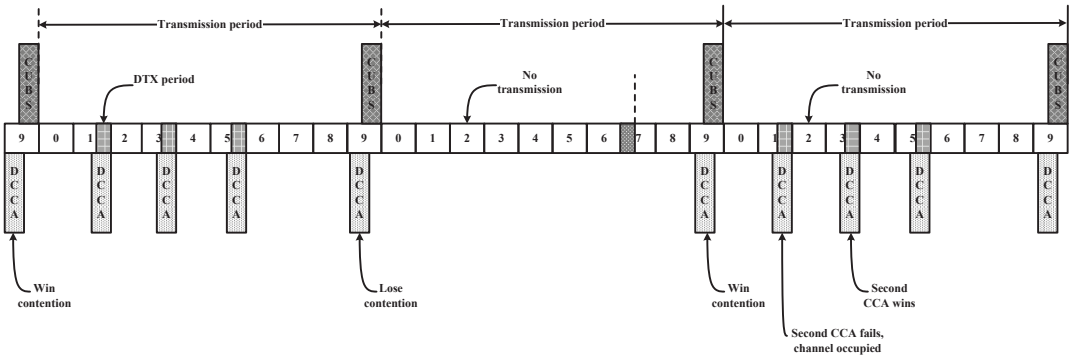

Figure 2.5: Illustration of DTX periods and DL CCA intervals. If the first CCA lose contention, the eNB will not transmit, nor will it perform any CCA until the next transmission period, either. On the contrary, if it wins contention, while the second CCA procedures fail during one DTX period, the transmission will stop until a subsequent second CCA indicates that the radio frequency band is available again.

2.3.4 Summary and Guidelines

Lessons Learnt from Different Coexistence Mechanisms Comparison

In general, for markets where no LBT is required, LTE-LAA's primary coexistence mechanisms can be summarized as duty-cycling, i.e., cycling LTE-LAA through ON/OFF periods. The main advantage of duty-cycling is that it requires fewer changes from LTE and does not require any ad-hoc standardization effort. The availability is attractive to operators who need to increase capacity in a short term, especially if they plan to deploy LTE-LAA in environments where there are free channels are available and hence fair coexistence with Wi-Fi is easy to achieve.

However, duty-cycling itself has some weakness, as stated in section 2.3.2, while using duty-cycling, it is the LTE-LAA cell that decides how much fairness to allow, and Wi-Fi networks can only adapt to the rules set by LTE-LAA. In other words, it is the LTE-LAA device that controls the ON/OFF cycle. Due to this situation, duty-cycling may lead to a poor performance of Wi-Fi devices. Furthermore, although longer LTE-LAA OFF times can lead to a lower percentage of errors and thus excellent throughput, for a better delay and latency performance of Wi-Fi devices, shorter LTE-ON time is needed. LTE-LAA duty-cycle parameters may affect Wi-Fi performance, thus selection of cycle period is critical to the performance on Wi-Fi network [158]. As shown in Fig. 2.3, data gaps that can be punctured into data punctured subframes and inserted

Table 2.5: Comparative study of LBT and Duty-cycling

	LBT	Duty-cycling
Advantage	More fair	1. Fewer changes from LTE; 2. No ad-hoc standardization requirement
Disadvantage	LTE performance degradation	Less Fair
Target Markets	With LBT reuirement (Europe and Japan)	Without LBT reuirement (UK, Korea and China)
Practicality	Release 13 was completed in Mar. 13, 2016; More onerous to implement	Based on Release 10-12; Can be deployed in a short term
MAC/PHY	Modifications required	Modifications required
Notes	1. Various LBT schemes (refer to Table 2.2); 2. LBT implementation has an impact on coexistence performance; 3. LBT with random backoff in a contention window of variable size is more attractive to Wi-Fi.	1. Short gaps lead to not only short latency, but also rate control problem; 2. Cycle period is critical to the performance.

periodically are also capable of resolving this conflict by minimizing latency impact to delay sensitive traffic on Wi-Fi. However, new challenges will arise with the introduction of this method. First, the introduction of these gaps can exacerbate the rate control problem. Second, delay-critical frames may not be transmitted during the short gaps.

Compared to duty-cycling, the addition of LBT will bring several benefits. For example, LTE-LAA with LBT requirement will degrade performance and hence reduce the benefits of LTE-LAA over Wi-Fi, thus will improve Wi-Fi throughput [55]. What's more, LBT itself allows for a distribution of spectrum resources that takes the traffic load of each coexisting network into account. On the other hand, LTE-LAA with LBT also has some weaknesses. As stated in Table 2.3, the LBT standardization was just completed in March 2016, so LBT is more onerous to implement than duty-cycling. What's more, the impact of Wi-Fi would vary on how LBT is implemented. In fact, 3GPP designs four kinds of channel access schemes [3]:

a) **No LBT:** No LBT procedure is performed by the transmitting entity.

b) **LBT without random backoff:** It means the duration of time that the channel is sensed to be idle before the transmitting entity transmits is deterministic.

c) **LBT with random backoff in a contention window of fixed size:** The LBT procedure has the following procedures as one of its components. The transmitting entity

draws a random number N within a contention window. The size of the contention window is specified by the minimum and maximum value of N. The size of the contention window is fixed. The random number N is used in the LBT procedure to determine the duration of time that the channel is sensed to be idle before the transmitting entity transmits on the channel.

d) **LBT with random backoff in a contention window of variable size:** The LBT procedure has the following procedures as one of its components. The transmitting entity draws a random number N within a contention window. The size of the contention window is specified by the minimum and maximum value of N. The transmitting entity can vary the size of the contention window when drawing the random number N, which is used in the LBT procedure to determine the duration of time that the channel is sensed to be idle before the transmitting entity transmits on the channel.

Wi-Fi performance itself benefits from a variable backoff periods. Nevertheless, 3GPP is also considering LTE-LAA using a fixed backoff periods. Table 2.2 further shows a comparative study of proposed LBT schemes.

Generally speaking, duty-cycling mechanisms are commonly regarded as being more aggressive and unfair than LBT because it does not abide by the same rules as Wi-Fi. However, adding LBT to LTE-LAA may takes away LTE advantages. It is also shown that the choice of channel access schemes real really makes sense, i.e., not all LBT schemes providing fair coexistence [3]. The introduction of LBT also requires MAC/PHY modifications, as discussed in section 2.3.3. For more details, refer to Table 2.5.

Lessons Learnt from Cognitive Radio

To ensure fairness, the unlicensed spectrum is supposed to be shared without preference. Although coexistence mechanisms have been designed to ensure that the existing systems are minimally interfered, potential interference could still appear in existing systems. The interference will occur when primary system begins to transmit right or shortly after the secondary system starts the transmission. For different RANs in unlicensed spectrum, the Wi-Fi users can be regarded as the primary users (PUs) since Wi-Fi is the prevalent technology using 5 GHz. If subsequent users such as LTE-LAA users, referred to as secondary users (SUs), want to use the occupied spectrum opportunistically or concurrently, an interference management mechanism should be established.

Since CR is initially designed in exploiting white spaces including unlicensed spectrum efficiently, it is nature to utilize the attributes of the CR to optimize LTE-LAA in 5 GHz. That means frequency-agile modems that can rapidly switch channels if interference is present, are needed.

The FCC defines CR as the radio that can change its transmission parameters based on interaction with the environment where it operates [159]. The main goal of CR is to identify the unused licensed spectrum for SU without causing interference to the PU. CR involves both spectrum sensing and channel switching techniques. Spectrum sensing is the ability to measure, sense and be aware of the parameters related to the radio channel characteristics. Spectrum sensing in CR networks is done for two purpose, one is to identify the spectrum opportunities, the other is to detect the interference in the spectrum. Channel switching techniques include predictive channel switching, random channel switching and optimal channel switching. Predictive channel switching mechanism calculates the remaining idle time of each channel and the channel with the largest remaining idle time is selected for switching. Random channel switching makes the selection in random manner when the interference occurs. In optimal channel switching scheme the channel that is free and offers longer remaining idle time is selected for switching.

LTE-LAA in 5 GHz can be regarded as a special case of OFDM-based CR systems. There are also several works focusing on LTE and LTE advanced networks along with CR. For example, in [160], CR is applied to sense the spectrum by using the conventional method of energy detection. In [161], the authors focus on improving resource efficiency in LTE network by considering CR device to device communication links. However, it seems the current available mathematically-optimal algorithms are not suitable for the implementation of LTE-LAA systems, due to potential iteration divergence and computation load [162]. I recommend that researchers focus on the LTE-LAA CR technique design.

2.4 Current Research on LTE and Wi-Fi Integration

Standards in which the Wi-Fi deals with authentication have been under consideration, such that the offloading from LTE to Wi-Fi will happen seemingly. Indeed, alongside LTE-LAA, recent work by the 3GPP on offloading to the WLAN is also being discussed. The inherent constraints of cellular networks, particularly due to cross-tier and co-tier

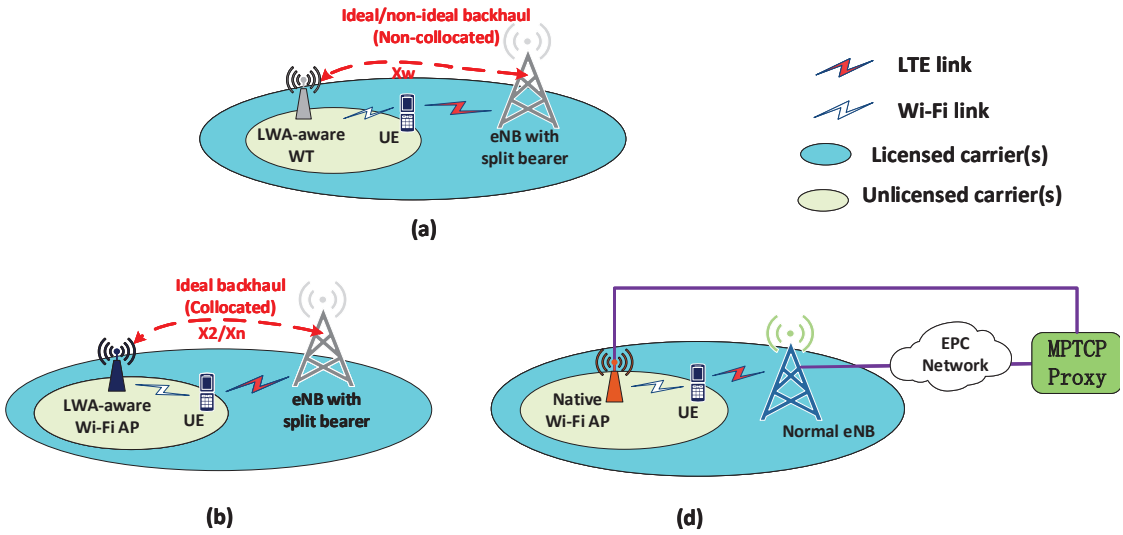

Figure 2.6: LTE-WLAN integration operation scenarios: (a) Non-collocated LWA operation scenario; (b) Collocated LWA operation scenario; (c) LWPA operation scenario. EPC refers to evolved packet core.

interference, motivate offloading some of the traffic to the Wi-Fi band, so as to alleviate the interference and ease congestion. 3GPP has defined several Wi-Fi offloading mechanisms which rely on the connection between the LTE and Wi-Fi.

With carrier Wi-Fi, Wi-Fi infrastructure can be utilized. Because with carrier Wi-Fi, LTE and Wi-Fi can be integrated in the core, operators can present a consistent set of policy and services. However, due to the different mobility, authentication, security, and management between LTE and Wi-Fi, there is still work ahead before achieving full integration.

2.4.1 LTE-WLAN Aggregation

LWA has been recently standardized in 3GPP Release 13 [16] to allow for boosting LTE data rates through leveraging 5 GHz Wi-Fi bands, such that Uplink (UL) traffic is carried on LTE and DL traffic to be aggregated at the Packet Data Convergence Protocol (PDCP) layer. PDCP re-ordering and PDCP aggregation features should be added to LWA UE.

The basic idea of LWA is that mobile operators use Wi-Fi for access, with Wi-Fi unlicensed band transmission integrated in the cellular network. This means that LWA can transmit LTE traffic through Wi-Fi APs that are connected to LTE BSs. At the same time, the Wi-Fi APs can use the LTE core network functions without a dedicated gateway. LWA reuses the LTE split-bear reordering mechanism to transmit PDCP packets

over LTE and to convey the remainders via Wi-Fi AP by encapsulating them in Wi-Fi frames in advance. The LTE evolved NodeB (eNB) will control the amount of traffic scheduled over Wi-Fi, and thereby will ensure proper load balancing between the LTE and Wi-Fi links. The received packets from both LTE and Wi-Fi will be aggregated at the PDCP layer of the LWA UE. A Wi-Fi AP can operate as a native Wi-Fi AP while not serving LWA purpose.

LWA supports both non-collocated and collocated scenarios, as shown in Fig. 2.6a and 2.6b. For the former, it features a new direct interface Xw, defined between LTE and WLAN. It may be noted that the Xw interface borrows many features from the X2 interface enhanced for dual connectivity, developed in Release 12 by 3GPP. The Xw interface is terminated at the WLAN termination (WT), which may be in control of one or more Wi-Fi APs.

Complementary to carrier Wi-Fi and LTE-LAA, LWA enables operators to integrate Wi-Fi. Moreover, LWA has several advantages. First, unlike LTE-LAA, it requires little intervention in existing networks and in devices since the WLAN radio link effectively becomes part of the E-UTRAN. Furthermore, because it uses ubiquitous Wi-Fi and LTE wireless interfaces, it can become commercially available in a short term. More works are required to quantify the performance comparison between LWA and LTE-LAA, especially if the LBT implementation is considered [10].

Additionally, Wi-Fi specifications continue to evolve. IEEE 802.11 is being adjusted towards 802.11ax which aims at increasing spectral efficiency in 2.4 and 5 GHz bands, particularly in dense deployments with a theoretical peak throughput up to 9.6 Gbps and 1.6 Gbps under more realistic conditions. In the millimetre wave band of 60 GHz, 802.11ad is a ratified amendment to 802.11 that defines a new physical layer for 802.11 networks and can offer up to 7 Gbps throughputs. 802.11ay is in the process of enhancing 802.11ad and aims at improving mobility, range and providing data rates of at least 20 Gbps. Even though LWA framework has been designed largely agnostic to 802.11 technologies, such increased data rates may require additional optimizations [52].

Currently Release 13 assumes no IEEE 802.11 impact and requires little coordination between 3GPP and IEEE. In Release 14, proactive cooperation and coordination between 3GPP and IEEE may allow LWA and IEEE 802.11 evolution to be more harmonious, further increasing the benefits of these technologies.

2.4.2 LTE-Wi-Fi Path Aggregation based on Multipath TCP

As an alternative to LWA at radio link level, LWPA is based on MPTCP which works differently as it is designed to aggregate multiple flows of data on transport layer.

The main design feature of LWPA is to transmit data using as many paths as possible while working with the existing Internet environment, without having to replace any part of it. MPTCP can establish multiple paths, and transmit data through them concurrently. Thus, LTE and Wi-Fi can be aggregated simply by adding an MPTCP gateway and upgrading the software on mobile devices, as shown in Fig. 2.6d. LWPA operates with the least knowledge of the network state, it provides performance improvement, and it is easy to implement.

2.4.3 Advantages of LTE-WLAN Integration

Wi-Fi has been widely used, due to easy deployment and low cost, making the integration of Wi-Fi in LTE networks feasible. Although Wi-Fi still needs enhancement in coverage, mobility and network efficiency similar to what LTE offers, it indeed has some advantages. Besides its wide AP footprint in the enterprise and in public venues, an additional advantage is its standardization and established ecosystem. Moreover, Wi-Fi specifications continue to evolve. IEEE 802.11 is being adjusted towards 802.11ax which aims at increasing the spectral efficiency in 2.4 and 5 GHz bands, particularly in dense deployments with a theoretical peak throughput of up to 9.6 Gbps, and 1.6 Gbps under more realistic conditions. 802.11ad is a ratified amendment to 802.11 that defines a new physical layer for 802.11 networks and can offer up to 7 Gbps throughput. 802.11ay is in the process of enhancing 802.11ad and aims at improving mobility, range and providing data rates of at least 20 Gbps.

The LWA, LWIP, and LWPA solutions seem to be promising for mobile network operators, as these technologies will have a smaller impact on infrastructure of both LTE and WLAN networks, compared to the use of LTE in the unlicensed bands. LTE-U, LTE-LAA, and MulteFire require 5 GHz LTE hardware on devices. On the other hand, existing eNBs and Wi-Fi APs can become LTE-WLAN Integration-enabled with software upgrades, which is a more cost efficient option than the use of LTE in the unlicensed spectrum, especially in the case of large-scale deployment. Moreover, LTE-WLAN integration allows mobile network operators to leverage existing investments in an extensive established base of Wi-Fi deployments. Being able to collocate SCs where

Wi-Fi APs already exist can speed up deployments and reduce cost and complexity. In addition, LTE-WLAN integration solutions do not cause issues regarding fair access as they permit only Wi-Fi use of unlicensed bands.

2.5 Modelling Considerations for LTE and Wi-Fi Inter-working System

2.5.1 With or Without an Anchor in the Licensed Band

As described in Section III.A, there are two deployment scenarios with respect to whether the licensed and unlicensed spectrum are aggregated or not. The choice between the two deployment options is dictated by the operator's existing assets and deployment plans.

Aggregating licensed and unlicensed spectrum for operator-controlled access to unlicensed spectrum that is well integrated to the LTE core network [3] can offer significant advantages. First, aggregating licensed and unlicensed bands can enable operators to leverage the existing LTE hardware in both the radio and core networks, thus, data offloading can be achieved in a seamless fashion. Moreover, to manage the different component carriers, the LTE eNB operating in the licensed spectrum can carry the control signaling which is granted the highest priority among nine Quality-of-Service (QoS) class identifiers defined by LTE. The signaling and control information is crucial not only to ensure the resource allocation is managed properly but also to maintain the robustness of the links. In some cases where there is a lot of interference and all the nodes are competing for resources, it is crucial to allocate the resources with an order. In addition, LTE macro cell can provide ubiquitous coverage for UEs. The above features make LTE able to facilitate opportunistic unlicensed access.

However, technologies requiring the operator to have an anchor in licensed spectrum may in practice limit the potential uses. A MulteFire network which is operating entirely in unlicensed spectrum seems to be promising for small businesses, enterprises, venue owners, and cable operators who lack licensed spectrum.

2.5.2 Radio Link-Level or TCP-level LTE-WLAN Integration

In radio link-level integration, LTE and Wi-Fi networks are closely coupled to potentially provide the highest performance, but with high implementation complexity. Compared to the TCP-level integration solution, where the transport layer has to infer the conges-

tion in the links using round trip delays and TCP acknowledgement loss, LWA and LWIP can improve system performance by managing radio resources in real time according to the radio frequency (RF) and load conditions of both LTE and Wi-Fi.

MPTCP proxy performs aggregation on top of the legacy networks, thus requiring no change in the legacy networks. A drawback to the radio link-level integration solution is investment costs for replacing less capable eNBs and Wi-Fi APs. On the contrary, LWPA based on MPTCP requires only modifications to operate software in the client devices and servers, and hence is easily implementable. It is also compatible with any legacy Wi-Fi APs. Since LTE and Wi-Fi have their own networks, the MPTCP proxy should identify ways to perform flow control on traffic forwarded to the respective network.

2.5.3 Comparison of Standardization Statuses

3GPP is making efforts to standardize LTE-LAA, LWA and LWIP in order to increase LTE rate through leveraging unlicensed Wi-Fi bands. In particular, LTE-LAA was approved as a Work Item (WI) for Release 13 in June 2015. 3GPP specified LTE-LAA for DL operation in Release 13 and is currently working on specifying LTE-LAA for UL operation in Release 14. Dual connectivity supporting spectrum aggregation between macro and small cells is another important LTE-LAA feature expected in Release 14 and beyond. LTE-LAA is standardized as a single global solution to be adopted by all regions with or without LBT requirements. The standardization process for LWA, including protocol architecture, solutions for aggregating data at the PDCP layer, signaling and interfaces between eNB and Wi-Fi AP, etc., was completed in March 2016. 3GPP also works on the enhanced LWA (eLWA) in Release 14. The eLWA is built on the Release 13 LWA framework without any change on the LWA architecture. Main topics include UL support, enhanced mobility, support for 60 GHz, and optimizations for high data rates 802.11 technologies, i.e., 802.11ax, 802.11ad and 802.11ay. Standardization for LWIP was formally completed in March 2016. The mobile operators can implement DL and UL functionality right away with LWIP.

The LTE-U forum has released LTE-U specifications including duty-cycle fair access solution since 2015. The LTE-U is a non-standard technology that employs a proprietary coexistence algorithm. The MulteFire Alliance released the MulteFire specification in 2016, which is built on elements of 3GPP Release 13 LTE-LAA for the DL and Release 14 enhanced LTE-LAA for the UL. Although standardization for MPTCP proxy began in

2009 when Internet Engineering Task Fore (IETF) MPTCP working group was formed, detailed architecture and deployment scenarios of MPTCP proxy-based aggregation, i.e., LWPA, have not been specified yet.

2.5.4 Further Research Directions

To meet the LTE and Wi-Fi inter-working challenges proposed in section 1.2.3, the community has proposed several coexistence mechanisms for both markets with and without LBT requirement. However, as will be discussed in the following sections, such a kind of coexistence is not going smoothly thus far. I summarize the key challenges related to the LTE and Wi-Fi cooperation as follows:

a) **Disputes over the effectiveness on current coexistence mechanisms are still the hot topic of the community.** As will be discussed in section 2.3.4, both duty-cycling and LTE-LAA with LBT are designed for specific markets. What's more, as stated in section 2.3.1 and 2.3.4, both mechanisms have their own weaknesses, and dispute remains over whether these mechanisms are valid in some specific scenarios. An agreement among the community is needed on one or more acceptable coexistence mechanisms.

b) **The lack of documented agreement on a definition of fairness is a big problem.** As stated in section 1.2.3, there exist different kinds of definition of fairness. The situation that Wi-Fi stakeholders tend to accept that fairness criteria means LTE-LAA should not impact Wi-Fi more enormous than another Wi-Fi network. Some 3GPP members believe that fair access means that LTE-LAA BS and IEEE 802.11 clients should have half of the bandwidth respectively. An agreement is required on the definition of fairness or a mechanism that achieves fairness.

c) **It is still too early to determine whether LTE-LAA is successful.** LTE-LAA is just one of a number of spectrum-sharing methods being used now with others in development or in test trials. The disagreement among different members in the community shows that there is no unified test platform. Furthermore, more researches concerning coexistence optimization are required. For example, new objective functions for optimizations problem formulations to guarantee the fair coexistence of LTE-LAA and Wi-Fi are needed. The attributes of the CR to optimize LTE-LAA in 5 GHz are also required. What's more, more complex tests on fairness, especially those based on a

range of realistic usage scenarios are urgently needed. That means, before drawing any conclusions, the community should first complete simulations representing more realistic usage scenarios.

d) **It lies in the features of specific scenarios that decide the coexistence is necessary or unnecessary.** That is to say, if it is not worthwhile for operators to deploy LTE-LAA from the perspective of various performance metrics, the coexistence is not necessary accordingly. From the view of market and technology, both LTE-LAA and Wi-Fi have their own benefits and cannot be replaced by each other. In this case, the choice of Wi-Fi or LTE-LAA is also related to the experience of operators and even financial and other factors.

2.6 Deployment Scenarios for the Coexistence and Scenario-oriented Decision-making

In previous sections, some coexistence-related features of LTE-LAA and Wi-Fi, as well as typical coexistence mechanisms on 5 GHz are discussed. They are fundamental for the discussion and investigation of the coexistence of two principal technologies in wireless communication systems. In this section, representative scenarios of deployment, which are of great significance, are being classified for the purpose of decision making for the coexistence of LTE-LAA and Wi-Fi in the next step. The concept of 'scenario-oriented coexistence' is presented and highlighted by dissecting an example of deployment scenario.

2.6.1 Influential Factors for the Classification of SC Scenarios

As stated in 3GPP TR 36.932 [163], in principle, the deploying scenarios can be classified from perspectives of eight factors affecting scenario deployment features of SC.

With/without Macro Coverage

Since Macro layer plays an important role in guaranteeing mobility, an SC may benefit from the presence of overlaid Macro cells. On the other hand, in such cases as deep indoor situations, an SC should also be able to work without Macro coverage. Thus, even for a space of similar size and for a building of same architectural structure and

Table 2.6: 5 GHz sub-bands for indoor/outdoor environment in some countries

Sub-bands	5.15-5.25 GHz	5.25-5.35 GHz	5.47-5.725 GHz	5.725-5.85 GHz
US/Canada	Indoor/Outdoor	Indoor/Outdoor	Indoor/Outdoor	Indoor/Outdoor
EU	Indoor	Indoor/Outdoor	Indoor/Outdoor	N/A
Korea	Indoor	Indoor/Outdoor	Indoor/Outdoor	Indoor/Outdoor
Japan	Indoor	Indoor	Indoor/Outdoor	N/A
China	Indoor	Indoor	N/A	Indoor/Outdoor
Australia	Indoor	Indoor/Outdoor	Indoor/Outdoor	Indoor/Outdoor
India	Indoor	Indoor	N/A	Indoor/Outdoor

interior furnishings, macro coverage will change deployment scenarios into different types compared with the case of absence of Macro cells.

Outdoor/indoor

A key difference between indoor and outdoor scenarios is the mobility support. In indoor scenarios such as offices and apartments, users normally stay stationary or move at very low speeds. In outdoor scenarios, however, to cover a large area like park or garden, a large number of SC nodes need to be set up to guarantee mobility everywhere. Relatively higher terminal speed can thus be expected in this situation.

Table 2.6 shows another notable fact that some sub-bands of 5 GHz are only available for indoor environment, and some others are useful for both indoor and outdoor cases due to specific considerations of these countries [50].

Ideal/non-ideal Backhaul

While considering the potentially large number of Wi-Fi APs and/or LTE-LAA STAs to be deployed, the link connecting the RAN and core network, also known as the backhaul is another key aspect of scenarios classification. The ideal backhaul, e.g., dedicated point-to-point connection using optical fibre or Line of Sight (LOS), is defined as latency less than 2.5 ms and a throughput of up to 10 Gbps. All other types of backhaul are non-ideal. Fig. 2.7 shows examples of both ideal and non-ideal backhaul deployments [50]. The unlicensed and licensed carriers in ideal backhaul deployments can be co-located or connected with each other with the help of the Remote Radio Head (RRH). While deploying non-ideal backhaul deployment, Multi-stream Aggregation (MSA) can

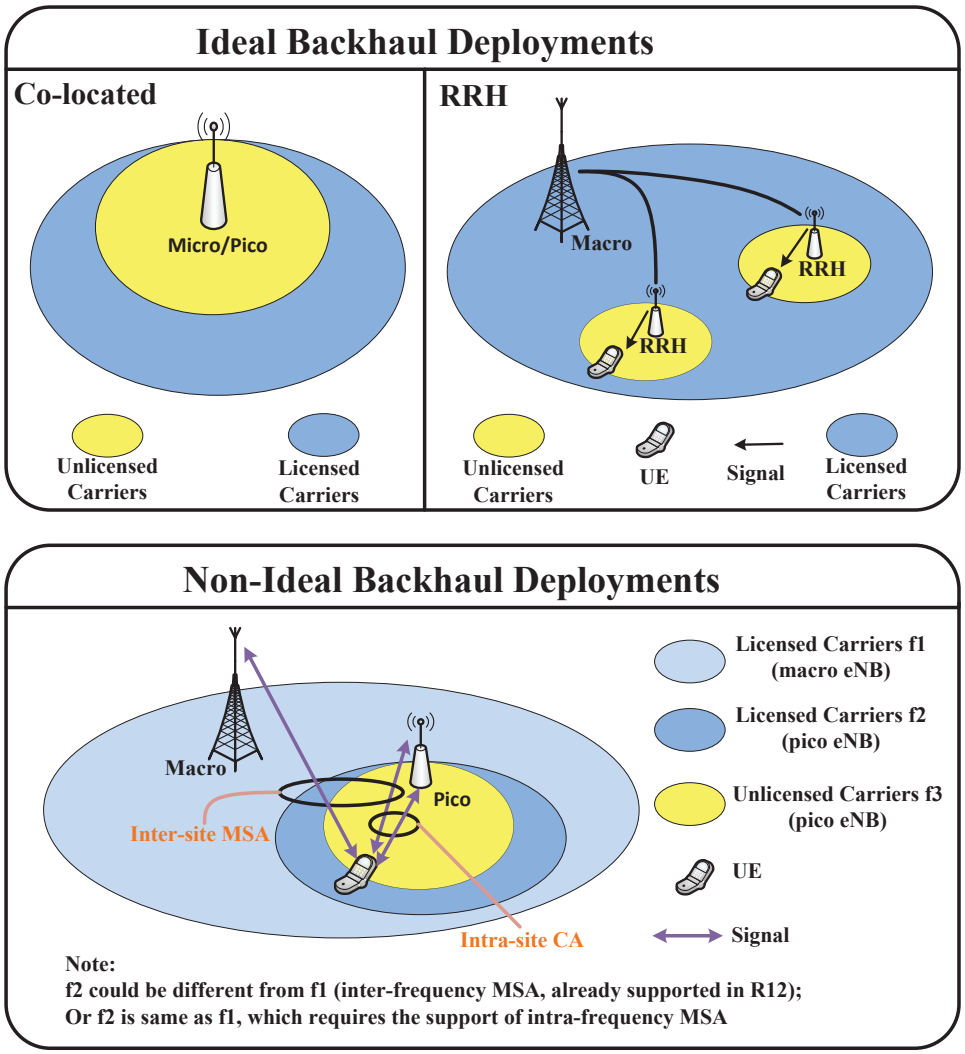

Figure 2.7: Ideal/non-ideal backhaul deployments.

enable data transmission without the need for additional signalling, thus maximizing utilization of system resources even when the user moves between different cell identifications [164]. MSA leverages the centralized integration of multiple RATs, carrier and intra-carrier ports to improve cell-edge throughput. In particular, with inter-RAT MSA, different RATs can be utilized to enhance user experience. Take the LTE/Wi-Fi scenario for example, LTE can act the host layer, with Wi-Fi acting as the boost layer. The former provides basic mobile services to the user, with an LTE host link remaining connected with the user. Wi-Fi then enhances user experience by providing a boost link between the user and Wi-Fi AP to boost data transmission rates. In addition, with inter-frequency MSA, a user is always anchored to the Macro cell through a host link even while dynamic connecting to other carriers through boost links for enhanced data

transmission.

Sparse/dense SC Deployment

In sparse scenarios, such as hotpot indoor/outdoor places, at most a few SC nodes are sparsely deployed. In dense scenarios, for example in a hypermarket or shopping mall, a large number of SC nodes are densely deployed to support huge traffic. Smooth future extension from small-area dense to large-area dense, or from normal dense to super-dense should be considered particularly.

Synchronized/asynchronous Connection

Both synchronized and asynchronous scenarios should be considered between LTE-LAA and/or Wi-Fi SCs as well as between SCs and Macro cell(s).

Spectrum

As to the spectrum factor in classifying scenario deployment, there are some example of spectrum configurations. The first case is when the carrier aggregation appears on the Macro layer with bands X and Y, only band X and Y, or only band X staying on the SC layer. Other two examples show that SCs supporting carrier aggregation bands are co-channel or not co-channel with the Macro layer, respectively.

One potential co-channel deployment scenario is dense outdoor co-channel SCs deployment, considering low mobility users and non-ideal backhaul.

Traffic

In an SC deployment, it is likely that the traffic will vary greatly since the number of users per SC node is typically not large due to the small coverage. It is also likely that the user distribution is very fluctuating among the SC nodes. The traffic is also expected to be highly asymmetrical, either DL or UL centric one. It should also be noted that traffic load distribution in the time-domain and spatial-domain could be uniform or non-uniform. Each case may correspond to a different scenario.

Backward Compatibility

Backward compatibility, i.e., the possibility for legacy (pre-Release 12) users to access an SC node/carrier, will be taken into account for SC deployments. The introduction

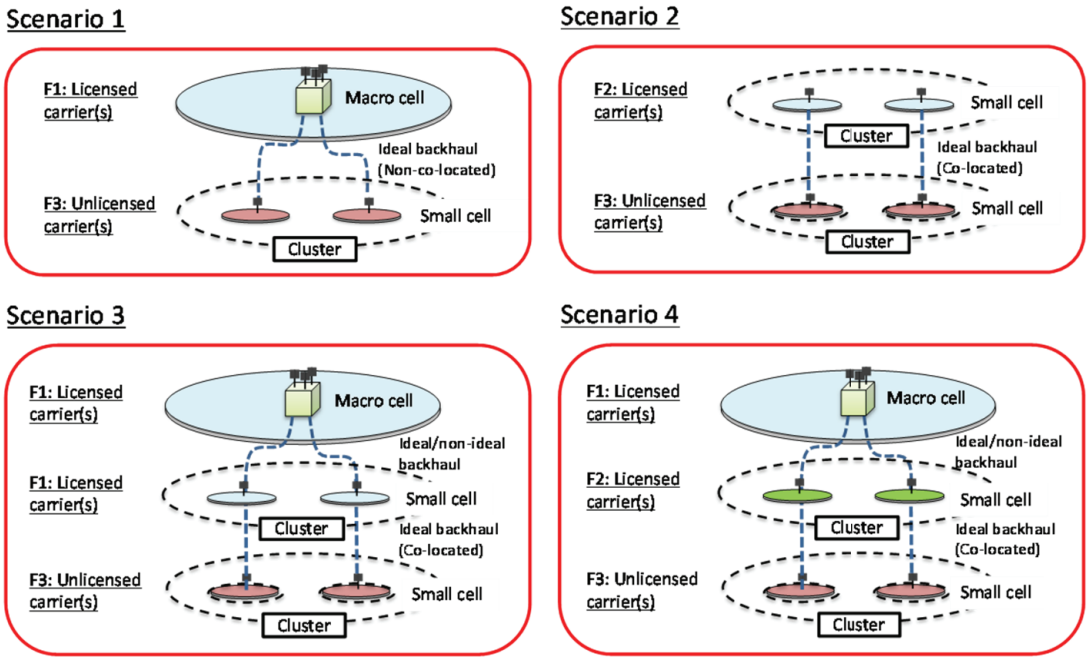

Figure 2.8: Four LTE-LAA deployment scenarios designed by 3GPP: a) scenario 1: carrier aggregation between licensed macro cell (F1) and unlicensed SC (F3); b) scenario 2: carrier aggregation between licensed SC (F2) and unlicensed SC (F3) without macro cell coverage; 3) scenario 3: licensed macro cell and SC (F1), with carrier aggregation between licensed SC (F1) and unlicensed SC (F3); 4) scenario 4: carrier aggregation between licensed macro cell (F1), licensed SC (F2) and unlicensed SC (F3) if there is ideal backhaul among macro cell and SC.

of non-backwards compatible features should be justified by sufficient gains. In another word, backward compatibility will be an important factor for distinguishing scenarios of deployment if the signal to/from an SC node is not strong to some extent.

2.6.2 Representative Deployment Scenarios

LTE-LAA Deployment Scenarios Designed by 3GPP

In an SC deployment, multiple scenarios are possible. The scenarios that 3GPP TR 36.889 envisages are shown in Fig. 2.8, and all include an LTE-LAA SC [142].

In the first scenario, the PCell is the Macro cell, and the LTE-LAA SC is not co-located, but linked to the Macro cell with ideal backhaul. In the other three scenarios, the LTE unlicensed cell is always co-located with a licensed SC, with the SC or the Macro cell acting as the primary carrier. The second scenario is most likely used in indoor environments. The choice of deployment scenario depends on the operators' strategy for

SCs and the availability of ideal backhaul.

By consolidating scene classification mentioned in the previous subsection, I concentrate on the following three representative scenarios of LTE-LAA and/or Wi-Fi deployment.

Office or CBD Buildings

A potential traffic offloading indoor environment is a multi-floor and multi-room office or Central Business District (CBD) building, where Wi-Fi APs and/or LTE-LAA BSs are set up for indoor coverage only. In each floor, a single floor/multi-room indoor scenario, adopted by both 3GPP and IEEE as a realistic scenario to represent residential and small office uncoordinated deployments, can be used for reference as illustrated in Fig. 2.9 [112]. Each floor consists of 2 rows of 10 rooms, each measuring 10m $\times$ 10m $\times$ 3m. The cross-floor signal needs to be calculated as well. Whether overlaid Macro cell(s) should be considered is decided by the Macro cell transmission power and features of the building structure, e.g., transmission loss condition of the external wall of building. As shown in Fig. 2.9, the outdoor coverage is ensured by setting up distributed antenna systems on the ground and directional antennas on the rooftop to cover high floors [165–167].

Public Establishments

Wi-Fi and/or LTE-LAA hotspots may be found in public establishments such as park, garden and coffee shops in many developed urban areas. In this situation, clustered Wi-Fi APs and LTE-LAA STAs are set up for outdoor coverage with overlaid Macro cell(s). All cells are distributed within a cluster in each Macro area. For closely located cells of different operators, additional minimum distance requirement is needed [168].

High Capacity Venues

High capacity venues refer to those scenarios with high dense users. In this case, with overlaid Macro cell(s), Wi-Fi APs are set up for indoor coverage, while LTE-LAA BSs are set up for indoor coverage. The stadium and train station are two typical examples of high capacity venues. Since UEs under those occasions are non-uniformly distributed, it is necessary to design the deployment of LTE-LAA STAs and Wi-Fi APs carefully to guarantee users coverage.

2.6.3 An Example of Scenario-oriented Coexistence Design with Representative Performance Evaluation Metrics and Scenarios

In this subsection I introduce a scenario-oriented decision-making procedure for the coexistence issue.

Scenario-oriented Coexistence Design

A prerequisite issue is whether or not the coexistence of the two technologies in the same unlicensed band is necessarily required. As far as the two aspects of this option are concerned, if the coexistence is inevitable, relevant coexistence mechanisms and parameters should be determined based on the specific scenario so as to settle the coexistence down. On the contrary, if there is no coexistence requirement, in view of the fact that LTE-LAA and Wi-Fi have their own benefits respectively, a question which technology should be chosen for the wireless communication also depends on various scenarios. That is to say, it is the particular scenario that makes sense while operators are considering how to deploy different technologies in 5 GHz UNII band no matter whether to take coexistence issue into account. In the very beginning of consideration for scenario-oriented coexistence, operators should determine whether the coexistence is certainly an uncontroversial choice. If the answer is NO, the feature of current deploying scenario can help choose either LTE-LAA or Wi-Fi. If operators are facing an answer of YES, they can also optimize coexistence mechanisms and parameters according to the communication traffic map of actual scenarios. For the convenience of understanding towards this kind of practical coexistence design, Fig. 2.10 is introduced to show a multi-floor and multi-room building with no Macro coverage, consisting of two sketches demonstrating the SC deployment plan in a single floor before and after optimization, respectively, as well as signal level traffic maps for both of a single floor and a multiple floor building.

Particularly, an analysis on the local communication traffic map is the essence of performance evaluation throughout the whole coexistence design process. In the example shown in Fig. 2.10, indoor co-floor and cross floor signal can be predicted with the help of an algorithm of environment modeling combined with radio propagation modeling. By executing the simulation and utilizing the prediction results of signal transmission, which could be calibrated with measurement data to ensure accuracy, the performance of LTE-LAA and/or Wi-Fi in this scenario can be evaluated correctly to a great extent.

To observe the details, for example, the simulation baseline or the first case is the

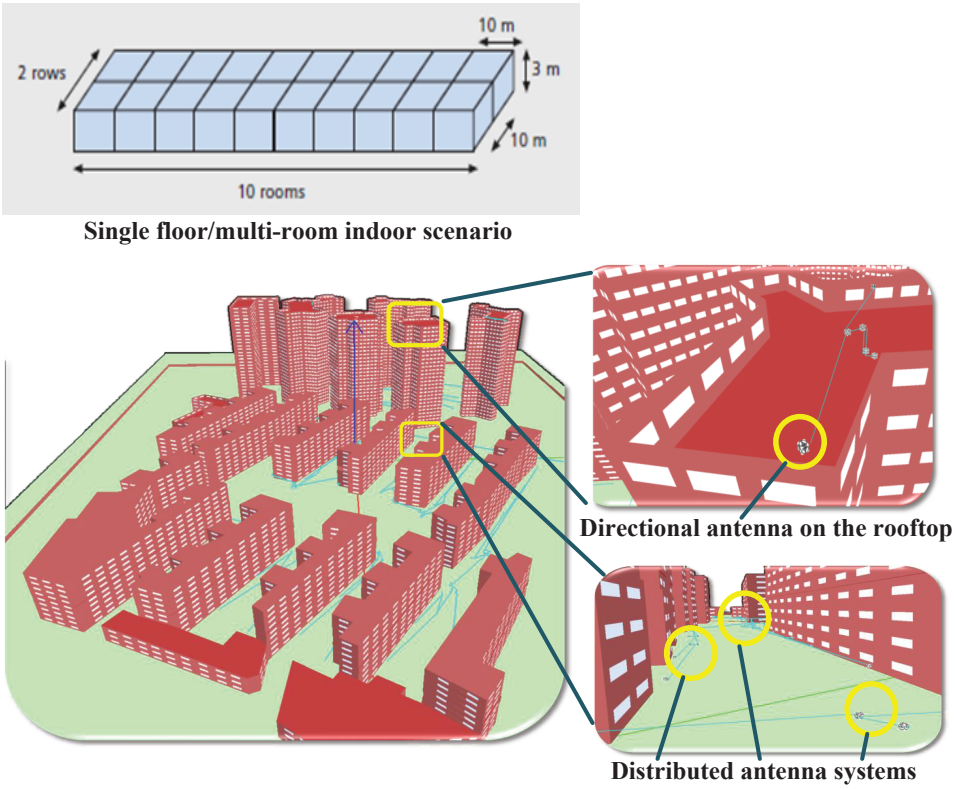

Figure 2.9: Office or CBD buildings.

one where all APs within a hotspot comply with Wi-Fi 802.11ac. The second case is a mixture of two groups with a specific coexistence mechanism, where one group is Wi-Fi and the other is LTE-LAA. In the third case, all Wi-Fi APs in the baseline are replaced by LTE-LAA nodes. The performance comparison of the two technologies among those three cases can help the operator determine whether considering the coexistence issue is the best choice before making further efforts. If the answer is 'NO', key factors of performance difference between LTE and Wi-Fi discussed before can assist the operator in choosing his/her favorite technology, i.e., either Wi-Fi or LTE-LAA. If the answer is in the affirmative, the performance of the whole system can be further optimized by adjusting one or more simulation parameters. The shadow of LTE-LAA interference on Wi-Fi can be shifted by several elements defined by [169]. For instance, it is concluded that LTE-LAA with smaller bandwidths may cause severe performance degradation of Wi-Fi. There is another fact that blocking LOS between LTE-LAA and Wi-Fi links can effectively decrease the impact of interference. Special care is thus required while simulating the coexistence channel model and designing mechanisms for channel/bandwidth selection. Moreover, multiple optimization methods shown in Fig. 2.10, e.g., adjusting

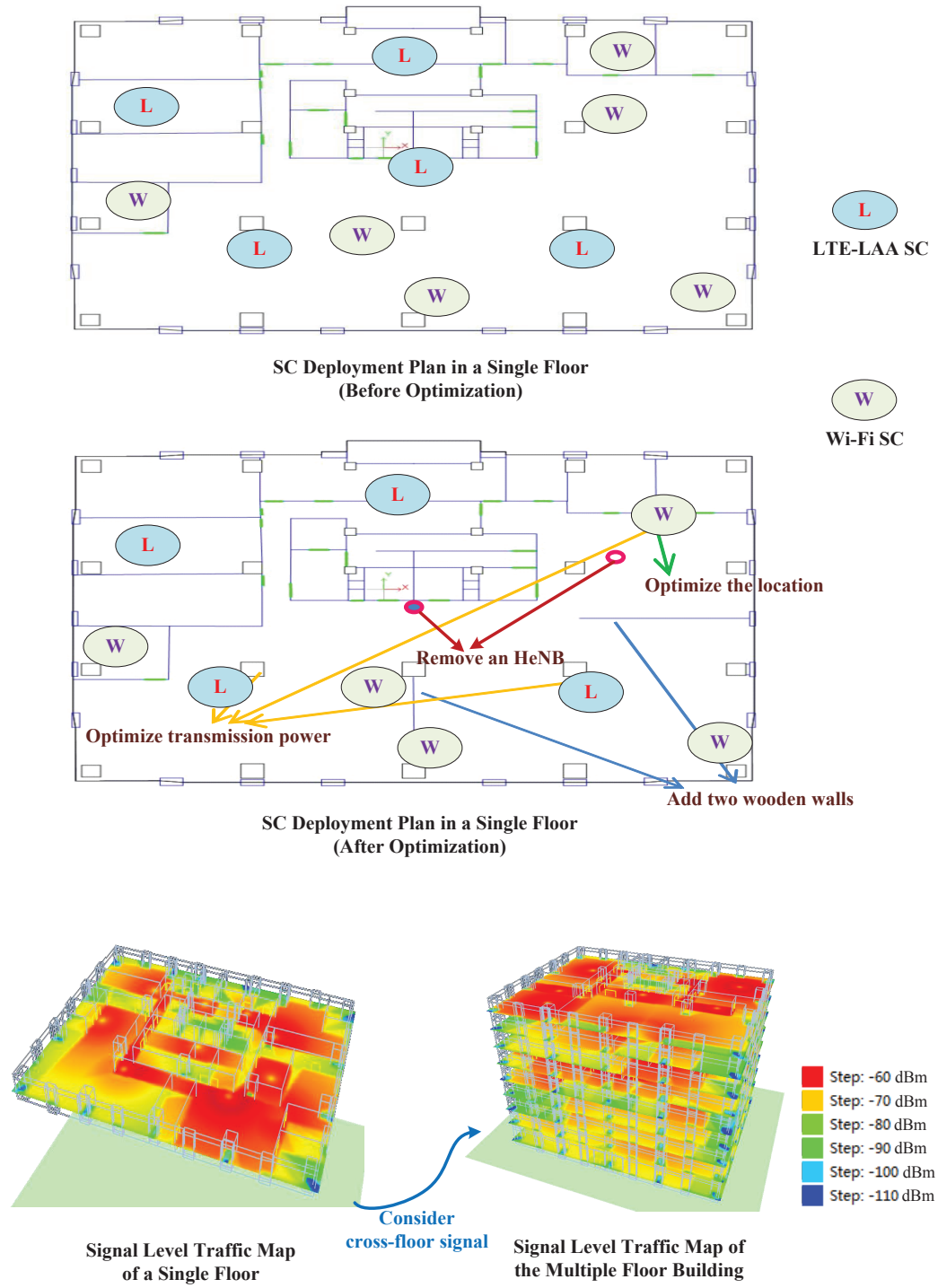

Figure 2.10: Scenario-oriented coexistence design for a realistic scenario.

locations of SCs, optimizing the transmission power of some HeNBs to reduce interference, adding walls for better interference isolation and removing unnecessarily deployed SCs, etc., can be used to improve the performance of indoor cells [170].

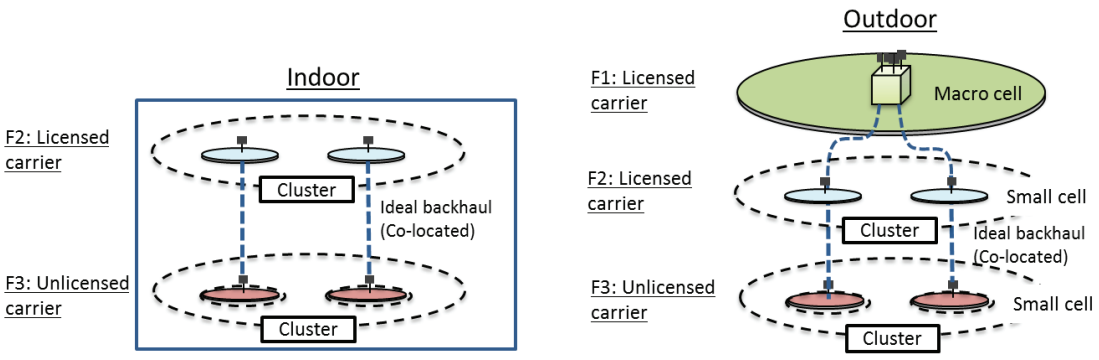

Figure 2.11: Two performance evaluation scenarios designed by 3GPP: a)indoor scenario; b) outdoor scenario, where the licensed carriers for the SC and macro cell are different.

Representative Performance Evaluation Scenarios

In this section, both indoor and outdoor scenarios for coexistence evaluations designed by 3GPP are discussed [142]. As shown in Fig. 2.11, the licensed carrier for the SCs is different with that for Macro cell in the outdoor scenario. Performance of user(s) attached to the Macro layer is not evaluated. More than one carrier can be considered for the unlicensed carrier. It should be noted that the evaluation scenarios designed by 3GPP do not restrict the design of target scenario for LTE-LAA. In the LTE and Wi-Fi coexistence case, in the first step, performance metrics for two Wi-Fi networks coexisting in a given evaluation scenario need to be evaluated and recorded. Then, in the second step, Wi-Fi is replaced with LTE-LAA for the group of eNBs and users served by one of the Wi-Fi operators. Performance metrics of the Wi-Fi network coexisting with the LTE-LAA network need to be evaluated and recorded too. A comparison of the performance metrics between two steps can be used to evaluate coexistence between LAA and Wi-Fi in an unlicensed band.

Recommended Performance Evaluation Metrics

The performance should be judged from different angles [171]. The most common criterion is the user throughput, which refers to the number of packets received for each LTE/Wi-Fi node during whole simulation time. The transmission success rate is also worth considering. The Signal to Interference plus Noise Ratio (SINR), Wi-Fi listen mode, as well as Wi-Fi transmit/receive mode also make sense. More researches are urgently needed on summarizing assessment techniques. The following typical metrics recommended by the community may be considered for coexistence performance eval-

uation in testing or simulation [7, 142, 148]:

a) **SINR:** The SINR of user m associated to SC x is appropriately written as:

$$SINR_m^k = \frac{P^{WiFi}(L_{m,x})^{-1}}{N_0 + \sum_{y \epsilon A_y^j} P^{WiFi}(L_{m,y})^{-1} + \sum_{y \epsilon B_y^j} P^{LAA}(L_{m,y})^{-1}}, \tag{2.1}$$

where $A_y^j = A^j \setminus A_x^j$, where A^j is the set of all Wi-Fi SCs transmitting on channel j and A_x^j is the contention domain of SC x. Similarly, $B_y^j = B^j \setminus B_x^j$, where B^j is the set of all LTE-LAA SCs transmitting on channel j and B_x^j is the contention domain of SC x. N_0 is the noise power. k can be LTE-LAA or Wi-Fi.

b) **User throughput:** It refers to the data rate over the time from the packet arrival to delivery during the interval divided by the interval period. The number of served bits of an unfinished file by the end of the simulation is divided by the served time. In actual operation, user throughput is the average of all its file throughputs. The interval periods recommended by [148] is to be at least 500 ms. We could further calculate the throughput of user m associated with SC x as:

$$R_m^k = \frac{1}{\left|A_x^j\right| + \left|B_x^j\right|} \rho_k(SINR_m^k), \tag{2.2}$$

where ρ_k is the auto-rate function specified in the IEEE 802.11ac standard.

c) **Latency:** Latency is defined as a time interval between time one and two, i.e., when a packet arrives at the entry point on the source until it is successfully delivered at the exit point on the destination. Latency is measured at the top of the MAC for simulation, but can be measured higher in the network stack for device studies. It is recommended that the number of users with the latency greater than 50 ms should be reported [142]. Due to practical limitations, it may only be possible to measure packet-by-packet latency for a few seconds. In such cases, the latency metric shall be measured for the longest duration.

d) **Average buffer occupancy:** Packet arrival rate for the measured buffer occupancy of the non-replaced Wi-Fi network in Wi-Fi and Wi-Fi coexistence scenario is used as the packet arrival rate in Wi-Fi and LTE-LAA coexistence evaluations.

e) **Loading on unlicensed layer:** Let $q_{m,x,h,t}$ be the size of the queue for the user m connected to the SC x for the operator h (h=1 or 2) at time t. Loading over the

unlicensed layer per SC can be defined as:

$$L_{x,h} = \frac{\sum_t 1(\sum_{m \epsilon \Omega} q_{m,x,h,t} > 0)}{T}, \tag{2.3}$$

where $1(.)$ is the indicator function, T refers to the total simulation time, and Ω is the set of users within 5 GHz coverage.

f) **Resource utilization on unlicensed layer:** Resource utilization can be defined as:

$$U_{x,h} = \frac{\sum_t 1(P_{x,h,t})}{T}, \tag{2.4}$$

where $P_{x,h,t} = 1$ if SC x of operator h is transmitting at time t over unlicensed layer (i.e., to one of the users in Ω).

g) **Packet loss:** A lost packet is defined as a packet that entered the source for transmission but was never received by the destination. The packet loss metric is calculated as a percentage of lost packets to the total packets attempted.

There are some other important metrics not captured in the current simulation and test, as well as proposed test plan, e.g. power save signalling loss and deferral. How well LTE-LAA and Wi-Fi play together in the real world will likely continue to be a point of industry contention.

Some Key Questions to Direct Future Researches in Scenario-oriented Coexistence Issue

A cooperation mechanism together with coexistence rather than a coexistence mechanism alone might become an option in future studies. Generally speaking, our suggestion is to firstly optimize the system performance based on the communication traffic map. Then, operators or even users can choose the best plan for the deployment of LTE-LAA and/or Wi-Fi in a specific scenario.

On the whole, as to the challenge of coexistence issues, a series of questions as follows could be summarized to direct future researches in this field.

1. For the purpose of performance maintenance, in which deployment scenario should either LTE-LAA or even Wi-Fi be used alone in 5 GHz UNII band without considering coexistence issue?

2. Otherwise, if coexistence is certainly needed, is it possible for the operator or the user to define the coexistence mechanisms and parameters based on the local communication traffic map?

3. On the other hand, is coexistence combined with cooperation mechanisms rather than coexistence alone a better choice to handle the interference among those different RANs?

2.7 Conclusion

For the top QoS of LTE-LAA and/or Wi-Fi in 5 GHz unlicensed band, I overviewed several key coexistence related features of the two technologies, and some key factors of performance difference between LTE and Wi-Fi. As a result, some valuable lessons have been learnt from LTE and Wi-Fi MAC comparison for the guideline of the choice of LTE-LAA and Wi-Fi. Furthermore, in section 2.3, to reach a better understanding of current consideration about the coexistence of LTE-LAA and Wi-Fi in the field of wireless communication and to evaluate the associated influence on wireless services, I first summarized the recent related works to present a stage picture of the research in the community. Coexistence mechanisms in both markets where LBT backoff mechanism is required or not have all been investigated. Meaningful lessons have been derived from different coexistence mechanisms comparison and CR, along with some important recommendations for ensuring fairness. Moreover, after summarizing eight primary influential factors for the classification of SC scenarios and concentrating on four representative scenarios of LTE-LAA and/or Wi-Fi deployment, I analyzed the whole procedure of design for an example scenario-oriented coexistence design by focusing on various coexistence schemes for different access applications. Accordingly, I further recommended performance evaluation scenarios and metrics. Besides, key challenges and research trends have all been put forward as our guidelines.

The contribution of this chapter mainly lies in a scenario-oriented decision-making procedure for the coexistence target, and recommendations related to LTE-LAA and Wi-Fi coexistence. I expect that this work could attract much more attention from the academia and industry to promote the corresponding research activities, especially future studies on cooperation-assisted coexistence mechanisms, and might provide helpful indications for deployment of LTE-LAA and/or Wi-Fi on 5 GHz UNII band.

Chapter 3

LTE-WLAN Aggregation: A Packet Level Analysis

3.1 Introduction

3.1.1 Background

One possible solution to address the increasing wireless data demand is traffic offloading from licensed Long Term Evolution (LTE) networks to the unlicensed spectrum [1]. One common approach for LTE to use the unlicensed band is to interwork with Wi-Fi. 3GPP has defined a tight interworking solution called LTE and Wi-Fi aggregation (LWA) [67] since Release 13 to support the access to both LTE and Wi-Fi networks simultaneously. LWA splits packet data convergence protocol (PDCP) packets of the same IP flow through both the LTE and Wi-Fi links, and is also able of aggregating received packets from both LTE and Wi-Fi at the user PDCP layer.

3.1.2 Main Results and Chapter Organization

The main contributions of this chapter can be summarized as follows. We investigate the effect of bursty LWA traffic on the throughput and the delay performance in an LWA-enabled network, where the LWA-mode Wi-Fi AP can simultaneously operate as the native-mode AP with the help of superposition coding. With congestion control on the LWA-mode AP, the native Wi-Fi AP not only utilizes the idle slots, but also transmits along with the LWA-mode AP by randomly accessing the channel. In this chapter, I first analyzes the characteristics of the queues at the LTE BS transmitter and the LWA-mode Wi-Fi AP transmitter. We model those queues as discrete time Markov Chains

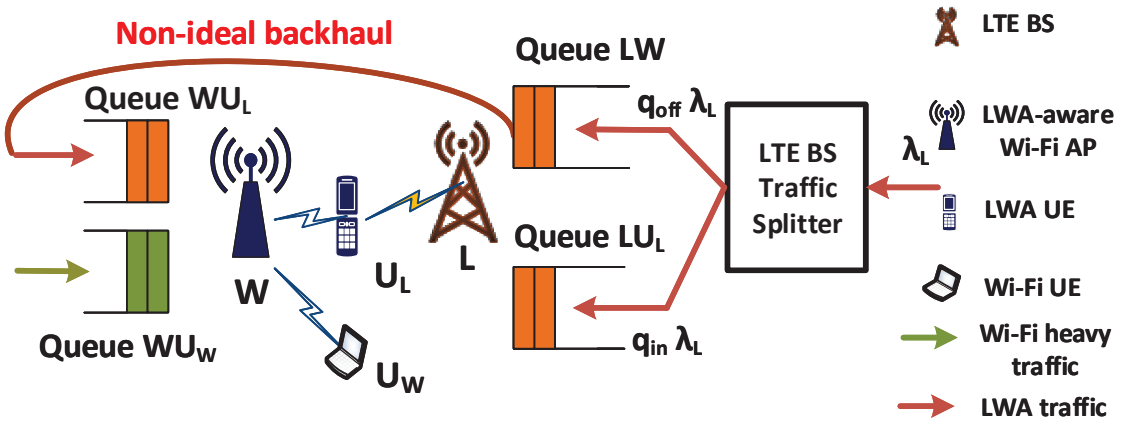

Figure 3.1: An example LWA network. LWA splits data units of the same bearer over the LTE and Wi-Fi link simultaneously. The AP W serves LWA purpose, and also operates as the native-mode Wi-Fi AP. The BS transmitter has queue LW and queue LU_L with packets intended to W and U_L, respectively. The AP transmitter has queue WU_L and queue WU_W containing the messages that are destined to U_L and U_W, respectively.

and obtain their stationary distributions. We then characterize the performance of the considered network in terms of the native Wi-Fi throughput and the LWA UE delay. More specifically, we derive the native Wi-Fi throughput and the delay of the LWA UE as functions of the native Wi-Fi AP access probability, the probability that the LWA UE chooses the LTE or Wi-Fi interface at one time slot, and the probability that an LTE packet to be routed through the LTE or the Wi-Fi link. To the best of our knowledge, similar results to this work have not been reported yet. Although our study builds on a simple network with four nodes (i.e., one LTE BS, one Wi-Fi AP, one LWA UE and one native Wi-Fi UE), the analysis can be used for further investigations in larger topologies.

The rest of this chapter is organized as follows. In Section 3.2, we present the considered system model including the network model, the physical layer model and the priority based Wi-Fi transmission scheme. In Section 3.3 and Section 3.4, we include the analysis for the queues, and show how to derive the LWA UE delay and the native Wi-Fi network throughput. Then we provide numerical evaluation of the presented results in Section 3.5. Finally we conclude this chapter in Section 3.6.

Table 3.1: Formulation symbols.

Probability	Explanation
q_{in}	probability that a packet generated at L to be routed through the LTE link
q_{off}	probability that a packet generated at L to be routed through the Wi-Fi link
$q_{\text{U}_L,\text{L}}$	probability that U_L chooses the LTE interface
$q_{\text{U}_L,\text{W}}$	probability that U_L chooses the Wi-Fi interface
$q_{\text{W, W}}$	probability that the native-mode Wi-Fi AP accesses the channel

3.2 System Model

3.2.1 Network Model

As shown in Fig. 3.1, we consider a scenario with one LTE BS and one Wi-Fi AP. The BS and the AP operate in different frequency bands, therefore there is no interference between them. We denote with L and W the BS and the AP, respectively. Packet traffic originates from L and W. In this work, we assume slotted time and the transmission of a packet requires one time slot. The ACKs are received instantaneously and error-free. The packet arrival processes at L are assumed to be Bernoulli with arrival rates λ_L. Note L and W are connected via a wireless non-ideal backhaul, which is used to offload packets from LTE to Wi-Fi. When a packet is generated at L, it has probability q_{in} to be routed through the LTE link, and q_{off} to be offloaded to W through the backhaul. To avoid the in-band interference, we further assume that the BS operates on 2.4 GHz to transmit packets through the LTE link, and offloads packets to W using the 3.5 GHz band. The BS has two different queues with packets intended for different receivers. Specifically, queue LW and queue LU_L contain packets generated at L, which are transmitted through Wi-Fi and LTE, respectively. Remark that the arrival rate at each queue denotes the probability of a new packet arrival in a time slot without accounting for the packets that are already in the queue. Obvious, the packets that enter LW and LU_L form two Bernoulli processes with arrival rates $\lambda_{LW} = q_{\text{off}}\lambda_L$ and $\lambda_{LU_L} = q_{\text{in}}\lambda_L$, respectively.

The AP can work in two modes. On the one hand, it can assist L's transmissions by keeping the offloaded packets in its queue WU_L, and trying to transmit them to the LWA UE in a later time slot. It is obvious that the packets enter WU_L form a Bernoulli process with arrival rates $\lambda_{WU_L} = \lambda_{LW}$. Note U_L is equipped with both LTE and Wi-Fi receivers, such like the current smartphone, and has the capability to aggregate traffic over L and W serving the LWA purpose. On each time slot, U_L may access either LTE or Wi-Fi access or both, and thus is assumed to have two options for receptions:

1. Both LTE and Wi-Fi receivers are activated, i.e., U_L can receive packets through both interfaces simultaneously.

2. UE U_L chooses randomly the LTE or the Wi-Fi receiver on each time slot.

Denote by $q_{\mathrm{U}_L,\mathrm{L}}$ and $q_{\mathrm{U}_L,\mathrm{W}}$ the probability that U_L chooses the LTE and Wi-Fi interface on each time slot, respectively. For the first case, $q_{\mathrm{U}_L,\mathrm{L}} = q_{\mathrm{U}_L,\mathrm{W}} = 1$. For the second case, $q_{\mathrm{U}_L,\mathrm{L}} + q_{\mathrm{U}_L,\mathrm{W}} = 1$.

On the other hand, W also has its own messages to transmit, and has the queue denoted by WU_W containing the packets destined to the native Wi-Fi UE, which can be served by W only. In this chapter, queue WU_W is saturated, i.e., has unlimited buffer size. In the later section, we will study the delay performance for U_L when U_W is under heavy traffic conditions. This is also a way to measure an upper bound for the delay faced by U_L.

3.2.2 Priority Based Wi-Fi Transmission Scheme

As illustrated in Fig. 3.2, a priority-based Wi-Fi transmission scheme is considered in this paper. Specifically, whether the native-mode Wi-Fi AP will access the channel depends on the size of WU_L, such that the native-mode Wi-Fi AP will not deteriorate the performance of the LWA-mode AP. Denote by Q_i the queue size of queue $i \in \{LW, LU_L, WU_L, WU_W\}$, measured in number of packets. Note that one packet can only appear in only one queue. We introduce a threshold M, which plays the role of a congestion limit for WU_L, and the activity of the native-mode and LWA-mode AP in a time slot are controlled in the following cases:

1. When $Q_{WU_L} = 0$, the LWA-mode AP has no packet to transmit, thus remains silent. In such case, the native-mode AP transmits a packet to U_W with probability 1.

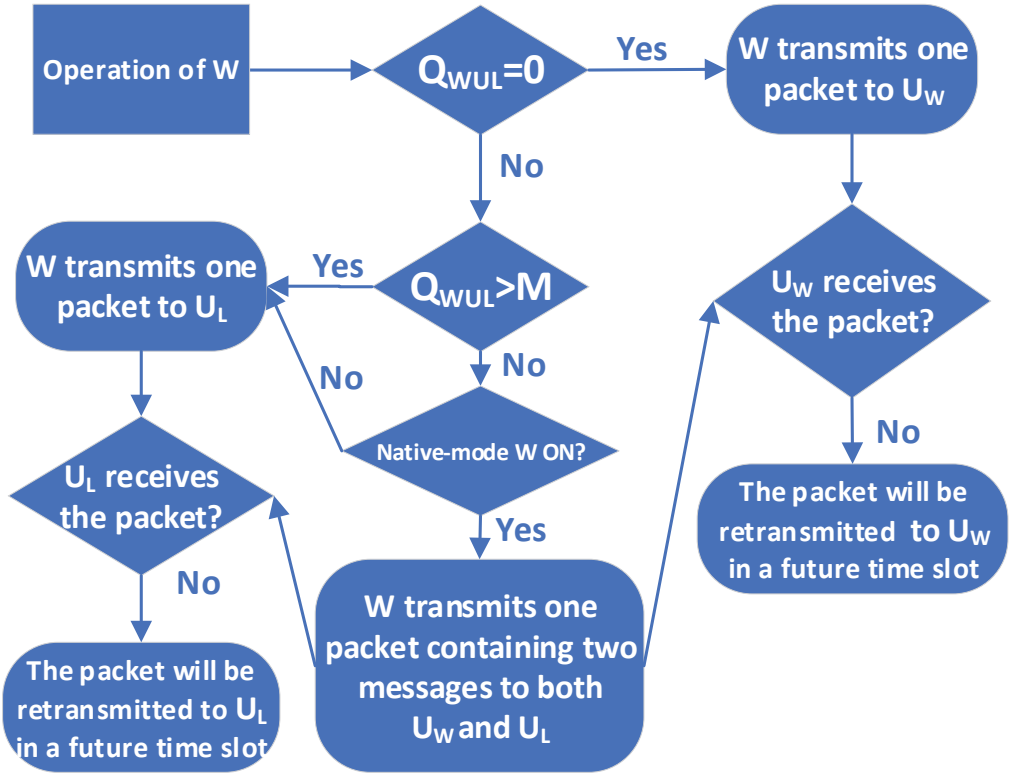

Figure 3.2: The operation of W in the described protocol.

2. When $1 \leqslant Q_{WU_L} \leqslant M$, the LWA-mode AP transmits one packet, and the native Wi-Fi AP accesses the channel with probability $q_{\mathrm{W,\,W}}$.

3. When $Q_{WU_L} > M$, the LWA-mode AP transmits one packet to U_L, and the native-mode AP remains silent.

For the second case, when WU_L and WU_W are not empty, the Wi-Fi AP will adopt the superposition coding scheme. More specifically, in this chapter, the AP can transmit one packet containing two messages, intended for the LWA UE and the native-mode Wi-Fi UE, respectively. We consider a decoding strategy where the UE with the better channel applies successive decoding and the other one treats interference as noise. We assume that the channel from W to U_L is better than that to U_W. The LWA UE decodes first the message intended for the native Wi-Fi UE, then subtracts it from the received signal. After that, U_L proceeds to decode its own message. The native Wi-Fi UE decodes its packets treating the superimposed additional layer just as noise. For more information about how to deploy the superposition coding method in Wi-Fi networks, refer to [70, 71].

Given a set of non-empty queues denoted by $\mathcal{T}$, let $\mathcal{S}_{j/\mathcal{T}}$ denote the event that UE j successfully decodes the packet transmitted from the queue that contains packets intended for j. For example, $\mathcal{S}_{U_W/WU_L,WU_W}$ refers to the event that UE U_W can decode the packet(s) from queue WU_W when both WU_L and WU_W are not empty, i.e., $\mathcal{T} = \{WU_L, WU_W\}$. Let $\mathcal{P}(\mathcal{B})$ represent the probability of occurrence of the event $\mathcal{B}$. It is reasonable to assume that no matter what the detection mechanism is, we always have $\mathcal{P}(\mathcal{S}_{U_W/WU_L,WU_W}) \leqslant \mathcal{P}(\mathcal{S}_{U_W/WU_W})$ and $\mathcal{P}(\mathcal{S}_{U_L/WU_L,WU_W}) \leqslant \mathcal{P}(\mathcal{S}_{U_L/WU_L})$.

In general, our scheme can be regarded as an extension of the Aloha random access scheme. We assume that there exists a coordinator, which exchange the information between the native-mode and LWA-mode AP. The coordinator also broadcasts the respective activity of the native-mode and LWA-mode AP depending on the queue size of WU_L. Although the exchange of information will introduce extra overhead to the LWA system operation, the proposed scheme is more flexible, and provides lower signaling overhead compared to fully centralized scheduling.

3.2.3 Physical Layer Model

The physical model is a generalized form of the packet erasure model. To be more clear, for the wireless link, a packet can be decoded correctly by the receiver if the signal-to-noise ratio (SNR) exceeds a prescribed threshold. Denote by p_{LW}, p_{LU_L}, p_{WU_L} and p_{WU_W} the success probability of the link $L \to W$, $L \to U_L$, $W \to U_L$ and $W \to U_W$, respectively. We consider the success probability of each link $k \to j$ based on its SNR, which can be represented as

$$\text{SNR}_{kj} = \frac{P_{kj}|h_{kj}|^2 d_{kj}^{-\alpha}}{\sigma^2}, \tag{3.1}$$

where P_{kj} denotes the transmission power of node k while serving j; h_{kj} refers to the small-scale channel fading from the transmitter k to the receiver j, which follows Rayleigh fading; σ^2 is the noise power; Here we assume a standard distance-dependent power law pass loss attenuation $d_{kj}^{-\alpha}$, where d_{kj} denotes the distance from the transmitter k to the receiver j, and α with $\alpha > 2$ refers to the pathloss exponent. A packet transmitted by i is successfully received by j if and only if $\text{SNR}_{kj} \geqslant \gamma_j$, where γ_j is the threshold regarding the transmission to node j. Denote p_{kj} as the success probability of

link $k \to j$, which can be represented as

$$p_{kj} = \mathcal{P}\{\mathrm{SNR}_{kj} \geqslant \gamma_j\} = \exp\left(-\frac{\gamma_j d_{kj}^{\alpha} \sigma^2}{P_{kj}}\right). \tag{3.2}$$

3.3 Network Performance Metrics

In this section, we define several relevant metrics for the performance evaluation of the considered LWA-enabled network with the priority based Wi-Fi transmission scheme.

3.3.1 Service Probability for the Queues

The service probability with a given SNR target can be defined as the probability of a successful packet transmission per time slot. The service probability for queue LU_L is

$$\mu_{LU_L} = q_{\mathrm{U}_L,\mathrm{L}} \cdot p_{\mathrm{LU}_L}. \tag{3.3}$$

Similarly, for queue LW, the service rate is represented as

$$\mu_{LW} = p_{\mathrm{LW}}. \tag{3.4}$$

In the following, we will show how to compute the service rate for queue WU_L and queue WU_W, respectively, depending on the value of Q_{WU_L}.

1. When $Q_{WU_L} = 0$, AP W has no data to transmit to U_L. In such case, the service rate seen at queue WU_W is

$$\mu_{WU_W,1} = \mathcal{P}(\mathcal{S}_{U_W/WU_W}). \tag{3.5}$$

   It is obvious that $\mathcal{P}(\mathcal{S}_{U_W/WU_W}) = p_{WU_W}$ holds.

2. When $1 \leqslant Q_{WU_L} \leqslant M$, the service rate seen at queue WU_W and queue WU_L are given by

$$\mu_{WU_W,2} = q_{\mathrm{w,w}} \cdot \mathcal{P}(\mathcal{S}_{U_W/WU_L,WU_W}), \tag{3.6}$$

$$\begin{aligned}\mu_{WU_L,1} = {} & (1 - q_{\mathrm{w,w}}) \cdot q_{\mathrm{U}_L,\mathrm{w}} \cdot \mathcal{P}(\mathcal{S}_{U_L/WU_L}) \\ & + q_{\mathrm{w,w}} \cdot q_{\mathrm{U}_L,\mathrm{w}} \cdot \mathcal{P}(\mathcal{S}_{U_L/WU_L,WU_W}).\end{aligned} \tag{3.7}$$

   Obviously, we have $\mathcal{P}(\mathcal{S}_{U_W/WU_W}) = p_{WU_W}$. In order to compute (3.6) and (3.7), we need to derive $\mathcal{P}(\mathcal{S}_{U_L/WU_L,WU_W})$ and $\mathcal{P}(\mathcal{S}_{U_W/WU_L,WU_W})$ first. Take the event

$\mathcal{S}_{U_L/WU_L,WU_W}$ for example. Remark that since WU_W is saturated, $Q_{WU_W} > 0$ always holds. The $\mathcal{S}_{U_L/WU_L,WU_W}$ is feasible when the received signal-to-interference-plus-noise ratio (SINR) is above a threshold γ_{U_L} and can be expressed by

$$\mathcal{S}_{U_L/WU_L,WU_W} = \left\{ \frac{P_{WU_L}|h_{WU_L}|^2 d_{WU_L}^{-\alpha}}{1 + P_{WU_W}|h_{WU_L}|^2 d_{WU_L}^{-\alpha}} \geqslant \gamma_{U_L} \right\}. \tag{3.8}$$

Remark that we consider a decoding strategy where the UE with the better channel (i.e., U_L) applies successive decoding and the other one (i.e., U_W) treats the message of U_L as noise. By (18) in [172], when $P_{WU_W} > P_{WU_L}\frac{\gamma_{U_W}(1+\gamma_{U_L})}{\gamma_{U_L}}$, we have

$$\mathcal{P}(\mathcal{S}_{U_L/WU_L,WU_W}) = \mathcal{P}(\mathcal{S}_{U_L/WU_L}) = \exp\left(- \frac{\gamma_{U_L} d_{WU_L}^{\alpha}}{P_{WU_L}} \right). \tag{3.9}$$

Otherwise, when $\gamma_{U_W} P_{WU_L} < P_{WU_W} \leqslant P_{WU_L}\frac{\gamma_{U_W}(1+\gamma_{U_L})}{\gamma_{U_L}}$, the following equation holds.

$$\mathcal{P}(\mathcal{S}_{U_L/WU_L,WU_W}) = \exp\left(- \frac{\gamma_{U_W} d_{WU_L}^{\alpha}}{P_{WU_W} - \gamma_{U_W} P_{WU_L}} \right). \tag{3.10}$$

By (15) in [172], the probability $\mathcal{P}(\mathcal{S}_{U_W/WU_L,WU_W})$ can be derived by

$$\begin{aligned} &\mathcal{P}(\mathcal{S}_{U_W/WU_L,WU_W}) = \\ &\mathbb{1}\{P_{WU_W} > \gamma_{U_W} P_{WU_L}\} \exp\left(- \frac{\gamma_{U_W} d_{WU_W}^{\alpha}}{P_{WU_W} - \gamma_{U_W} P_{WU_L}} \right). \end{aligned} \tag{3.11}$$

For the sake of simplicity, in the reminder of this chapter, we assume that $\gamma_{U_W} P_{WU_L} < P_{WU_W} \leqslant P_{WU_L}\frac{\gamma_{U_W}(1+\gamma_{U_L})}{\gamma_{U_L}}$ always holds.

3. When $Q_{WU_L} > M$, the service rate seen at queue WU_L can be represented by

$$\mu_{WU_L,2} = q_{\mathrm{U_L,W}} \cdot \mathcal{P}(\mathcal{S}_{U_L/WU_L}). \tag{3.12}$$

Remark that by definition, the service probability for WU_W only accounts for the case with $Q_{WU_L} \leqslant M$.

In summary, when the RS scheme is adopted, the average service rate seen at queue WU_L is given by

$$\bar{\mu}_{WU_L} = \frac{T_{WU_L}}{\mathcal{P}(1 \leqslant Q_{WU_L} \leqslant M) + \mathcal{P}(Q_{WU_L} > M)}, \tag{3.13}$$

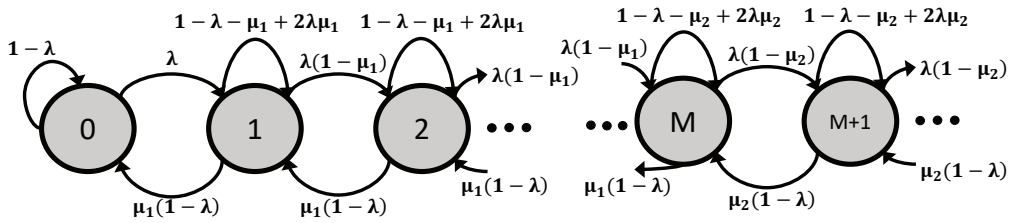

Figure 3.3: The Discrete Time Markov Chain which models the i-th queue evolution ($i \in \{LU_L, LW, WU_L\}$). When $i \in \{LU_L, LW\}$, $M \to \infty$ holds.

where

$$\begin{aligned} T_{WU_L} =& \mathcal{P}(1 \leqslant Q_{WU_L} \leqslant M) \cdot \mu_{WU_L,1} \\ &+ \mathcal{P}(Q_{WU_L} > M) \cdot \mu_{WU_L,2}. \end{aligned} \tag{3.14}$$

3.3.2 Native Wi-Fi throughput

For the considered shared access Wi-Fi networks, we aim at evaluating the throughput of the native Wi-Fi network, abbreviated as native Wi-Fi throughput, denoted by T_{WU_W}, which can be represented as

$$\begin{aligned} T_{WU_W} =& \mathcal{P}(Q_{WU_L} = 0) \cdot \mu_{WU_W,1} \\ &+ \mathcal{P}(1 \leqslant Q_{WU_L} \leqslant M) \cdot \mu_{WU_W,2}. \end{aligned} \tag{3.15}$$

3.3.3 LWA UE Delay

The delay experienced by the LWA UE is a critical metric for the performance of the LWA system with delay-sensitive applications. As mentioned before, we focus on the delay experienced by U_L when traffic at Wi-Fi UE U_W is heavy. To be more specific, denote by $\bar{D}$ the average delay per packet at UE U_L under heavy Wi-Fi traffic. The delay $\bar{D}$ is constitutive of LTE link delay and Wi-Fi link delay, denoted by $\bar{D}_L$ and $\bar{D}_W$, respectively. Thus the formal definition of D is

$$\bar{D} = q_{\text{in}}\bar{D}_L + q_{\text{off}}\bar{D}_W, \tag{3.16}$$

where D_L can be represented as

$$\bar{D}_L = D_{LU_L}. \tag{3.17}$$

D_W equals to the sum of delay at queue LW and WU_L. Denote by D_i the average delay at queue i ($i \in \{LW, LU_L, WU_L, WU_W\}$) per packet, thus we have

$$\bar{D}_W = D_{LW} + D_{WU_L}. \tag{3.18}$$

Note that D_i ($i \in \{LU_L, WU_L, WU_W, LW\}$) consists of the queueing delay and the transmission delay. From Little's law [173], we obtain the queueing delay that is related to the average queue size per packet arrival. The transmission delay is inversely proportional to the service rate. In general, the following equation holds.

$$D_i = \frac{\bar{Q}_i}{\lambda_i} + \frac{1}{\bar{\mu}_i}, i \in \{LU_L, WU_L, WU_W, LW\}, \tag{3.19}$$

where $\bar{Q}_i$ and $\bar{\mu}_i$ are the average queue size and the average service probability of the i-th queue, respectively.

3.4 Analysis of Native Wi-FI Network Throughput and LWA UE Delay

By the definition of the metrics proposed in Section 3.3, the delay seen at U_L depends on $\bar{Q}_{WU_L}$, $\bar{Q}_{LW}$ and $\bar{Q}_{LU_L}$. In addition, native Wi-Fi throughput depends on the state of the queue size of queue WU_L. In this section, we first derive $\mathcal{P}(Q_i = 0)$ and $\mathcal{P}(1 \leqslant Q_i \leqslant M)$ ($i \in \{LU_L, LW, WU_L\}$). Then the average queue size of LU_L, LW and WU_L will be analyzed. After that, we will derive T_{WU_W} and $\bar{D}$.

3.4.1 Analysis of the Queues

We first provide the definition of queue stability.

Definition 1. *Denote by Q_i^t the length of queue i at the beginning of time slot t. The queue is said to be stable if $\lim_{t\to 0} \mathcal{P}(Q_i^t < x) = F(x)$ and $\lim_{x\to\infty} F(x) = 1$.*

Although we will not make explicit use of this definition, here we take advantage of its corollary, namely Loynes' theorem [174], which states that if the average arrival rate is less than the average service rate, the queue will be stable. Otherwise, the queue is unstable and the value of Q_i^t approaches infinity.

We model queue $i \in \{LU_L, WU_L, LW\}$ as a discrete time Markov Chain (DTMC), which describes the queue evolution and is presented in Fig. 3.3. Note that when $i \in \{LU_L, LW\}$, $M \to \infty$ always holds. In Fig. 3.3, for the sake of convenience, for queue LU_L and LW, we use λ to represent λ_i, while $\mu_1 = \mu_2 = \mu_i$. For queue WU_L, we use λ to represent λ_{WU_L}, while μ_1 refers to the service rate of queue WU_L when $1 \leqslant Q_{WU_L} \leqslant M$, and μ_2 represents the service rate of queue WU_L when $Q_{WU_L} > M$.

Each state is denoted by an integer and represents the queue size. The metrics related to the rate are measured by the average number of packets per time slot.

Denote by π the stationary distribution of the DTMC, where $\pi(m) = \mathcal{P}(Q = m)$ is the probability that the queue has m packets in its steady state. Let Q represent the queue size.

Lemma 1. *The stationary distribution of the DTMC described in Fig. 3.3 is*

1. *For* $1 \leq Q \leq M$*, we have*

$$\pi(m) = \frac{\lambda^m (1-\mu_1)^{m-1}}{(1-\lambda)^m \mu_1^m} \pi(0). \tag{3.20}$$

2. *For* $Q > M$*, we have*

$$\pi(m) = \frac{\lambda^m (1-\mu_1)^M (1-\mu_2)^{m-M-1}}{(1-\lambda)^m \mu_1^m \mu_2^{m-M}} \pi(0), \tag{3.21}$$

where $\pi(0)$ *is the probability that the queue is empty, given by*

1. *If* $\lambda \neq \mu_1$*, we have*

$$\pi(0) = \frac{(\mu_1 - \lambda)(\mu_2 - \lambda)}{\mu_1\mu_2 - \lambda\mu_1 - \lambda \left[\frac{\lambda(1-\mu_1)}{(1-\lambda)\mu_1}\right]^M (\mu_2 - \mu_1)}. \tag{3.22}$$

2. *If* $\lambda = \mu_1$*, we have*

$$\pi(0) = \frac{\mu_2 - \mu_1}{\mu_1 + (\mu_2 - \mu_1)\frac{M+1-\mu_1}{1-\mu_1}}. \tag{3.23}$$

Proof. From the DTMC described in Fig. 3.3, we obtain the following balance equations:

$$\pi(0) = \pi(0)(1-\lambda_i) + \pi(1)\mu_1(1-\lambda)$$
$$\Leftrightarrow \pi(1) = \frac{\lambda}{\mu_1(1-\lambda)}\pi(0).$$
$$\pi(1) = \pi(0)\lambda + \pi(1)(1-\lambda-\mu_1+2\lambda\mu_1) + \pi(2)\mu_1(1-\lambda)$$
$$\Leftrightarrow \pi(2) = \left(\frac{\lambda}{\mu_1(1-\lambda)}\right)^2 (1-\mu_1)\pi(0).$$

In summary, for $1 \leq Q \leq M$ we can derive (3.20), and for $Q > M$, the (3.21) follows.

In addition, we have that $\sum_{m=0}^{\infty} \pi(m) = 1$ holds. This, together with (3.20) and (3.21), shows that the (3.22) holds when $\lambda \neq \mu_1$. When $\lambda = \mu_1$, denote by $x(\lambda)$ and $y(\lambda)$ the nomination and denominator of $\pi(0)$. We can derive $\pi(0)$ as

$$\pi(0) = \lim_{\lambda \to \mu_1} \frac{x'(\lambda)}{y'(\lambda)}. \tag{3.24}$$

Then the equation (3.23) follows by applying 1'Hôpital's rule. □

Lemma 2. *The queue in Fig. 3.3 is stable if and only if $\lambda < \mu_2$ holds.*

Proof. From $\sum_{m=0}^{\infty} \pi_i(m) = 1$, the condition that the series is converging when $\lambda < \mu_2$, which is also the condition that the DTMC is an aperiodic irreducible Markov Chain, showing that the queue is stable.

In addition, the condition $0 \leqslant \pi(0) \leqslant 1$ should also be satisfied. In the following, we consider the three specific cases:

1. If $\lambda < \mu_1$, consider the equation (3.22), obviously $\pi(0) > 0$. In addition, we have the denominator $y(\lambda) > \mu_2(\mu_1 - \lambda)$, thus $\pi(0) < \frac{\mu_2 - \lambda}{\mu_2} < 1$ holds.

2. If $\lambda = \mu_1$, consider the equation (3.23), obviously $0 < \pi(0) < 1$ holds.

3. If $\mu_1 < \lambda < \mu_2$, consider the equation (3.22), obviously the nominator $x(\lambda) < 0$. we also have $\frac{\lambda(1-\mu_1)}{(1-\lambda)\mu_1} > 1$. Since both $\left(\frac{\lambda}{\mu_1}\right)^{M+1} > 1$ and $\left(\frac{1-\lambda}{1-\mu_1}\right)^{M} \cdot \frac{\mu_2 - \lambda}{\mu_2 - \mu_1} < 1$ hold, we have $y(\lambda) < 0$. Therefore $\pi(0) > 0$. Similar to the case $\lambda < \mu_1$, we still have $\pi(0) < 1$.

Therefore the conclusion that $0 < \pi(0) < 1$ always holds.

□

With Lemma 1, the probability for $1 \leqslant Q \leqslant M$ and $Q > M$ when the queue is stable can be derived as in the following theorem. For the sake of simplicity, in the rest of this work, we only consider the case where $\lambda \neq \mu_1$. The result for $\lambda = \mu_1$ can be derived in a similar way. For convenience, in the reminder of this chapter, let $\phi \triangleq \frac{\lambda(1-\mu_1)}{(1-\lambda)\mu_1}$.

Theorem 1. *When the queue in Fig. 3.3 is stable, i.e., $\lambda < \mu_2$, and $\lambda \neq \mu_1$, the following two equations hold:*

$$\mathcal{P}(1 \leqslant Q \leqslant M) = \frac{\lambda(1-\phi^M)(\mu_2 - \lambda)}{\mu_1\mu_2 - \lambda\mu_1 - \lambda\phi^M(\mu_2 - \mu_1)}. \tag{3.25}$$

$$\mathcal{P}(Q > M) = \frac{\lambda\phi^M(\mu_1 - \lambda)}{\mu_1\mu_2 - \lambda\mu_1 - \lambda\phi^M(\mu_2 - \mu_1)}. \tag{3.26}$$

Proof. By Lemma 1, when $\lambda < \mu_2$, we have

$$\begin{aligned} \mathcal{P}(1 \leq Q \leq M) =& \sum_{m=1}^{M} \pi(m) \\ =& \frac{\pi(0)}{1-\mu_1} \sum_{m=1}^{M} \phi^m = \frac{\pi(0)\lambda(1-\phi^M)}{\mu_1 - \lambda}. \end{aligned} \tag{3.27}$$

Combined with (3.22), then the (3.25) follows. In addition, since

$$\mathcal{P}(Q > M) = 1 - \sum_{m=0}^{M} \pi(m) \tag{3.28}$$

holds, the (3.26) follows. Hence the conclusion. □

Corollary 1.1. *When $M \to \infty$, $\mathcal{P}(Q \geqslant 1)$ is given by*

$$\mathcal{P}(Q \geqslant 1) = \frac{\lambda}{\mu_1}. \tag{3.29}$$

Theorem 2. *The average queue size of the queue in Fig. 3.3 is given by*

$$\bar{Q} = \frac{K_1 + K_2}{\mu_1\mu_2 - \lambda\mu_1 - \lambda\phi^M(\mu_2 - \mu_1)}, \tag{3.30}$$

where

$$K_1 = \phi^M \lambda(\mu_1 - \lambda)\left[M + \frac{(1-\lambda)\mu_2}{\mu_2 - \lambda}\right], \tag{3.31}$$

and

$$K_2 = \lambda(1-\lambda)\mu_1 \frac{\mu_2 - \lambda}{\mu_1 - \lambda}\left[M\phi^{M+1} - \phi^M(M+1) + 1\right]. \tag{3.32}$$

Proof. The average queue size of the queue is

$$\begin{aligned}
\bar{Q} &= \sum_{m=1}^{\infty} m\pi(m) = \sum_{m=1}^{M} m\pi(m) + \sum_{m=M+1}^{\infty} m\pi(m) \\
&= \sum_{m=1}^{M} m\pi(m) + \sum_{m=1}^{\infty}(M+m)\cdot\pi(M+m) \\
&= \sum_{m=1}^{M} m\pi(m) + M\sum_{m=1}^{\infty}\pi(M+m) + \sum_{m=1}^{\infty} m\pi(M+m).
\end{aligned} \tag{3.33}$$

In the following, we will show how to compute the three terms on the right side when $\lambda < \mu_2$ and $\lambda \neq \mu_1$. For the first term,

$$\begin{aligned}
\sum_{m=1}^{M} m\pi(m) &= \sum_{m=1}^{M} m\pi(0)\frac{\lambda^m(1-\mu_1)^{m-1}}{(1-\lambda)^m\mu_1^m} \\
&= \frac{\lambda\pi(0)}{\mu_1(1-\lambda)}\sum_{m=1}^{M}\phi' \\
&= \frac{\lambda\pi(0)}{\mu_1(1-\lambda)}\frac{M\phi^{M+1} - \phi^M(M+1) + 1}{(1-\phi)^2}.
\end{aligned} \tag{3.34}$$

For the second term, by (3.26), we have

$$\begin{aligned}
M\sum_{m=1}^{\infty}\pi(M+m) &= M\mathcal{P}(Q > M) \\
&= \frac{\lambda M\phi^M(\mu_1 - \lambda)}{\mu_1\mu_2 - \lambda\mu_1 - \lambda\phi^M(\mu_2 - \mu_1)}
\end{aligned} \tag{3.35}$$

For the third term, by (3.21), we have

$$\begin{aligned}\sum_{m=1}^{\infty} m\pi(M+m) &= \sum_{m=1}^{\infty} \frac{\phi^M \pi(0)\lambda}{(1-\lambda)\mu_2} \left(\left[\frac{\lambda(1-\mu_2)}{\mu_2(1-\lambda)} \right]^i \right)' \\ &= \frac{\lambda(1-\lambda)\mu_2 \frac{\mu_1-\lambda}{\mu_2-\lambda}\phi^M}{\mu_1\mu_2 - \lambda\mu_1 - \lambda\phi^M(\mu_2-\mu_1)}.\end{aligned} \tag{3.36}$$

Substituting (3.34), (3.35) and (3.36), then (3.30) follows. □

Corollary 2.1. *The average queue size of the queue in Fig. 3.3 when $M \to \infty$ is given by*

$$\bar{Q} = \frac{\lambda(1-\lambda)}{\mu_1 - \lambda}. \tag{3.37}$$

Proof. The average queue size of the queue is

$$\bar{Q} = \sum_{m=1}^{\infty} m\pi(m). \tag{3.38}$$

Combined with (3.20), we have

$$\bar{Q} = \frac{\mu_1 - \lambda}{\mu_1} \cdot \frac{\lambda}{\mu_1(1-\lambda)} \cdot \sum_{m=1}^{\infty} m \left(\frac{\lambda(1-\mu_1)}{\mu_1(1-\lambda)} \right)^{m-1}. \tag{3.39}$$

Note that $\sum_{m=1}^{\infty} m\alpha^{m-1} = \frac{1}{(1-\alpha)^2}$ holds for $\alpha < 1$. Therefore (3.37) follows. □

3.4.2 Analysis of the Native Wi-Fi Throughput

From Lemma 1, Theorem 2 and (3.15), we have

$$\begin{aligned}T_{WU_W} =& \mathcal{P}(Q_{WU_L} = 0) \cdot \mu_{WU_W,1} \\ &+ \mathcal{P}(1 \leqslant Q_{WU_L} \leqslant M) \cdot \mu_{WU_W,2} \\ =& \frac{N_1 \cdot (N_2 + N_3)}{N_4 - N_5},\end{aligned} \tag{3.40}$$

where

$$N_1 = \mu_{WU_L,2} - \lambda_{WU_L}, \tag{3.41}$$

$$N_2 = \mu_{WU_W,1}(\mu_{WU_L,1} - \lambda_{WU_L}), \tag{3.42}$$

$$N_3 = \mu_{WU_W,2}\lambda_{WU_L}(1 - \xi^M), \tag{3.43}$$

$$N_4 = \mu_{WU_L,1}(\mu_{WU_L,2} - \lambda_{WU_L}), \tag{3.44}$$

and

$$N_5 = \lambda_{WU_L}\xi^M(\mu_{WU_L,2} - \mu_{WU_L,1}). \tag{3.45}$$

The ξ is represented by

$$\xi \triangleq \frac{\lambda_{WU_L}(1-\mu_{WU_L,1})}{(1-\lambda_{WU_L})\mu_{WU_L,1}}. \tag{3.46}$$

A special case is when $M \to \infty$. In such case, by Corollary 1.1 and (3.15), the equation (3.40) can be transformed to

$$T_{WU_W} = (1-\frac{\lambda_{WU_L}}{\mu_{WU_L,1}}) \cdot \mu_{WU_W,1} + \frac{\lambda_{WU_L}}{\mu_{WU_L,1}} \cdot \mu_{WU_W,2} \tag{3.47}$$

3.4.3 Analysis of the LWA UE Delay

From Theorem 2 and Corollary 2.1, we have

$$\begin{aligned} D_{LU_L} &= \frac{\bar{Q}_{LU_L}}{\lambda_{LU_L}} + \frac{1}{\mu_{LU_L}} \\ &= \frac{1-\lambda_{LU_L}}{\mu_{LU_L}-\lambda_{LU_L}} + \frac{1}{\mu_{LU_L}}, \end{aligned} \tag{3.48}$$

$$\begin{aligned} D_{LW} &= \frac{\bar{Q}_{LW}}{\lambda_{LW}} + \frac{1}{\mu_{LU_L}} \\ &= \frac{1-\lambda_{LW}}{\mu_{LW}-\lambda_{LW}} + \frac{1}{\mu_{LW}}, \end{aligned} \tag{3.49}$$

$$\begin{aligned} D_{WU_L} &= \frac{\bar{Q}_{WU_L}}{\lambda_{WU_L}} + \frac{1}{\bar{\mu}_{WU_L}} \\ &= \frac{L_1+L_2}{L_3} + \frac{1}{\bar{\mu}_{WU_L}}, \end{aligned} \tag{3.50}$$

where

$$L_1 = \xi^M(\mu_{WU_L,1}-\lambda_{WU_L}) \left[M + \frac{(1-\lambda_{WU_L})\mu_{WU_L,2}}{\mu_{WU_L,2}-\lambda_{WU_L}} \right], \tag{3.51}$$

$$\begin{aligned} L_2 =& (1-\lambda_{WU_L})\mu_{WU_L,1}\frac{\mu_{WU_L,2}-\lambda_{WU_L}}{\mu_{WU_L,1}-\lambda_{WU_L}} \\ & \cdot \left[M\xi^{M+1} - \xi^M(M+1)+1 \right], \end{aligned} \tag{3.52}$$

$$\begin{aligned} L_3 =& \mu_{WU_L,1}\mu_{WU_L,2} - \lambda_{WU_L}\mu_{WU_L,1} \\ & - \lambda_{WU_L}\xi^M(\mu_{WU_L,2}-\mu_{WU_L,1}). \end{aligned} \tag{3.53}$$

Also, remark that $\lambda_{WU_L} \neq \mu_{WU_L,1}$, from (3.13) and the result of Theorem 1, we have

$$\bar{\mu}_{WU_L} = \frac{\mu_{WU_L,1}H_1 + \mu_{WU_L,2}H_2}{H_1+H_2}, \tag{3.54}$$

where

$$H_1 = \lambda_{WU_L}(1-\xi^M)(\mu_{WU_L,2}-\lambda_{WU_L}) \tag{3.55}$$

$$H_2 = \lambda_{WU_L}\xi^M(\mu_{WU_L,1}-\lambda_{WU_L}) \tag{3.56}$$

Table 3.2: System Parameters.

Parameters	Values
LTE link distance (d_{LU_L})	300 m
Native Wi-Fi link distance (d_{WU_W})	20 m
LWA-mode Wi-Fi link distance (d_{WU_L})	20 m
Backhaul distance (d_{LW})	200 m
Pathloss exponent (α)	4
LTE BS transmission power(P_{LU_L}, P_{LW})	200 mw
Wi-Fi AP transmission power (P_{WU_W})	20 mw
Noise power ($sigma^2$)	-113.97 dbm
SNR target (γ_j, $\forall j$)	0 dB

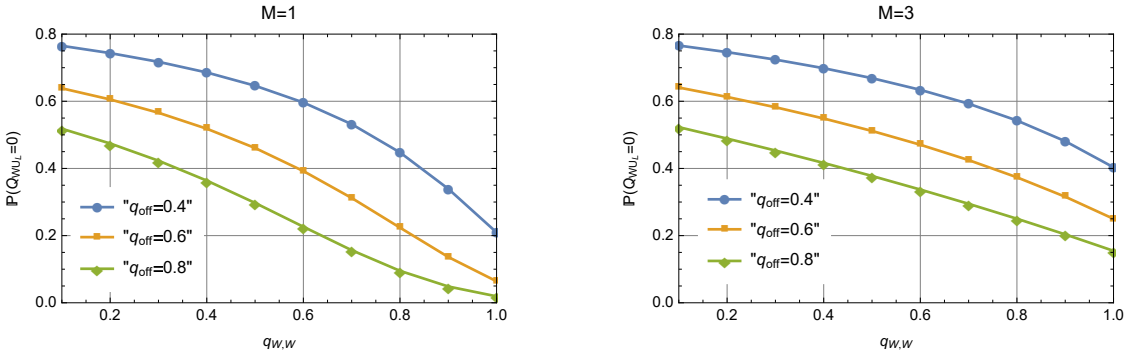

Figure 3.4: $\mathcal{P}(Q_{WU_L} = 0)$ vs. $q_{W,W}$.

Please note that when $M \to \infty$, similar to (3.48), the equation (3.50) can be transformed to

$$\begin{aligned} D_{WU_L} &= \frac{\bar{Q}_{WU_L}}{\lambda_{WU_L}} + \frac{1}{\mu_{WU_L,1}} \\ &= \frac{1 - \lambda_{WU_L}}{\mu_{WU_L,1} - \lambda_{WU_L}} + \frac{1}{\mu_{WU_L,1}}, \end{aligned} \tag{3.57}$$

Remark the LWA UE delay D can be computed using (3.16), (3.17) and (3.18).

3.5 Numerical Results

In this section, we provide numerical evaluation of the results presented in the previous sections. To be more specific, we plot the native Wi-Fi throughput and the delay of the LWA UE as functions of the native Wi-Fi AP access probability, the probability that the LWA UE chooses the LTE or Wi-Fi interface at one time slot, and the probability that an

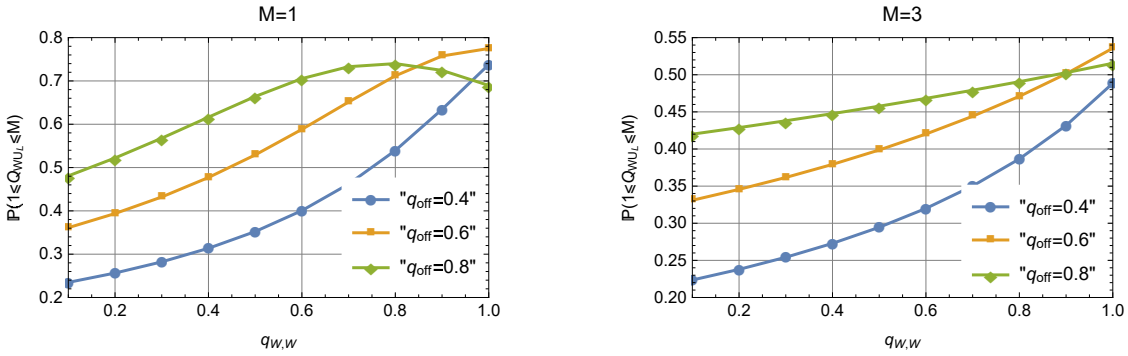

Figure 3.5: $\mathcal{P}(1 \leqslant Q_{WU_L} \leqslant M)$ vs. $q_{W,W}$.

LTE packet to be routed through the LTE or the Wi-Fi link. The values of the simulation parameters are given in Table 3.2. The success probabilities p_{kj} of link $k \rightarrow j$ can be derived by (3.2). Note that all the results below are obtained where the queue stability condition is satisfied.

3.5.1 Native Wi-Fi Throughput

By (3.15), the native Wi-Fi throughput depends heavily on the value of $\mathcal{P}(Q_{WU_L} = 0)$ and $\mathcal{P}(1 \leqslant Q_{WU_L} \leqslant M)$. In Fig. 3.4, we plot the probability that the queue size of Q_{WU_L} is 0 with respect to $q_{W,W}$ for the two cases with $M = \{1, 3\}$. As expected, with $q_{W,W}$ increasing, $\mathcal{P}(Q_{WU_L} = 0)$ decreases. Larger q_{off} leads to lower $\mathcal{P}(Q_{WU_L} = 0)$. We also observe that larger M leads to higher $\mathcal{P}(Q_{WU_L} = 0)$, because it leads to weaker congestion control, with which the LWA-mode Wi-Fi AP will remain silent with higher probability. We also plot the probability that the queue size of Q_{WU_L} is between 1 and M with respect to $q_{W,W}$, as illustrated in Fig. 3.5. The first important observation is that $\mathcal{P}(1 \leqslant Q_{WU_L} \leqslant M)$ is not always a monotonic function of $q_{W,W}$. Second, it is not always the highest q_{off} that gives the largest $\mathcal{P}(1 \leqslant Q_{WU_L} \leqslant M)$, since with M increasing, the probability that queue WU_L is empty decreases. Third, larger M leads to smaller $\mathcal{P}(1 \leqslant Q_{WU_L} \leqslant M)$. This is because when q_{off} is relatively low, the arrival rates λ_{WU_W} is also low, in which case M does not really affect the system, since the probability that WU_L is not empty decreases. In Fig. 3.6, we present the probability that the queue size of Q_{WU_L} is 0 with respect to $q_{U_L,W}$ for the two cases with $M = \{1, 3\}$. From this figure, with $q_{U_L,W}$ increasing, $\mathcal{P}(Q_{WU_L} = 0)$ increases at first, then saturates. However, when $q_{U_L,W}$ becomes larger, $\mathcal{P}(Q_{WU_L} = 0)$ has smaller variation with respect to the variations of q_{off}. Another important observation is that larger M does not increase the maximum $\mathcal{P}(Q_{WU_L} = 0)$. Fig. 3.7 show the relationship between $\mathcal{P}(1 \leqslant Q_{WU_L} \leqslant$

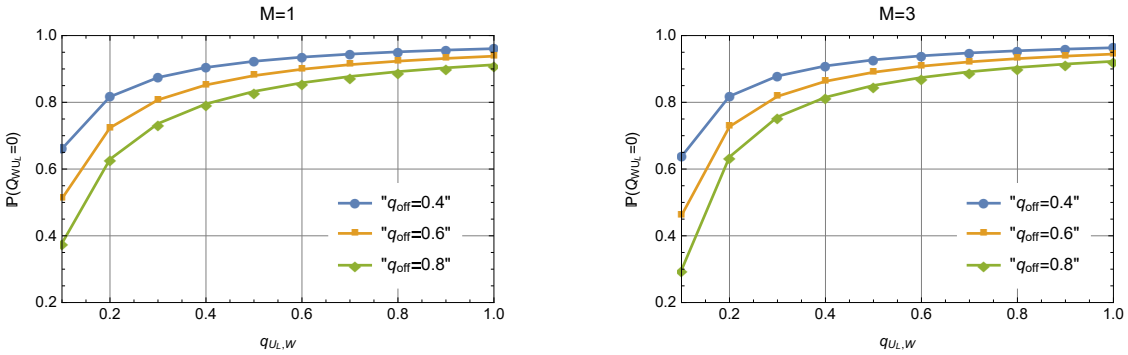

Figure 3.6: $\mathcal{P}(Q_{WU_L} = 0)$ vs. $q_{U_L,W}$.

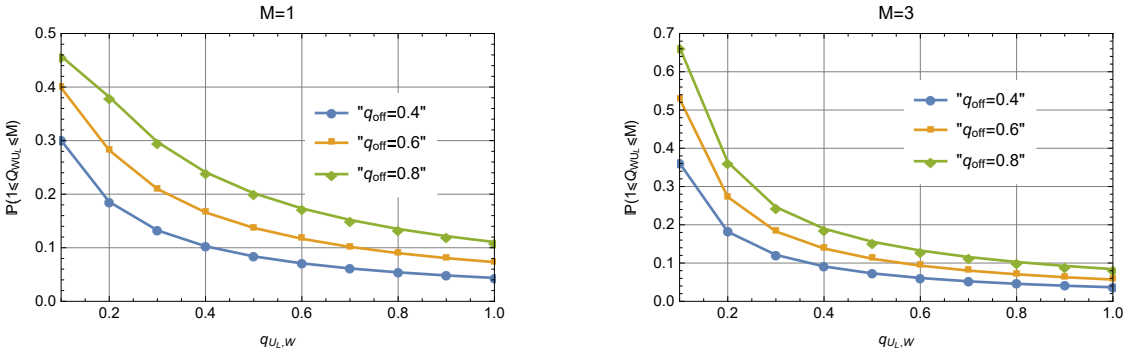

Figure 3.7: $\mathcal{P}(1 \leqslant Q_{WU_L} \leqslant M)$ vs. $q_{U_L,W}$.

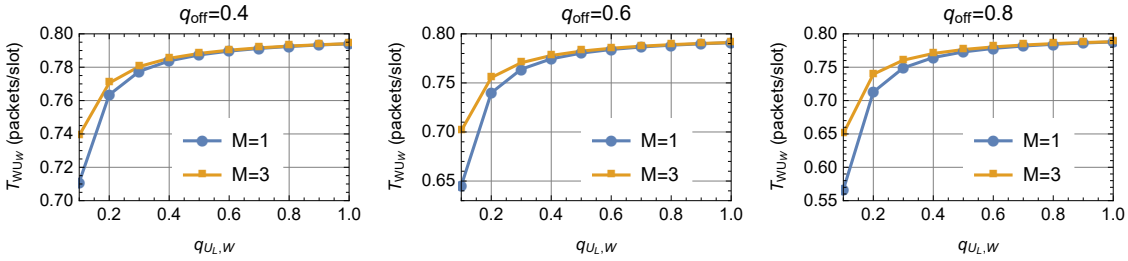

Figure 3.8: Native Wi-Fi throughput vs. $q_{U_L,W}$.

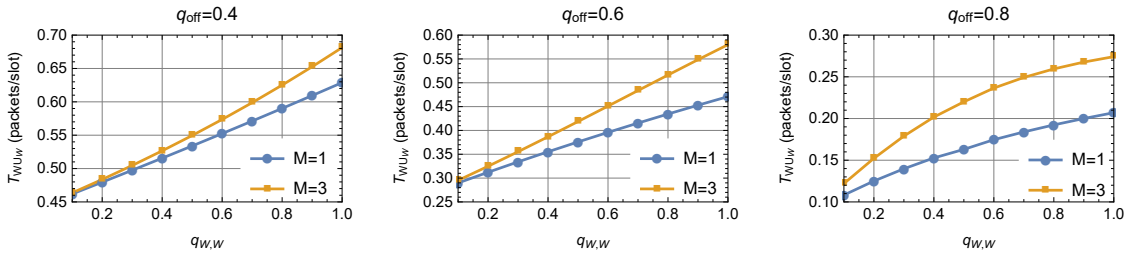

Figure 3.9: Native Wi-Fi throughput vs. $q_{W,W}$.

M) and $q_{U_L,W}$. As expected, larger $q_{U_L,W}$ leads to lower $\mathcal{P}(1 \leqslant Q_{WU_L} \leqslant M)$. However, when the value of $q_{U_L,W}$ becomes higher, $\mathcal{P}(1 \leqslant Q_{WU_L} \leqslant M)$ has smaller variation with respect to the variations of M.

In Fig. 3.8, we plot the native Wi-Fi throughput with respect to the probability that

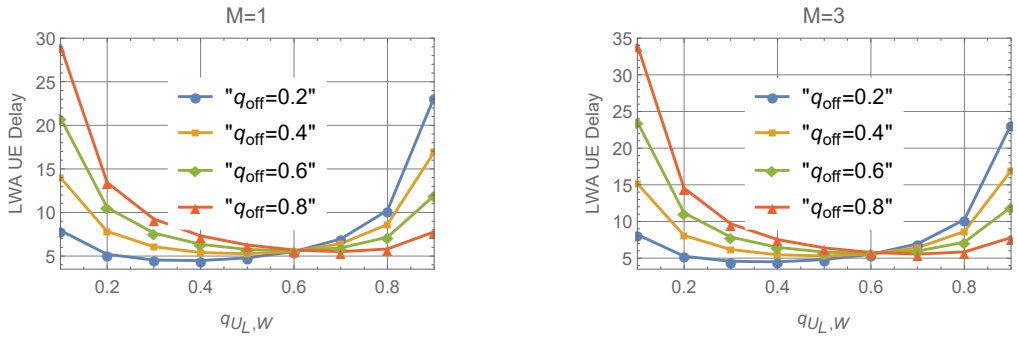

Figure 3.10: LWA UE delay vs. $q_{U_L,W}$.

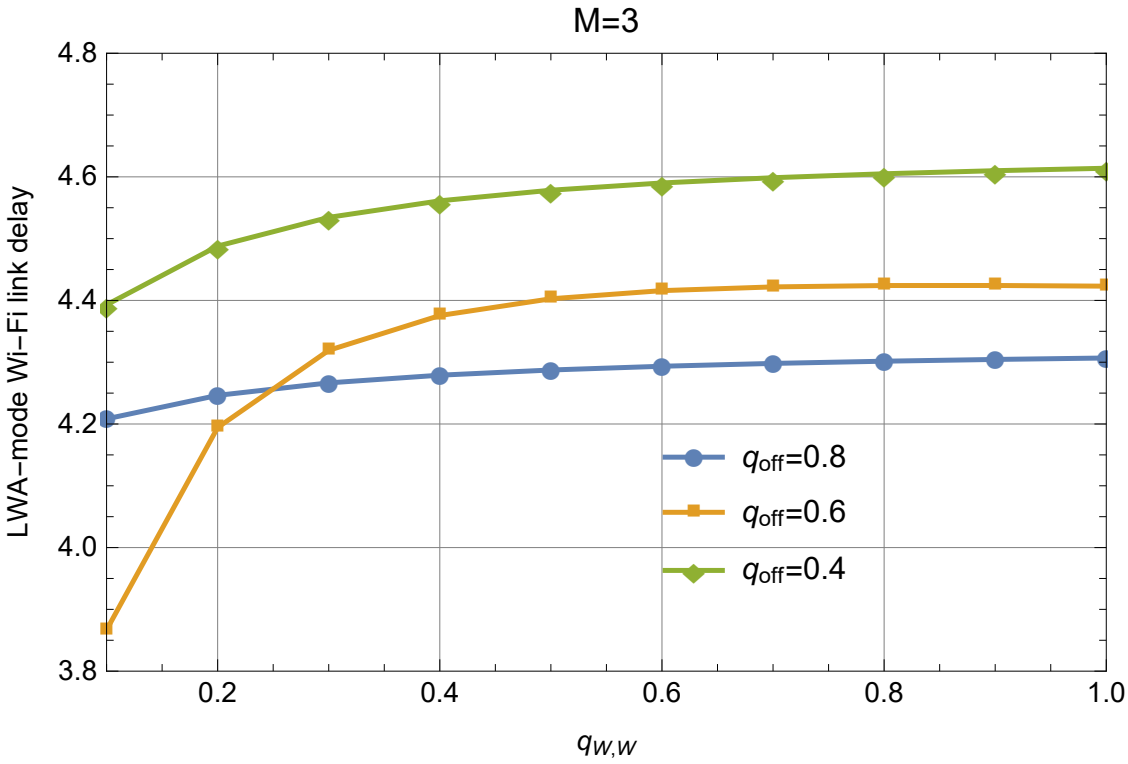

Figure 3.11: LWA-mode Wi-Fi link delay vs. $q_{U_L,W}$.

the LWA UE activates the LTE interface only to receive packet on each time slot. The results are presented with congestion threshold $M = \{1, 3\}$ and $q_{\text{off}} = \{0.4, 0.6, 0.8\}$. Our first remark is that, with $q_{U_L,W}$ increasing, the native Wi-Fi throughput increases rapidly at first, then saturates. We also observe that larger M provides higher potential improvement for the native Wi-Fi throughput, as the native Wi-Fi link is more likely to be active. However, when $q_{U_L,W}$ becomes larger, T_{WU_W} has smaller variation with respect to variations of M, since the probability that queue WU_L is empty increases. In such case, due to the low utilization, choosing $M = 1$ in our protocol is beneficial. In addition, comparing the sub-figures in Fig. 3.8, the maximum throughput of the native

Wi-Fi network remains the same with different q_{off}.

In Fig. 3.9 we draw the native Wi-Fi throughput with respect to $q_{W,W}$. We observe that the native Wi-Fi throughput increases with $q_{W,W}$, as otherwise it decreases. Another interesting observation is that for the same q_{off}, the difference between the native Wi-Fi throughput with $M = 1$ and that with $M = 3$ increases with $q_{W,W}$, since with M increasing, the probability that queue WU_L is empty decreases. It can be observed from Fig. 3.9 that, for the same value of $q_{W,W}$, increasing q_{off} will also increase the difference between the native Wi-Fi throughput with $M = 1$ and that with $M = 3$. This is because when q_{off} is relatively low, the arrival rates λ_{WU_W} is also low, in which case M does not really affect the system, since the probability that WU_L is not empty decreases.

3.5.2 LWA UE Delay

To illustrate the impact of different parameters on the LWA UE delay. We first plot Fig. 3.10 to present the LWA UE delay as a function of $q_{U_{L,W}}$ for different values of M and q_{off}. The first observation is that the LWA UE delay is not a monotonic function of $q_{U_{L,W}}$. There exists an optimal point that gives the minimum LWA UE delay among the feasible choice of $q_{U_{L,W}}$. Second, comparing the sub-figures in Fig. 3.10, we observe that larger M results in higher LWA UE delay. However, once $q_{U_{L,W}}$ reaches a certain level, e.g. $q_{U_{L,W}} = 0.2$ in Fig. 3.10, $\bar{D}$ has very little variation with respect to the variation of M. The reason is the probability that queue WU_L is empty increases with $q_{U_{L,W}}$. In such case, due to the low utilization, choosing $M = 1$ in our protocol is beneficial. Third, it is not always the highest q_{off} that gives the largest $\bar{D}$. The first reason is that larger q_{off} leads to higher D_{WU_L}, but smaller D_{LU_L} and D_{LW}. Another reason is that the success probability for the link $W \rightarrow U_L$ is not constant, but depends on the specific value of M and $q_{U_{L,W}}$, as described in Section 3.3. To be more specific, the value of M affects the probability of the queue size of WU_L to fall in the three different cases, and the value of $q_{U_{L,W}}$ affects the queue size of WU_L in cases $1 \leqslant Q_{WU_L} \leqslant M$ and $Q_{WU_L} > M$.

We then plot Fig. 3.11 to present $\bar{D}_W$ as a function of $q_{W,W}$ for different values of q_{off}. An interesting observation is that the LWA UE delay increases rapidly at first, then saturates. Higher q_{off} leads to lower saturated delay. The reason is when q_{off} is very high, the native Wi-Fi AP will not be allowed to transmit with high probability, as the queue size of WU_L falls in the case $Q_{WU_L} > M$. Then, with high success probability, the LWA-mode Wi-Fi transmission is almost interference-free.

3.6 Conclusion

This chapter investigated an LWA-enabled network consisting of an LTE BS and a Wi-Fi AP. The LTE BS has bursty arrivals, and transmits packets to the Wi-Fi AP through a non-ideal backhaul. The AP can operate in LWA mode and native Wi-Fi mode simultaneously with the help of superposition coding. We proposed a priority-based Wi-Fi transmission scheme with congestion control and studied the throughput of the native Wi-Fi network, as well as the LWA UE delay when the native Wi-Fi UE is under heavy traffic conditions. We further studied the impact of the scheme design parameters on the throughput and delay performance. Our results provide fundamental insights in the throughput and delay behavior of the considered network, which are essential for further investigation of this topic in larger topologies.

Chapter 4

Modeling and Analysis of MPTCP Proxy-based LTE-WLAN Path Aggregation

4.1 Introduction

There is an increasing demand for high data rate in wireless communications systems due to the fact that mobile traffic is expected to become 8.2 times larger in 2020 than what it was in 2015. Since the new licensed spectrum bands are rare and expensive, an interesting proposition is to enable a better use of different types of spectrum traffic offload, including the unlicensed bands. It is estimated that up to thirty percent of broadband access in cellular networks can be offloaded to unlicensed bands which are primarily used by WiFi networks [124].

There have been attempts to develop Long Term Evolution (LTE)-Wireless Local Area Network (WLAN) Path Aggregation (LWPA) based on Multi-path Transmission Control Protocol (MPTCP) [6, 175]. The LWAP design allows the aggregation of LTE and Wi-Fi, and the increase of download speeds can be acquired simply by adding an MPTCP gateway on mobile device, without causing changes in legacy Internet infrastructure or applications. Unlike LTE-WLAN carrier aggregation solutions like the LTE-Licensed Assisted Access (LAA), LWAP eliminates the controversial fairness issues between LTE and Wi-Fi and it does not require the deployment of new access networks[1]. LWPA can be potentially incorporated with Quality-of-Service (QoS)-related applications, such as Scalable Video Coding (SVC). For instance, the basic layer data can be

delivered through a reliable LTE connection and the enhancement layer data can be transmitted through a Wi-Fi AP to increase the quality of video streaming.

In this work, a stochastic geometry framework is proposed to evaluate the performance of LWPA in large-scale networks. We take into account the possibility to have closed-access Wi-Fi APs that are not available to be aggregated and whose performance are not allowed to be affected. The activation conditions of a LWPA-mode Wi-Fi are determined by the user density, the CSMA distance, and their relevant locations to nearby closed-access Wi-Fi APs. Using existing results from stochastic geometry analysis, we propose three approximations for the density of active LWPA Wi-Fi as a function of different network parameters. We also characterize the performance improvements of the considered network in terms of the aggregate data rate and the area spectral efficiency (ASE) of a Wi-Fi band. These improvements validate the advantages of LWPA as a promising method to improve the spectrum usage in unlicensed bands.

4.2 System Model

We consider a two-Radio Access Technology (RAT) network consisting of cellular BSs and WLAN APs. The LTE BSs are scattered on the two-dimensional Euclidian plane $\mathbb{R}^2$ according to a homogeneous PPP, denoted by Φ_L with intensity λ_L [176]. The coverage region of an LTE BS can be modeled via a Voronoi tessellation. Similarly, the WLAN APs are modeled to follow a homogeneous PPP Φ_W with intensity λ_W. We divide the WLAN APs into two tiers/groups, depending on whether or not they are accessible for the network operators to improve the QoS of cellular networks. The open-access Wi-Fi APs are available for path aggregation with the LTE BSs to serve cellular users simultaneously through parallel data flows. The closed-access Wi-Fi are occupied by private individuals, hence, they are accessible to only Wi-Fi users with the access rights. We assume that each WiFi AP has a probability p to be occupied by closed-access Wi-Fi users, and probability $1-p$ to be open-access.[1] As a result, the WiFi locations can also be modeled as two independent PPPs Φ_{W1} and Φ_{W2} for the open-access and closed-access Wi-Fi tiers, respectively, with corresponding densities $\lambda_{W1} = (1-p)\lambda_W$ and $\lambda_{W2} = p\lambda_W$. The LTE users are also assumed to be distributed according to another homogeneous PPP Φ_u with density ξ_u. We suppose that each cellular user is associated with the closest LTE BS. The distribution of users connected to closed-access Wi-Fi will

[1]The probability p denotes the percentage of closed-access WiFi among all the WiFi APs.

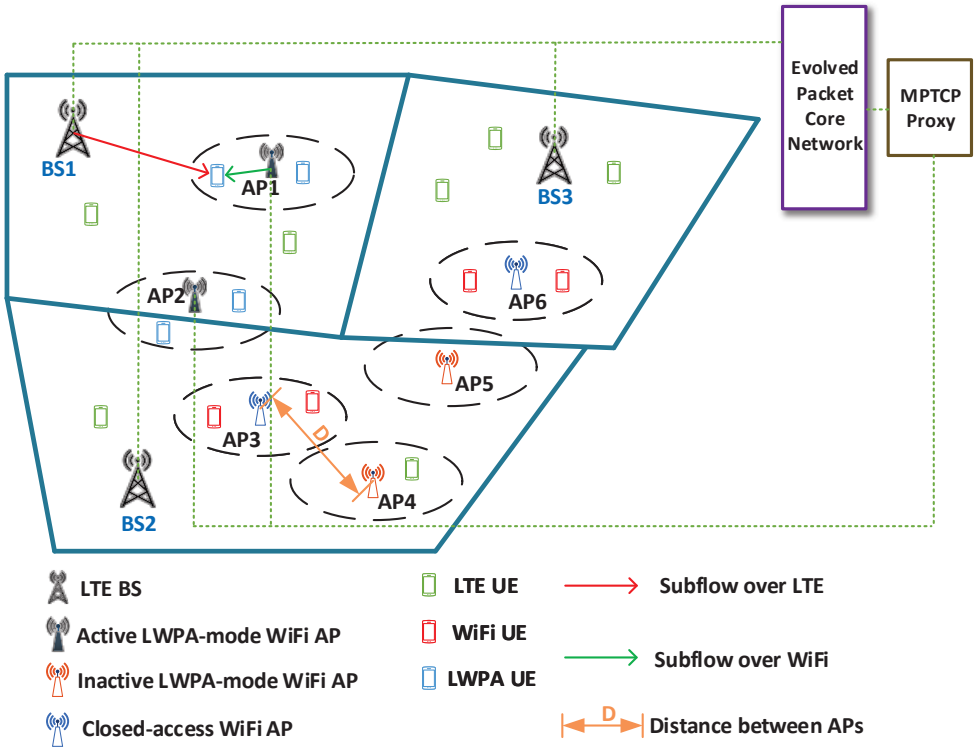

Figure 4.1: Two-RAT HetNet consisting of LTE BSs, active LWPA-mode Wi-Fi APs, inactive LWPA-mode Wi-Fi APs in the cellular RAT, and closed-access Wi-Fi APs in the WLAN RAT. The backhaul is shown by the dotted lines. AP1 and AP2 are active LWPA-mode Wi-Fi APs since they both meet the conditions. AP3 and AP6 are not available for LWPA mode because they are closed-access Wi-Fi. Although AP4 and AP5 are open-access Wi-Fi, they are inactive LWPA-mode Wi-Fi APs because there is no cellular user closer to AP5 than distance R, while the distance between AP4 and the active Wi-Fi AP3 is shorter than δ.

not affect the performance of LWPA, thus it is not specified in our system model.

For the LTE cellular network, each LTE BS utilizes the total available spectrum of B_c-Hz universal frequency reuse in the Downlink (DL), which is partitioned into a number of radio Resource Blocks (RBs). Each RB occupies a bandwidth of b_c Hz, and the RBs are allocated equally among all users. Assuming having N users inside a LTE cell, then each user is assigned B_c/b_cN RBs. The Wi-Fi APs utilize the unlicensed spectrum with a total bandwidth of B_w Hz.

In this work, we consider MHCP of type II to model the distribution of Wi-Fi APs using CSMA-CA MAC protocol [92]. The key point is that two active Wi-Fi APs operating in the same frequency band cannot be closer to each other than a threshold dis-

tance δ, which can be seen as setting up guard zones with a radius δ around the active transmitters. The distribution of active closed-access Wi-Fi APs without the presence of LWPA-mode Wi-Fi is denoted by $\widetilde{\Phi}_{W2}$. In order to ensure the QoS of closed-access WiFi users, the activation of LWA-mode Wi-Fi APs must not create any backoff/contention to any active closed-access Wi-Fi. According to this setup, a potential LWPA-mode Wi-Fi AP can be active only when there is no closed-access Wi-Fi AP or other active LWPA-mode Wi-Fi AP within distance δ. The distribution of active LWPA-mode Wi-Fi APs is a thinned version of the initial homogeneous PPP Φ_{W1}, where the thinning procedure involves conditions imposed by the cellular user density, the locations of closed-access Wi-Fi and other LWA-mode Wi-Fi APs. Fig. 4.1 presents a two-RAT HetNet consisting of LTE BSs in the cellular RAT and active LWPA-mode Wi-Fi APs, inactive LWPA-mode Wi-Fi APs, as well as closed-access Wi-Fi APs in the WLAN RAT.

Summarizing, an active LWPA-mode Wi-Fi AP must satisfy the four conditions below:

1. It must be open-access;
2. At least one LTE user is inside its service range, i.e., within distance R;
3. Any closed-access Wi-Fi AP must be at least outside distance δ;
4. Two active LWPA-mode Wi-Fi APs cannot be closer to each other than δ.

When all these conditions are satisfied, an open-access Wi-Fi AP can work in LWPA mode and serve the cellular user within its coverage together with the LTE BS.

Using existing results on the density of MHCP and Poisson Hole Process (PHP), we can obtain the following approximations on the density of active LWPA-mode Wi-Fi APs in our considered model.

(a) From the first and the second conditions, the probability of a point in Φ_{W1} being retained is the probability that there is at least one point from Φ_u within distance R. The retaining probability is [176]

$$P_1 = 1 - \exp(-\xi_u \pi R^2). \tag{4.1}$$

Considering the CSMA/CA operation of the WLAN RAT, the Wi-Fi APs in the same tier are assumed to be installed with respect to a minimum distance δ between each other, thus the resulted distribution of closed-access Wi-Fi APs forms an MHCP

$\widetilde{\Phi}_{W2}$ with intensity $\widetilde{\lambda}_{W2} = (1-\exp(-p\lambda_W \pi\delta^2))/\pi\delta^2$ [91]. Based on the first and the third conditions, the probability of a point in Φ_{W1} being retained is the probability that there is no point from $\widetilde{\Phi}_{W2}$ within distance δ. The resulted intensity of retained points can be approximated by the density of a Poisson Hole Process (PHP). The corresponding retaining probability is

$$\begin{aligned} P_2 &= \exp(-\widetilde{\lambda}_{W2}\pi\delta^2) \\ &= \exp(\exp(-p\lambda_W\pi\delta^2) - 1). \end{aligned} \tag{4.2}$$

Note that this approximation is accurate only when $\widetilde{\lambda}_{W2} < P_1\lambda_{W1}$ [177]. Thus, the distribution of open-access Wi-Fi APs from Φ_{W1} meeting the second and third conditions forms $\widetilde{\Phi}_{W1}$ with intensity $\widetilde{\lambda}_{W1} = P\lambda_{W1}$, where the retaining probability is $P = P_1P_2$. Because of the fourth condition the resulted distribution of active LWPA-mode Wi-Fi APs can be further regarded as an MHCP Φ_A^1 with intensity [91]

$$\lambda_A^1 \approx \frac{1 - \exp(-\widetilde{\lambda}_{W1}\pi\delta^2)}{\pi\delta^2}. \tag{4.3}$$

(b) Due to the fourth condition, we have that the resulted distribution of open-access Wi-Fi APs based on Φ_{W1} forms an MHCP $\widehat{\Phi}_{W1}$ with intensity $\widehat{\lambda}_{W1} = \frac{1-\exp(-\lambda_{W1}\pi\delta^2)}{\pi\delta^2}$. Thus, the active LWPA-mode Wi-Fi APs refer to those from $\widehat{\Phi}_{W1}$ meeting the second and third conditions. The effective density of active LWPA-mode Wi-Fi APs modeled as Φ_A^2 is

$$\lambda_A^2 \approx P_1P_2\widehat{\lambda}_{W1}, \tag{4.4}$$

when $\widetilde{\lambda}_{W2} < P_1\widehat{\lambda}_{W1}$ holds. Φ_{A2} is obtained by thinning the MHCP $\widehat{\Phi}_{W1}$ with the retaining probability $P = P_1P_2$.

(c) We first assume that the distribution of Wi-Fi APs meeting the fourth condition forms an MHCP $\widetilde{\Phi}_W$ with intensity $\widetilde{\lambda}_W = \frac{1-\exp(-\lambda_W\pi\delta^2)}{\pi\delta^2}$. Then, the intensity of open-access Wi-Fi APs from $\widetilde{\Phi}_W$ can be written as $(1-p)\widetilde{\lambda}_W$. The active LWPA-mode Wi-Fi APs refer to the open-access Wi-Fi APs from $\widetilde{\lambda}_W$ meeting the second condition, and they are modeled as Φ_A^3 with intensity

$$\lambda_A^3 \approx P_1(1-p)\widetilde{\lambda}_W, \tag{4.5}$$

which is obtained by thinning the MHCP $\widetilde{\Phi}_W$ with the retaining probability $(1-p)P_1$.

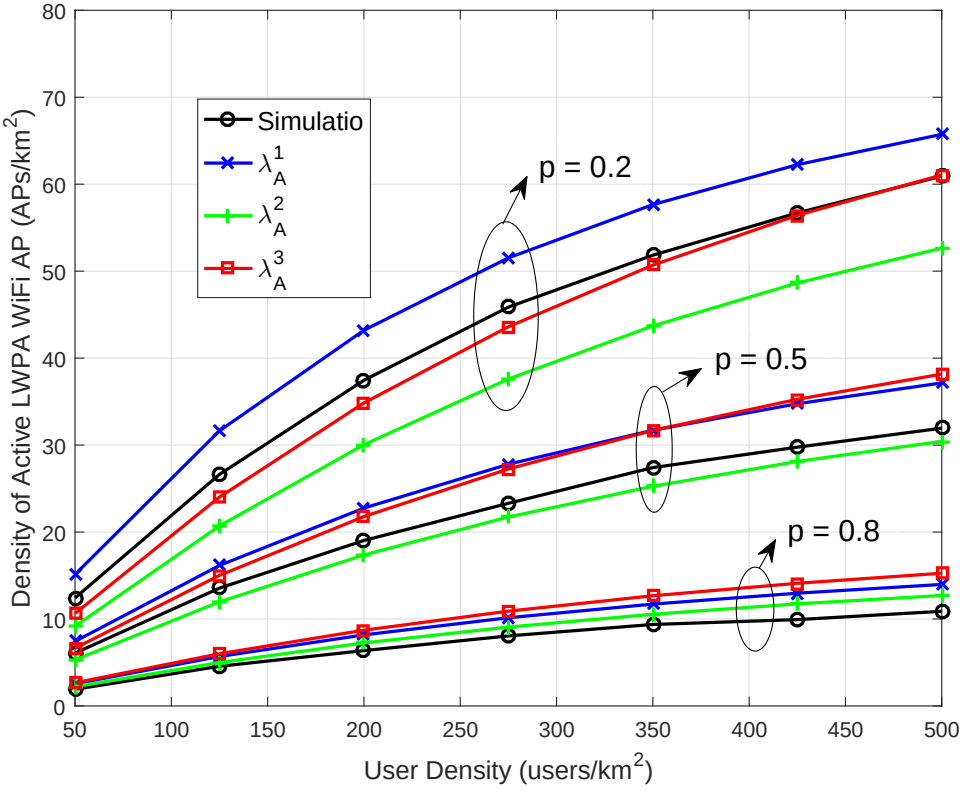

Figure 4.2: Density of active LWPA WiFi APs vs. user density with $p = 0.2, 0.5, 0.8$ and $\delta = 50$ m.

Fig. 4.2 shows the density of active LWPA-mode Wi-Fi APs versus the user density in cases when p equals to 0.2, 0.5 and 0.8, respectively. The approximated density is calculated with $\lambda_L = 100/\text{km}^2$, $\lambda_W = 200/\text{km}^2$ and $R = 30$ m. The results shown in blue lines are generated from (4.3). The red lines correspond to the approximation results obtained via (4.4). The green lines refer to the results generated via (4.5). We can observe from the results that the three approximations are all relevant, and the accuracy of these approximations depends heavily on the network parameters, such as δ and p. The gaps between the approximations and simulation results also come from the fact that the existing density functions of MHCP and PHP also contain certain approximation errors. When p is low, the red curve is closest to the simulation curve. However, when p increases, the red cure is not always the best. For simplicity, in the remainder of this chapter, we consider $\lambda_A = \lambda_A^3$ to represent the density of active LWPA-mode Wi-Fi APs.

4.3 Performance Analysis

In this section, we evaluate the performance gain of LWPA, in terms of the improved data rate and the area spectral efficiency.

4.3.1 Success Probability Analysis

In this work, we assume that in each time slot, at most one user will be served by an LWPA-mode Wi-Fi. Due to the randomness of point processes, for each active LWPA-mode Wi-Fi, its served cellular user can be considered as randomly and uniformly distributed within its service range. Without loss of generality, we consider a typical LWPA user centered at the origin with its associated LWPA-mode Wi-Fi AP W_o at a random distance l away, the SINR of its received signal is given by

$$\mathrm{SINR}_W = \frac{P_W h_W l^{-\alpha}}{\sum_{j \in \Phi_A \cup \widetilde{\Phi}_{W2} \setminus \{W_o\}} P_W h_j d_j^{-\alpha} + \sigma^2}, \tag{4.6}$$

where P_W denotes the transmitting power of Wi-Fi AP. h_W and h_j refer to small-scale fading from the typical LWPA-mode Wi-Fi AP, and the j-th interfering Wi-Fi AP to the typical LWPA user, respectively. σ^2 represents the noise power. We assume that all users experience Rayleigh fading, i.e. $h_W, h_j \sim \exp(1)$. d_j denotes the distance from the j-th interfering Wi-Fi AP to the typical LWPA user. We consider a standard distance-dependent pathloss attenuation, i.e. $r^{-\alpha}$, where $\alpha > 2$ is the pathloss exponent.

Similarly, for a typical LTE user located at the origin with its associated LTE BS L_o at a random distance r away, the SINR of its received signal is given by

$$\mathrm{SINR}_L = \frac{P_L g_L r^{-\alpha}}{\sum_{i \in \Phi_L \setminus \{M_o\}} P_L g_i l_i^{-\alpha} + \sigma^2}, \tag{4.7}$$

where P_L denotes the transmit power of LTE BS. g_L and g_i refer to small-scale power fading from the typical LTE BS, and the i-th interfering LTE BS to the typical LTE user, respectively. g_L and g_i follow the exponential distribution with unit mean (Rayleigh fading). l_i denotes the distance from the i-th interfering Wi-Fi AP to the typical LTE user.

As discussed in Section 4.2, the interference received by the typical LWPA user is caused the transmitting nodes distributed outside the guard zone centered at its associated transmitter. When $\delta \geq l$, there is a minimum distance between a typical LWPA user to its nearest interfering Wi-Fi AP, as shown in Fig. 4.3. The probability density function (PDF) of the link distance l is $f(l) = \frac{2l}{R^2}$ for $0 \leq l \leq R$, as a result of the randomly and

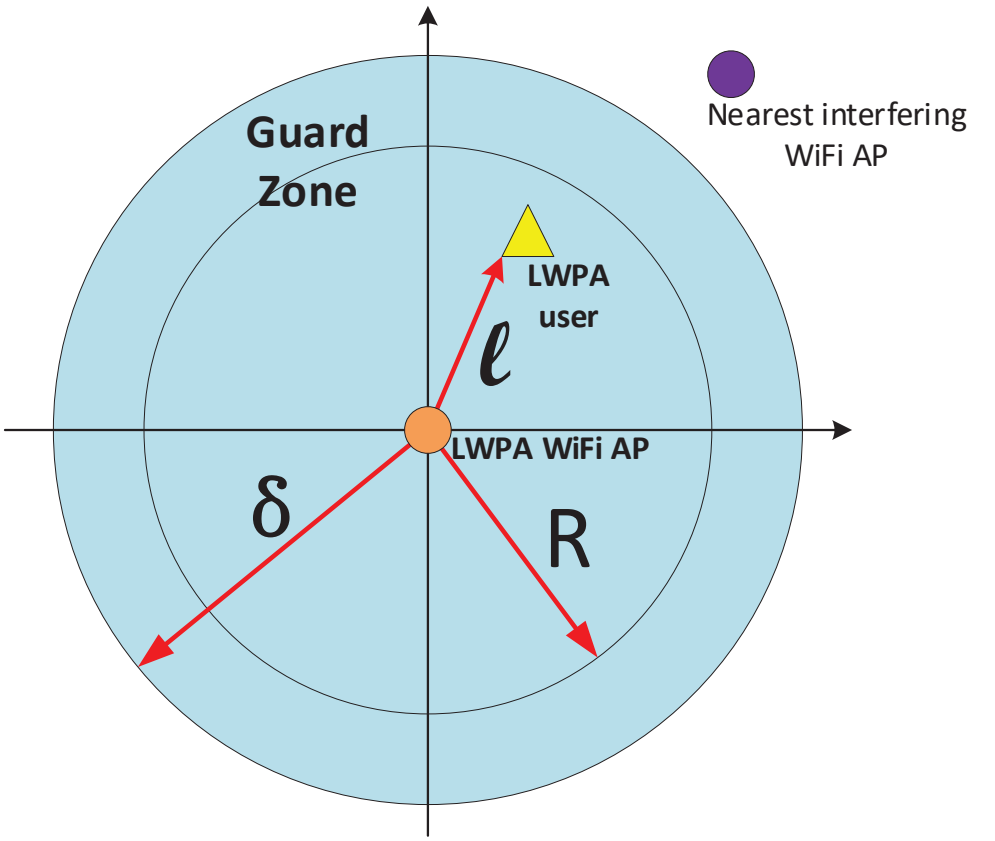

Figure 4.3: Guard Zone with radius δ of a typical active LWPA-mode WiFi AP centered at the origin with its users uniformly distributed in a disk $B(0, R)$. According to the system model, no active open-access or closed-access WiFi AP can lie in the circle of radius δ centered at the origin, thus the distance from the nearest WiFi AP to the typical LWPA user is at least $\delta - l$.

uniformly distributed user within the service range of an LWPA-mode Wi-Fi AP. For a given SINR threshold θ, the success probability of a typical active LWPA-mode Wi-Fi link in our considered network is given by

$$\begin{aligned} P_{suc}^{WiFi}(\theta, \lambda) =& \mathbb{P}(\mathrm{SINR}_W > \theta) \\ =& \mathbb{E}_l \left[\mathcal{L}_{I_W|\delta-l}(\theta l^\alpha) \cdot \exp\left(-\frac{\theta \sigma^2 l^\alpha}{P_W} \right) \right] \\ \approx& \int_0^R \frac{2l}{R^2} \cdot \mathcal{L}_{I_W|\delta-l}(\theta l^\alpha) \cdot \exp\left(-\frac{\theta \sigma^2 l^\alpha}{P_W} \right) \mathrm{d}l, \end{aligned} \tag{4.8}$$

where $I_W = \sum_{j \in \Phi_A \cup \widetilde{\Phi}_{W2} \setminus \{W_o\}} h_j d_j^{-\alpha}$ denotes the interference from other active Wi-Fi APs with normalized transmit power, $\mathcal{L}_{I_W|x}(s)$ refers to the Laplace transform of the interference coming from other Wi-Fi APs located out of a circle area $B(0,x)$ and is given by [99]

$$\begin{aligned}\mathcal{L}_{I_W|x}(s) =& \mathbb{E}\left[\exp\left(-s\sum_{j\in\Phi_A\setminus B(0,x)} h_j d_j^{-\alpha}\right)\right] \\ =& \exp\left(-\pi\lambda s^{\frac{2}{\alpha}}\int_{\frac{x^2}{s^{2/\alpha}}}^{\infty}\frac{1}{1+w^{\frac{\alpha}{2}}}\mathrm{d}w\right),\end{aligned} \tag{4.9}$$

where $\lambda = \lambda_A + \widetilde{\lambda}_{W2}$.

As a result of the nearest LTE BS association, the PDF of a typical LTE link distance is $f(r) = 2\pi\lambda_L r \cdot e^{-\pi\lambda_L r^2}$ for $0 \le r < \infty$[87]. Similarly, for a given SINR threshold θ, the success probability of a typical LTE link in our considered network is given by

$$\begin{aligned}P_{suc}^{LTE}(\theta) =& \mathbb{P}(\mathrm{SINR}_L > \theta) \\ =& \mathbb{E}_r\left[\widetilde{\mathcal{L}}_{I_L|r}(\theta r^\alpha)\cdot\exp\left(-\frac{\theta\sigma^2 r^\alpha}{P_L}\right)\right] \\ =& \int_0^\infty 2\pi\lambda_L r\cdot e^{-\pi\lambda_L r^2}\cdot\widetilde{\mathcal{L}}_{I_L|r}(\theta r^\alpha) \\ & \times\exp\left(-\frac{\theta\sigma^2 r^\alpha}{P_L}\right)\mathrm{d}r,\end{aligned} \tag{4.10}$$

where $I_L = \sum_{i\in\Phi_L\setminus\{M_o\}} g_i l_i^{-\alpha}$ denotes the interference from other LTE BSs with normalized transmit power, $\widetilde{\mathcal{L}}_{I_L|x}(s)$ refers to the Laplace transform of interference coming from other LTE BSs located out of a circle area $B(0,x)$, given by [99]

$$\begin{aligned}\widetilde{\mathcal{L}}_{I_L|x}(s) =& \mathbb{E}\left[\exp\left(-s\sum_{i\in\Phi_L\setminus B(0,x)} g_i l_i^{-\alpha}\right)\right] \\ =& \exp\left(-\pi\lambda_L s^{\frac{2}{\alpha}}\int_{\frac{x^2}{s^{2/\alpha}}}^{\infty}\frac{1}{1+w^{\frac{\alpha}{2}}}\mathrm{d}w\right).\end{aligned} \tag{4.11}$$

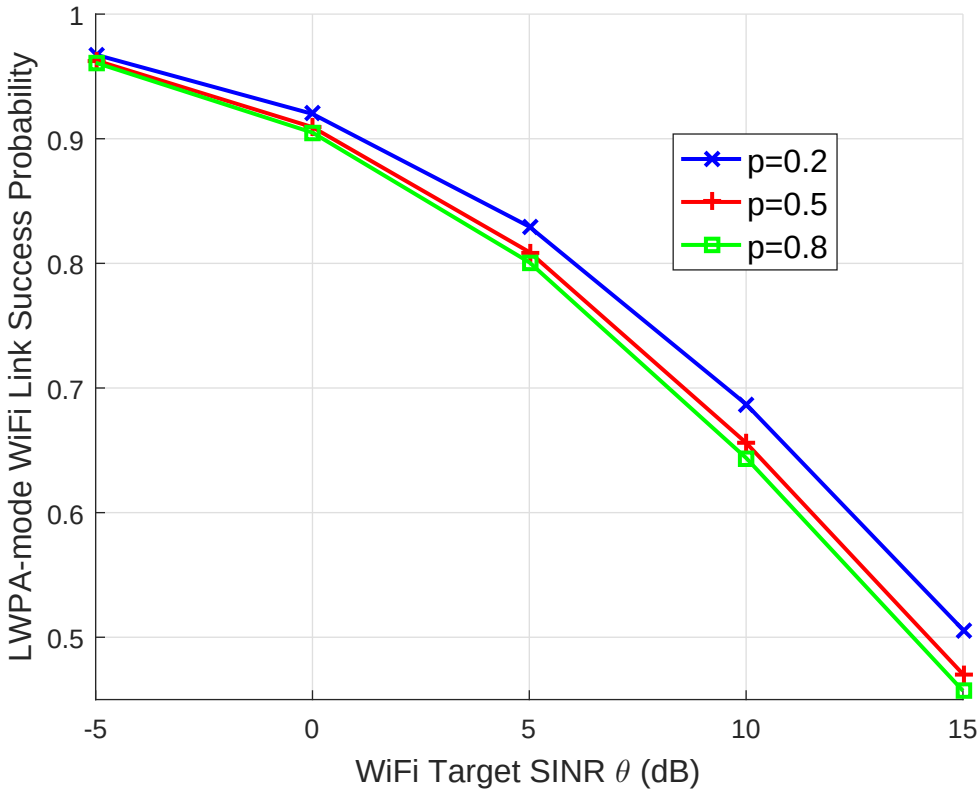

Figure 4.4: LWPA-mode Wi-Fi link success probability vs. θ with $p = \{0.2, 0.5, 0.8\}$, $\delta = 50$ m.

4.3.2 Cellular Rate Improvement

Without LTE-WLAN path aggregation, assuming i.i.d. Gaussian codebooks, the ergodic rate of a LTE link can be given by

$$\begin{aligned} R_{LTE} =& \mathbb{E}[\log_2(1+\mathrm{SINR}_L)] \\ =& \int_0^\infty \frac{P_{suc}^{LTE}(\theta)}{1+\theta}\mathrm{d}\theta, \end{aligned} \tag{4.12}$$

which can be obtained with the help of the SIR distribution given in (4.10). Similarly, when the user is connected to a nearby LWPA-mode WiFi AP, the ergodic rate can be obtained by

$$R_{WiFi} = \int_0^\infty \frac{P_{suc}^{WiFi}(\theta,\lambda)}{1+\theta}\mathrm{d}\theta. \tag{4.13}$$

As mentioned in Section 4.2, the RBs are equally assigned to the LTE users. In an LTE cell with total available bandwidth B_c, regardless of the number of users inside its coverage, the aggregate data rate averaging over all possible locations of users can be obtained as $B_c R_{LTE}$. With path aggregation, in addition to the data rate received from LTE BS, each active LWPA-mode Wi-Fi AP can provide an average rate equal to

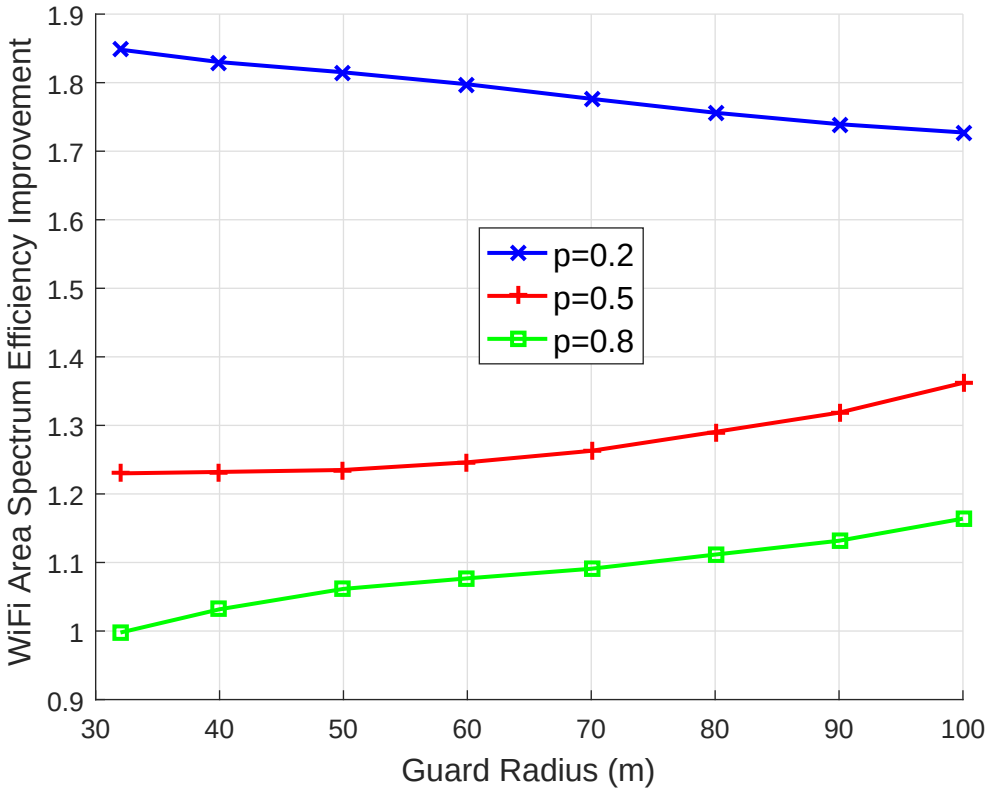

Figure 4.5: Wi-Fi ASE improvement vs. guard zone radius with $p = \{0.2, 0.5, 0.8\}$.

$B_w R_{WiFi}$ to the LTE users inside its service range. Therefore, in a random LTE cell, the percentage of cellular rate improvement can be expressed as

$$P_{CI} = \frac{B_w \cdot R_{WiFi} \cdot N_W}{B_c \cdot R_{LTE}}. \tag{4.14}$$

where $N_W = \frac{\lambda_A}{\lambda_L}$ is the average number of active LWPA-mode WiFi APs per LTE cell.

4.3.3 Area Spectral Efficiency Improvement of the WiFi Band

The ASE is an important metric to evaluate the spatial reuse of spectrum, measured by average data rate per Hz per unit area. For the considered network model, the ASE for Wi-Fi spectrum can be expressed as

$$\begin{aligned} \mathcal{T} =& (\lambda_A + \widetilde{\lambda}_{W2}) \mathbb{E}[\log_2(1 + \mathrm{SINR}_W)] \\ =& (\lambda_A + \widetilde{\lambda}_{W2}) \int_0^\infty \frac{P_{suc}^{WiFi}(\theta, \lambda_A + \widetilde{\lambda}_{W2})}{1+\theta} \mathrm{d}\theta. \end{aligned} \tag{4.15}$$

Specifically, if $\lambda_A = 0$, i.e. there is no active LWPA-mode Wi-Fi in the network, the ASE for Wi-Fi spectrum can be expressed as

$$\widetilde{\mathcal{T}} = \widetilde{\lambda}_{W2} \int_0^\infty \frac{P_{suc}^{WiFi}(\theta, \lambda_{W2})}{1+\theta} \mathrm{d}\theta. \tag{4.16}$$

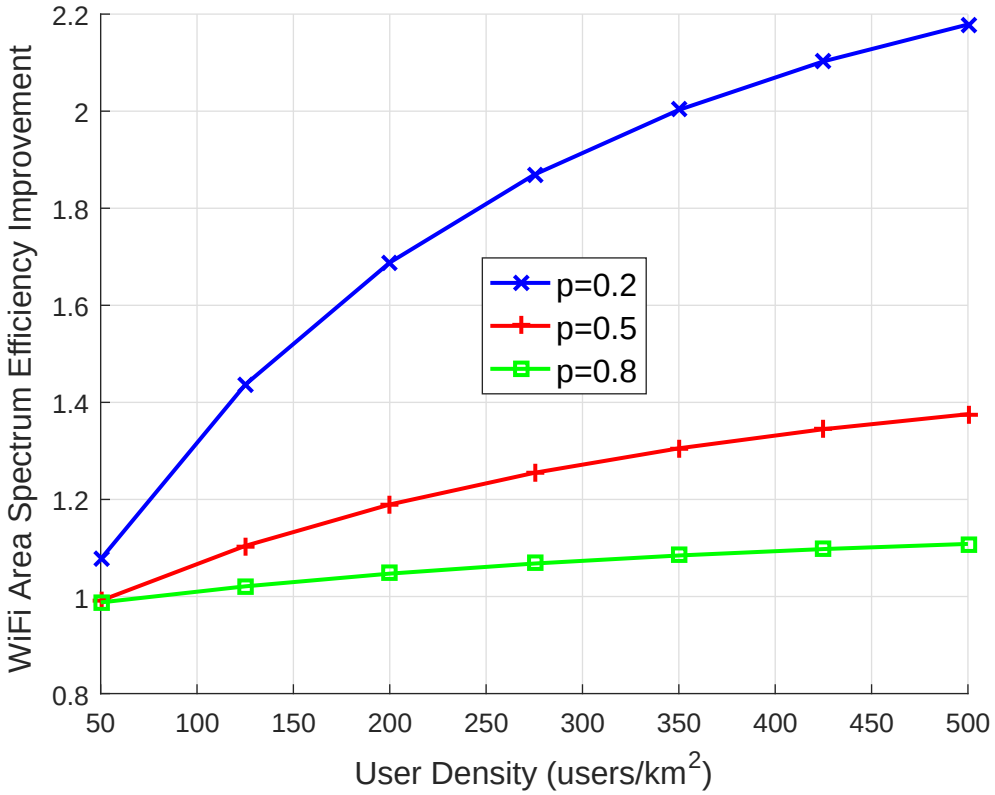

Figure 4.6: Wi-Fi ASE improvement vs. user density with $p = \{0.2, 0.5, 0.8\}$, and here δ= 50 m.

Thus, the ASE improvement of the Wi-Fi band is

$$P_{SI} = \frac{\mathcal{T} - \mathcal{T}}{\widetilde{\mathcal{T}}}. \tag{4.17}$$

The improvement/ratio of ASE provides a quantitative measure on how much network throughput gain in Wi-Fi band we can expect by allowing LWPA without affecting the activity of closed-access Wi-Fi APs.

4.4 Numerical Results

In this section, we present the LWPA-mode Wi-Fi link success probability, the cellular rate and the ASE improvement of the Wi-Fi band through numerical evaluations for $p = \{0.2, 0.5, 0.8\}$. The densities of the LTE BSs and Wi-Fi APs are $\lambda_L = 100/\text{km}^2$ and $\lambda_W = 200/\text{km}^2$, respectively. The cellular and WLAN bandwidth are both set to be 10 MHz. The transmit power of LTE BS and Wi-Fi AP are set to be 22 dBm and 18 dBm, respectively, and the noise power on both licensed and unlicensed bands is -95

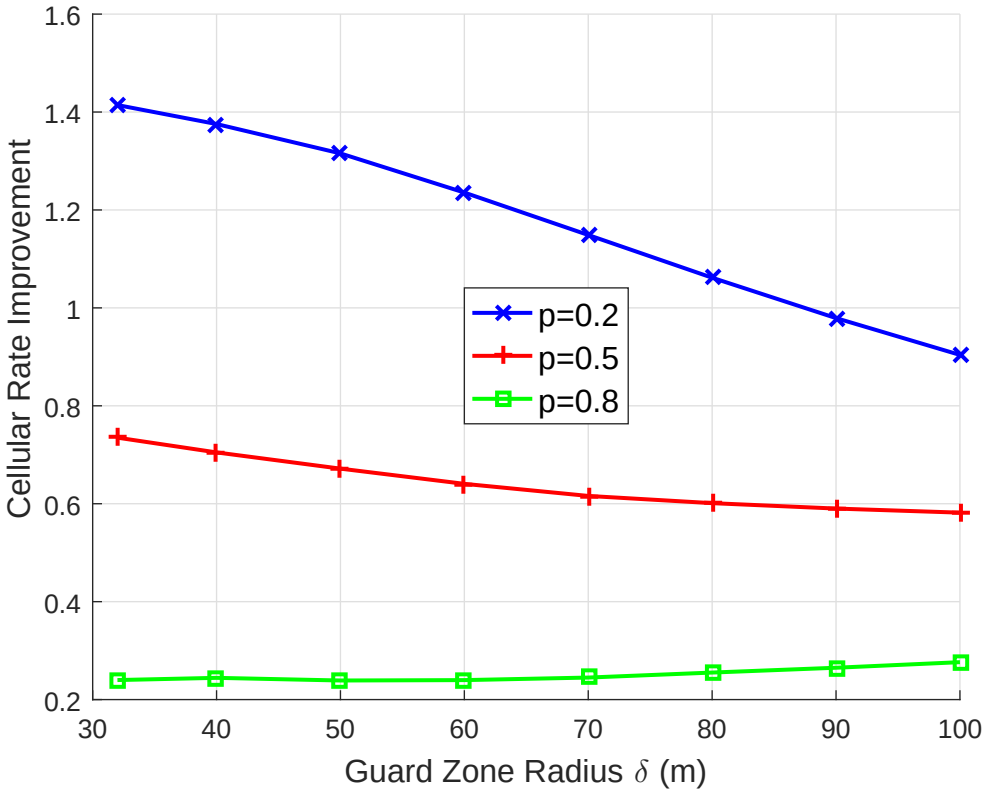

Figure 4.7: Cellular rate improvement vs. guard radius with $p = \{0.2, 0.5, 0.8\}$.

dBm. Rayleigh fading model is adopted for both cellular and WiFi links with $\mathbb{E}[h] = 1$. The pathloss exponent is $\alpha = 4$.

4.4.1 LWPA-mode WiFi Link Success Probability

In Fig. 4.4, we show the approximated success probability of the LWPA-mode Wi-Fi link as a function of the SINR threshold θ. The results are generated from (4.8). We observe that the value of p has little impact on the success probability of LWPA-mode Wi-Fi link. With smaller closed-access Wi-Fi percentage p, the success probability is slightly higher. This means that in the case with smaller p, the total density of active Wi-Fi will be slightly smaller.

4.4.2 WiFi ASE Improvement

Based on the approximated LWPA-mode Wi-Fi link success probability, we present the the percentage of Wi-Fi ASE improvement versus the guard zone radius as well as the user density in Fig. 4.5 and Fig. 4.6, respectively. The results are generated from (4.17). As expected, with smaller closed-access Wi-Fi percentage p, the Wi-Fi ASE

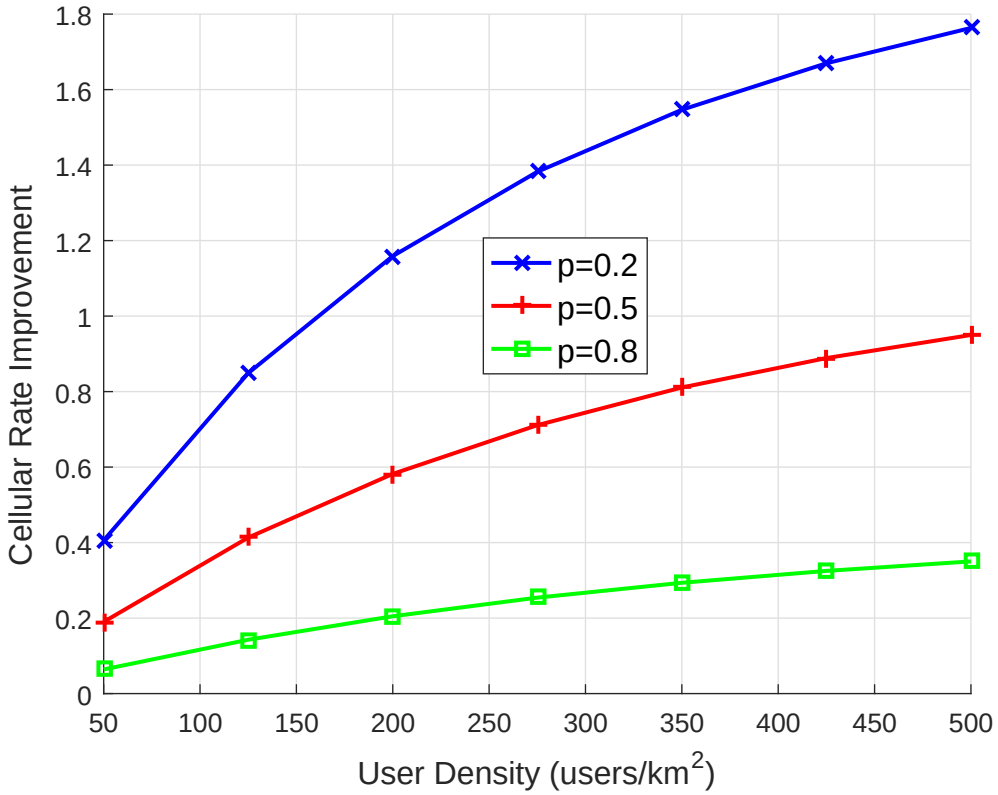

Figure 4.8: Cellular rate improvement vs. user density with $p = \{0.2, 0.5, 0.8\}$, and here $\delta = 50$ m.

improvement is higher. Another interesting observation from Fig. 4.5 is that when $p = 0.5$ and 0.8, the percentage of improved ASE increases along with the guard radius, while when $p = 0.2$, a different trend can be observed. This is due to the fact that increasing the guard radius will decrease the density of not only active LWPA-mode Wi-Fi APs, but also closed-access Wi-Fi APs. From (4.17) it is not obvious how the ASE improvement would evolve with the guard radius, which gives the opportunity to optimize the guard radius under specific network conditions. From Fig. 4.6, we see that the ASE improvement becomes very limited when the percentage of closed-access Wi-Fi p is higher. With smaller p, the ASE improvement increases rapidly with the user density, meaning that the advantage of LWPA is more obvious in the dense user regime with less closed-access Wi-Fi APs.

4.4.3 Cellular Rate Improvement

Fig. 4.7 and Fig. 4.8 present the percentage of cellular rate improvement versus the guard radius δ and versus the user density, respectively. The results are generated from

(4.14). Similar to the trend observed for Wi-Fi ASE improvement, with smaller value of p, the data rate received by the cellular users can be further improved. It is worth noticing that enabling LWPA can significantly improve the downloading rates of the LTE users without causing much interference to the existing closed-access Wi-Fi users.

4.5 Conclusion

In this chapter, a stochastic geometry model was used to model and analyze the performance of an MPTCP Proxy-based LWPA network with intra-tier and cross-tier dependencies. Under the considered network model and the activation conditions of LWPA-mode Wi-Fi, we obtained three approximations for the density of active LWPA-mode Wi-Fi APs through different approaches. Performance metrics including the success probability, the cellular rate improvement and the area spectral efficiency have been analytically derived and numerically evaluated. The impact of different parameters on the network performance have been analyzed, validating the significant gain of using LWPA in terms of boosted data rate and improved spectrum reuse.

Chapter 5

Resource Optimization for Joint LWA and LTE-U in Load-coupled and Multi-Cell Networks

5.1 Introduction

We present a system framework for capacity optimization in Wi-Fi and load-coupled LTE networks, where LWA and LTE-U are jointly used. The novelties consist in both data aggregation by LWA as well as spectrum sharing by LTE-U. To the best of our knowledge, the properties of load-coupling when the amount of resource is variable have not been studied in the literature. In our work, the LTE and Wi-Fi systems are interconnected by spectrum sharing. Thus not only should we consider the load coupling among all LTE cells, but each cell is also required to ensure the performance of the Wi-Fi network at the same time. Applying the solution approaches proposed by literature [102–105] to the scenario with spectrum sharing guarantees neither feasibility nor optimality.

Given a base data demand of the users, the optimization task is to maximize the common scaling factor [102], via optimizing the spectrum sharing of LTE and Wi-Fi, while accounting for the resource limits as well interference. We provide theoretical analysis, resulting in an algorithm that achieves global optimality. Thus we can effectively use numerical results to characterize the gain by joint LWA and LTE-U.

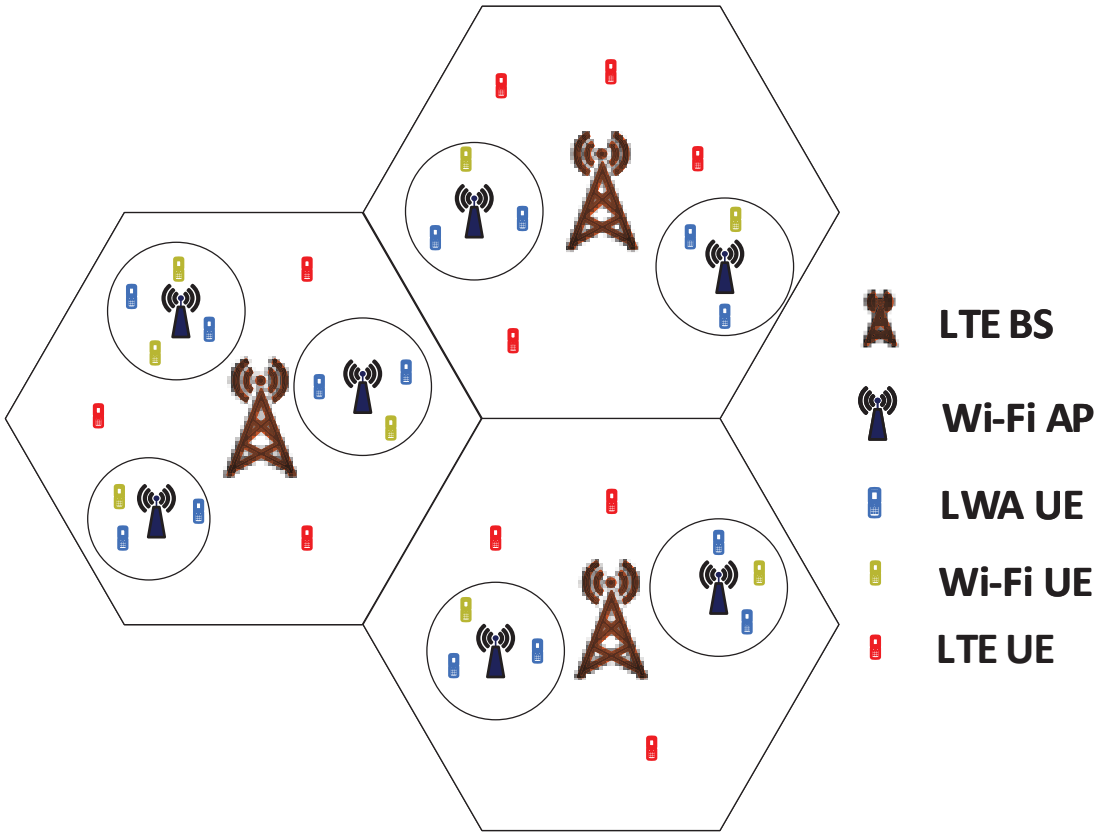

Figure 5.1: System model for LTE-U and LWA.

5.2 System Model and Problem Formulation

5.2.1 Network Model

As illustrated in Fig. 5.1, we consider a scenario with I LTE BSs, $\mathcal{I} = \{1, 2, \cdots, I\}$, and H Wi-Fi APs, $\mathcal{H} = \{1, 2, \cdots, H\}$. There can be one or multiple Wi-Fi APs inside an LTE cell. The coverage areas of the Wi-Fi APs are non-overlapping, and thus there is no interference among the APs. The Wi-Fi network deploys the IEEE 802.11ax protocol, and operates in the 5 GHz unlicensed band. The IEEE 802.11ax Task Group has defined the uplink and downlink orthogonal frequency division multiple access (OFDMA) [178]. In the conventional Wi-Fi setup, e.g., IEEE 802.11n, the capacity can be analyzed using a discrete-time Markov chain (DTMC) model, e.g., [113]. However, this is less reasonable in our case, since the DTMC model does not consider the actual signal-to-interference-and-noise ratio (SINR), which is a key parameter in case of OFDMA. There are J^{LTE} LTE user equipments (UEs), forming set $\mathcal{J}^{\text{LTE}} = \{1, 2, \cdots, J^{\text{LTE}}\}$. The UE group served by BS $i \in \mathcal{I}$ is denoted by $\mathcal{J}_i^{\text{LTE}}$. All LTE UEs and are able to aggregate LTE and Wi-Fi traffic. An LTE UE is served by an LTE BS and a Wi-Fi AP by LWA, if it is in the

coverage area of the latter. The LTE UE group covered by the h-th Wi-Fi AP is denoted by $\mathcal{J}_h^{\text{LTE}}$. There also exist native Wi-Fi UEs, i.e., UEs served by Wi-Fi only. This UE set is denoted by $\mathcal{J}_h^{\text{WiFi}}$ for AP h.

By LTE-U, LTE can share the unlicensed band with Wi-Fi via an inter-system coordinator [179]. Channel access schemes to deal with LTE and Wi-Fi coexistence are based on duty-cycle or listen-before-talk (LBT) [1]. In our work, the duty-cycle method is employed. The unlicensed band is periodically divided into two time periods among LTE and Wi-Fi. Denote by $\theta \in [0, 1)$ the proportion of unlicensed band allocated for LTE. The residual $1 - \theta$ is for Wi-Fi. The presence of Wi-Fi native UEs implies $\theta < 1$. The minimum unit for both LTE and IEEE 802.11ax Wi-Fi resource allocation is referred to as resource unit (RU). Denote by M^{L} and M^{U} the number of RUs in licensed and unlicensed bands, respectively.

5.2.2 LTE Load Coupling

For LTE, we use ρ_i to denote the fraction of RU consumption in cell i, used for serving UEs, also referred to as cell load. The network-wise load vector is $\boldsymbol{\rho} = (\rho_1, \rho_2, \ldots, \rho_I)^T$. In the load-coupling model [101], the SINR at UE $j \in \mathcal{J}_i^{\text{LTE}}$ is

$$\gamma_j(\boldsymbol{\rho}) = \frac{p_i g_{ij}}{\sum_{k \in \mathcal{I} \setminus \{i\}} p_k g_{kj} \rho_k + \sigma^2}. \tag{5.1}$$

Here, p_i is the transmit power per RU of BS i, g_{ij} is the power gain between cell i and UE j, and the term σ^2 refers to the noise power. Note that g_{kj}, $k \neq i$, represents the power gain from the interfering BSs. For any RU in cell i, ρ_k is intuitively interpreted as the likelihood that the served UEs of cell i receive interference from k. The term $\sum_{k \in \mathcal{I} \setminus \{i\}} p_k g_{kj} \rho_k$ is interpreted as the interference that UE j experiences.

For UE $j \in \mathcal{J}^{\text{LTE}}$, the data rate achieved, if all the $M^{\text{L}} + \theta M^{\text{U}}$ LTE RUs are given to j, is expressed below, where B denotes one RU's bandwidth.

$$C_j^{\text{LTE}}(\boldsymbol{\rho}, \theta) = (M^{\text{L}} + \theta M^{\text{U}}) B \log_2(1 + \gamma_j(\boldsymbol{\rho})). \tag{5.2}$$

Denote by r_j the baseline demand of UE j. We would like to scale up r_j by a demand scaling factor $\alpha > 0$. We remark that the maximum demand scaling factor can be regarded as the satisfaction ratio of the UE demands. In general, delivering more demands leads to higher satisfaction. Given base demand r_j and the resource limit, the solution α^*

obtained by solving (6.17) is the maximum achievable ratio of r_j with the resource limits. If r_j can be satisfied, we must have $\alpha^* \geqslant 1$, as otherwise the network is overloaded and α^* is a satisfiable proportion of the demands r_j ($j \in \mathcal{J}$). The physical meaning of α will be discussed in Section 5.2.4. If j is served by LTE only, then $\alpha r_j / C_j^{\text{LTE}}(\boldsymbol{\rho}, \theta)$ gives the proportion of required LTE RUs for satisfying αr_j. If j is served by both systems, we use coefficient β_j ($\beta_j \in [0, 1]$) to denote the proportion of demand to be delivered by LTE. This coefficient can be set via for example a look-up table based on the relative signal strengths of the two systems[1]. The proportion of required LTE RUs for satisfying the (scaled) demand is $\alpha r_j \beta_j / C_j^{\text{LTE}}(\boldsymbol{\rho}, \theta)$. The required proportion of RUs by cell i to meet the (scaled) demand of UE j reads

$$\mathrm{f}_{ij}(\boldsymbol{\rho}, \theta, \alpha) = \begin{cases} \dfrac{\alpha r_j \beta_j}{C_j^{\text{LTE}}(\boldsymbol{\rho}, \theta)}, \forall j \in \mathcal{J}_h^{\text{LTE}}, h \in \mathcal{H} \\ \dfrac{\alpha r_j}{C_j^{\text{LTE}}(\boldsymbol{\rho}, \theta)}, \forall j \in \mathcal{J}^{\text{LTE}} \setminus \cup_{h \in \mathcal{H}} \mathcal{J}_h^{\text{LTE}}. \end{cases} \tag{5.3}$$

The sum of (5.3) over cell i's UEs gives the following function for cell i, which we also present in vector form for the network.

$$\mathrm{f}_i(\boldsymbol{\rho}, \theta, \alpha) = \sum_{j \in \mathcal{J}_i^{\text{LTE}}} \mathrm{f}_{ij}(\boldsymbol{\rho}, \theta, \alpha), \tag{5.4}$$

$$\mathbf{f}(\boldsymbol{\rho}, \theta, \alpha) = [\mathrm{f}_1(\boldsymbol{\rho}, \theta, \alpha), \mathrm{f}_2(\boldsymbol{\rho}, \theta, \alpha), \ldots, \mathrm{f}_I(\boldsymbol{\rho}, \theta, \alpha)]. \tag{5.5}$$

Given θ and α, $\mathbf{f}(\boldsymbol{\rho})$ is a standard interference function (SIF) [180]. Denote by $\mathbf{f}^k$ ($k > 1$) the function composition of $\mathbf{f}(\mathbf{f}^{k-1}(\boldsymbol{\rho}))$ (with $\mathbf{f}^0(\boldsymbol{\rho}) = \boldsymbol{\rho}$). If $\lim_{k \to \infty} \mathbf{f}^k(\boldsymbol{\rho})$ exists, it is unique. Let ρ_{ij} represent the proportion of RUs allocated to UE j by j's serving cell i. The load of any cell $i \in \mathcal{I}$ is $\rho_i = \sum_{j \in \mathcal{J}_i^{\text{LTE}}} \rho_{ij}$. The load-coupling model reads $\rho_i = \mathrm{f}_i(\boldsymbol{\rho}, \theta, \alpha), \forall i$. This model leads to a non-linear equation system. In particular, the load vector $\boldsymbol{\rho}$ appears in both sides of the equation and cannot be readily solved in closed form, since the load ρ_i for cell i affects the load ρ_k of other cells $k \neq i$, which would in turn affect the load ρ_i. Therefore, analysis using the load-coupling model is not straightforward.

[1] Our work focuses on network level resource allocation with spectrum sharing. An exntension is to consider β_j as optimization variable as well. However, this changes the problem scope – optimization is then at the level of individual UEs. Moreover, a much larger amount of control overhead will be involved to communicate the optimization results to all individual UEs.

5.2.3 Rate and Resource Characterization for Wi-Fi

For Wi-Fi, the counterpart of (5.3) for UE j of AP h reads

$$\mathrm{m}_{hj}(\theta,\alpha)=\begin{cases}\dfrac{\alpha r_j(1-\beta_j)}{C_j^{\text{WiFi}}(\theta)},\forall j\in\mathcal{J}_h^{\text{LTE}},h\in\mathcal{H}\\ \dfrac{\alpha r_j}{C_j^{\text{WiFi}}(\theta)},\forall j\in\mathcal{J}_h^{\text{WiFi}},h\in\mathcal{H}\end{cases}\tag{5.6}$$

where $C_j^{\text{WiFi}}(\theta)=(1-\theta)M^{\text{U}}B\log(1+\frac{p_h g_{hj}}{\sigma^2})$, with $(1-\theta)M^{\text{U}}$ being the total number of Wi-Fi RUs. The terms p_h and g_{hj} denote the transmit power per RU of AP h and the power gain between AP h and UE j, respectively. Based on (5.6), we define the following entities of required resource consumption.

$$\mathrm{m}_h(\theta,\alpha)=\sum_{j\in\mathcal{J}_h^{\text{LTE}}\cup\mathcal{J}_h^{\text{WiFi}}}\mathrm{m}_{hj}(\theta,\alpha).\tag{5.7}$$

$$\mathbf{m}(\theta,\alpha)=[\mathrm{m}_1(\theta,\alpha),\mathrm{m}_2(\theta,\alpha)\ldots,\mathrm{m}_H(\theta,\alpha)].\tag{5.8}$$

Let x_{hj} denote the proportion of RUs allocated to UE j. The load of AP h is $x_h=\sum_{j\in\mathcal{J}_h^{\text{LTE}}\cup\mathcal{J}_h^{\text{WiFi}}}x_{hj},\forall h\in\mathcal{H}$. The values of x_h is bounded by $x^{\max}$. Moreover, to meet the demand requirement, $x_h=\mathrm{m}_h(\theta,\alpha)$. We define $\boldsymbol{x}=(x_1,x_2,\ldots,x_H)^T$.

5.2.4 Problem Formulation

Given a baseline demand distribution, the maximum α shows how much increase can still be accommodated by the network. In this sense, maximizing the demand scaling factor is equivalent to maximizing the network capacity. The optimization problem is formalized in (5.9).

$$\alpha'=\max_{\theta,\boldsymbol{\rho},\boldsymbol{x}}\quad\alpha\tag{5.9a}$$

$$\text{s.t.}\quad\boldsymbol{\rho}=\mathbf{f}(\boldsymbol{\rho},\theta,\alpha),\boldsymbol{x}=\mathbf{m}(\theta,\alpha)\tag{5.9b}$$

$$\boldsymbol{\rho}\leqslant\boldsymbol{\rho}^{\max},\boldsymbol{x}\leqslant\boldsymbol{x}^{\max},\theta\in[0,1)\tag{5.9c}$$

The objective is to maximize α, which is the satisfaction ratio of the UE demands. Given the baseline demand and the resource limit, the solution obtained by solving (5.9a) is the maximum achievable ratio of r_j with the resource limit. Namely, $\alpha'\geqslant 1$ if r_j can be satisfied, as otherwise the network is overloaded. Constraints (5.9b) ensures that sufficient amount of RUs are allocated to deliver the UE's demands, taking into account α. Constraints (5.9c) imposes the resource limits, and the range of θ. The resource limit is assumed to be uniform.

5.3 Solution Approach

Assume first θ is given. Denote by α^* the optimum for this restricted setup. Consider maximum demand scaling for LTE and Wi-Fi separately. That is, for each of the two systems, demand scaling is performed for its native UEs' demand and the demand proportions, $r_j\beta_j$ or $r_j(1-\beta_j)$, for any UE j served by both systems. Denote the corresponding optimal values by α^{LTE} and α^{WiFi}, respectively.

Lemma 3. *For any given θ, $\alpha^* = \min\{\alpha^{\text{LTE}}, \alpha^{\text{WiFi}}\}$.*

Proof. First, $\min\{\alpha^{\text{LTE}}, \alpha^{\text{WiFi}}\}$ obviously gives a feasible α of (5.9) for the given θ, thus $\alpha^* \geqslant \min\{\alpha^{\text{LTE}}, \alpha^{\text{WiFi}}\}$. Next, observe that, by definition, for any UE j served by both LTE and Wi-Fi, the scaled demand served by LTE is $\alpha^* r_j\beta_j$ and that by Wi-Fi is $\alpha^* r_j(1-\beta_j)$, at the optimum of (5.9) for the given θ. Moreover, the achieved scaling for all Wi-Fi native users is α^*. Hence α^* is achievable when Wi-Fi is considered separately, giving $\alpha^* \leqslant \alpha^{\text{WiFi}}$. Similarly, $\alpha^* \leqslant \alpha^{\text{LTE}}$. Therefore $\alpha^* \leqslant \min\{\alpha^{\text{LTE}}, \alpha^{\text{WiFi}}\}$, and the result follows. □

Next, we address the computation of α^{LTE} and α^{WiFi}. For LTE, given θ, denote by $\boldsymbol{\rho}^*$ the optimal load vector, for which α^{LTE} is achieved. At least one element of $\boldsymbol{\rho}^*$ equals $\rho^{\max}$, as otherwise all cells have spare resource and α^{LTE} would not be optimal. The condition can be stated as $\|\boldsymbol{\rho}\|_\infty = \rho^{\max}$, where $\|\cdot\|_\infty$ is the maximum norm. All functions in $\mathbf{f}(\boldsymbol{\rho}, \alpha)$ under fixed θ are strictly concave in $\boldsymbol{\rho}$ for $\boldsymbol{\rho} \geqslant 0$ [101]. As $\mathbf{f}$ is linear in α, $\frac{1}{\alpha}\boldsymbol{\rho} = \mathbf{f}(\boldsymbol{\rho}, 1)$ is equivalent to $\boldsymbol{\rho} = \mathbf{f}(\boldsymbol{\rho}, \alpha)$. Moreover, $\|\cdot\|_\infty$ is monotone. Thus, the system $\{\|\boldsymbol{\rho}\|_\infty = \rho^{\max}, \frac{1}{\alpha}\boldsymbol{\rho} = \mathbf{f}(\boldsymbol{\rho}, 1), \boldsymbol{\rho} \in \mathbb{R}_+^I\}$ is a conditional eigenvalue problem for concave mapping. This can be solved using normalized fixed point iteration [102]. Given $\boldsymbol{\rho}^k$ ($k \geqslant 0$) and any $\boldsymbol{\rho}^0 \in \mathbb{R}_+^I$, one such iteration computes the next iterate $\boldsymbol{\rho}^{k+1}$ by $\boldsymbol{\rho}^{k+1} = \rho^{\max}\mathbf{f}(\boldsymbol{\rho}^k, 1)/\|\boldsymbol{\rho}\|_\infty$, and, if $\lim_{k\to\infty} \rho^{\max}\mathbf{f}(\boldsymbol{\rho}^k, 1)/\|\boldsymbol{\rho}\|_\infty$ exists, the sequence $\boldsymbol{\rho}^0, \boldsymbol{\rho}^1, \ldots,$ converges to $\boldsymbol{\rho}^*$ which is unique. Moreover, equality holds for all rows of $\frac{1}{\alpha}\boldsymbol{\rho} = \mathbf{f}(\boldsymbol{\rho}, 1)$. Thus α^{LTE} is

$$\alpha^{\text{LTE}} = \rho_i^*/\mathrm{f}_i(\boldsymbol{\rho}^*, 1), \forall i \in \mathcal{I}. \tag{5.10}$$

For Wi-Fi, since the APs do not overlap and there is no interference among them, maximum demand scaling within each AP can be studied independently, and the bottleneck AP with the smallest achievable scaling factor gives α^{WiFi}. Denote by α_h^{WiFi} the

value for AP h, $\forall h \in \mathcal{H}$, we hence have

$$\alpha^{\text{WiFi}} = \min\{\alpha_1^{\text{WiFi}}, \alpha_2^{\text{WiFi}}, \ldots, \alpha_H^{\text{WiFi}}\}. \tag{5.11}$$

Consider $\mathrm{m}_h(\theta, \alpha)$, and we drop parameter θ that for the moment is given. From (5.6) and (5.7), $\mathrm{m}_h(\alpha)$ is linearly increasing in α. Therefore, $\mathrm{m}_h(\alpha_h^{\text{WiFi}}) = x^{\max}$ for $h \in \mathcal{H}$, as otherwise α_h^{WiFi} can be increased further. This, together with the linearity, implies that α_h^{WiFi} is the ratio between the amount of available resource and the required resource consumption by the baseline demand with $\alpha = 1$, i.e., $\alpha_h^{\text{WiFi}} = x^{\max}/\mathrm{m}_h(1)$.

Thus far, the results apply to fixed spectrum allocation θ. In the following, we consider θ as optimization variable, and study $\alpha^{\text{LTE}}(\theta)$ and $\alpha^{\text{WiFi}}(\theta)$ as functions of θ, to enable the characterization of optimal θ. The formal definition of $\alpha^{\text{LTE}}(\theta)$ is given below, and $\alpha^{\text{WiFi}}(\theta)$ is defined similarly for Wi-Fi.

$$\alpha^{\text{LTE}}(\theta) = \max_{\boldsymbol{\rho}} \ \alpha \text{ s.t. } \boldsymbol{\rho} = \mathbf{f}(\boldsymbol{\rho}, \theta, \alpha), \boldsymbol{\rho} \leqslant \boldsymbol{\rho}^{\max} \tag{5.12}$$

Lemma 4. *$\alpha^{\text{LTE}}(\theta)$ is continuous and monotonically increasing in θ.*

Proof. Given any $\theta \in [0, 1)$, denote the optimum of (5.12) by $\dot{\boldsymbol{\rho}}$. Consider $\theta' \geqslant \theta$. By (5.3) and (5.4), $\mathbf{f}(\dot{\boldsymbol{\rho}}, \theta, \alpha^{\text{LTE}}(\theta)) \geqslant \mathbf{f}(\dot{\boldsymbol{\rho}}, \theta', \alpha^{\text{LTE}}(\theta))$. Hence $\dot{\boldsymbol{\rho}}$ along with θ' is feasible to (5.12), and by (5.3) and (5.4) it leads to the objective no smaller than $\alpha^{\text{LTE}}(\theta)$, thus, $\alpha^{\text{LTE}}(\theta) \leqslant \alpha^{\text{LTE}}(\theta')$, hence monotonicity follows. We then prove continuity. By (5.3) and (5.4), for any sufficiently small positive number ε, there exists $\boldsymbol{\delta} = (\delta_1, \delta_2, \ldots, \delta_I)^T$, such that $\mathrm{f}_i(\dot{\boldsymbol{\rho}}, \theta, \alpha^{\text{LTE}}(\theta)) = \mathrm{f}_i(\dot{\boldsymbol{\rho}}, \theta - \delta_i, \alpha^{\text{LTE}}(\theta) - \varepsilon)$, $\forall i \in \mathcal{I}$. Let $\delta_{\min} = \min_{i \in I} \delta_i$, we have $\mathrm{f}_i(\dot{\boldsymbol{\rho}}, \theta - \delta_{\min}, \alpha^{\text{LTE}}(\theta) - \varepsilon) \leqslant \mathrm{f}_i(\dot{\boldsymbol{\rho}}, \theta - \delta_i, \alpha^{\text{LTE}}(\theta) - \varepsilon) = \mathrm{f}_i(\dot{\boldsymbol{\rho}}, \theta, \alpha^{\text{LTE}}(\theta))$, $\forall i \in \mathcal{I}$. Since $\mathbf{f}(\dot{\boldsymbol{\rho}}, \theta - \delta_{\min}, \alpha^{\text{LTE}}(\theta) - \varepsilon) \leqslant \mathbf{f}(\dot{\boldsymbol{\rho}}, \theta, \alpha^{\text{LTE}}(\theta)) = \dot{\boldsymbol{\rho}}$, we have $\mathbf{f}^{k+1}(\dot{\boldsymbol{\rho}}, \theta - \delta_{\min}, \alpha^{\text{LTE}}(\theta) - \varepsilon) \leqslant \mathbf{f}^{k}(\dot{\boldsymbol{\rho}}, \theta - \delta_{\min}, \alpha^{\text{LTE}}(\theta) - \varepsilon)$, $\forall k \geqslant 0$. Let $\boldsymbol{\rho}' = \lim_{k \to \infty} \mathbf{f}^k(\dot{\boldsymbol{\rho}}, \theta - \delta_{\min}, \alpha^{\text{LTE}}(\theta) - \varepsilon)$. At convergence, $\boldsymbol{\rho}' = \mathbf{f}(\boldsymbol{\rho}', \theta - \delta_{\min}, \alpha^{\text{LTE}}(\theta) - \varepsilon) \leqslant \dot{\boldsymbol{\rho}}$. Hence $\boldsymbol{\rho}'$ along with $\theta - \delta_{\min}$ is feasible to (5.12) and leads to $\alpha^{\text{LTE}}(\theta) - \varepsilon$, thus $\alpha^{\text{LTE}}(\theta - \delta_{\min}) \geqslant \alpha^{\text{LTE}}(\theta) - \varepsilon$. Similarly, $\alpha^{\text{LTE}}(\theta + \delta_{\min}) \leqslant \alpha^{\text{LTE}} + \varepsilon$. By the monotonicity, for any θ' with $\theta - \delta_{\min} < \theta' < \theta + \delta_{\min}$, $\alpha^{\text{LTE}}(\theta) - \varepsilon < \alpha^{\text{LTE}}(\theta') < \alpha^{\text{LTE}}(\theta) + \varepsilon$, proving continuity. Hence the conclusion follows. □

By (5.6) and (5.11), $\alpha^{\text{WiFi}}(\theta)$ is linearly decreasing in θ. This with Lemma 2 shows that at most one intersection point of $\alpha^{\text{WiFi}}(\theta)$ and $\alpha^{\text{LTE}}(\theta)$ exists, yielding the following result.

Theorem 3. *The optimum of (5.9) is the intersection point of* $\alpha^{\text{WiFi}}(\theta)$ *and* $\alpha^{\text{LTE}}(\theta)$ *if* $\alpha^{\text{WiFi}}(0) \geqslant \alpha^{\text{LTE}}(0)$. *Otherwise the optimum is* $\alpha^{\text{WiFi}}(0)$.

Proof. By (5.6), (5.7) and (5.11), $\lim_{\theta \to 1} \alpha^{\text{WiFi}}(\theta) = 0$. By Lemma 2, $\lim_{\theta \to 1} \alpha^{\text{LTE}}(\theta) > 0$, i.e., $\lim_{\theta \to 1} \alpha^{\text{LTE}}(\theta) > \lim_{\theta \to 1} \alpha^{\text{WiFi}}(\theta)$. If $\alpha^{\text{WiFi}}(0) \geqslant \alpha^{\text{LTE}}(0)$, there exists a point where $\alpha^{\text{WiFi}}(\theta)$ and $\alpha^{\text{LTE}}(\theta)$ intersect. This point is the optimum α of (5.9) by Lemma 3. Otherwise, if $\alpha^{\text{WiFi}}(0) < \alpha^{\text{LTE}}(0)$, no intersection point exists. The optimum is $\min\{\alpha^{\text{LTE}}(0), \alpha^{\text{WiFi}}(0)\}$, i.e., $\alpha^{\text{WiFi}}(0)$ due to Lemma 1. Hence the result. □

Algorithm 1 Maximum demand scaling

Input: $\check{\theta}$, $\hat{\theta}$, ϵ_θ

1: $\theta \leftarrow 0$, $\check{\theta} \leftarrow 0$, $\hat{\theta} \leftarrow 1$
2: Compute $\alpha^{\text{LTE}}(\theta)$ by (5.10) and $\alpha^{\text{WiFi}}(\theta)$ by (5.11)
3: **if** $\alpha^{\text{WiFi}}(\theta) \geqslant \alpha^{\text{LTE}}(\theta)$ **then**
4: **repeat**
5: $\theta \leftarrow (\check{\theta} + \hat{\theta})/2$
6: Compute $\alpha^{\text{LTE}}(\theta)$ and $\alpha^{\text{WiFi}}(\theta)$
7: **if** $\alpha^{\text{WiFi}}(\theta) \geqslant \alpha^{\text{LTE}}(\theta)$ **then**
8: $\check{\theta} \leftarrow \theta$
9: **if** $\alpha^{\text{WiFi}}(\theta) < \alpha^{\text{LTE}}(\theta)$ **then**
10: $\hat{\theta} \leftarrow \theta$
11: **until** $\hat{\theta} - \check{\theta} \leqslant \epsilon_\theta$

return $\alpha^{\text{WiFi}}(\theta)$

By the theoretical results, we present Algorithm 1 for solving (5.9). If $\alpha^{\text{WiFi}}(0) < \alpha^{\text{LTE}}(0)$, then $\alpha^{\text{WiFi}}(0)$ is the optimum. Otherwise a bi-section search of θ is performed, where ϵ_θ is the accuracy tolerance. Note that in Line 6, while computing $\alpha^{\text{LTE}}(\theta)$, by (5.10), $\boldsymbol{\rho}^*$ needs to be calculated first.

5.4 Simulation Results

The network consists of seven LTE cells. In each cell, five APs are randomly and uniformly distributed. The ranges of a BS and AP are 500 m and 50 m, respectively. Each AP serves two native Wi-Fi UEs located randomly within the range. For every LTE cell, the UEs are of two groups. One consists of LWA UEs, served by both Wi-Fi and LTE

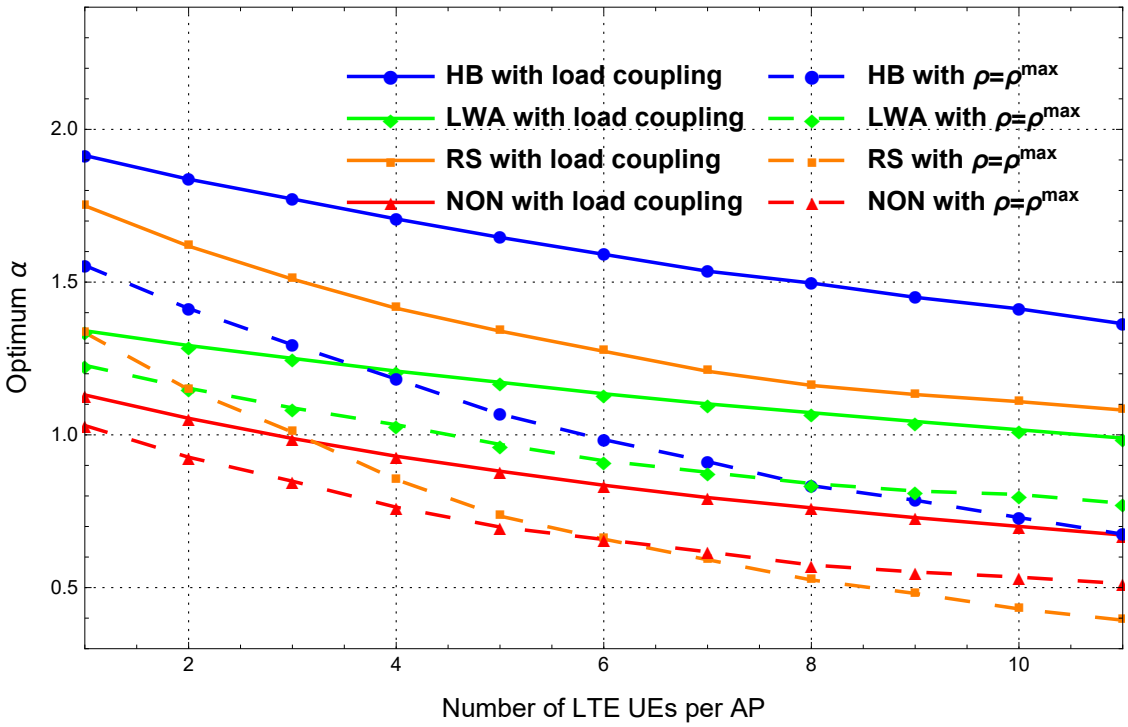

Figure 5.2: Optimum α with respect to the number of LTE UEs per Wi-Fi AP.

simultaneously. The other group consists of 30 native LTE UEs. Both licensed and unlicensed spectrum have a bandwidth of 20 MHz. The transmit power per RU for LTE and Wi-Fi are 200 mW and 20 mW, respectively. The noise power spectral density is -174 dBm/Hz. The simulation settings follow the 3GPP and IEEE 802.11ax standardization [16, 178]. For any LWA UE, the demand split coefficient $\beta = 0.4$. The path loss follows the COST-231-HATA model. The shadowing coefficients are generated by the log-normal distribution with 6 dB and 3 dB standard deviation for LTE and Wi-Fi, respectively. Both $\rho^{\max}$ and $x^{\max}$ equal to one. The simulations have been averaged over 1000 realizations, with $\epsilon_\theta = 10^{-6}$.

We refer to HB as the proposed hybrid method with both offloading via LWA and sharing of unlicensed spectrum. RS stands for using spectrum sharing only; this is equivalent to setting $\beta = 0$. LWA can be regarded as a special case of HB with demand split but no spectrum sharing ($\theta = 0$). Finally, NON is the baseline scheme with no demand split nor spectrum sharing. Fig. 5.2 shows the capacity in the achievable maximum scaling α with respect to the number of LTE UEs per AP. Compared to the worst case (i.e., $\boldsymbol{\rho} = \boldsymbol{\rho}^{\max}$), the load coupling model gives a more realistic picture. In particular, the maximum demand scaling with load coupling is considerably higher compared to the worst case. For HB and LWA, the optimal α value is given by Algorithm 1. For RS and NON,

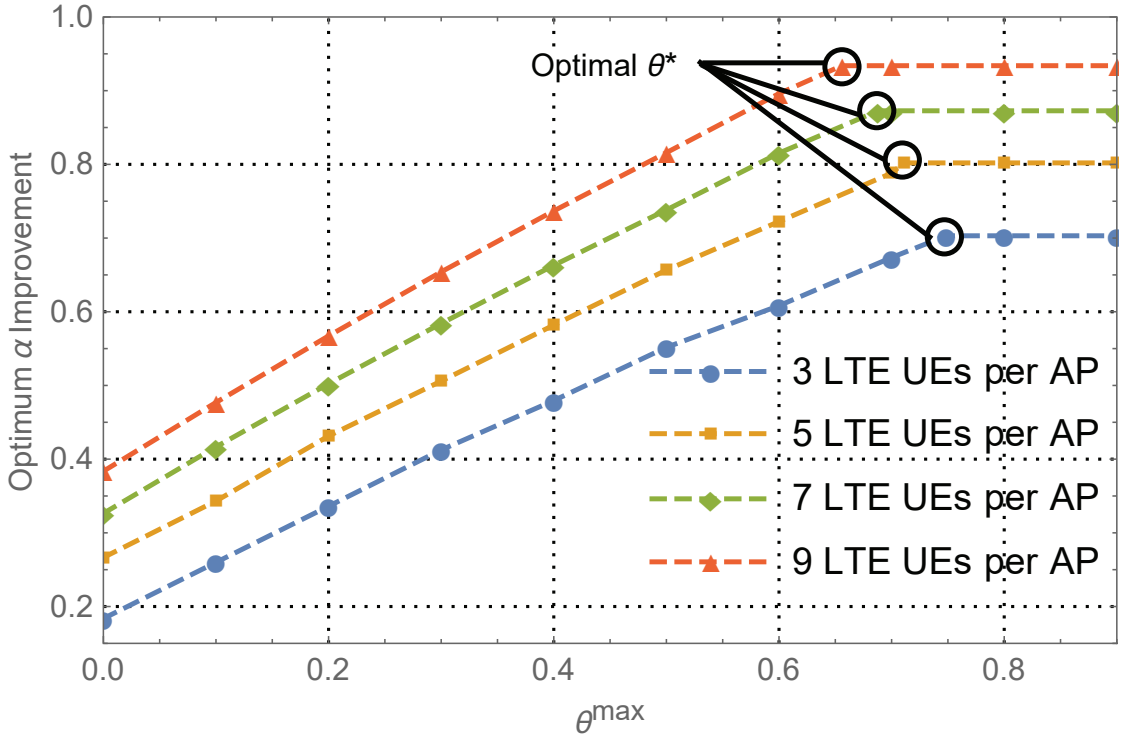

Figure 5.3: Percentage improvement of HB over NON in respect of available θ.

the optimum is $\min\{\alpha^{\text{LTE}}(0), \alpha^{\text{WiFi}}(0)\}$. From the figure, HB, RS, and LWA all outperform the baseline scheme NON. Note that HB has a clear effect of leveraging synergy of LWA and spectrum sharing, showing clearly better performance than LWA and RS. One benefit of having $\beta > 0$, which is the case of HB, is the reduction of interference in the LTE network, and this is particularly beneficial if the system is interference limited. Moreover, RS performs better than LWA, indicating the lack of spectrum is a bottleneck (for the LTE native UEs). Furthermore, the advantage of LWA is more obvious in denser user regime, where more UEs could be served by LTE and Wi-Fi simultaneously.

Fig. 5.3 reveals the impact of the amount of unlicensed spectrum made available to LTE. We introduce $\theta^{\max}$ and require $\theta \leqslant \theta^{\max}$. The vertical axis represents the percentage improvement of HB over NON. From the figure, $\theta^{\max}$ has a clear effect on performance. The improvement curves are approximately linear, until $\theta^{\max}$ reaches θ^*, after which the curves become flat, i.e., the Wi-Fi system is now the bottleneck. Moreover, it is apparent that the optimal allocation, i.e., θ^*, varies by the number of UEs served by Wi-Fi, demonstrating the significance of the optimizing spectrum allocation when LTE-U and LWA are jointed used.

5.5 Conclusion

We have derived an optimization algorithm for the performance of adopting both LWA and LTE-U. The results demonstrate that the improvement is very significant from a capacity enhancement standpoint. A future work is to include the demand split coefficient into the optimization.

Chapter 6

Performance Optimization for Joint Wi-Fi Offloading and LTE-U in Multi-Cell Networks

6.1 Introduction

6.1.1 Background and Motivation

Unlicensed spectrum utilization in LTE networks is a promising technique to meet the massive traffic demand [1]. There are two effective methods to use unlicensed bands for delivering LTE traffic. One is called Wi-Fi offloading, which focuses on offloading LTE traffic to Wi-Fi. An alternative method is LTE-unlicensed (LTE-U), which aims to directly use LTE protocols and infrastructures over the unlicensed spectrum. In two recent surveys [1, 181], it has been pointed out that addressing the above two methods simultaneously could further improve the system performance. Motivated by this, we consider joint Wi-Fi offloading and LTE-U, and examine the resulting performance potential for capacity enhancement.

6.1.2 Main Results and Chapter Organization

The main contributions of this work are summarized as follows. We present a new system framework for computing the maximum demand scaling factor for all UEs in both Wi-Fi and multi-cell LTE networks. The LTE and Wi-Fi systems are inter-connected by Wi-Fi offloading and inter-system spectrum sharing. More specifically, similar to [111],

the power gain-based UE offloading scheme is investigated in this chapter. Furthermore, we employ the orthogonal spectrum sharing scheme to address the coexistence issue of LTE and Wi-Fi in unlicensed bands. The LTE cells in our work are subject to load-coupling due to inter-cell interference. Our framework is a significant extension of the one used in [101–103, 105, 119–123]. Based on this framework, we jointly optimize UE association and inter-system spectrum sharing, while accounting for the resource limits as well as inter-cell interference. To solve the proposed problem, we first consider a restricted UE offloading scheme, and then prove that this problem restriction leads to no loss of optimality and generality. Next we provide theoretical analysis for the restricted optimization problem, resulting in an algorithm that achieves global optimality. Finally, we show numerically how the joint optimization scheme can be used to scale up UE demands. The obtained results reveal how joint LTE-U and Wi-Fi offloading improve the network capacity.

In the following, we discuss the fundamental differences between our investigated problems and those, e.g., [111] considering the single-cell scenario. In our case, not only each LTE cell needs to ensure the performance of the Wi-Fi network within its coverage, but the load-coupling among all cells is also required to be considered. For load-coupled cells, the interference that one cell generates to other cells depends on the resource allocation in this cell. The amounts of resource to meet the demand requirement for all cells are coupled together, but not independent to each other. Thus optimizing joint UE association and inter-system spectrum sharing within one cell leads to a chain reaction among other cells. In summary, in this chapter, the time-frequency resource allocation, the UE association and spectrum sharing between LTE and Wi-Fi in all cells are coupled together. Therefore, each cell cannot be optimized independently, and applying the solution approach proposed by the single cell case to the load-coupled multi-cell case guarantees neither feasibility nor optimality.

The rest of this chapter is organized as follows. The system model is given in Section 6.2. Section 6.3 formulates the problem. Section 6.4 presents the problem reduction with restricted UE offloading scheme. Section 6.5 derives our solution method for the problem solving. After discussing the numerical results in Section 6.6, we conclude the chapter in Section 6.7.

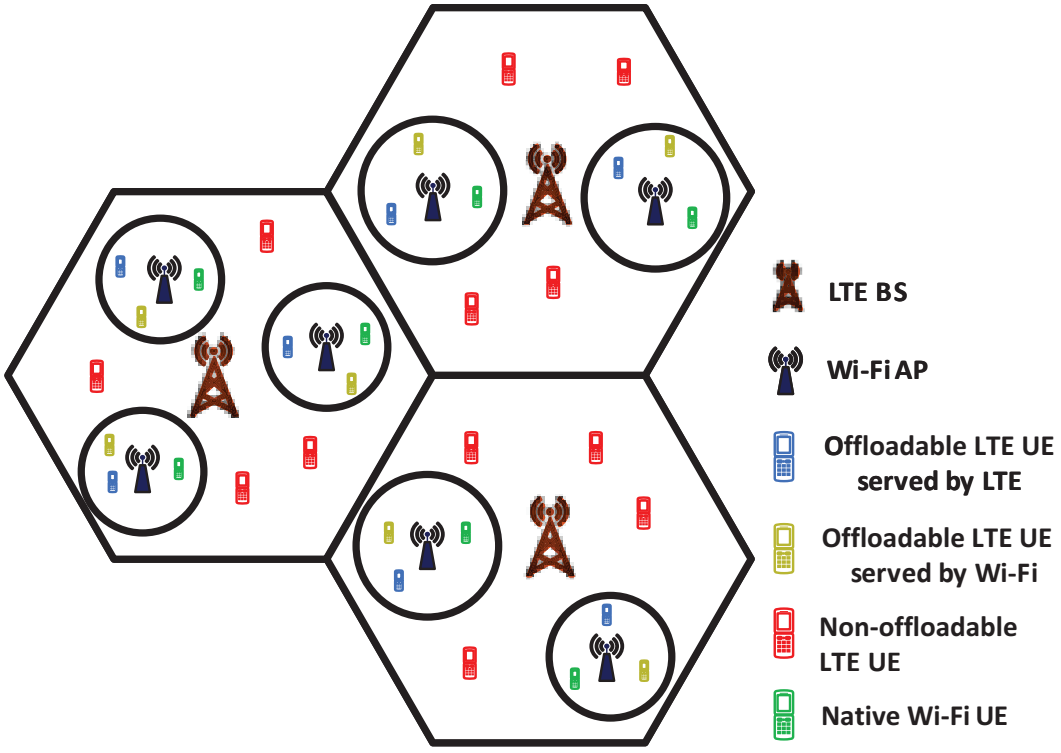

Figure 6.1: System model for joint LTE-U and Wi-Fi Offloading.

6.2 System Model

6.2.1 Network Model

As illustrated in Fig. 6.1, we consider a scenario with I LTE BSs, $\mathcal{I} = \{1, 2, \cdots, I\}$, and H Wi-Fi APs, $\mathcal{H} = \{1, 2, \cdots, H\}$. There can be one or multiple APs inside an LTE cell, and each AP is located entirely in one cell. The coverage areas of the APs do not overlap, and therefore there is no interference among the APs. This assumption has also been adopted in the literature, such as [182, 183]. An LTE BS is able to offload UEs to those APs within its coverage. Denote by $\mathcal{J}$ the set of UEs. The LTE UEs are of two groups. One consists of offloadable LTE UEs, that are inside the Wi-Fi coverage areas. There are J^{OFF} offloadable LTE UEs in total, forming set $\mathcal{J}^{\text{OFF}} = \{1, 2, \cdots, J^{\text{OFF}}\}$. The offloadable LTE UEs covered by cell $i \in \mathcal{I}$ is denoted by $\mathcal{J}_i^{\text{OFF}}$. Denote by $\mathcal{J}_h^{\text{OFF}}$ the set of LTE UEs that can be offload to AP $h \in \mathcal{H}$. The other group consists of non-offloadable LTE UEs. This LTE UE set is denoted by $\mathcal{J}_i^{\text{LTE}}$ for cell i. There also exist native Wi-Fi UEs, which are served by Wi-Fi only. Denote by $\mathcal{J}_h^{\text{WiFi}}$ the set of native Wi-Fi UEs served by AP h.

The Wi-Fi deploys the IEEE 802.11ax protocol, and works in the 5 GHz unlicensed

spectrum. Note the IEEE 802.11ax Task Group has defined the uplink and downlink Orthogonal Frequency-division Multiple Access (OFDMA). In our work, the resource unit (RU) refers to the minimum unit for both LTE and IEEE 802.11ax Wi-Fi resource allocation in OFDMA. The LTE system operates on the licensed band, and at the same time shares the unlicensed band with Wi-Fi by LTE-U. A cell or AP serves its UEs by orthogonal (i.e., non-overlapping) use of RUs. Denote by M^{L} and M^{U} the numbers of RUs in licensed and unlicensed bands, respectively.

To avoid inter-system interference, we assume orthogonal spectrum allocation by employing the duty-cycle method as in [100, 184], where the unlicensed band is periodically divided into two time periods for the LTE and Wi-Fi systems. We use an optimization variable $\theta \in (0, 1]$ to represent the proportion of unlicensed band allocated for Wi-Fi. Therefore the rest $1-\theta$ is for LTE. The existence of native Wi-Fi UEs implies $\theta > 0$.

In this chapter, we investigate the power gain-based UE offloading scheme. To be more specific, if UE $k \in \mathcal{J}_h^{\text{OFF}}$ is offloaded to AP $h \in \mathcal{H}$, any UE $j \in \mathcal{J}_h^{\text{OFF}} \backslash \{k\}$ that has a same or larger power gain with respect to h compared to k is also served by h. For any UE $j \in \mathcal{J}^{\text{OFF}}$, denote by z_j the offloading indicator variable where $z_j = 1$ shows that UE j is served by Wi-Fi and $z_j = 0$ by LTE otherwise. Denote by g_{hj} the power gain between AP h and UE j. Specifically,

$$z_j \geqslant z_k \; \forall j, k \in \mathcal{J}_h^{\text{OFF}} : g_{hj} \geqslant g_{hk}, \forall h \in \mathcal{H}. \tag{6.1}$$

We assume that there exists an inter-system coordinator, which performs the UE offloading and resource allocation of the unlicensed band, as in [184, 185]. Remark that the joint optimization of UE association and unlicensed bands resource allocation will be investigated in the reminder of this chapter.

6.2.2 LTE Load Coupling

For LTE, let ρ_j represent the proportion of RUs allocated to UE j by j's serving cell i, and denote by ρ_i the fraction of RU consumption in cell $i \in \mathcal{I}$ that are scheduled for serving its UEs. The entity ρ_i complies to the definition of the cell load [101]. By the definition of ρ_i ($i \in \mathcal{I}$), we have

$$\rho_i = \sum_{j \in \mathcal{J}_i^{\text{LTE}}} \rho_j + \sum_{j \in \mathcal{J}_i^{\text{OFF}} : z_j = 0} \rho_j. \tag{6.2}$$

Network-wisely, $\boldsymbol{\rho} = (\rho_1, \rho_2, \ldots, \rho_I)^T$, with uniform upper limit $\rho^{\max}$ that is at most one. We need to keep $\rho_i \leqslant \rho^{\max}$ ($i \in \mathcal{I}$), otherwise the network is overloaded, meaning that the available resource is not sufficient for delivering the demands. In the load-coupling model, to take into account inter-cell interference, the signal-to-interference-and-noise ratio (SINR) computation over one RU uses the cell load levels. In particular, the SINR at UE j served by cell i is modeled as [101]

$$\gamma_j(\boldsymbol{\rho}) = \frac{p_i g_{ij}}{\sum_{k \in \mathcal{I} \setminus \{i\}} p_k g_{kj} \rho_k + \sigma^2}, \tag{6.3}$$

where p_i represents the transmit power per RU of BS i, g_{ij} refers to the power gain between cell i and UE j, and σ^2 is the noise power. The term g_{kj}, $k \neq i$, refers to the power gain from the interfering BSs. Intuitively for any RU in cell i, ρ_k is interpreted as the likelihood that the served UEs of cell i receive interference from k. Note that interference is zero if cell k is not utilizing any resource. By the load-coupling model in [102, 103, 105, 119], the interference that UE j receives from other cells is modeled by the term $\sum_{k \in \mathcal{I} \setminus \{i\}} p_k g_{kj} \rho_k$.

Given the SINR, the achieved data rate for LTE UE j served by cell i, if all the $M^{\mathrm{L}} + (1-\theta)M^{\mathrm{U}}$ LTE RUs are given to j, is expressed as

$$C_j^{\mathrm{LTE}}(\boldsymbol{\rho}, \theta) = (M^{\mathrm{L}} + (1-\theta)M^{\mathrm{U}}) B \log_2(1 + \gamma_j(\boldsymbol{\rho})), \tag{6.4}$$

where B denotes the bandwidth of one RU.

Denote by r_j the baseline demand of UE $j \in \mathcal{J}$. We would like to scale up r_j by a demand scaling factor $\alpha > 0$. The physical meaning of α will be discussed in detail in Section 6.3. If UE j is served by LTE, then $\alpha r_j / C_j^{\mathrm{LTE}}(\boldsymbol{\rho}, \theta)$ gives the proportion of required LTE RUs for satisfying the scaled demand. The formal definition of the minimum proportion of RUs that cell i needs to satisfy the scaled demand of UE j is

$$\mathrm{f}_j(\boldsymbol{\rho}, z_j, \theta, \alpha r_j) = \begin{cases} \dfrac{\alpha r_j (1 - z_j)}{C_j^{\mathrm{LTE}}(\boldsymbol{\rho}, \theta)}, \forall j \in \mathcal{J}_i^{\mathrm{OFF}} \\ \dfrac{\alpha r_j}{C_j^{\mathrm{LTE}}(\boldsymbol{\rho}, \theta)}, \forall j \in \mathcal{J}_i^{\mathrm{LTE}}. \end{cases} \tag{6.5}$$

Taking the sum of (6.5) over cell i's UEs gives the required proportion of resource consumption in cell i, i.e.,

$$\mathrm{f}_i(\boldsymbol{\rho}, \boldsymbol{z}, \theta, \alpha \boldsymbol{r}) = \sum_{j \in \mathcal{J}_i^{\mathrm{LTE}} \cup \mathcal{J}_i^{\mathrm{OFF}}} \mathrm{f}_j(\boldsymbol{\rho}, z_j, \theta, \alpha r_j). \tag{6.6}$$

We present (6.6) in vector form for the LTE network as below.

$$\begin{aligned}&\mathbf{f}(\boldsymbol{\rho}, \boldsymbol{z}, \theta, \alpha\boldsymbol{r})\\&= [\mathrm{f}_1(\boldsymbol{\rho}, \boldsymbol{z}, \theta, \alpha\boldsymbol{r}), \mathrm{f}_2(\boldsymbol{\rho}, \boldsymbol{z}, \theta, \alpha\boldsymbol{r}), \ldots, \mathrm{f}_I(\boldsymbol{\rho}, \boldsymbol{z}, \theta, \alpha\boldsymbol{r})].\end{aligned} \tag{6.7}$$

Given $\boldsymbol{z}$, θ, α and $\boldsymbol{r}$, $\mathbf{f}(\boldsymbol{\rho})$ is a standard interference function (SIF) [180]. Given $\boldsymbol{\rho}^{(t)}$ ($t \geqslant 0$) and any $\boldsymbol{\rho}^{(0)} \in \mathbb{R}_+^I$, one fixed point iteration computes the next iterate $\boldsymbol{\rho}^{(t+1)}$ by $\boldsymbol{\rho}^{(t+1)} = \mathbf{f}(\boldsymbol{\rho}^{(t)})$. If $\lim_{t\to\infty} \mathbf{f}(\boldsymbol{\rho}^{(t)})$ exists, it is unique for any $\boldsymbol{\rho}^{(0)} \geqslant 0$, and also the unique solution of $\boldsymbol{\rho} = \mathbf{f}(\boldsymbol{\rho})$.

For allocating sufficient proportion of RUs to satisfy UE j's scaled demand, we have

$$\rho_j = \mathrm{f}_j(\boldsymbol{\rho}, z_j, \theta, \alpha r_j), \forall j \in \mathcal{J}_i^{\text{LTE}} \cup \mathcal{J}_i^{\text{OFF}}. \tag{6.8}$$

Putting the pieces together, we have

$$\rho_i = \mathrm{f}_i(\boldsymbol{\rho}, \boldsymbol{z}, \theta, \alpha\boldsymbol{r}), \forall i \in \mathcal{I}. \tag{6.9}$$

In vector form, we obtain the load coupling equation as follows

$$\boldsymbol{\rho} = \mathbf{f}(\boldsymbol{\rho}, \boldsymbol{z}, \theta, \alpha\boldsymbol{r}). \tag{6.10}$$

The equation (6.10) cannot be readily solved in closed form, as the load $\boldsymbol{\rho}$ appears in both sides of the equation. To be more specific, the load ρ_i for cell i affects the load ρ_k of other cells $k \neq i$, which would in turn affect the load ρ_i. Therefore, the load-coupling model leads to a non-linear equation system, and analysis using this model is not straightforward.

6.2.3 Rate and Resource Characterization for Wi-Fi

The capacity of a Wi-Fi network deploying the conventional protocol, e.g., IEEE 802.11n can be analyzed using a discrete-time Markov chain (DTMC) model, e.g., [113]. However, in our case, it is less reasonable to analyze the Wi-Fi capacity using queueing theory, since the DTMC model does not consider the actual SINR, which is a key parameter in case of OFDMA.

For IEEE 802.11ax Wi-Fi, the required proportion of resource consumption that AP $h \in \mathcal{H}$ has to use to meet the scaled demand of UE j reads

$$\mathrm{m}_j(z_j, \theta, \alpha r_j) = \begin{cases} \dfrac{\alpha r_j z_j}{C_j^{\text{WiFi}}(\theta)}, \forall j \in \mathcal{J}_h^{\text{OFF}} \\ \dfrac{\alpha r_j}{C_j^{\text{WiFi}}(\theta)}, \forall j \in \mathcal{J}_h^{\text{WiFi}}, \end{cases} \tag{6.11}$$

where $C_j^{\text{WiFi}}(\theta) = \theta M^{\text{U}} B \log(1 + \frac{p_h g_{hj}}{\sigma^2})$, with θM^{U} referring to the total number of Wi-Fi RUs. Denote by p_h the transmit power per RU of AP h. The sum of (6.11) over AP h's UEs gives the following function of AP h, which we also present in vector form for the Wi-Fi network.

$$\mathrm{m}_h(\boldsymbol{z}, \theta, \alpha\boldsymbol{r}) = \sum_{j \in \mathcal{J}_h^{\text{OFF}} \cup \mathcal{J}_h^{\text{WiFi}}} \mathrm{m}_j(z_j, \theta, \alpha\boldsymbol{r}). \tag{6.12}$$

$$\mathbf{m}(\boldsymbol{z}, \theta, \alpha\boldsymbol{r}) = [\mathrm{m}_1(\boldsymbol{z}, \theta, \alpha\boldsymbol{r}), \mathrm{m}_2(\boldsymbol{z}, \theta, \alpha\boldsymbol{r}) \ldots, \mathrm{m}_H(\boldsymbol{z}, \theta, \alpha\boldsymbol{r})]. \tag{6.13}$$

Denote by x_{hj} the proportion of RUs allocated to UE j. The level of resource consumption in any AP $h \in \mathcal{H}$ is

$$x_h = \sum_{j \in \mathcal{J}_h^{\text{WiFi}}} x_j + \sum_{j \in \mathcal{J}_h^{\text{OFF}}: z_j = 1} x_j. \tag{6.14}$$

The value in (6.14) is bounded by $x^{\max}$ that is at most one (i.e., all RUs are used), i.e., $x_h \leqslant x^{\max}$ ($h \in \mathcal{H}$). For later use, we define $\boldsymbol{x} = (x_1, x_2, \ldots, x_H)^T$. Similar to (6.9), we have that

$$x_h = \mathrm{m}_h(\boldsymbol{z}, \theta, \alpha\boldsymbol{r}), \forall h \in \mathcal{H} \tag{6.15}$$

holds in order to meet the scaled demand requirement. Network-wisely, we have

$$\boldsymbol{x} = \boldsymbol{m}(\boldsymbol{z}, \theta, \alpha\boldsymbol{r}). \tag{6.16}$$

6.3 Problem Formulation and Description

Given the same UE and baseline demand distribution but the increase in the demand requirement, the optimization task is to compute the maximum demand scaling factor α. The maximum α shows how much increase can still be accommodated by the network. In this sense, maximizing demand scaling factor is equivalent to maximizing the network capacity. We jointly optimize spectrum sharing between LTE and Wi-Fi as well as UE association, while accounting for the resource limits and interference between LTE cells.

The optimization problem can be formalized as

$$\alpha^* = \max_{\boldsymbol{\rho},\boldsymbol{x},\boldsymbol{z},\theta} \ \alpha \tag{6.17a}$$

$$\text{s.t.} \quad z_j \geqslant z_k \ \forall j,k \in \mathcal{J}_h^{\text{OFF}} : g_{hj} \geqslant g_{hk}, \forall h \in \mathcal{H} \tag{6.17b}$$

$$\boldsymbol{\rho} = \mathbf{f}(\boldsymbol{\rho}, \boldsymbol{z}, \theta, \alpha\boldsymbol{r}) \tag{6.17c}$$

$$\boldsymbol{x} = \boldsymbol{m}(\boldsymbol{z}, \theta, \alpha\boldsymbol{r}) \tag{6.17d}$$

$$\boldsymbol{\rho} \leqslant \boldsymbol{\rho}^{\max} \tag{6.17e}$$

$$\boldsymbol{x} \leqslant \boldsymbol{x}^{\max} \tag{6.17f}$$

$$\theta \in (0,1], z_j \in \{0,1\}, \forall j \in \mathcal{J}^{\text{OFF}} \tag{6.17g}$$

Constraint (6.17b) imposes the power gain-based UE offloading scheme. Constraints (6.17c) and (6.17d) ensure that sufficient time-frequency resources are allocated for satisfying the UE's demands, taking into account the scaling factor α. As imposed by (6.17c) and (6.17d), the UEs in $\mathcal{J}$ can be viewed as being throughput-oriented, and delivering more demands leads to higher satisfaction. Thus solving (6.17) yields a network-level evaluation for UE data rate enhancement. Constraints (6.17e) and (6.17f) represent the resource limits. For compactness, entities $\boldsymbol{\rho}$, $\boldsymbol{x}$, $\boldsymbol{z}$ and $\boldsymbol{r}$ in the constraints are in vector form.

Note solving (6.17) is indeed identical to optimize the level of quality-of-service (QoS) satisfaction subject to the max-min fairness. More specifically, define β_{LTE} and β_{WiFi} the minimum level of QoS satisfaction among all LTE links and all Wi-Fi links, respectively. The level of QoS satisfaction is equivalent to the ratio of the feasible transmission rate to the required baseline demand. The formal definition of β_{LTE}, β_{WiFi} are

$$\beta_{\text{LTE}} = \min_{j \in \mathcal{J}^{\text{LTE}} \cup \mathcal{J}^{\text{OFF}} : z_j = 0} \frac{C_j^{\text{LTE}}(\boldsymbol{\rho}, \theta)\rho_j}{r_j}, \tag{6.18}$$

$$\beta_{\text{WiFi}} = \min_{j \in \mathcal{J}^{\text{WiFi}} \cup \mathcal{J}^{\text{OFF}} : z_j = 1} \frac{C_j^{\text{WiFi}}(\theta)x_j}{r_j}. \tag{6.19}$$

Let $\beta = \min\{\beta_{\text{LTE}}, \beta_{\text{WiFi}}\}$. Thus the utility β represents the minimum level of QoS satisfaction among all links. Consider the optimization problem below.

$$\max_{\boldsymbol{\rho},\boldsymbol{x},\boldsymbol{z},\theta} \ \beta \tag{6.20a}$$

$$\text{s.t.} \quad (6.17\text{b}), (6.17\text{e}) - (6.17\text{g})$$

$$\boldsymbol{\rho} = \beta\mathbf{f}(\boldsymbol{\rho}, \boldsymbol{z}, \theta, \boldsymbol{r}) \tag{6.20b}$$

$$\boldsymbol{x} = \beta\boldsymbol{m}(\boldsymbol{z}, \theta, \boldsymbol{r}) \tag{6.20c}$$

By (6.5) and (6.6), we have $\beta \mathbf{f}(\boldsymbol{\rho}, \boldsymbol{z}, \theta, \boldsymbol{r}) = \mathbf{f}(\boldsymbol{\rho}, \boldsymbol{z}, \theta, \beta\boldsymbol{r})$. Similarly by (6.11) and (6.12), $\beta \boldsymbol{m}(\boldsymbol{z}, \theta, \boldsymbol{r}) = \boldsymbol{m}(\boldsymbol{z}, \theta, \beta\boldsymbol{r})$. Thus obviously the optimum of (6.20) is optimal to (6.17).

In addition, the maximum demand scaling factor can be regarded as the satisfaction ratio of the UE demands. Given base demand r_j and the resource limit, the solution α^* obtained by solving (6.17) is the maximum achievable ratio of r_j with the resource limit. If r_j can be satisfied, we must have $\alpha^* \geqslant 1$, as otherwise the network is overloaded and α^* is a satisfiable proportion of the demands r_j ($j \in \mathcal{J}$).

As α is a scalar, the natural approach for obtaining α^* is to perform a bi-section search on an interval $[\check{\alpha}, \hat{\alpha}]$ confining α^*. For each trial of α, one needs to determine whether there exists θ and $\boldsymbol{z}$ such that both LTE and Wi-Fi have sufficient resource for delivering the scaled demand, accounting for the interference among LTE cells. Enumerating all θ and $\boldsymbol{z}$ gives the answer whether a trial α can be achieved or not. However, this exhaustive search does not scale, as θ is continuous and the size of the solution space of $\boldsymbol{z}$ is exponential in the number of APs. In the following, we will first consider a restricted UE offloading scheme in Section 6.4, and prove that this restricted problem does not lead to any loss of optimality or generality. We then show how to obtain the optimum for the problem restriction in Section 6.5. In general, our approach indeed provides a global optimum.

6.4 Problem Reduction with Restricted UE Offloading Scheme

To define the restricted UE offloading scheme, we index the UEs in set $\mathcal{J}^{\text{OFF}}$ in a specific way, as discussed below.

Consider first an arbitrary UE offloading solution, and let UE $j \in \mathcal{J}^{\text{OFF}}$ denote the UE offloaded to Wi-Fi AP $h \in \mathcal{H}$, i.e., $z_j = 1$, such that j has the smallest power gain with respect to AP h among all LTE UEs offloaded to this AP. In other words, for UE $k \in \mathcal{J}_h^{\text{OFF}}$, $z_k = 1$ if $g_{hk} \geqslant g_{hj}$ and $z_k = 0$ otherwise. Let $\theta_j(\alpha)$ represent the minimum proportion of unlicensed band required by Wi-Fi to meet the scaled demand of UEs served by the h-th Wi-Fi AP for scaling α. Note that in the rest of the chapter, unless otherwise specified, for each UE $j \in \mathcal{J}^{\text{OFF}}$, the index of the AP that covers j is omitted with no ambiguity. This is because an offloadable LTE UE is served by at most one AP, and the coverage areas of the APs are non-overlapping.

We now consider all the UEs in set $\mathcal{J}^{\text{OFF}}$. We order the UEs $j \in \mathcal{J}^{\text{OFF}}$ in the

ascending order of $\theta_j(\alpha)$, where $\theta_1(\alpha) \leqslant \theta_2(\alpha) \leqslant, \ldots, \leqslant \theta_{J^{\text{OFF}}}(\alpha)$. The UE index also represents its position in the sequence without loss of generality. Note that this ordering is used throughout the rest of this chapter. We address the computation of $\theta_j(\alpha)$ as follows. The formal definition of $\theta_j(\alpha)$ is

$$\theta_j(\alpha) = \min_{x_h, \theta} \ \theta \tag{6.21a}$$

$$\text{s.t.} \quad z_k = 1 \quad \forall k \in \mathcal{J}_h^{\text{OFF}} : g_{hj} \leqslant g_{hk} \tag{6.21b}$$

$$z_k = 0 \quad \forall k \in \mathcal{J}_h^{\text{OFF}} : g_{hj} > g_{hk} \tag{6.21c}$$

$$x_h = m_h(\boldsymbol{z}, \theta, \alpha) \tag{6.21d}$$

$$x_h \leqslant x^{\max} \tag{6.21e}$$

Consider $m_h(\boldsymbol{z}, \theta, \alpha)$. From (6.11), (6.12) and the definition of $C_j^{\text{WiFi}}(\theta)$, $m_h(\boldsymbol{z}, \theta, \alpha)$ is linearly increasing in $1/\theta$. Therefore, $m_h(\boldsymbol{z}, \theta_j(\alpha), \alpha) = x^{\max}$ holds at optimum of (6.21), as otherwise $\theta_j(\alpha)$ can be decreased further. Thus $\theta_j(\alpha)$ is the ratio between the required resource consumption with $\theta = 1$, and the amount of available resource, i.e.,

$$\theta_j(\alpha) = m_h(\boldsymbol{z}, 1, \alpha)/x^{\max} \text{ s.t. (6.21b), (6.21c).} \tag{6.22}$$

Lemma 5. *$\theta_j(\alpha)$ is linearly increasing in α, $\forall j \in \mathcal{J}^{OFF}$.*

Proof. It follows from (6.11) and (6.12) that $m_h(\boldsymbol{z}, 1, \alpha)$ is linearly increasing in α, $\forall h \in \mathcal{H}$. Then from (6.22), for any $j \in \mathcal{J}^{\text{OFF}}$, $\theta_j(\alpha)$ is linearly increasing in α as well. □

Lemma 6 shows that the ordering of $j \in \mathcal{J}^{\text{OFF}}$ is independent of α.

Lemma 6. *For any $\alpha_1, \alpha_2 > 0$, if $\theta_j(\alpha_1) \leqslant \theta_k(\alpha_1)$, then $\theta_j(\alpha_2) \leqslant \theta_k(\alpha_2)$, $\forall j, k \in \mathcal{J}^{\text{OFF}}$.*

Proof. By Lemma 5, for any $j, k \in \mathcal{J}^{\text{OFF}}$, both $\theta_j(\alpha)$ and $\theta_k(\alpha)$ are linearly increasing in α, thus there exists at most one point where $\theta_j(\alpha)$ and $\theta_k(\alpha)$ intersect, and $\lim_{\alpha \to 0} \theta_j(\alpha) = \lim_{\alpha \to 0} \theta_k(\alpha) = 0$. Therefore there is no point of intersection of $\theta_j(\alpha)$ and $\theta_k(\alpha)$ since $\alpha > 0$. In other words, the size relationship of $\theta_j(\alpha)$ and $\theta_k(\alpha)$ remains unchanged with α. Hence the conclusion follows. □

The considered restricted UE offloading scheme is defined as follows. That is, if the UE $k \in \mathcal{J}^{\text{OFF}}$ is offloaded to the Wi-Fi system, any UE $j \in \mathcal{J}^{\text{OFF}} \backslash \{k\}$ that has a smaller UE index than k is also served by Wi-Fi. Specifically we have

$$z_j \geqslant z_k \ \forall j, k \in \mathcal{J}^{\text{OFF}} : j \leqslant k. \tag{6.23}$$

In Section 6.5, we will maximize α under the above restricted UE offloading scheme, as formulated below

$$\alpha' = \max_{\boldsymbol{\rho},\boldsymbol{x},\boldsymbol{z},\theta} \alpha \text{ s.t. (6.17c)} - \text{(6.17g)}, \text{(6.23)}. \tag{6.24}$$

Recall that for the original problem defined in (6.17), for any AP $h \in \mathcal{H}$, the number of the candidate offloading solutions equals to the number of offloadable LTE UEs inside h. The exhaustive search on $\boldsymbol{z}$ does not scale in (6.17), since one needs to consider all the possible combinations of the offloading solutions of the APs. In other words, the solution space of $\boldsymbol{z}$ in (6.17) is exponential in the number of APs. The optimization problem (6.24) is a restriction of (6.17). In (6.24), the size of the solution space of $\boldsymbol{z}$ is $J^{\text{OFF}} + 1$, thus the exhaustive search of solutions in $\boldsymbol{z}$ does scale.

As shown in Lemma 7, we prove that the problem restriction does not lead to any loss of optimality, i.e., $\alpha^* = \alpha'$.

Lemma 7. *The optimum of* (6.24) *is optimal to* (6.17).

Proof. We first prove $\alpha^* \geqslant \alpha'$. For any two UEs $k, j \in \mathcal{J}^{\text{OFF}}$ covered by $h \in \mathcal{H}$, if $k \leqslant j$, i.e., $\theta_k(\alpha) \leqslant \theta_j(\alpha)$, then by the definition of $\theta_k(\alpha)$ and $\theta_j(\alpha)$, we have $g_{hk} \geqslant g_{hj}$. Therefore, any solution that fulfils (6.23) also satisfies (6.17b). In other words, the solution space of (6.24) is a subspace of that of (6.17). Hence we have $\alpha^* \geqslant \alpha'$.

We then prove $\alpha^* \leqslant \alpha'$. Suppose that $\langle \boldsymbol{\rho}^*, \boldsymbol{x}^*, \boldsymbol{z}^*, \theta^* \rangle$ is an optimal solution of (6.17). Without loss of generality, suppose in $\boldsymbol{z}^*$, UE j has the largest UE index among all LTE UEs offloaded to Wi-Fi. Let h denote the AP serving j. If $\boldsymbol{z}^*$ satisfies (6.23), obviously $\langle \boldsymbol{\rho}^*, \boldsymbol{x}^*, \boldsymbol{z}^*, \theta^* \rangle$ is feasible in (6.24), and hence $\alpha^* \leqslant \alpha'$. Otherwise, if $\boldsymbol{z}^*$ does not fulfil (6.23), then in $\boldsymbol{z}^*$, there exists some UE $k \in \mathcal{J}^{\text{OFF}}$ with $k < j$, $k \notin \mathcal{J}_h^{\text{OFF}}$ and $z_k^* = 0$. In such case, consider another offloading solution $\boldsymbol{z'}$, where UEs $1, 2, \ldots, j$ are offloaded. Obviously, $\boldsymbol{z'}$ fulfils (6.23). Consider replacing $\boldsymbol{z}^*$ with $\boldsymbol{z'}$. In both $\boldsymbol{z'}$ and $\boldsymbol{z}^*$, since UE j has the largest UE index among all LTE UEs offloaded to Wi-Fi, as proved earlier, it has the smallest power gain with respect to AP h among all LTE UEs offloaded to this AP. Therefore, we have $m_h(\boldsymbol{z}^*, \theta^*, \alpha^*) = m_h(\boldsymbol{z'}, \theta^*, \alpha^*)$. In $\boldsymbol{z'}$, for the same reason, for any UE k offloaded to Wi-Fi, $\theta_k(\alpha^*) \leqslant \theta_j(\alpha^*)$ holds. This, together with (6.22), shows that for any $h' \in \mathcal{H}$, $m_{h'}(\boldsymbol{z'}, 1, \alpha^*) \leqslant m_h(\boldsymbol{z'}, 1, \alpha^*)$. From (6.11), (6.12) and the definition of $C_j^{\text{WiFi}}(\theta)$, both $m_h(\boldsymbol{z}, \theta, \alpha)$ and $m_{h'}(\boldsymbol{z}, \theta, \alpha)$ are linearly increasing in $1/\theta$. Therefore, $m_{h'}(\boldsymbol{z'}, \theta^*, \alpha^*) \leqslant m_h(\boldsymbol{z'}, \theta^*, \alpha^*)$ also holds. Since $m_h(\boldsymbol{z}^*, \theta^*, \alpha^*) \leqslant x^{\max}$ holds by definition and $m_h(\boldsymbol{z}^*, \theta^*, \alpha^*) = m_h(\boldsymbol{z'}, \theta^*, \alpha^*)$, we have $m_{h'}(\boldsymbol{z'}, \theta^*, \alpha^*) \leqslant$

$x^{\max}$. Let $\boldsymbol{x'} = \boldsymbol{m}(\boldsymbol{z'}, \theta^*, \alpha^*)$, we have $\boldsymbol{x'} \leqslant \boldsymbol{x}^{\max}$. In addition, from (6.4)-(6.7), we have $\boldsymbol{\rho^*} = \mathbf{f}(\boldsymbol{\rho^*}, \boldsymbol{z^*}, \theta^*, \alpha^*) > \mathbf{f}(\boldsymbol{\rho^*}, \boldsymbol{z'}, \theta^*, \alpha^*)$. Let $\boldsymbol{\rho^*} = \mathbf{f}(\boldsymbol{\rho^*}, \boldsymbol{z'}, \theta^*, \alpha^+)$. By (6.5) and (6.6), we have $\alpha^+ > \alpha^*$. In summary, $\langle \boldsymbol{\rho^*}, \boldsymbol{x'}, \boldsymbol{z'}, \theta^* \rangle$ is feasible in (6.24) and leads to an objective larger than α^*. Therefore $\alpha' \geqslant \alpha^*$. Hence the conclusion $\alpha^* = \alpha'$ follows. □

6.5 Optimization Under Restricted UE Offloading Scheme

Lemma 7 shows that solving (6.24) is equivalent to solving (6.17). In this section, we will present how to obtain the optimum α' of (6.24). Similar to (6.17), the natural approach for obtaining α' is to perform a bi-section search.

Consider an arbitrary trial α in the bi-section search process. Given $\boldsymbol{z}$, if there exists a solution $\langle \boldsymbol{\rho}, \boldsymbol{x}, \boldsymbol{z}, \theta \rangle$ such that (6.17c)-(6.17g) can be satisfied, then this α can be achieved by $\boldsymbol{z}$, otherwise not. Enumerating all $\boldsymbol{z}$ gives the answer whether α can be achieved or not. Since the size of the solution space of $\boldsymbol{z}$ in (6.24) is $J^{\text{OFF}} + 1$, this exhaustive search does scale. In the following, we consider a generic UE offloading solution $\bar{\boldsymbol{z}}$ satisfying (6.23), Without loss of generality, suppose in $\bar{\boldsymbol{z}}$, UEs up to $j \in \{0, 1, 2, \cdots, J^{\text{OFF}}\}$ are offloaded, i.e., for UE $k \in \mathcal{J}^{\text{OFF}}$, $\bar{z}_k = 1$ if $k \leqslant j$, otherwise $\bar{z}_k = 0$.

Denote by $\bar{\theta}_j(\alpha)$ the minimum proportion of unlicensed spectrum resource required by Wi-Fi for satisfying α. The formal definition of $\bar{\theta}_j(\alpha)$ is

$$\bar{\theta}_j(\alpha) = \min_{\boldsymbol{x}, \theta} \ \theta \tag{6.25a}$$

$$\text{s.t.} \quad \boldsymbol{x} = \boldsymbol{m}(\bar{\boldsymbol{z}}, \theta, \alpha) \tag{6.25b}$$

$$\boldsymbol{x} \leqslant \boldsymbol{x}^{\max} \tag{6.25c}$$

$$\bar{z}_k = 1, \forall k \in \mathcal{J}^{\text{OFF}} : k \leqslant j \tag{6.25d}$$

$$\bar{z}_k = 0, \forall k \in \mathcal{J}^{\text{OFF}} : k > j. \tag{6.25e}$$

Recall that the coverage areas of the APs do not overlap, and there is no interference among the APs. Therefore, solving (6.25) can be carried out separately for the APs , and the bottleneck AP with the largest value gives $\bar{\theta}_j(\alpha)$. Taking into account the effects of (6.25b) and (6.25c), we hence have

$$\bar{\theta}_j(\alpha) = \max_{h \in \mathcal{H}} \ m_h(\bar{\boldsymbol{z}}, 1, \alpha)/x^{\max} \text{ s.t. (6.25d), (6.25e).} \tag{6.26}$$

Note that Wi-Fi has enough resource for delivering the demand with α if and only if $\bar{\theta}_j(\alpha) \leqslant 1$.

Lemma 8. *$\bar{\theta}_j(\alpha)$ is linearly increasing in α, $\forall j \in \{0, 1, 2, \cdots, J^{OFF}\}$.*

Proof. The proof is similar to that of Lemma 5. □

For the same offloading solution $\bar{\boldsymbol{z}}$ and demand scaling α, the proportion of unlicensed spectrum resource that LTE can use is no more than $1 - \bar{\theta}_j(\alpha)$, as otherwise scaling α cannot be achieved by the UEs served by Wi-Fi. From (6.4), (6.5) and (6.6), $\mathbf{f}(\boldsymbol{\rho}, \boldsymbol{z}, \theta, \alpha)$ is monotonically increasing in θ. Thus by (6.24), for the LTE system, α can be achieved by the offloading solution $\bar{\boldsymbol{z}}$ together with $\bar{\theta}_j(\alpha)$ and the resulting $\boldsymbol{\rho}$ if

$$\boldsymbol{\rho} = \mathbf{f}(\boldsymbol{\rho}, \bar{\boldsymbol{z}}, \bar{\theta}_j(\alpha), \alpha) \tag{6.27}$$

and

$$\boldsymbol{\rho} \leqslant \boldsymbol{\rho}^{\max}. \tag{6.28}$$

Given $\bar{\boldsymbol{z}}$, $\bar{\theta}_j(\alpha)$ and α, $\mathbf{f}(\boldsymbol{\rho})$ is an SIF [180]. The main property of an SIF is that a fixed point of (6.27), if exists, is unique and can be computed via fixed point iterations. Specifically, a vector $\boldsymbol{\rho}$ satisfying $\boldsymbol{\rho} = \mathbf{f}(\boldsymbol{\rho}, \bar{\boldsymbol{z}}, \bar{\theta}_j(\alpha), \alpha)$, if exists, is unique and can be obtained by the iterations $\boldsymbol{\rho}^{(t+1)} = \mathbf{f}(\boldsymbol{\rho}^{(t)}, \bar{\boldsymbol{z}}, \bar{\theta}_j(\alpha), \alpha)$ ($t \geqslant 0$) with any non-negative $\boldsymbol{\rho}^{(0)}$.

The theoretical derivations above enable Algorithm 2 for solving (6.24). The basic idea of Algorithm 2 is to perform a bi-section search on an interval $[\check{\alpha}, \hat{\alpha}]$ confining α'. For each trial of α, the algorithm goes through all the candidate UE offloading solutions to examine if there exists some $j \in \{0, 1, 2, \cdots, J^{\text{OFF}}\}$ such that 1) $\bar{\theta}_j(\alpha) \leqslant 1$; 2) $\boldsymbol{\rho} = \mathbf{f}(\boldsymbol{\rho}, \bar{\boldsymbol{z}}, \bar{\theta}_j(\alpha), \alpha)$ has a solution, which is no larger than $\boldsymbol{\rho}^{\max}$. If such j exists, then α can be achieved. In the algorithm, we use indi_j to denote the demand scaling indicator where $\text{indi}_j = 1$ shows that the demand scaling can be satisfied in $\bar{\boldsymbol{z}}$, as otherwise $\text{indi}_j = 0$.

To be more specific, for any $j \in \{0, 1, 2, \cdots, J^{\text{OFF}}\}$, Algorithm 2 first obtains $\bar{\theta}_j(\alpha)$ in Line 9, and finds out whether $\bar{\theta}_j(\alpha) > 1$ in Line 10. If yes, Wi-Fi does not have enough resource to deliver the scaled demand by $\bar{\boldsymbol{z}}$, i.e., $\text{indi}_j = 0$. Otherwise, if $0 < \bar{\theta}_j(\alpha) \leqslant 1$, starting from any non-negative $\boldsymbol{\rho}^{(0)}$, we compute $\lim_{t\to\infty} \mathbf{f}(\boldsymbol{\rho}^{(t)}, \bar{\boldsymbol{z}}, \bar{\theta}_j(\alpha), \alpha)$ iteratively. Note that the convergence rate of fixed point point iterations on $\mathbf{f}(\boldsymbol{\rho}, \bar{\boldsymbol{z}}, \bar{\theta}_j(\alpha), \alpha)$ is linear [186]. Fixed point iterations using $\mathbf{f}(\boldsymbol{\rho}, \bar{\boldsymbol{z}}, \bar{\theta}_j(\alpha), \alpha)$ are applied in Lines 13-18. Then the algorithm checks whether $\boldsymbol{\rho}^{(t)} \leqslant \boldsymbol{\rho}^{\max}$ in Line 19. If not, then at least one cell will be overloaded for meeting UE demands, i.e., $\text{indi}_j = 0$. Otherwise, the α under consideration can be satisfied by both LTE and Wi-Fi using $\bar{\boldsymbol{z}}$, i.e., $\text{indi}_j = 1$.

Algorithm 2 Maximum Demand Scaling

Input: $\boldsymbol{\rho}^{\max}$, $\mathbf{f}(\cdot)$, $\check{\alpha}$, $\hat{\alpha}$, ϵ_α, ϵ_ρ.

stat $\leftarrow$ achievable, $\text{indi}_j \leftarrow 1, \forall j \in \{0, 1, 2, \cdots, J^{\text{OFF}}\}$
repeat
  $\alpha \leftarrow (\check{\alpha} + \hat{\alpha})/2$
  for $j \in \{0, 1, 2, \cdots, J^{\text{OFF}}\}$ **do**
    $z_k \leftarrow 1, \forall k \in \mathcal{J}^{\text{OFF}} : k \leqslant j$
    $z_k \leftarrow 0, \forall k \in \mathcal{J}^{\text{OFF}} : k > j$
    if stat $=$ achievable and $\text{indi}_j = 0$ **then**
    else
      Compute $\bar{\theta}_j(\alpha)$ using (6.26)
      if $\bar{\theta}_j(\alpha) > 1$ **then**
        stat $\leftarrow$ unachievable, $\text{indi}_j \leftarrow 0$
      else
        $t \leftarrow 0$, $\boldsymbol{\rho}^{(0)} \leftarrow \boldsymbol{\rho}^{\max}$
        repeat
          $t \leftarrow t + 1$
          for $i \in \mathcal{I}$ **do**
            $\rho_i^{(t)} \leftarrow \mathrm{f}_i(\boldsymbol{\rho}^{(t-1)}, \boldsymbol{z}, \bar{\theta}_j(\alpha), \alpha)$
        until $\|\boldsymbol{\rho}^{(t)} - \boldsymbol{\rho}^{(t-1)}\|_\infty \leqslant \epsilon_\rho$
        if $\boldsymbol{\rho}^{(t)} \leqslant \boldsymbol{\rho}^{\max}$ **then**
          $\check{\alpha} \leftarrow \alpha$, stat $\leftarrow$ achievable, $\text{indi}_j \leftarrow 1$
          break
        else
          stat $\leftarrow$ unachievable, $\text{indi}_j \leftarrow 0$
  if stat $=$ unachievable **then**
    $\hat{\alpha} \leftarrow \alpha$
until $\hat{\alpha} - \check{\alpha} \leqslant \epsilon_\alpha$

Return α

Theorem 4. *The problem* (6.24) *can be optimally solved by Algorithm 2.*

Proof. Recall that α is a scalar. Suppose that $\langle \boldsymbol{\rho'}, \boldsymbol{x'}, \bar{\boldsymbol{z}}, \bar{\theta}_j(\alpha) \rangle$ is an optimal solution of (6.24). By (6.4), (6.5) and (6.6), $\mathbf{f}(\boldsymbol{\rho}, \boldsymbol{z}, \theta, \alpha)$ is monotonically increasing in θ and α. This, together with Lemma 8, shows that $\langle \boldsymbol{\rho'}, \boldsymbol{x'}, \bar{\boldsymbol{z}}, \bar{\theta}_j(\alpha - \phi) \rangle$ is also feasible to (6.24). In addition, Lemma 8 also shows that, for any positive value ϕ, if $\bar{\theta}_j(\alpha) > 1$, then $\bar{\theta}_j(\alpha + \phi) > 1$ also holds. In other words, if α cannot be satisfied with $\bar{\boldsymbol{z}}$, a higher demand scaling is also not achievable in the same offloading solution. Hence the conclusion. □

6.6 Simulation Results

In this section, we will present numerical results to verify our analysis and validate the performance of the proposed algorithm. The network for simulation consists of 19 hexagonal LTE cells, each of which has one BS in the center. In each cell, 5 APs are randomly and uniformly distributed. The ranges of a BS and an AP are 500 m and 50 m, respectively. Each cell serves 30 non-offloadable LTE UEs that are randomly and uniformly located within the range. Inside each AP, 5 native Wi-Fi UEs are randomly and uniformly distributed. Both licensed and unlicensed spectrum have a bandwidth of 20 MHz. The bandwidth of each RU is set to be 180 KHz. For LTE and Wi-Fi, the transmit power per RU are 200 mW and 20 mW, respectively. The noise power spectral density is set to be -174 dBm/Hz. The simulation settings follow the 3GPP and IEEE 802.11ax standardization [3, 178]. The path loss follows the COST-231-HATA model, with the shadowing coefficients generated by the log-normal distribution with 6 dB and 3 dB standard deviation for LTE and Wi-Fi, respectively. The resource limit $\rho^{\max}$ and $x^{\max}$ both equal to one. The simulations have been averaged over 1000 realizations, with convergence tolerances $\epsilon_\alpha = \epsilon_\rho = 10^{-6}$.

We refer to HB as the proposed hybrid method, i.e., LTE can offload UEs to Wi-Fi via Wi-Fi offloading and simultaneously share the unlicensed spectrum with Wi-Fi. Refer to NON as the baseline scheme with no spectrum sharing nor Wi-Fi offloading. The UE demand is set such that for the baseline, with $\alpha = 1$, there is at least one cell $i \in \mathcal{I}$ reaching the load limit ($\rho_i = \rho^{\max}$). RS stands for the use of inter-system spectrum sharing only; this can be regarded as a special case of HB with $\boldsymbol{z} = \mathbf{0}$. WO stands for using Wi-Fi offloading only; this is equivalent to setting $\theta = 1$. For the above four

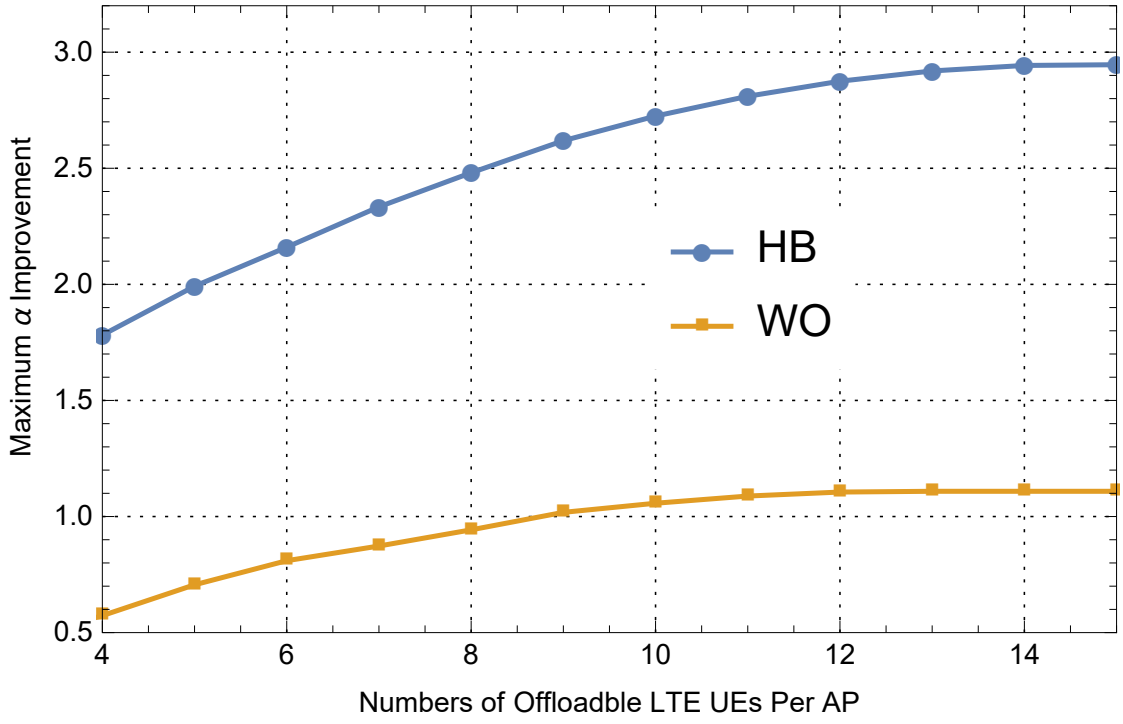

Figure 6.2: Percentage improvement of HB and WO over NON in respect of the number of offloadable LTE UEs per Wi-Fi AP.

schemes, the optimal α value is given by Algorithm 2.

Fig. 6.2 shows the percentage improvement of HB and WO over NON in terms of demand scaling α with respect to the number of offloadable LTE UEs per AP. From Fig. 6.2, both HB and WO outperform the baseline scheme NON. HB is better than WO, showing that optimizing the spectrum sharing between LTE and Wi-Fi can improve the capacity performance of the network. Another observation is that, for both HB and WO, with the number of offloadable LTE UEs increasing, the percentage improvement of achievable α increases at first, then saturates. Specifically, when Wi-Fi has enough resource for external offloading, the advantage of Wi-Fi offloading is more obvious in denser user regime, in which case more UEs could be offloaded to Wi-Fi. On the contrary, when Wi-Fi has no spare resource for external offloading, no more offloadable LTE UE is allowed to be offloaded to Wi-Fi, as otherwise the Wi-Fi network will be overloaded. In the latter case, adding more offloadable LTE UEs to the network leads to virtually no capacity improvement of HB and WO over NON.

We then study the impact of the maximum amount of unlicensed spectrum that Wi-Fi and LTE can use. Fig. 6.2 shows the percentage improvement of HB and RS over NON in terms of demand scaling α with respect to the percentage of available unlicensed

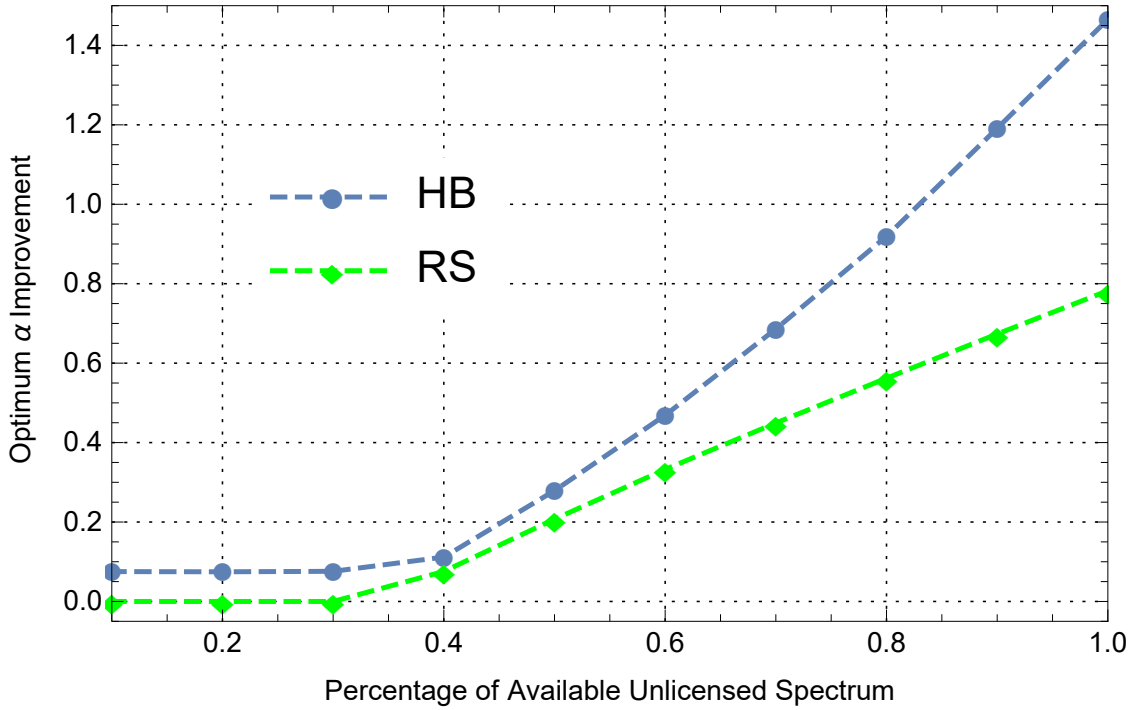

Figure 6.3: Percentage improvement of HB and RS over NON in respect of the percentage of available unlicensed spectrum.

spectrum. From the figure, both HB and RS are better than NON. HB also outperforms RS. One benefit of having $\boldsymbol{z} \neq \mathbf{0}$ is the reduction of interference in the LTE network; this is beneficial especially if the LTE network is interference limited. In general, though either Wi-Fi offloading and inter-system spectrum sharing helps in boosting capacity, the combination HB has a better performance than any of the two, since it has a clear effect of leveraging synergy. Another interesting observation from Fig. 6.2 is that utilizing more unlicensed RUs can increase the improvement of HB and RS over NON only when the number of unlicensed RUs is large enough. The percentage of available unlicensed spectrum has little impact on the improvement of HB and RS over NON when it is small (e.g. less than 0.2). In such case, Wi-Fi has to use all the unlicensed spectrum to meet the optimal α,.

Fig. 6.4 reveals the impact of the amount of unlicensed spectrum made available to Wi-Fi. Here we introduce $\theta^{\min}$ and require $\theta > \theta^{\min}$. The vertical axis represents the percentage improvement of HB over NON in terms of demand scaling. From the figure, $\theta^{\min}$ has a clear effect on performance. The percentage improvement of HB over NON increases when $\theta^{\min}$ becomes smaller, until $\theta^{\min}$ reaches θ^{*}, after which the curves becomes flat, i.e., the Wi-Fi system is now the bottleneck. Moreover, from the figure, it is

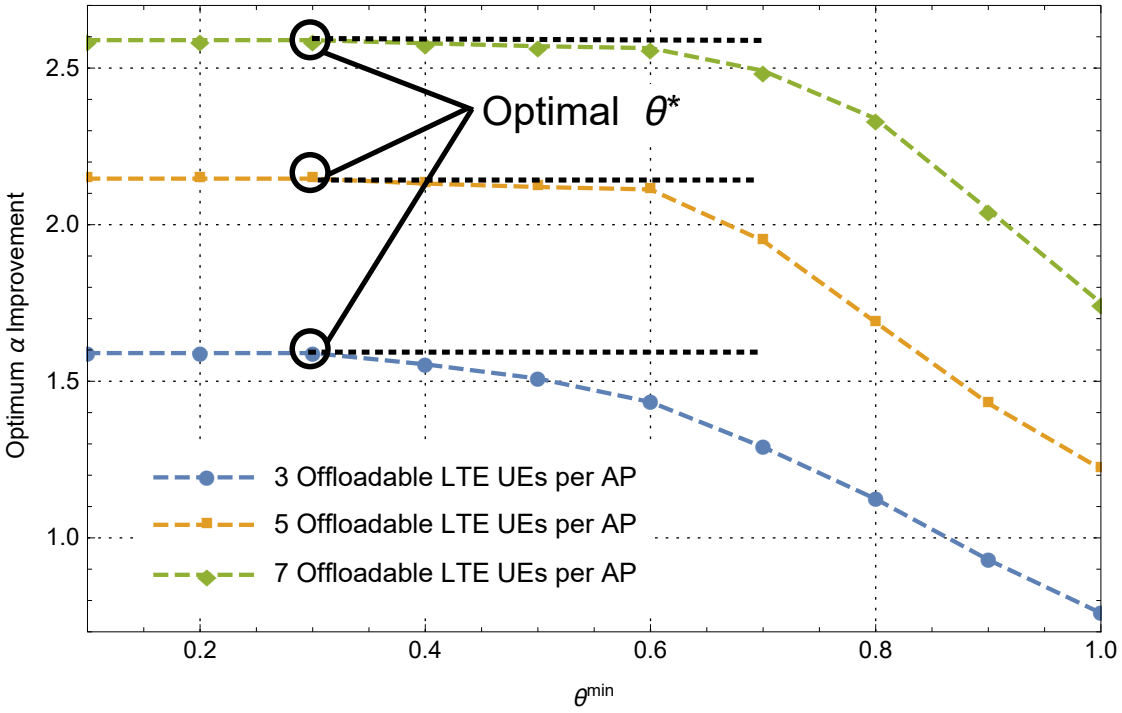

Figure 6.4: Percentage improvement of HB over NON in respect of the percentage of available θ.

apparent that the optimal allocation, i.e., θ^*, does not vary by the number of offloadable LTE UEs. This is because the value of θ^* is indeed equal to the minimum proportion of unlicensed spectrum resource required for satisfying the optimal α when there is no LTE UE offloaded to Wi-Fi.

6.7 Conclusion

In this chapter, we have derived an optimization algorithm to study the performance of adopting both Wi-Fi offloading and LTE-U. The results demonstrate that the improvement is very significant from a capacity enhancement standpoint and hence the joint approach is promising for future networks.

Chapter 7

Conclusions and Outlook

In this chapter, I summarize the contribution as well as the highlights of this thesis. The perspectives regarding the future work related to the topics presented in this thesis has also been discussed.

7.1 General Conclusions

This thesis mainly investigated several emerging technologies towards unlicensed spectrum utilization in LTE networks. The related research involves two major directions, including data offloading to the IEEE 802.11 based WLAN and the direct usage of LTE based networks over the unlicensed spectrum. In general, how to avoid severe performance degradation of the Wi-Fi network is a challenging issue of utilizing unlicensed spectrum in LTE networks. Specifically, first, the inter-system spectrum sharing, or, more specifically, the coexistence of LTE and Wi-Fi in the same unlicensed spectrum is the major challenge of implementing LTE-U. Second, to use the LTE and Wi-Fi integration approach, mobile operators have to manage two disparate networks in licensed and unlicensed spectrum. Third, optimization for joint data offloading to Wi-Fi and LTE-U in multi- cell scenarios poses more challenges because inter-cell interference must be addressed.

To solve the above challenges, first of all, two advanced technologies enabling LTE data offloading to the IEEE 802.11 based WLAN have been studied. It has been shown that a stochastic geometry model can be used to model and analyze the performance of an MPTCP Proxy-based LWPA network with intra-tier and cross-tier dependencies in large scale networks. An important feature of such network was studied, that is, the

activation conditions of a LWPA-mode Wi-Fi are determined by the user density, the CSMA distance, and their relevant locations to nearby closed-access Wi-Fi APs. The numerical results illustrate the impact of different network parameters on the performance of LWPA networks, which can be useful for further performance optimization. In the meantime, the performance of the LTE and Wi-Fi aggregation (LWA)-enabled network has also been studied using stochastic geometry. The previous LWA studies are based on one common assumption: a Wi-Fi AP serving LWA purpose is only able to offload bearers from LTE, and does not have its own UEs to serve. I motivate the use of superposition coding, so as to allow the Wi-Fi AP serving the purpose of LWA can simultaneously operate as the native-mode AP that serves Wi-Fi users only. When assuming bursty packet arrivals at the LTE node, I proposed a congestion control protocol and introduced queueing analysis in such network. The impact of the design parameters of the shared access protocol on the native Wi-Fi throughput has been analyzed. The results are essential for further investigations in larger topologies.

This thesis also takes a significant step of analyzing joint data offloading and the direct usage of LTE based networks over the unlicensed spectrum. There only exists a few works analyzing the joint use of these two technologies, and none of them considered multi-cell scenarios with arbitrary topologies. The performance optimization of multi-cell networks with LWA and LTE-U with sharing of the unlicensed band has been considered. This network model has also been extended to a more complex scenario, where UE association needs to be considered. In both chapters, Theoretical conclusions were derived to enable algorithms that achieve global optimality. Numerical results show the algorithms effectiveness and benefits of joint use of data offloading and the direct use of LTE over the unlicensed band. The main results of this thesis answered the question about how to model joint optimization for data offloading and inter-system spectrum sharing in joint Wi-Fi and load-coupled LTE networks and how to solve the resulting problems to optimality.

7.2 Highlight and Future Research Directions

In this section, I summarize the highlights in this thesis as well as those experiences learnt that will be useful for the future studies.

In general, LTE specifications may have to go beyond regulatory requirements to meet the levels of fairness that Wi-Fi stakeholders expect, namely that the impact of an

LTE SC is not greater than that of a Wi-Fi AP. That is because of the fact that the standards body for LTE represents the mobile operator and vendor ecosystems and indirectly the Wi-Fi performance. The backoff time defined in LTE-LAA plays an important role in how the traffic will be split between Wi-Fi and LTE-LAA and, hence, is a factor in how fair the coexistence will be [10].

There are many unexploited research topics related to my Ph.D thesis and further extensions of the studies that I have accomplished. In this section, I give a brief overview of the perspectives and possible extensions of this thesis.I provide several recommendations that may be useful to future research on LTE and Wi-Fi inter-working systems as well as the working process for LTE working in the unlicensed band.

a) **All technologies in the 5 GHz unlicensed band should have equal control for access to the medium.** Duty-cycling mechanisms targeting at the market with no LBT requirement allow the LTE-LAA to statically or dynamically define the proportion of a cycle allocated to LTE-LAA and the proportion allocated to Wi-Fi. It is unacceptable for an unlicensed spectrum that is supposed to be shared with preference. It is recommended that any sharing scheme should treat LTE-LAA and Wi-Fi as equals in future decisions about medium access.

b) **LTE-LAA medium sharing algorithms should be dynamically designed, and respond quickly to changing conditions.** A static medium sharing algorithms like LTE muting discussed in section 2.3.2 can cause unfairness and inefficiency. I recommend that any unlicensed medium sharing algorithms should be designed to dynamically respond to the changing needs of all users. In addition, the CSAT ON/OFF period varies from 50 ms to 200 ms in past design. These designs are not able to meet the requirement of Wi-Fi, which is more reactive to changes in load and contention, adjusting on a packet by packet basis. I further recommend that any unlicensed medium sharing algorithms should be designed to respond to load changes within a few packets transmission.

c) **More complex tests on fairness, especially those based on a range of realistic usage scenarios are needed.** The tests and simulation already done by LTE-U Forum and 3GPP are only based on relatively simple scenarios [7, 142]. In particular, both LTE-U Forum and Wi-Fi evaluate the performance of LTE-LAA and Wi-Fi coexistence, only with respect to indoor/outdoor scenarios. In fact, as will be discussed

in section 2.3.1, outdoor/indoor is just one of eight influential factors for the classification of SC scenarios. Studies in a range of realistic deployment scenarios and network densities are still missing. What's more, simulations done by 3GPP and LTE-U Forum consider limited traffic types. For example, It appears to be the simulation case with many obvious high density, high channel load missing from the set of simulations so far. In addition, there are some important metrics not captured in the current simulation and test, including packet loss, frame retransmission rate, packet loss and jitter, etc. I recommend researchers interested in this area refer to the performance evaluation metrics and scenarios organised in section 2.6, as well as test plan proposed by [146]. The community should also ensure that realistic simulation scenarios with both UL and DL traffic are considered.

d) **More researches on mechanisms for scenarios where LTE-LAA and Wi-Fi hear each other at a moderate interference level are required.** As discussed in section 2.3.1, some industry members believe that there is no effective coexistence technique to handle scenarios where LTE-LAA and Wi-Fi devices hear each other at moderate interference levels [143]. There are some reasons for their understanding. First, the Wi-Fi devices are not aware of the duty-cycled nature of the interference. When the interference is below Wi-Fi's energy detection threshold, Wi-Fi will attempt to transmit, even in the presence of significant interference not formally detected by the Wi-Fi. Transmitting during LTE-LAA's ON time leads to greater error rates and causes Wi-Fi to slow down. Second, the LTE-LAA interference is on the same order as the Wi-Fi signal, so that while LTE-LAA is on, the Wi-Fi communication can be very limited, even not possible at all. In fact, if the Wi-Fi client and AP hear the LTE eNB below/above energy detection, respectively, a hidden node scenario where only a few Wi-Fi devices can transmit data frames will appear. Their conclusion is congested by the rest of the community [144], which explains that the divergence in results was caused by the fact that the testing done in [143] is based on extremely pessimistic and impractical assumptions. Their disagreement shows at least two shortcomings of current research. First, there is no unified version of the exact values of both LTE-LAA and Wi-Fi energy detection threshold. Second, there is no unified test platform for the coexistence. Our recommendation is that future researches should focus on solving the above two problems.

e) **The community should seek a balance between fairness and performance.** As

stated above, coexistence such as LBT that increases fairness can have a negative effect on performance. The historical approach the Wi-Fi industry utilizes is to agree on the CSMA/CA access method instead of making an agreement on a definition of fairness. I recommend that LTE in the unlicensed band considers using a similar level of fairness that is common in Wi-Fi networks to reach a balance between fairness and performance.

f) **More researches concerning coexistence optimization are required.** In [24], fairness allocation between LTE-LAA and Wi-Fi is studied through theoretical and simulation analysis. However, literature is scarce and better mechanisms analysis might be needed. In general, while discussing the fairness, an objective function should be created to evaluate the user access or network serving. For markets with LBT requirement, researchers can refer the Wi-Fi scheduling fairness functions to create their own, since the LBT scheme is a simplified version of DCF. However, for markets without LBT, there is a need for new objective functions for optimization problem formulations to guarantee the fair coexistence of LTE-LAA and Wi-Fi. I also recommend researchers to optimize the coexistence of LTE-LAA and Wi-Fi separately rather than jointly. Optimizing LTE-LAA and Wi-Fi jointly requires information exchange between the two RANs, which further needs the LTE-LAA and Wi-Fi aggregation.

g) **More realistic traffic flow splitting and aggregation schemes are required.** The common feature among LWA , LWPA is that the network data traffic is traversing through LTE and WLAN links simultaneously. In chapter 3 and 4, I only consider a simple yet traffic flow splitting and aggregation scheme. In fact, various techniques and approaches for traffic flow splitting between the LTE and WLAN links have been considered in the literature. Multiple data traffic flows are aggregated at user terminal by different aggregation techniques, depending on at which level the aggregation between LTE and WLAN is effectuated. For each aggregation type, the protocol design and performance investigation will follow different approaches. For instance, in LWA, as a result of radio link aggregation that splits the bearers at PDCP level, an efficient bearer splitting and packet scheduling policy could maximize the advantages of LWA. While with LTE-WiFi path aggregation, the modeling and analysis on traffic splitting are mainly based on how to divide and aggregate the transport-layer data flow. Potential improvement can be achieved by developing scheduling algorithms

that take into account the instantaneous or average channel conditions, the packet arrival rate, the buffer state, and the users QoS requirement.

h) **More advanced coexistence mechanisms are required.** Chapter 5 and 6 considered a very simple coexistence mechanism. It is very interesting to consider more realistic mechanisms mentioned in Chapter 2. Indeed, the main issue in LTE-U and LTE-LAA types of networks is the coexistence between LTE and WiFi in unlicensed bands. The challenge is to design an adequate coexistence scheme to keep a balance in the unlicensed spectrum ecosystem and provide benefits to all the stakeholders. Existing mechanisms such as LBT and duty cycles could act as basic schemes for the interference coordination and fairness management. Therein, the design parameters of the LBT or duty-cycle play a critical role in the performance of these schemes. For instance, due to the transmitting power disparity between LTE stations and WiFi APs, applying LBT in LTE-U or LTE-LAA networks might significantly degrade the performance of existing Wi-Fi systems. The choice of the contention window and backoff time for LTE and WiFi users are extremely important to balance the expected performance between LTE and WiFi users. With duty-cycle techniques, the duty cycle period and the fraction of duty cycle to assign to LTE/WiFi users are the most important parameters. Depending on the goals of the coexistence scheme, the design parameters can be tuned in a way that certain utility functions are optimized under some practical constraints on the available resources. Besides the advantages of LBT and duty-cycle techniques, their functionality in LTE-LAA networks might degrade the advantages of LTE in terms of the scheduled transmissions. The tradeoff between fairness and other performance metrics is an important research direction in this area.

Bibliography

[1] B. Chen, J. Chen, Y. Gao, and J. Zhang, "Coexistence of LTE-LAA and Wi-Fi on 5 GHz with corresponding deployment scenarios: A survey," *IEEE Communications Surveys and Tutorials*, vol. 19, no. 1, pp. 7–32, Jan. 2017.

[2] A. K. Sadek, T. Kadous, K. Tang *et al.*, "Extending LTE to unlicensed band-merit and coexistence," in *Proc. 2015 IEEE Inter. Conf. on Commun. (ICC) Workshop on LTE in Unlicensed Bands (LTE-U)*, London, 2015.

[3] 3rd Generation Partnership Project; Feasibility Study on Licensed-Assisted Access to Unlicensed Spectrum; Study on Licensed-Assisted Access to Unlicensed Spectrum (Release 13), *3GPP TR 36.889 V13.0.0*, July. 2015.

[4] S. Hajmohammad and H. Elbiaze, "Unlicensed spectrum splitting between Femtocell and Wi-Fi," in *IEEE International Conference on Communications (ICC)*, Budapest, Jun. 2013.

[5] N. DOCOMO, "Views on LAA for Unlicensed Spectrum Scenarios and Initial Evaluation Results," *3GPP RAN1 standard contribution - (RWS-140026)*, Jun. 2014.

[6] S. Barr, C. Paasch, and O. Bonaventure, "Multipath TCP: From theory to practice," in *IFIP Networking, Valencia*, May 2011.

[7] Alcatel-Lucent, Ericsson, Qualcomm Technologies Inc., and Samsung Electronics & Verizon, "LTE-U Technical Report Coexistence Study for LTE-U SDL V1.3," Tech. Rep., Nov. 2015. [Online]. Available: http://www.lteuforum.org/uploads/3/5/6/8/3568127/lte-u_forum_lte-u_sdl_coexistence_specifications_v1.3.pdf

[8] R. Zhang, M. Wang, L. Cai *et al.*, "LTE-unlicensed: The future of spectrum ag-

gregation for cellular networks," *IEEE Wireless Commun.*, vol. 22, no. 3, pp. 150–159, Jun. 2015.

[9] Interdigital, "A Look at the Requirements for LTE in the Unlicensed Spectrum," *3GPP RAN1 standard contribution - (RWS-140006)*, Jun. 2014.

[10] "LTE unlicensed and Wi-Fi: Moving beyond coexistence," Report, Senza Fili, 2015. [Online]. Available: http://apps.fcc.gov/ecfs/document/view?id=60001076664

[11] Ericsson, "LTE Licensed Assisted Access," Jan. 2015. [Online]. Available: http://www.ericsson.com/res/thecompany/docs/press/media_kits/ericsson-license-assisted-access-laa-january-2015.pdf

[12] J. Jeon, H. Niu, Q. Li *et al.*, "LTE with listen-before-talk in unlicensed spectrum," in *Proc. 2015 IEEE Inter. Conf. on Commun. (ICC) Workshop on LTE in Unlicensed Bands (LTE-U)*, London, 2015, to be published.

[13] 3rd Generation Partnership Project; Evolved Universal Terrestrial Radio Access (E-UTRA); Carrier Aggregation; Base Station (BS) Radio Transmission and Reception (Rel 10), *3GPP TR 36.808 V10.1.0*, Jul. 2013.

[14] 3rd Generation Partnership Project; Evolved Universal Terrestrial Radio Access (E-UTRA); Carrier aggregation enhancements; User Equipment (UE) and Base Station (BS) radio transmission and reception (Rel 11), *3GPP TR 36.823 V11.1.0*, Nov. 2013.

[15] 3rd Generation Partnership Project; Requirements for further advancements for Evolved Universal Terrestrial Radio Access (E-UTRA) (LTE-Advanced) (Rel 12), *3GPP TR 36.913 V12.0.0*, Oct. 2014.

[16] 3rd Generation Partnership Project; Evolved Universal Terrestrial Radio Access (E-UTRA) and Evolved Universal Terrestrial Radio Access Network (E-UTRAN); Overall description; Stage 2 (Rel 13), *3GPP TR 36.300 V13.0.0*, Jul. 2015.

[17] AT&T, "Assisted Access for LTE," *3GPP RAN1 standard contribution - (RWS-140003)*, Jun. 2014.

[18] Y. Lee, T. C. Chuah, J. Loo, and A. Vine, "Recent Advances in Radio Resource Management for Heterogeneous LTE/LTE-A Networks," *IEEE Communications Surveys and Tutorials*, vol. 16, pp. 2142–2180, 2014.

[19] M. Wang, J. Zhang, B. Ren, W. Yang, J. Zou, M. Hua, and X. You, "The Evolution of LTE Physical Layer Control Channels: A Tutorial," *IEEE Communications Surveys and Tutorials*, vol. PP, pp. 1–1, 2015.

[20] G. Ku and J. M. Walsh, "Resource Allocation and Link Adaptation in LTE and LTE Advanced: A Tutorial," *IEEE Communications Surveys and Tutorials*, vol. 17, pp. 1605–1633, 2015.

[21] F. Ghavimi and H. Chen, "M2M Communications in 3GPP LTE/LTE-A Networks: Architectures, Service Requirements, Challenges, and Applications," *IEEE Communications Surveys and Tutorials*, vol. 17, pp. 525–549, 2015.

[22] A. Laya and L. Alonso and J. AlonsoZarate, "Is the Random Access Channel of LTE and LTE-A Suitable for M2M Communications? A Survey of Alternatives," *IEEE Communications Surveys and Tutorials*, vol. 16, pp. 4–16, 2014.

[23] A. Babaei, J. Andreoli-Fang, and B. Hamzeh, "On the impact of LTE-U on Wi-Fi performance," in *Proc. 2014 IEEE 25th Int. Symp. PIMRC*, Washington DC, Sept. 2014, pp. 1621–1625.

[24] A. K. Sadek, "Carrier sense adaptive transmission (CSAT) in unlicensed spectrum," U.S. Patent 20 150 085 841A1, Mar. 2015.

[25] A. Molisch, *Wireless Communications*. Wiley-IEEE Press, 2011, pp. 665–698.

[26] M. Mehaseb, Y. Gadallah, A. Elhamy, and H. ElHennawy, "Classification of LTE Uplink Scheduling Techniques: an M2M Perspective," *IEEE Communications Surveys and Tutorials*, vol. PP, pp. 1–1, 2015.

[27] J. Liu, N. Kato, J. Ma, and N. Kadowaki, "Device-to-Device Communication in LTE-Advanced Networks: A Survey," *IEEE Communications Surveys and Tutorials*, vol. 17, pp. 1923–1940, 2015.

[28] "Technical Specification Group Radio Access Network; Evolved Universal Terrestrial Radio Access (E-UTRA); Physical channels and mod-

ulation," Report, Sophia-Antipolis, Sept. 2012. [Online]. Available: http://www.3gpp.org/DynaReport/36.211.htm

[29] J. Zhang, L. Yang, L. Hanzo, and H. Gharavi, "Advances in Cooperative Single-Carrier FDMA Communications: Beyond LTE-Advanced," *IEEE Communications Surveys and Tutorials*, vol. 17, pp. 730–756, 2015.

[30] N. AbuAli, A. Taha, M. Salah, and H. Hassanein, "Uplink Scheduling in LTE and LTE-Advanced: Tutorial, Survey and Evaluation Framework," *IEEE Communications Surveys and Tutorials*, vol. 16, pp. 1239–1265, 2014.

[31] H. Lee and S. Vahid and K. Moessner, "A Survey of Radio Resource Management for Spectrum Aggregation in LTE-Advanced," *IEEE Communications Surveys and Tutorials*, vol. 16, pp. 745–760, 2014.

[32] *Part 11: Wireless LAN Medium Access Control (MAC) and Physical Layer (PHY) Specification*, IEEE Std. 802.11, 2013.

[33] J. Jeon, H. Niu, Q. Li *et al.*, "LTE in the unlicensed spectrum: Evaluating coexistence mechanisms," in *Proc. IEEE GLOBECOM Workshop 2014*, Austin, TX, Dec. 2014, pp. 740–745.

[34] N. Rupasinghe and I. Guvenc, "Licensed-assisted access for WiFi-LTE coexistence in the unlicensed spectrum," in *Proc. IEEE GLOBECOM Workshop 2014*, Austin, TX, Dec. 2014, pp. 894–899.

[35] E. Perahia and R. Stacey, *Next Generation Wireless LANs: Throughput, Robustness, and Reliability in 802.11n*. Cambridge University, 2008.

[36] C. Chen, R. Ratasuk, and A. Ghosh, "Downlink performance analysis of LTE and WiFi coexistence in unlicensed bands with a simple listen-before-talk scheme," in *Proc. 2015 IEEE 81st Vehic. Technol. Conf. (VTC)*, Glasgow, May. 2015, pp. 1–5.

[37] J. Cao and M. Ma and H. Li and Y. Zhang and Z. Luo, "A Survey on Security Aspects for LTE and LTE-A Networks," *IEEE Communications Surveys and Tutorials*, vol. 16, pp. 283–302, 2014.

[38] D. Xenakis and N. Passas and L. Merakos and C. Verikoukis, "Mobility Management for Femtocells in LTE-Advanced: Key Aspects and Survey of Handover

Decision Algorithms," *IEEE Communications Surveys and Tutorials*, vol. 16, pp. 64–91, 2014.

[39] G. Y. Li and J. Niu and D. Lee and J. Fan and Y. Fu, "Multi-Cell Coordinated Scheduling and MIMO in LTE," *IEEE Communications Surveys and Tutorials*, vol. 16, pp. 761–775, 2014.

[40] F. Capozzi and G. Piro and L. A. Grieco and G. Boggia and P. Camarda, "Downlink Packet Scheduling in LTE Cellular Networks: Key Design Issues and a Survey," *IEEE Communications Surveys and Tutorials*, vol. 15, pp. 678–700, 2013.

[41] E. Pateromichelakis and M. Shariat and A. ulQuddus and R. Tafazolli, "On the Evolution of Multi-Cell Scheduling in 3GPP LTE / LTE-A," *IEEE Communications Surveys and Tutorials*, vol. 15, pp. 701–717, 2013.

[42] R. Ratasuk, M. Uusitalo, N. Mangalvedhe *et al.*, "License-exempt LTE deployment in heterogeneous network," in *Proc. IEEE 2012 Int. Symp. on Wireless Communication Systems(ISWCS)*, Paris, Aug. 2012, pp. 246–250.

[43] R. Ratasuk, N. Mangalvedhe, and A. Ghosh, "LTE in unlicensed spectrum using licensed-assisted access," in *Proc. IEEE GLOBECOM 2014*, Austin, TX, Dec. 2014, pp. 746–751.

[44] A. Bhorkar, C. Ibars, A. Papathanassiou, and P. Zong, "Medium access design for lte in unlicensed band," in *Proc. 2015 IEEE Int. Workshop on Wireless Communications and Networking Conference (WCNC)*, New Orleans, LA, Mar. 2015, pp. 369–373.

[45] 3rd Generation Partnership Project; Evolved Universal Terrestrial Radio Access (E-UTRA); Further advancements for E-UTRA physical layer aspects (Rel 9), *3GPP TR 36.814 V9.0.0*, Mar. 2010.

[46] C. Kosta, B. Hunt, A. U. Quddus, and R. Tafazolli, "On Interference Avoidance Through Inter-Cell Interference Coordination (ICIC) Based on OFDMA Mobile Systems," *IEEE Communications Surveys and Tutorials*, vol. 15, pp. 973–995, 2013.

[47] E. Pateromichelakis, M. Shariat, A. U. Quddus, and R. Tafazolli, "On the Evo-

lution of Multi-Cell Scheduling in 3GPP LTE / LTE-A," *IEEE Communications Surveys and Tutorials*, vol. 15, pp. 701–717, 2013.

[48] A. S. Hamza, S. S. Khalifa, H. S. Hamza, and K. Elsayed, "A Survey on Inter-Cell Interference Coordination Techniques in OFDMA-Based Cellular Networks," *IEEE Communications Surveys and Tutorials*, vol. 15, pp. 1642–1670, 2013.

[49] A. Al-Dulaimi, S. Al-Rubaye, and E. Sousa, "5G communications race: Pursuit of more capacity triggers LTE in unlicensed band," *IEEE Trans. Commun.*, vol. 10, no. 1, pp. 43–51, Mar. 2015.

[50] Huawei, "Scenarios, spectrum considerations and preliminary assessment results of U-LTE," *3GPP RAN1 standard contribution - (RWS-140005)*, Jun. 2014.

[51] D. Ricker, *Echo Signal Processing*. Springer, 2003, p. 23.

[52] E. Charfi, L. Chaari, and L. Kamoun, "PHY/MAC Enhancements and QoS Mechanisms for Very High Throughput WLANs: A Survey," *IEEE Communications Surveys and Tutorials*, vol. 15, pp. 1714–1735, 2013.

[53] N. Valliappan and A. K. Sadek, "Long term evolution interference management in unlicensed bands for Wi-Fi operation," U.S. Patent 20 150 105 067A1, Apr. 2015.

[54] F. Chaves, E. Almeida, R. Vieira, A. Cavalcante, F. Abinader, S. Choudhury, and K. Doppler, "LTE UL power control for the improvement of LTE/Wi-Fi coexistence," in *Proc. 2013 IEEE 78th Vehic. Technol. Conf. (VTC)*, Las Vegas, NV, Sep. 2013, pp. 1–6.

[55] Nokia, "LTE in Unlicensed Spectrum : European Regulation and Co-Existence Considerations," *3GPP RAN1 standard contribution - (RWS-140002)*, Jun. 2014.

[56] Alcatel Lucen, "On the Standardisation of LTE in Unlicensed Spectrum," *3GPP RAN1 standard contribution - (RWS-140014)*, Jun. 2014.

[57] P. Nuggehalli, "LTE-WLAN Aggregation [Industry Perspectives]," *IEEE Wireless Communications*, vol. 23, no. 4, pp. 4–6, Aug. 2016.

[58] D. Laselva *et al.*, "3GPP LTE-WLAN Aggregation Technologies: Functionalities and Performance Comparison," *IEEE Communications Magazine*, vol. 56, no. 3, pp. 195–203, Mar. 2018.

[59] Q. Zhu *et al.*, "A Digital Polar Transmitter with DC-DC Converter Supporting 256-QAM WLAN and 40-MHz LTE-A Carrier Aggregation," *IEEE J. Solid-State Circuits*, vol. 52, no. 5, pp. 1196–1209, Mar. 2017.

[60] D. Lopez-Perez, D. Laselva, E. Wallmeier, P. Purovesi, and P. Lunden, "Long Term Evolution-Wireless Local Area Network Aggregation Flow Control," *IEEE Access*, vol. 4, pp. 9860–9869, Jan. 2017.

[61] Y. Lin, Y. Shih, and P. Chao, "Design and Implementation of LTE RRM With Switched LWA Policies," *IEEE Trans. on Veh. Technol.*, vol. 67, no. 2, pp. 1053–1062, Feb. 2018.

[62] Y. Ohta *et al.*, "Link Layer Structure for LTE-WLAN Aggregation in LTE-advanced and 5G Network," in *Proc. IEEE Conf. Standards Commun. Netw. (CSCN)*. IEEE, Oct. 2015, pp. 83–88.

[63] S. Singh *et al.*, "Optimal Traffic Aggregation in Multi-RAT Heterogeneous Wireless Networks," in *Proc. IEEE Int. Conf. Commun. Wksp. (ICC)*. IEEE, May 2016, pp. 626–631.

[64] H. Zhang *et al.*, "Inter-eNB Flow Control for Heterogeneous Networks with Dual Connectivity," in *Proc. IEEE Veh. Technol. Conf. (VTC)*. IEEE, May 2015, pp. 1–5.

[65] S. Borst *et al.*, "Optimal Path Selection in Multi-RAT Wireless Networks," in *Proc. IEEE INFOCOM Wksp.* IEEE, Apr. 2016, pp. 592–597.

[66] B. Liu *et al.*, "Delay-Aware LTE WLAN Aggregation in Heterogeneous Wireless Network," *IEEE Access*, vol. 6, pp. 14 544–14 559, Apr. 2016.

[67] 3GPP, "TS 36.300 V. 13.3.0 Evolved Universal Terrestial Radio Access Network (E-UTRAN) Evolved Universal Terrestrial Radio Access (EUTRA) and Evolved Universal Terrestrial Radio Access Network (E-UTRAN); Overall Description; Stage 2," Tech. Rep., 2016.

[68] IEEE 802.11: Wireless LAN Medium Access Control(MAC) and Physical Layer (PHY) Specifications, *IEEE-SA, DOI:10.1109/IEEESTD.2012.6178212*, Apr. 2012.

[69] D. Tse *et al.*, *Fundamentals of wireless communication*. Cambridge University, 2005.

[70] S. Vanka *et al.*, "Superposition Coding Strategies: Design and Experimental Evaluation," *IEEE Trans. Wireless Commun.*, vol. 11, no. 7, pp. 2628–2639, July 2012.

[71] S. M. R. Islam *et al.*, "Power-Domain Non-Orthogonal Multiple Access (NOMA) in 5G Systems: Potentials and Challenges," *IEEE Commun. Surveys Tuts.*, vol. 19, no. 2, pp. 721–742, Second Quarter 2012.

[72] T. Cover, "An Achievable Rate Region for the Broadcast Channel," *IEEE Transactions on Information Theory*, vol. 21, no. 4, pp. 399–404, July 1975.

[73] Q. Zhao, L. Tong, A. Swami, and Y. Chen, "Decentralized Cognitive MAC for Opportunistic Spectrum Access in Ad Hoc Networks: A POMDP Framework," *IEEE Journal on Sel. Areas in Commun.*, vol. 25, no. 3, pp. 589–600, Apr. 2007.

[74] R. Urgaonkar and M. Neely, "Opportunistic Scheduling with Reliability Guarantees in Cognitive Radio Networks," *IEEE Trans. on Mobile Computing*, vol. 8, no. 6, pp. 766–777, June 2009.

[75] A. Fanous and A. Ephremides, "Stable Throughput in a Cognitive Wireless Network," *IEEE Journal on Sel. Areas in Commun.*, vol. 31, no. 3, pp. 523–533, Mar. 2013.

[76] S. Ghez and S. Verdu, "Stability Property of Slotted Aloha with Multipacket Reception Capability," *IEEE Trans. Autom. Control*, vol. 33, no. 7, pp. 640–649, Jul. 1988.

[77] V. Naware, G. Mergen, and L. Tong, "Stability and Delay of Finite-user Slotted Aloha with Multipacket Reception," *IEEE Trans. Inf. Theory*, vol. 51, no. 7, pp. 2636–2656, Jul. 2005.

[78] A. Rabbachin, T. Q. S. Quek, H. Shin, and M. Z. Win, "Cognitive Network Interference," *IEEE Journal on Sel. Areas in Commun.*, vol. 29, no. 2, pp. 480–493, Feb. 2011.

[79] S. Kompella, G. D. Nguyen, C. Kam, J. E. Wieselthier, and A. Ephremides, "Cooperation in Cognitive Underlay Networks: Stable Throughput Tradeoffs," *IEEE/ACM Trans. Netw.*, vol. 22, no. 6, pp. 1756–1768, Dec. 2014.

[80] N. Pappas and Kountouris, "Throughput of a Cognitive Radio Network under Congestion Constraints: A Network-Level Study," in *Proc. IEEE Intl. Conf. on Cognitive Radio Oriented Wireless Networks and Commun., Oulu, Finland*, June Oct. 1998.

[81] A. E. Ewaisha and C. Tepedelenlioglu, "Throughput Optimization in Multichannel Cognitive Radios with Hard-deadline Constraints," *IEEE Trans. on Veh. Technology*, vol. 65, no. 4, pp. 2355–2638, Apr. 2016.

[82] S. Singh *et al.*, "Proportional Fair Traffic Splitting and Aggregation in Heterogeneous Wireless Networks," *IEEE Commun. Letters*, vol. 20, no. 5, pp. 1010–1013, May. 2016.

[83] F. Mehmeti and T. Spyropoulos, "Performance Analysis of Mobile Data Offloading in Heterogeneous Networks," *IEEE Trans. on Mobile Computing*, vol. 16, no. 2, pp. 482–497, Feb. 2017.

[84] C. Hua *et al.*, "Online Packet Dispatching for Delay Optimal Concurrent Transmissions in Heterogeneous Multi-RAT Networks," *IEEE Trans. Wireless Commun.*, vol. 15, no. 7, pp. 5076–5085, July 2016.

[85] Z. Zhou, D. Guo, and M. L. Honig, "Licensed and Unlicensed Spectrum Allocation in Heterogeneous Networks," *IEEE Trans. Commun.*, vol. 65, no. 4, pp. 1815–1827, Apr. 2016.

[86] A. Ephremides and B. Hajek, "Information Theory and Communication Networks: an Unconsummated Union," *IEEE Trans. on Inform. Theory*, vol. 44, no. 6, pp. 2416–2434, Oct. 1998.

[87] J. G. Andrews, F. Baccelli, and R. K. Ganti, "A Tractable Approach to Coverage and Rate in Cellular Networks," *IEEE Transactions on Communications*, vol. 59, no. 11, pp. 3122–3134, Nov. 2011.

[88] H. S. Dhillon, R. K. Ganti, F. Baccelli, and J. G. Andrews, "Modeling and analysis of k-tier downlink heterogeneous cellular networks," *IEEE J. Sel. Areas Commun.*, vol. 30, no. 3, pp. 550–560, 2012.

[89] H. S. Dhillon, R. K. Ganti, and J. G. Andrews, "Load-aware modeling and analy-

sis of heterogeneous cellular networks,," *IEEE Trans. Wireless Commun.*, vol. 12, no. 4, pp. 1666–1677, 2013.

[90] S. Mukherjee, "Distribution of downlink SINR in heterogeneous cellular networks," *IEEE J. Sel. Areas Commun.*, vol. 30, no. 3, pp. 575–585, 2012.

[91] M. Haenggi, "Mean interference in hard-core wireless networks," *IEEE Communications Letters*, vol. 15, no. 8, pp. 792–794, August 2011.

[92] H. Q. Nguyen, F. Baccelli, and D. Kofman, "A stochastic geometry analysis of dense IEEE 802.11 networks," in *IEEE INFOCOM*, May 2007, pp. 1199–1207.

[93] Y. Gao, B. Chen, X. Chu, and J. Zhang, "Resource allocation in lte-laa and wifi coexistence: a joint contention window optimization scheme," in *Proceedings of IEEE Global Communications Conference*, 2017, pp. 1–6.

[94] C. H. Lee and M. Haenggi, "Interference and outage in poisson cognitive networks," *IEEE Transactions on Wireless Communications*, vol. 11, no. 4, pp. 1392–1401, Apr. 2012.

[95] Z. Yazdanshenasan, H. S. Dhillon, M. Afshang, and P. H. J. Chong, "Poisson Hole Process: Theory and Applications to Wireless Networks," *IEEE Trans. Wireless Commun.*, vol. 15, no. 11, pp. 7531–7546, 2016.

[96] M. Kountouris and N. Pappas, "Approximating the interference distribution in large wireless networks," in *11th International Symposium on Wireless Communications Systems (ISWCS)*, Aug 2014, pp. 80–84.

[97] Z. Chen and M. Kountouris, "Decentralized opportunistic access for D2D underlaid cellular networks." [Online]. Available: http://arxiv.org/abs/1607.05543

[98] N. Pappas and M. Kountouris, "Performance analysis of distributed cooperation under uncoordinated network interference," in *IEEE International Conference on Acoustics, Speech and Signal Processing (ICASSP)*, May 2014, pp. 6181–6185.

[99] Z. Chen and M. Kountouris, "Guard zone based d2d underlaid cellular networks with two-tier dependence," in *IEEE International Conference on Communication Workshop (ICCW)*, June 2015, pp. 222–227.

[100] Q. Chen, G. Yu, H. Shan, A. Maaref, G. Y. Li, and A. Huang, "Cellular Meets WiFi: Traffic Offloading or Resource Sharing?" *IEEE Trans. Wireless. Commun.*, vol. 15, no. 5, pp. 3354–3367, May. 2016.

[101] I. Siomina and D. Yuan, "Analysis of Cell Load Coupling for LTE Network Planning and Optimization," *IEEE Trans. Wireless. Commun.*, vol. 11, no. 6, pp. 2287–2297, Feb. 2012.

[102] ——, "Optimizing Small-Cell Range in Heterogeneous and Load-Coupled LTE Networks," *IEEE Trans. Veh. Technol.*, vol. 64, no. 5, pp. 2169–2174, May 2015.

[103] R. L. G. Cavalcante *et al.*, "Max-min Utility Optimization in Load Coupled Interference Networks," *IEEE Trans. Wireless. Commun.*, vol. 16, no. 2, pp. 705–716, Nov. 2017.

[104] H. Klessig *et al.*, "A Performance Evaluation Framework for Interference-Coupled Cellular Data Networks," *IEEE Trans. Wireless. Commun.*, vol. 15, no. 2, pp. 938–950, Feb. 2015.

[105] Z. Yang, W. Xu, J. Shi *et al.*, "Association and Load Optimization with User Priorities in Load-Coupled Heterogeneous Networks," *IEEE Trans. Wireless. Commun.*, vol. 17, no. 1, pp. 324–338, Jan. 2018.

[106] Q. Ye, "User Association for Load Balancing in Heterogeneous Cellular Networks," *IEEE Trans. Wireless Commun.*, pp. 2706–2716, Jun. 2013.

[107] B. H. Jung, N. Song, and D. K. Sung, "A Network-assisted User-centric WiFi-offloading Model for Maximizing Per-user Throughput in a Heterogeneous Network," *IEEE Trans. Veh. Technol.*, vol. 63, no. 4, pp. 1940–1945, May. 2014.

[108] M. H. Cheung and J. Huang, "DAWN: Delay-aware Wi-Fi Offloading and Network Selection," *IEEE J. Sel. Areas Commun.*, vol. 33, no. 6, pp. 1214–1223, Jun. 2015.

[109] H. Deng and I.-H. Hou, "On the Capacity-performance Trade-off of Online Polocy in Delayed Mobile Offloading," *IEEE Trans. Wireless Commun.*, vol. 16, no. 1, pp. 526–537, Jan. 2017.

[110] H. Ko, J. Lee, and S. Pack, "Performance Optimization of Delayed Wi-Fi Offloading and Network Selection," *IEEE J. Sel. Areas Commun.*, vol. 66, no. 10, pp. 9436–9447, Oct. 2017.

[111] Q. Chen, G. Yu, A. Maaref *et al.*, "Rethinking Mobile Data Offloading for LTE in Unlicensed Spectrum," *IEEE Trans. Wireless. Commun.*, vol. 15, no. 7, pp. 4987–5000, July. 2016.

[112] F. Abinader, E. Almeida, F. Chaves *et al.*, "Enabling the coexistence of LTE and Wi-Fi in unlicensed bands," *IEEE Commun. Mag.*, vol. 52, no. 11, pp. 54–61, Nov. 2014.

[113] G. Bianchi, "Performance Analysis of IEEE 802.11 Distributed Coordination Function," *IEEE J. Sel. Areas Commun.*, vol. 18, no. 3, pp. 535–547, Mar. 2000.

[114] H. Zhang, X. Chu, W. Guo *et al.*, "Coexistence of Wi-Fi and Heterogeneous Small Cell Networks Sharing Unlicensed Spectrum," *IEEE Commun. Mag.*, vol. 54, pp. 158–164, 2015.

[115] Y. Wu, W. Guo, H. Yuan *et al.*, "Device-to-device meets LTE-unlicensed," *IEEE Commun. Mag.*, vol. 54, no. 5, pp. 154–159, May 2016.

[116] Y. Li, F. Baccelli, J. G. Andrews, T. D. Novlan *et al.*, "Modeling and Analyzing the Coexistence of Wi-Fi and LTE in Unlicensed Spectrum," *IEEE Trans. Wireless Commun.*, vol. 15, no. 9, pp. 6310–6326, Sept. 2016.

[117] X. Wang, T. Q. Quek, M. Sheng *et al.*, "Throughput and fairness analysis of Wi-Fi and LTE-U in unlicensed band," *IEEE J. Sel. Areas Commun.*, vol. 35, no. 1, pp. 63–78, Jan. 2017.

[118] C. Liu and H. Tsai, "Traffic Management for Heterogeneous Networks With Opportunistic Unlicensed Spectrum Sharing," *IEEE Trans. Wireless Commun.*, vol. 16, no. 9, pp. 5717–5731, Sept. 2017.

[119] C. K. Ho *et al.*, "Data Offloading in Load Coupled Networks: A Utility Maximization Framework," *IEEE Trans. Wireless. Commun.*, vol. 13, no. 4, pp. 1921–1931, Apr. 2014.

[120] H. Klessig, D. Ohmann, A. J. Fehske *et al.*, "A Performance Evaluation Framework for Interference-Coupled Cellular Data Networks," *IEEE Trans. Wireless. Commun.*, vol. 15, no. 2, pp. 938–950, Feb. 2015.

[121] L. You and D. Yuan, "Load Optimization With User Association in Cooperative and Load-Coupled LTE Networks," *IEEE Trans. Wireless. Commun.*, vol. 16, no. 5, pp. 3218–3231, May 2017.

[122] B. Chen, L. You, D. Yuan *et al.*, "Resource Optimization for Joint LWA and LTE-U in Load-coupled and Multi-Cell Networks," *IEEE Commun. Letters*, pp. 1–1, Sept. 2018.

[123] Q. Liao, "Dynamic Uplink/Downlink Resource Management in Flexible Duplex-Enabled Wireless Networks," in *2017 ICC Workshop*, Oct. 2017.

[124] A. Bleicher, "A surge in small cell sites," *IEEE Spectrum*, vol. 50, no. 1, pp. 38–39, Jan. 2013.

[125] "Cisco Virtual Networking Index: Global Mobile Data Traffic Forecast Update, 2011-2016," White Paper, Cisco, 2012. [Online]. Available: http://www.cisco.com

[126] D.Flore, "Chairman Summary," *3GPP RAN1 standard contribution - (RWS-140029)*, Jun. 2014.

[127] "LTE in Unlicensed Spectrum : Harmonious Coexistence with WiFi," White Paper, Qualcomm, 2012. [Online]. Available: https://www.qualcomm.com

[128] Sony, "Requirements and coexistence topics for LTE-U," *3GPP RAN1 standard contribution - (RWS-140010)*, Jun. 2014.

[129] "Evolved Universal Terrestrial Radio Access (E-UTRA); Physical layer procedures," Report, 3GPP, Jan. 2016. [Online]. Available: http://www.3gpp.org/dynareport/36213.htm

[130] R. Yin, G. Yu, A. Maaref, and G. Li, "Adaptive LBT for Licensed Assisted Access LTE Networks," in *2015 IEEE Global Communications Conference (GLOBECOM)*, San Diego, 2015.

[131] A. Baswade and B. Tamma, "Channel sensing based dynamic adjustment of contention window in LAA-LTE networks," in *2016 8th International Conference on Communication Systems and Networks (COMSNETS)*, Bangalore, 2016.

[132] C. Kim, C. Yang, and C. Kang, "Adaptive Listen-Before-Talk (LBT) Scheme for LTE and Wi-Fi Systems Coexisting in Unlicensed Band," in *2016 13th IEEE Annual Consumer Communications and Networking Conference (CCNC)*, Las Vegas, 2016.

[133] H. Ko, J. Lee, and S. Pack, "A Fair Listen-Before-Talk Algorithm for Coexistence of LTE-U and WLAN," *IEEE Transactions on Vehicular Technology*, p. 1, 2016.

[134] Y. Li, J. Zheng, and Q. Li, "Enhanced Listen-before-talk Scheme for Frequency Reuse of Licensed-assisted Access Using LTE," in *2015 IEEE 26th International Symposium on Personal, Indoor and Mobile Radio Communications (PIMRC): Mobile and Wireless Networks*, Hong Kong, 2016.

[135] A. Mukherjee, "System architecture and coexistence evaluation of licensedassisted access. LTE with IEEE 802.11," in *Proc. 2015 IEEE Inter. Conf. on Commun. (ICC) Workshop on LTE in Unlicensed Bands (LTE-U)*, London, 2015.

[136] C. Cano and D. Leith, "Coexistence of Wi-Fi and LTE in unlicensed bands: A proportional fair allocation scheme," in *Proc. 2015 IEEE Inter. Conf. on Commun. (ICC) Workshop on LTE in Unlicensed Bands (LTE-U)*, London, 2015.

[137] T. Nihtila, V. Tykhomyrov, O. Alanen *et al.*, "System performance of LTE and IEEE 802.11 coexisting on a shared frequency band," in *Proc. 2013 IEEE Int. Workshop on Wireless Communications and Networking Conference (WCNC)*, Shanghai, Apr. 2013, pp. 1038–1043.

[138] O. Sallent, J. Perez-Romero, R. Ferrus, and R. Agusti, "Learning-based Coexistence for LTE Operation in Unlicensed Bands," in *Proc. 2015 IEEE Inter. Conf. on Commun. (ICC) Workshop on LTE in Unlicensed Bands (LTE-U)*, London, 2015.

[139] B. Jia and M. Tao, "A channel sensing based design for LTE in unlicensed bands," in *Proc. 2015 IEEE Inter. Conf. on Commun. (ICC) Workshop on LTE in Unlicensed Bands (LTE-U)*, London, 2015.

[140] A. Cavalcante, "Performance evaluation of LTE and Wi-Fi coexistence in unlicensed bands," in *Proc. 2013 IEEE 77th Vehi. Technol. Conf. (VTC) Spring*, Dresden, Jun. 2013, pp. 1–6.

[141] C. Cano and D. J. Leith, "Coexistence of WiFi and LTE in unlicensed bands: A proportional fair allocation scheme," in *Proc. 2015 IEEE Inter. Conf. on Commun. (ICC) Workshop on LTE in Unlicensed Bands (LTE-U)*, London, 2015.

[142] 3rd Generation Partnership Project; Technical Specification Group Radio Access Network; Study on Licensed-Assisted Access to Unlicensed Spectrum; (Release 13), *3GPP TR 36.889 V13.0.0*, Jun. 2015.

[143] "LTE and Wi-Fi in Unlicensed Spectrum: A Coexistence Study," White Paper, Google, Jun. 2015. [Online]. Available: http://apps.fcc.gov/ecfs/document/view?id=60001078145

[144] "Reply Comments of Ericsson," White Paper, Ericsson, Jun. 2015. [Online]. Available: http://apps.fcc.gov/ecfs/document/view?id=60001104806

[145] "Reply Comments of Qualcomm Incorporated," White Paper, Qualcomm, Jun. 2015. [Online]. Available: http://apps.fcc.gov/ecfs/comment/view?id=60001084962

[146] Wi-Fi Alliance, "Coexistence Test Plan Version 0.8.2," Tech. Rep., 2016. [Online]. Available: https://www.wi-fi.org

[147] FCC. (2016) Trends in LTE-U and LAA Technology. [Online]. Available: http://apps.fcc.gov

[148] Wi-Fi Alliance, "Coexistence Guidance Version 2.0," Tech. Rep., Feb. 2016. [Online]. Available: https://www.wi-fi.org/download.php?file=/sites/default/files/private/CoX_Guidelines_v2.0.pdf

[149] E. Almeida, A. Cavalcante, R. Paiva *et al.*, "Enabling LTE/WiFi coexistence by LTE blank subframe allocation," in *Proc. 2013 IEEE Inter. Conf. on Commun. (ICC)*, Budapest, Jun. 2013, pp. 5083–5088.

[150] A. K. Sadek, "Carrier sense adaptive transmission (CSAT) in unlicensed spectrum," U.S. Patent 201 500 858 684A1, Mar. 2015.

[151] S. Sagari, I. Seskar, and D. Raychaudhuri, "Modeling the coexistence of LTE and Wi-Fi heterogeneous," in *Proc. 2015 IEEE Inter. Conf. on Commun. (ICC) Workshop on LTE in Unlicensed Bands (LTE-U)*, London, 2015.

[152] F. Liu, E. Bala, E. Erkip, R. Yang *et al.*, "A framework for femtocells to access both licensed and unlicensed bands," in *Proc. 2011 Int. Symp. WiOpt*, Princeton, NJ, May. 2011, pp. 6809–6814.

[153] N. Zhang, M. Saisai, X. Jing *et al.*, "Unlicensed spectrum usage method for cellular communication systems," in *Proc. 2012 8th Int. Conf. WiCOM*, Shanghai, Sept. 2012, pp. 1–5.

[154] S. Hajmohammad, H. Elbiaze, and W. Ajib, "Fine-tuning the femtocell performance in unlicensed bands: Case of Wi-Fi co-existence," in *Proc. 2014 Int. Conf. WiCOM*, Nicosia, Aug. 2014, pp. 250–255.

[155] A. Damnjanovic, "Techniques for assessign clear channel in an unlicensed radio frequency spectrum band," U.S. Patent 20 150 098 397A1, Apr. 2015.

[156] T. Ji, N. Bhushan, Y. Wei *et al.*, "LTE-U clear channel assessment operations," U.S. Patent 20 150 099 525A1, Apr. 2015.

[157] P. Xia, Z. Teng, and J. Wu, "How loud to talk and how hard to listen-before-talk in unlicensed LTE," in *Proc. 2015 IEEE Inter. Conf. on Commun. (ICC) Workshop on LTE in Unlicensed Bands (LTE-U)*, London, 2015.

[158] Cablelabs, "CableLabs Perspectives on LTE-U Coexistence with Wi-Fi and Operational Modes for LTE-U," *3GPP RAN1 standard contribution - (RWS-140004)*, Jun. 2014.

[159] S. Haykin, "Cognitive radio: Brain-empowered Wireless Communications," *IEEE Journal on Selected Areas in Communications*, vol. 23, pp. 201–220, 2005.

[160] P. Karunakaran, T. Wagner, A. Scherb, and W. Gerstacker, "Sensing for Spectrum Sharing in Cognitive LTE-A Cellular Networks," in *Wireless Communications and Networking Conference (WCNC)*, Istanbul, 2005.

[161] G. Singh and P. Mehta, "Review on Analysis of LTE and Cognitive Radio Network using OFDM signal," *International Journal on Recent and Innovation Trends in Computing and Communication*, vol. 2.

[162] W. Xu, B. Li, Y. Xu, and J. Lin, "Lower-Complexity Power Allocation for LTE-U Systems: A Successive Cap-Limited Waterfilling Method," in *Vehicular Technology Conference (VTC Spring), 2015 IEEE 81st*, Glasgow, 2015.

[163] 3rd Generation Partnership Project; Scenarios and requirements for small cell enhancements for E-UTRA and E-UTRAN (Rel 12), *3GPP TR 36.932 V13.0.0*, Dec. 2015.

[164] "MSA: A key technology for the evolution of future wireless networks," Jun. 2013. [Online]. Available: http://www.huawei.com/en/static/HW-267909.pdf

[165] "The Role and Benefits of RF and Performance Modelling Tools in the HetNet Era," White Paper, Ranplan, Sept. 2014. [Online]. Available: https://www.ranplan.co.uk/downloads/resources/Value_of_planning_tools.pdf

[166] "Outdoor LTE Small Cell Deployment on Lampposts: A Paris City Study," White Paper, Ranplan, Jun. 2014. [Online]. Available: https://www.ranplan.co.uk/whitepaper/OutdoorSmallCellRanplan_v4.pdf

[167] "Small Cell Deployments: Recent Advances and Research Challenges," White Paper, Ranplan, Nov. 2012. [Online]. Available: https://www.ranplan.co.uk/whitepaper/FemtoSON_Paper.pdf

[168] Samsung, "Performance Evaluation of LTE in Unlicensed Spectrum," *3GPP RAN1 standard contribution - (RWS-140016)*, Jun. 2014.

[169] Y. Jian, C.-F. Shih, B. Krishnaswamy, and R. Sivakumar, "Coexistence of Wi-Fi and LTE-LAA: experimental evaluation, analysis and insights," in *Proc. 2015 IEEE Inter. Conf. on Commun. (ICC) Workshop on LTE in Unlicensed Bands (LTE-U)*, London, 2015.

[170] "Small Cell Deployment in HetNets," White Paper, Ranplan, Jun. 2012. [Online]. Available: https://www.ranplan.co.uk/SmallCellDeployHetNetSCWS.pdf

[171] A. Bhorkar, C. Ibars, and P. Zong, "Performance evaluation of LTE and Wi-Fi coexistence in unlicensed spectrum," in *Proc. 2015 IEEE Inter. Conf. on Commun. (ICC) Workshop on LTE in Unlicensed Bands (LTE-U)*, London, 2015.

[172] N. Pappas, M. Kountouris, A. Ephremides, and V. Angelakis, "Stable Throughput Region of the Two-User Broadcast Channel," *IEEE Trans. Commun.*, pp. 1–1, May 2018.

[173] W. Szpankowski, "Stability Conditions for Some Distributed Systems: Buffered Random Access Systems," *Advances in Applied Probability*, vol. 26, no. 2, pp. 498–515, Jun. 1994.

[174] R. Loynes, "The stability of a queue with non-independent inter-arrival and service times," in *Proc. Camb. Philos. Soc*, July 1962.

[175] D. Kaspar, "Multipath aggregation of heterogeneous access networks," *ACM SIGMultimedia Records*, vol. 4, no. 1, pp. 27–28, 2012.

[176] M. Haenggi, *Stochastic geometry for wireless networks*. Cambridge University Press, 2012.

[177] Z. Yazdanshenasan, H. S. Dhillon, M. Afshang, and P. H. J. Chong, "Poisson Hole Process: Theory and Applications to Wireless Networks," *IEEE Transactions on Wireless Communications*, vol. 15, no. 11, pp. 7531–7546, Nov. 2016.

[178] M. S. Afaqui *et al.*, "IEEE 802.11ax: Challenges and Requirements for Future High Efficiency WiFi," *IEEE Wireless. Commun.*, vol. 24, no. 3, pp. 130–137, Jun. 2016.

[179] S. Sagari, "Coordinated Dynamic Spectrum Management of LTE-U and Wi-Fi Networks," in *Proc. IEEE Int. Symp. Dyn. Spectr. Access Netw. (DySPAN), Stockholm, Sweden*, Sept. 2015.

[180] R. Cavalcante *et al.*, "Toward Energy-efficient 5G Wireless Communications Technologies: Tools for Decoupling the Scaling of Networks from the Growth of Operating Power," *IEEE Signal Process. Mag.*, vol. 31, no. 6, pp. 24–34, Nov. 2014.

[181] Q. Chen, G. Yuan, H. M. Elmaghraby *et al.*, "Embedding LTE-U within Wi-Fi Bands for Spectrum Efficiency Improvement," *IEEE Netw.*, vol. 31, no. 2, pp. 72–79, Mar. 2017.

[182] K. Xin, Y. K. Chia, S. Sun *et al.*, "Mobile Data Offloading through a third-party Wi-Fi Access Points: An Opterator's Perspective," *IEEE Trans. Wireless Commun.*, vol. 13, no. 10, pp. 5340–5351, Oct. 2014.

[183] F. Liu, E. Bala, E. Erkip, M. Beluri, and R. Yang, "Small Cell Traffic Balancing over Licensed and Unlicensed Bands," *IEEE Trans. Veh. Technol.*, vol. 64, no. 12, pp. 5850–5865, Dec. 2015.

[184] Q. Chen, G. Yu, and Z. Ding, "Optimizing Unlicensed Spectrum Sharing for LTE-U and WiFi Network Coexistence," *IEEE J. Sel. Areas Commun.*, vol. 34, no. 10, pp. 2562–2574, Oct. 2016.

[185] M. Ismail and W. Zhuang, "A Distributed Multi-service Resource Allocation Algorithm in Heterogeneous Wireless Access Medium," *IEEE J. Sel. Areas Commun.*, vol. 30, no. 2, pp. 425–432, Feb. 2012.

[186] H. R. Feyzmahdavian, M. Johansson, and T. Charalambous, "Contractive Interference Functions and Rates of Convergence of Distributed Power Control Laws," *IEEE Trans. Wireless Commun.*, vol. 11, no. 12, pp. 4494–4502, 2012.